ALTERED HEPARAN SULFATE IN AGEING AND DEMENTIA: A POTENTIAL AXIS FOR THE DYSREGULATION OF BACE-1 IN ALZHEIMER'S DISEASE

Thesis submitted in accordance with the requirements of the University of Liverpool for the degree of Doctor of Philosophy

2017

HANNAH ELIZABETH CLARKE

Supervisors:

Professor Jerry Turnbull

Doctor Olga Vasieva

(Institute of Integrative Biology, University of Liverpool)

Funded by Alzheimer's Research UK

0.1 Acknowledgments

There are lots of people I would like to thank for their support and guidance over the last 3 years. They have all helped me hugely and without them I would not be sitting here now writing the acknowledgements for my thesis so thank you!

I would firstly like to take this opportunity to thank Alzheimer's Research UK for their funding, without which this project would not have been possible. I would also like to thank my supervisor Professor Jerry Turnbull, for not only giving me the opportunity to complete this PhD in the first place but also for all of his help and guidance throughout the whole process. I have learnt a great deal during my time with Jerry and am very grateful for the opportunities he gave me along the way, thank you! Thanks must also go to Dr. Olga Vasieva for her help and guidance with completing the informatics aspect of this project, something I was a complete novice at when I started!

I would also like to say a big thank you to the members of lab B past and present, for all of their help, support and friendship throughout the last 3 years. Special thanks to Dr. Scott Guimond and Dr Becky Miller for teaching me all there is to know about HS and for showing me the ropes in the lab when I first joined the group and had no idea what I was doing! Thank you to both of them for introducing me to Hank and Sheila and all things chromatography! Also a special thank you to Rachel and Fi for being amazing lab buddies and being there for much needed Starbucks trips and distraction from thesis writing when needed. Thanks to them for keeping me sane, I couldn't have done it without them!

Huge thanks must also go to Dr. Linda Troeberg and Dr. Tas Chanalaris at the University of Oxford for their collaboration, help and friendship this last year. Thanks to them for all of their help with the TaqMan® array analysis, without which chapter 3 wouldn't have happened. They let me visit on a number of occasions with boxes of samples to run and included little surprises in the parcels they sent me. I would like to thank them for their patience with my endless questions and for making me smile with deliveries of chocolate whilst writing my thesis.

Thanks must also go to my "fellow PhD buddies"; to Charlotte, Becca, Zoe, Hannah, Melissa W and Clarissa who even though may be studying at different universities, have been there when things haven't gone quite right and when we didn't know which stats test to use. Thanks to them for the catch ups over wine and all the science chat. I must also mention Melissa S, who whilst choosing not to do a PhD, deserves one just for listening to us every time we meet up!

Big thank you must also go to my Mum, Dad and brother - the best family in the world for supporting me not just through this PhD but always. Thanks to them for always being on the end of

the phone when I needed to talk and for telling me not to give up and to keep going when things got tough. I am the luckiest to have them. Also a huge thank you to my wonderful boyfriend Rich who has been there the whole time. Thanks to him for putting up with my early mornings and late nights and helping me switch off when all I could think about was science. Thanks also to Rich for always listening and encouraging me. I promise all the science chat can stop now!

Thank you everyone!

0.2 Abstract

Alzheimer's disease (AD) is characterised by amyloid plaques composed of amyloid-beta (Aß), the cleavage product of the amyloid precursor protein (APP) by the protease beta-secretase (BACE-1). Heparan sulfate (HS) inhibits BACE-1 and holds potential as a new drug discovery target; *in vivo* HS may act as a brake on the generation of Aß via regulation of BACE-1. Previous work has identified the sulfate moieties in HS as key determinants in the efficacy of BACE-1 inhibition. Structural changes in HS are known to occur with ageing and we hypothesised that these changes could result in reduced BACE-1 inhibition and ultimately elevated production of Aß.

Strong anion exchange chromatography was used to assess disaccharide composition of HS from AD (n=20) and age-matched control (n=15) brain tissue. TaqMan® array profiling of HS-related genes was also carried out to explore expression levels of HS-related genes that may be responsible for downstream HS structural changes. HS purified from AD and age-matched control samples was assessed for its ability to inhibit BACE-1 using FRET-based BACE-1 activity assays and finally, manipulation of endogenous HS in HEKSweAPP cells with RNAi was carried out to explore the possibility of modulating generation of the toxic Aß species.

HS from AD tissue was found to carry a significantly decreased proportion of the di-sulfated ΔUA-GlcNS(6S) disaccharide vs. controls ($p<0.01$) and increased levels of the lesser-sulfated ΔUA-GlcNAc(6S) unit vs. controls ($p<0.05$). Furthermore, significantly more total HS was present within control brain tissue (122.3µg/100mg) vs. AD (78.6µg/100mg) ($p<0.01$). TaqMan® array analysis revealed significant alteration in expression of HS biosynthetic genes with AD including up-regulation of *HS6ST1* ($p<0.05$) and a strong trend for down regulation of *HS6ST3*, coupled with up regulation of *SULF1*. These changes may go some way to explain changes in the level of sulfation of HS particularly, 6-O sulfation, as observed by structural analysis. Most noticeably, BACE-1 activity assays revealed a significant reduction of BACE-1 inhibition efficacy by HS from AD patients ($p<0.05$). In addition, knockdown of SULF1 in HEKSweAPP cells, which would be expected to elevate 6-O sulfation, generated a significant reduction in Aß.

Our observation that AD brain HS contains fewer di-sulfated ΔUA-GlcNS(6S) disaccharides, alongside observed upstream gene expression changes, would be consistent with a less sulfated HS chain with reduced ability to inhibit BACE-1 thus generating more Aß as observed in AD. The observed reduction in BACE-1 inhibition efficacy by HS with AD confirms our hypothesis that structural changes in HS may contribute to modulating AD pathogenesis in patients. Finally, these studies support the idea that HS-based therapeutics might provide the basis for novel disease modifying drugs that could prove beneficial in future efforts to treat an underlying cause of AD.

0.3 Table of Contents

0.4. Table List

0.5. Figure List

0.6 Abbreviations

A

Aβ – Amyloid Beta
AD – Alzheimer's disease
AGRN – Agrin
AMAC – 2-Aminoacridone
APP – Amyloid Precursor Protein

B

BACE-1 – Beta-Site APP Cleaving Enzyme
BBB – Blood Brain Barrier
BDR – Brains for Dementia Research
BODIPY - 4,4-Difluoro-4-Bora-3a,4a-Diaza-S-Indacene

C

CBD – Cortical Basal Degeneration
CD44 – CD44
CERAD – Consortium to Establish a Registry for Alzheimer's disease
COL18A1 – Type 18 Collagen
CS – Chondroitin Sulfate
CSF – Cerebral Spinal Fluid
CT – Computed Tomography

D

DEAE - Diethylaminoethanol
DNA – Deoxyribonucleic Acid
DS – Dermatan Sulfate

E

EDTA – ethylene-di-amine-tetra-acetic acid
EEG – Electroencephalogram
EST –Expressed Sequence Tag Analysis
EXT1 – Exostose-1
EXT2 – Exostose-2
EXTL3 – Exostose-like-3

F

FGF-2 – Fibroblast Growth Factor-2
FTDP-17 – Frontal-Temporal Dementia leading to Parkinsonism on chromosome 17

G

GAG – Glycosaminoglycan
GALT1 – Galactosyltransferase 1
GALT2 – Galactosyltransferase 2
GlcA – Glucuronic acid
GLCE – C5-Epimerase
GlcNAc – N-acetyl-glucosamine
GlcNS – N-sulfate-glucosamine
GPC1 – Glypican-1
GPC2 – Glypican-2
GPC3 – Glypican-3
GPC4 – Glypican-4
GPC5 – Glypican-5
GPC6 – Glypican-6

H

HA – Hyaluronic acid
HS – Heparan Sulfate
HPLC – High Performance Liquid Chromatography
HPSE - Heparinase
HS6ST1 – Heparan Sulfate 6-O Sulfotransferase-1
HS6ST2 – Heparan Sulfate 6-O Sulfotransferase-2
HS6ST3 – Heparan Sulfate 6-O Sulfotransferase-3
HS2ST1 – Heparan Sulfate 2-O Sulfotransferase-1
HS3ST1 – Heparan Sulfate 3-O Sulfotransferase-1
HS3ST2 – Heparan Sulfate 3-O Sulfotransferase-2
HS3ST4 – Heparan Sulfate 3-O Sulfotransferase-4
HS3ST5 – Heparan Sulfate 3-O Sulfotransferase-5
HS3ST6 – Heparan Sulfate 3-O Sulfotransferase-6
HSPG – Heparan Sulfate Proteoglycan
HSPG2 – Perlecan

I

IdoA – Iduronic Acid

J

K

KS – Keratan Sulfate

L

M

MMSE – Mini Mental State Exam
MPSS – Massively Parallel Signature Sequence Tag Analysis
MRC – Medical Research Council
MRI – Magnetic Resonance Imaging
MS – Mass Spectrometry

N

NaCl – Sodium Chloride
NaOH – Sodium Hydroxide
NDST1 – N-Deacetylase/N-Sulfotransferase-1
NDST2 – N-Deacetylase/N-Sulfotransferase-2
NDST3 – N-Deacetylase/N-Sulfotransferase-3
NDST4 – N-Deacetylase/N-Sulfotransferase-4
NFTs – Neurofibrillary Tangles
NIA – National Institute of Ageing
NIH – National Institute of Health
NIHR – National Institute of Health Research
NRP1 – Neuropilin-1
NINCDS-ADRDA – National Institute of Neurological and Communicative Disorders and Stroke and the Alzheimer's disease and Related Disorders Association
NO – Nitric Oxide

O

P

PBS – Phosphate Buffered Saline
PET – Positron Emission Tomography
PHF – Paired Helical Filaments
PIMH – Porcine Intestinal Mucosal Heparin
PMD – Post Mortem Delay
PSP – Progressive Supranuclear Palsy

Q

R

ROS – Reactive Oxygen Species
RNS – Reactive Nitrogen Species
RNA – Ribonucleic Acid
RP-HPLC – Reverse Phase High Performance Liquid Chromatography
RT-PCR – Real Time Polymerase Chain Reaction

S

SAGE – Serial Analysis of Gene Expression
SAX – Strong Anion Exchange
SAX-HPAEC – Strong Anion Exchange – High Performance Chromatography
SAXS – Small Angle X-Ray Scattering
SULF1 – Sulfatase 1
SULF2 – Sulfatase 2
SDC1 – Syndecan-1
SDC2 – Syndecan-2
SDC3 – Syndecan-3
SDC4 – Syndecan-4
SRGN - Serglycin

T

TLC – Thin Layer Chromatography
TBFBR3 – Beta-glycan

U

UV – Ultraviolet

V

W

X

XYLT1 – Xylosyltransferase-1
XYLT2 – Xylosyltransferase-2

Y

Z

Chapter 1: Introduction to Alzheimer's disease and heparan sulfate

1. Chapter 1

1.1 Introduction to glycosaminoglycans

Glycosaminoglycans (GAGs) are complex polysaccharides that are made up of repeating units of disaccharide entities that may vary in their sequence, linkage motif and modification pattern; i.e. the degree of sulfated and acetylated motifs that may be present along the length of the GAG chain. The extent of variability between members of the GAG family is considerable and as such these molecules are found to be involved in mediating a significant proportion of biological processes and pathways within the body. The size of GAG chains is not well defined and may be as long as 25,000 disaccharide units in length in the case of hyaluronic acid (HA) (Handel*, et al.* 2005). GAGs are localised to a number of regions of the cell, found free within cells, but also bound to membrane surfaces as proteoglycans or shed as a soluble ectodomain (Capila and Linhardt 2002). The structural diversity afforded by GAG chains makes them potent modulators of biological functions and changes in their structure (and hence binding affinity with specific protein ligands), confers substantial variation in the efficacy of these physiological reactions. As such, understanding GAG chain complexity and functionality offers a great deal of insight into molecular mechanisms and indeed disease pathogenesis. The heterogeneity and complex regulation of GAGs present analysis challenges resulting in some distinct gaps in our understanding of their biology. Advances in carbohydrate chemistry in recent years however has alleviated some of these difficulties and has begun to allow elucidation of the role of GAG chains *in vivo* with respect to health and disease (Handel*, et al.* 2005).

Members of the GAG family include heparan sulfate (HS), chondroitin sulfate (CS), dermatan sulfate (DS) (Sugahara*, et al.* 2003), keratan sulfate (KS) (Funderburgh 2000), hyaluronic acid (HA) and heparin (Capila and Linhardt 2002). These GAGs differ in their structural characteristics and protein binding affinities and as such play very different physiological roles within the body.

1.2 Heparan sulfate

HS is the most ubiquitous of the GAG chains and comprises between 50% and 90% of total endothelial proteoglycans (PGs) (Handel*, et al.* 2005). Furthermore, HS presents the most highly heterogeneous structural capacity of all GAGs and may exert its function both on the cell surface, in the matrix, and in soluble form, making its role within the body wide and varied. HS consists of repeating disaccharide units of alternating glucuronic/iduronic acid (GlcA/IdoA) and glucosamine (GlcNAc). (Esko 2001). One or more HS chains can covalently bind to a core protein forming a

heparan sulfate proteoglycan (HSPG) (Bernfield*, et al.* 1999). HSPGs play central roles in both normal physiology and development. Within the structure, variably sulfated and acetylated motifs exist that confer different binding properties to protein ligands via electrostatic forces of attraction. Consequently, HS is able to regulate metabolism, transport, support, and information transfer (Bishop*, et al.* 2007).

1.2.1 HS biosynthesis

1.2.1.1 HS chain initiation

The biosynthesis of HS has been more conclusively understood in recent years and molecular cloning of specific HS biosynthetic enzymes has allowed scientists to better understand the function of this biosynthetic machinery, as well as the complexity and regulation of HS chain production. HS chain biosynthesis is initiated by the formation of a linkage region that links the HS chain to a core protein. The core proteins, which carry HS chains, include syndecan (SDC), glypican (GPC), agrin (AGRN), perlecan (HSPG2) and collagen XVIII (COL18A1). Other HSPGs exist that only carry the HS chains under certain circumstances are referred to as "part time" HSPGs and include CD44, betaglycan (TGFBR3) and testican (SPOCK) (Parish 2006). The relative amounts of these proteins may act as a limiting factor in the synthesis of HS. Likewise, regulatory domains within these proteins, other than the HS binding sites themselves, may have important regulatory function (Chen and Lander 2001). HS biosynthesis begins with the generation of a tetrasaccharide glucuronic acid-galactose-galactose-xylose linker region. Xylotransferase enzymes, XYLT or XYLT2, add xylose to a serine residue on the core HS protein to initiate this linker formation. The addition of two galactose residues by galactosyltransferases GALT-1 and GALT-2 follows and the linker is completed by a final addition of GlcA via the action of GlcAT-1 transferase (Kreuger and Kjellen 2012, Zhang*, et al.* 1995). The linker region generated in this instance for HS synthesis is identical to that generated for CS. Elongation of the HS chain occurs via the action of a family of glycosyltransferases, EXTLs. The enzymes work by catalysing the addition of GlcNAc to the non-reducing end of the tetrasaccharide linker to begin the elongation of the HS chain. Following this, a polymerase complex of EXT1 and EXT2 enzymes add alternating GlcA and GlcNAc residues to the HS chain. At this point, the HS chain becomes a substrate for chain modification by a number of enzymes and addition of the first GlcNAc residue limits the chain to the HS pathway. These enzymes are numerous and exhibit different substrate specificity, which is not entirely understood as yet (Esko and Selleck 2002). Furthermore, not all of these modification reactions will go to completion along the HS chain, further conferring structural heterogeneity between different GAG chains (**Figure 1.1**).

1.2.1.2 HS chain modification

Modification of the HS chain begins with N-deacetylation/N-sulfation of GlcNAc residues by the family of NDST enzymes (NDST1-4). The action of this family is the first committed reaction in HS chain modification and is a pre-requisite for all subsequent modifications that the HS chain may undergo. The members of the NDST family of enzymes all share reasonably high sequence specificity and overall structure however the ratio of deacetylase and sulfotransferase activity differs significantly between the family isoforms. NDST2 for example, exhibits a higher ratio of N-deacetylase/N-sulfotransferase activities vs. NDST1. Furthermore, NDST3 and NDST4 have starkly different ratios of activity compared to NDST1 and NDST2. NDST3 has a much greater efficiency at removing acetyl groups at the N- position whilst conversely; NDST4 exhibits robust sulfotransferase activity (Aikawa*, et al.* 2001). Interestingly whilst *NDST1* and *NDST2* genes are expressed ubiquitously, expression of *NDST3* and *NDST4* genes are restricted to the adult brain and fetal tissues (Aikawa and Esko 1999, Toma*, et al.* 1998). The differential expression of these genes alongside other HS-related genes would suggest that the synthesis of GAG chains is a tightly regulated process akin to processes such as the translation of fibroblast growth factors like FGF-2 (Kevil*, et al.* 1995).

1.2.1.3 HS domain structure

Modification by the NDST enzymes is not carried out to completion at all N-positions along the HS chain. As a result, N-sulfated regions will be interspersed with N-acetylated regions, giving rise to so-called "NS-domains" and "NA-domains" respectively along the HS chain (Esko and Lindahl 2001, Turnbull and Gallagher 1991) (**Figure 1.1**). These domains may occur in a multitude of conformations and hence provide the HS chain with a macroscopic structural heterogeneity. Likewise, the level of modification to individual disaccharides within the chain can vary substantially. Overall, these structural alterations confer a wide variety of protein ligand binding potential.

1.2.1.4 Epimerisation of the HS chain

Action of the C5-epimerase enzyme, GLCE, follows modification by the NDST enzyme family and subsequently epimerises some (but not all) of the GlcA units to IdoA. Previous research has indicated that epimerisation in this fashion does not occur on those units that are already O-sulfated, nor those adjacent to O-sulfated GlcNAc residues (Backstrom*, et al.* 1979). These findings thus suggest that epimerisation occurs after N-deacetylation/N-sulfation but before sulfation at the 6-O and 3-O position (Lindahl*, et al.* 1976). Indeed, it has been suggested that the extent to which IdoA residues are generated along the HS chain is restricted by the degree of N-deacetylation/N-

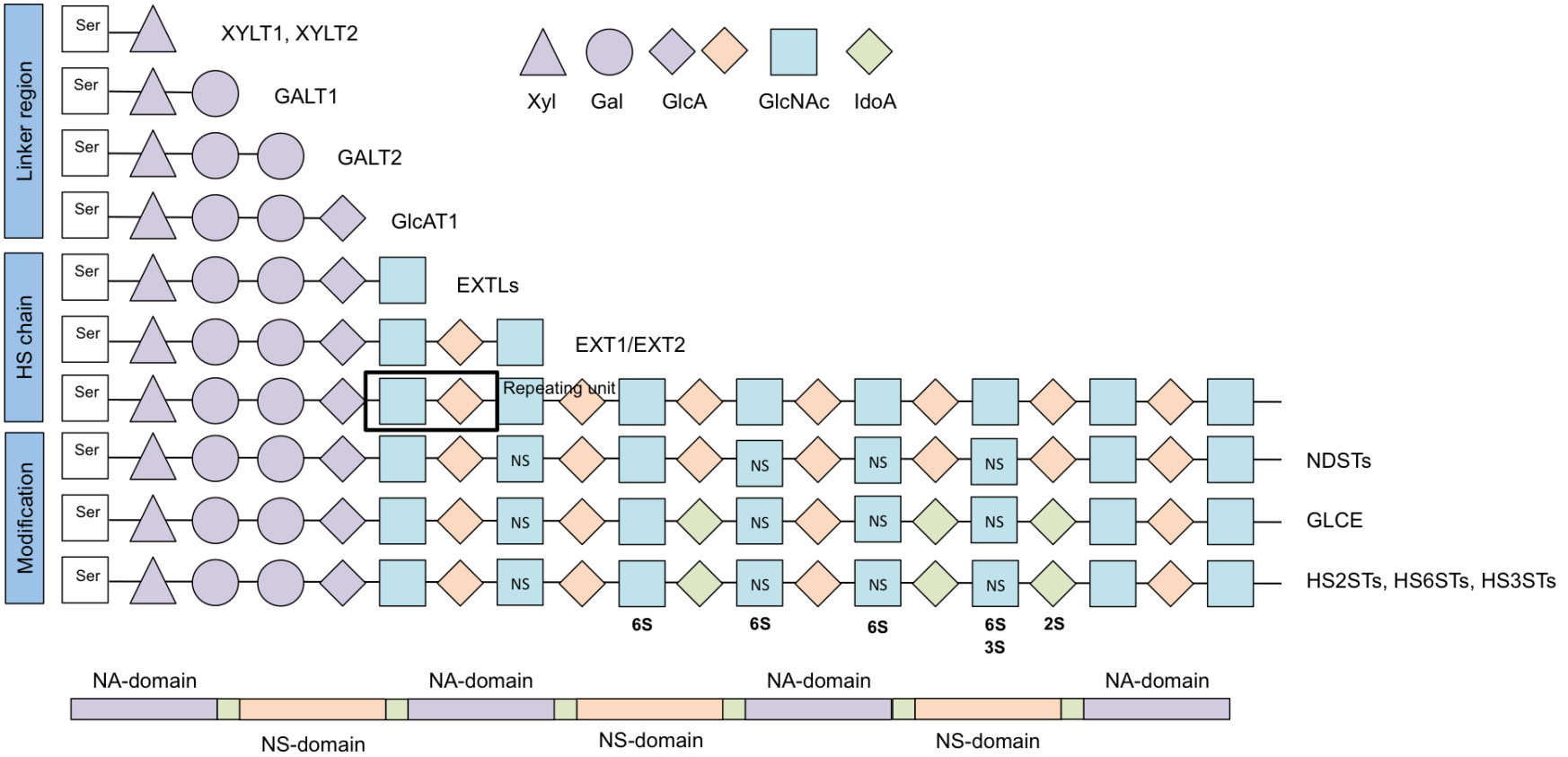

Figure 1.1: The different stages in the biosynthesis of HS. Diagram to show a simplified scheme of chain formation and modification involved in the synthesis of HS. Enzymes responsible for each change are shown at respective steps. Formation of the HS chain occurs first followed by considerable modification via a number of different enzymes. Abbreviations: Xyl; Xylose, Gal; Galactose, GlcA; Glucuronic acid, GlcNAc; N-acetylated glucosamine, IdoA; Iduronic acid, XYLT1/2; Xylosyltransferase 1/2, GALT1/2; Galactosyltransferase 1/2, GlcAT1; Glycosyltransferase 1, EXT1/2; Exostosin Glycosyltransferase 1/2, EXTL; Exostosin Glycosyltransferase Like, NDSTs; N-Deacetylase/N-Sulfotransferase, GLCE; C5 Epimerase, HS2ST1; Heparan sulfate 2-O sulfotransferase, HS6ST; Heparan Sulfate 6-O Sulfotransferase, HS3ST; Heparan Sulfate 3-O Sulfotransferase, NS; N-sulfated GlcN, 6S; 6-O-sulfated GlcN, 2S; 2-O-sulfated IdoA, 3S; 3-O-sulfated GlcN, Ser; serine.

sulfation that has occurred previously (Esko and Selleck 2002). This variable regulation of epimerisation as evidenced by domain distribution alongside NDST modification and expression of the *GLCE* gene will further contribute to the structural heterogeneity observed within HS.

1.2.1.5 Sulfation at the 2-O, 6-O and 3-O position

Addition of further sulfate groups may occur at various positions along the HS chain at the 2-O, 6-O and 3-O position by 2-O sulfotransferases, 6-O sulfotransferases and 3-O sulfotransferases respectively. Addition of sulfate groups in this way can occur in multiple locations on the constituent HS residues (Smeds*, et al.* 2003).

A 2-O sulfotransferase enzyme, HS2ST1 acts to transfer a sulfate group to the 2-OH position of both an IdoA and GlcA residues; however shows preferential efficacy for the IdoA (Esko and Selleck 2002) to form 2-OS IdoA or 2-OS GlcA. The IdoA-2-OS residues have been shown to have physiological functions and this structural motif is particularly important for the stimulation of growth factor mediated signal transduction pathways (Kreuger*, et al.* 2001). The HS2ST1 enzyme has also been implicated in axon migration and guidance in nervous system development (Kinnunen*, et al.* 2005) and knockdown of the *HS2ST1* gene is compensated for with enhanced sulfation at the 6-O position. In addition, research suggests that the HS2ST1 enzyme is able to utilise structural elements along the HS chain to distinguish particular sulfation patterns to determine substrate specificity (Liu*, et al.* 2014). It is believed that this may drive the way and extent to which the HS chain is modified. Furthermore, prominence of 2-O sulfation appears to be somewhat linked with the extent of C5-epimerisation and N-deacetylation/N-sulfation suggesting that these modification events may at least in some way occur simultaneously (Esko and Selleck 2002).

The addition of a sulfate group at the 6-O position has been shown to take place via the action of three 6-O sulfotransferases, HS6ST1, HS6ST2 and HS6ST3. These enzymes catalyse the transfer of a sulfate group to the GlcNAc/GlcNS residues of the HS chain. The activity of each isoform is not fully understood however there is some evidence that each family member has different specificity of action depending on the nature of the residue it acts upon. Previous work has indicated that HS6ST1 prefers the IdoA-GlcNS unit whilst HS6ST2 shows preference for the GlcA-GlcNS and IdoA-GlcNS units. Finally, the HS6ST3 isoform will act on either residue regardless of substrate availability (Habuchi*, et al.* 2000). Similarly, the 3-O sulfotransferase family of enzymes is made up of 7 isoforms. This group is responsible for the rare addition of a sulfate group to the 3-OH position of a N-sulfated glucosamine or an N-acetylated glucosamine to form 3-O glucosamine. It is believed that the different isoforms exhibit varying specificity for different substrates and the activity of each result in very different structures of HS (Moon*, et al.* 2012).

1.2.1.6 Removal of sulfate groups at the 6-O position

In addition to those modification events that transfer a sulfate group on to the HS chain, the sulfatase family of enzymes (post synthetic modification enzymes), SULF1 and SULF2 catalyse the hydrolysis of the sulfate ester bond at the carbon-6 position of the GlcNAc residues on the HS chain (Morimoto-Tomita*, et al.* 2002, Nagamine*, et al.* 2012). Previous work has discovered that removal of 6-O sulfate groups in this manner can both activate and attenuate important cell signaling pathways within the body (Dhoot*, et al.* 2001, Lai*, et al.* 2003). The subtle changes in HS structure that SULF1 and SULF2 thus afford make them key players in the regulation of key physiological processes such as cell proliferation, differentiation and migration (Lamanna*, et al.* 2007). Studies suggest that SULF1 and SULF2 enzymes prefer the highly sulfated substrates of the tri-sulfated ΔUA2S-GlcNS6S and di-sulfated ΔUA-GlcNS6S residues (Frese*, et al.* 2009, Lamanna*, et al.* 2008).

Together, the action of these biosynthetic enzymes generates HS with great structural heterogeneity, which in turn confers a diverse ligand binding capacity and thus functional repertoire within the body (**Figure 1.1**). In particular, its interaction with such a plethora of protein ligands makes it a target for further elucidating functional mechanisms in both normal physiology and disease pathogenesis. More recently, HS has been identified as a key mediator of Alzheimer's pathology and understanding its role in the pathogenesis of this neurodegenerative disease may prove fundamental in understanding its pathological pathways and symptom onset.

1.3 Alzheimer's disease

1.3.1 Background

Alzheimer's disease (AD) is a neurological condition that leads to progressive degeneration of brain function and is the leading cause of dementia amongst the elderly today (Allan*, et al.* 2009). AD was first described in 1906 by German neuropathologist and psychiatrist Alois Alzheimer after the death of one of his patients Auguste. D, a fifty year-old woman he had been studying since 1901 when she came to him presenting symptoms of memory loss, disorientation and personality deficits. Alzheimer went on to name the condition and made it a clinically recognised disease (Berchtold and Cotman 1998). The incidence of AD is rapidly increasing and in 2006 there were 26.6 million people suffering from this condition globally. This is predicted to increase so that by 2050, 1 in 85 people around the world will be diagnosed with AD (Brookmeyer*, et al.* 2007). Indeed, AD is becoming a rapidly expanding burden for the global economy and in some instances; the cost of care giving to those afflicted exceeds the capacities of some developing countries.

1.3.2 Diagnosis

The difficulties associated with the diagnosis of AD may be part of the reason that to date there exists no curative treatment for this condition. Detection and clinical diagnosis of AD is particularly challenging and currently only 100% certain diagnosis can be achieved at post mortem meaning treatment strategies are often initiated too late on in disease progression. There are a number of different medical criteria that can be used to diagnose AD however the most commonly used is that of the collaborative efforts of the National Institute of Neurological and Communicative Disorders and Stroke and the Alzheimer's disease and Related Disorders Association (NINCDS-ADRDA) (McKhann*, et al.* 1984). These criteria distinguish between definite, probable and possible cases of AD. Diagnosis of definite AD occurs when both the clinical features of probable AD are present and can also be confirmed with histopathological investigation at biopsy or autopsy. Probable AD is diagnosed after a thorough neurophysical examination of the individual with a battery of tests. The Mini Mental State Examination (MMSE) is the most widely used test despite criticism that it is not suitable for the diagnosis of more mild forms of dementia. Deficits in areas of cognition including progressive deterioration in memory in the absence of symptoms of delirium coupled with onset between the ages of 40 and 90 are considered indicative of AD. Other symptoms that may contribute to the diagnosis of probable AD include difficulties with language, perception and trouble with activities important to daily living. Signs of these deficits alongside a family history of dementia may be confirmed with spinal fluid examination, electroencephalography (EEG) and computerized tomography (CT). Variations in the onset of AD, presentation of symptoms or clinical manifestation may lead to the diagnosis of possible AD or in those cases where a secondary brain disease or injury has been previously identified (Cummings*, et al.* 1998).

No laboratory test currently exists to confirm diagnosis of AD. The National Institute on Ageing (NIA) and National Institute of Neurological and Communicative Disorders and Stroke (NINCDS) (Mirra*, et al.* 1993) have established another set of criteria to categorise and classify the neuropathology implicated in AD. These require the presence of age-adjusted neocortical plaque densities but do not distinguish between plaque type and their location within the cortex. Furthermore, the Consortium to Establish a Registry for Alzheimer's disease (CERAD) requires both the presence of age-adjusted plaque densities that can be at least semi-quantified and a clinical diagnosis of AD following extensive neurological examination (Mirra*, et al.* 1991). Opponents have argued that these criteria are falling behind in light of the advances in reliable biomarkers that can be used in conjunction with Magnetic Resonance Imaging (MRI) techniques and Positron Emission Tomography (PET) (Dubois*, et al.* 2007). Amendments to these criteria now require at least one biomarker of AD alongside the still very important clinical analysis of cognition. The use of MRI allows visualisation of atrophy in areas of the hippocampus and the entorhinal cortex and may be useful in determining the rate of progression of AD and the extent of cognitive decline that may

follow. Likewise, the use of PET-based imaging techniques has become popular in the diagnosis of AD as it allows observation of glucose metabolism within different regions of the brain. A diminished oxygen metabolism in the cingulated region of the brain is commonly used as a marker for the diagnosis of AD. Indeed, the use of radiotracers in PET imaging is becoming common practice in not just dementia diagnosis but also other types of psychiatric disorders (Brooks 2009). Agents to detect amyloid-plaque deposits within the brain are still under development but could prove particularly beneficial in the early detection of AD (Salawu*, et al.* 2011).

1.3.2.1 Biomarkers

There have been calls for a combination of these guidelines alongside the use of biomarkers. Biomarkers refer to both fluid and imaging measures that may clarify the identification of AD pathology in patients. Presently, biomarkers are divided into two main categories; 1) the biomarkers identifying accumulation of Aβ (to be discussed). These biomarkers include disease-specific tracer retention using PET imaging and also low levels of cerebral spinal fluid (CSF) Aβ42 and 2) biomarkers which indicate the presence of neuronal injury of degeneration. These include elevated levels of CSF tau, atrophy of cortices as determined with MRI and decrease fluorodeoxyglucose uptake on PET in a temporal fashion (Jack*, et al.* 2011). Several other types of biomarker have been identified however are yet to be validated by the AD criteria as defined by the Alzheimer's Association, NIA and National Institute of Health (NIH). Examples include diagnosis based on electroencephalogram (Dauwels*, et al.* 2010) signaling whereby traces from AD patients present slowing of the EEG, perturbations in EEG synchrony and reduced complexity of overall signal (Dauwels*, et al.* 2010). Furthermore, studies indicate that implications of altered resting state functional network connectivity in patients suffering from AD may also be invaluable as a marker of this disease (Buckner*, et al.* 2005). Biomarkers will ultimately prove the most useful diagnostic marker for AD, avoiding current difficulties associated with somewhat subjective cognitive evaluation testing. A combination of these alongside pre-established mental examination may prove to be optimal in the detection of this type of dementia.

1.3.3 Neuropathology and pathophysiology

There are two fundamental hallmarks of pathology associated with AD, the presence of intracellular neurofibrillary tangles (NFTs) comprised of hyperphosphorylated tau and extracellular senile plaques composed of the amyloid-beta peptide (Aβ) (Hyman and Gomez-Isla 1997). These two key features of AD may also be accompanied by the loss of synapses and degeneration of neurons as well as granulovascular degeneration, AMY plaques (non beta-amyloid plaque-like deposits) (Lippa,

et al. 2000) and amyloid angiopathy (Cummings*, et al.* 1998) (the formation of amyloid deposits within the walls of the blood vessels of the central nervous system (CNS)) (Revesz*, et al.* 2002).

1.3.3.1 Neurofibrillary tangles (NFTs)

Some studies have suggested that the presence of NFTs within the neurons of the brain correlate well with the symptoms of dementia (Arriagada*, et al.* 1992). AD alongside other conditions such as Corticobasal Degeneration (CBD), Progressive Supranuclear Palsy (PSP) and Pick's disease make up a group of neurodegenerative diseases referred to as tauopathies, and are characterized by extensive neuronal loss, brain atrophy and age-progressing dementia (Yue*, et al.* 2011). Indeed the term tauopathy is rather a generic term describing the accumulation of abnormally phosphorylated tau (Buee*, et al.* 2000).

Tau (MAPτ) is a microtubule-associated protein that plays an important role in the pathology that accompanies AD. In its normal state, tau is a microtubule binding protein found in the cytoplasm of cells. It is a soluble protein found within the human CNS and exists in 6 main isoforms. Tau plays an important role in the assembly (Weingarten*, et al.* 1975) and stabilisation of axons and effectively acts as the "train tracks" by which cell transport of organelles such as mitochondria and other synaptic components occurs along (Trojanowski and Lee 2005).

In healthy individuals, tau is phosphorylated dynamically in a process that enables its interaction with microtubules and this facilitates axonal transport. However in tauopathies like AD, tau becomes hyperphosphorylated (Brunden*, et al.* 2009). In this condition, already phosphorylated sites under healthy physiological conditions are further phosphorylated into a hyperphosphorylated state. Furthermore, specific additional residue sites including a proline-directed serine/threonine sites (Buee*, et al.* 2000) become phosphorylated in a disease-specific manner. It is the phosphorylation of these specific sites on microtubules that results in a reduced affinity of tau for microtubules, and coincidently causes the protein's dissociation, negatively impacting microtubule stability (Gotz*, et al.* 2008). Rather than bind to microtubules, tau in the disease state, forms insoluble deposits. These inclusions are usually in the form of fibrils and are most commonly found within the dendrites of neurons as well as their cell bodies (**Figure 1.2**).

Pathological tau inclusions usually exist in the form of paired helical filaments (PHFs). These filaments are held together by strong disulfide bonds that crosslink at several sites to create large insoluble fibrous inclusions that cannot be broken down easily (Mazanetz and Fischer 2007). These lesions have been found to accumulate with a progressive nature that is both spatial and temporal, spreading systemically from the transentorhinal cortex, to the limbic cortical regions and finally to

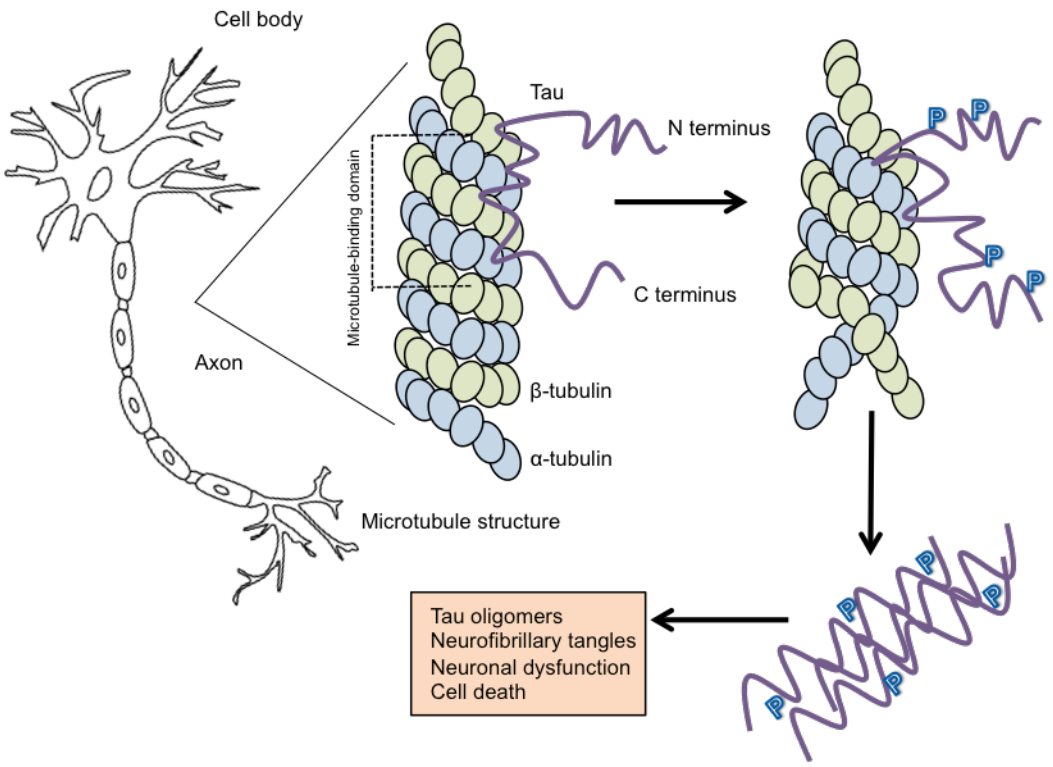

Figure 1.2: Tau and neurodegeneration. Microtubules form the basis of axonal transport and are made from both α- and β-tubulin. It is these "railway tracks" along axons that provide structural support to neurons. Tau is an important microtubule-associated protein that stabilises microtubules through binding to specific binding sites comprised of 18 amino-acid motifs. In the pathological condition, tau becomes hyperphosphorylated resulting in reduced affinity of the tau protein for microtubules, ultimately leading to destabilisation of the microtubule. Tau dissociates as a consequence and accumulation of abnormal tau settles in the neurons. Commonly, these aggregations exist as paired helical filaments (PHFs). Following the appearance of this fibrous pathological tau, tau oligomers and insoluble tangles occur due to further proteolytic processing. Tau in this pathological conformation ultimately leads to neuronal degeneration and cell death. Adapted from (Mazanetz and Fischer 2007)

the neocortical areas (Terry*, et al.* 1991). In doing so, these tangles are thought to contribute to the degradation of neurons within the brain and ultimately compromise cognitive function.

1.3.3.2 Amyloid pathology

The presence of insoluble amyloid plaques within the brain forms a second key hallmark of AD. These deposits are formed principally of the β-amyloid protein (Aβ), a polypeptide of 40-42 amino acid residues (Glenner and Wong 2012). The Aβ protein is generated through the cleavage of the amyloid precursor protein (APP), a single-pass transmembrane protein with a large extracellular domain. APP is localised to chromosome 21; the chromosome found in triplicate in those with Down's syndrome, a condition that invariably leads to the onset of AD (Kang*, et al.* 1987, Robakis*, et al.* 1987). This was the first primary evidence for the role of Aβ as the primary step in the onset and

progression of AD pathogenesis. The primary component of amyloid plaques within the brain, the Aβ peptide is formed as a result of cleavage of a larger precursor protein called the amyloid precursor protein (APP). This is a large protein that is made in the cells and transported to the membrane where it undergoes cleavage. The cleavage of APP can occur via two pathways. Most APP is processed via the non-amyloidogenic pathways. In this way, the formation of Aβ is not possible and generation of amyloid plaque densities is precluded. During this process, APP is cleaved by a α-secretase at the plasma membrane, an enzyme belonging to the disintegrin and metalloproteinase family (ADAM). 3 candidates have been identified for this cleavage step; ADAM9, ADAM10 and ADM17 (LaFerla*, et al.* 2007). Cleavage by this secretase occurs within the Aβ domain itself thus precluding the generation of a toxic Aβ domain. Two fragments are released, a large sAPPα ectodomain released into the extracellular space and a carboxyl-terminal fragment (C83) that remains within the membrane. Following this, γ-secretase cleaves the C83 fragment to generate a second, smaller P3 fragment (LaFerla*, et al.* 2007) (**Figure 1.3**).

Unprocessed APP can be internalised into early endosomes, where it can become a substrate for the β-site APP-cleaving enzyme 1 (BACE1) (these endosomes have the optimum pH for BACE-1 activity). Cleavage of APP by BACE-1 results in a sAPPβ ectodomain and C99 domain composed of the first 99 amino acids of APP that is retained within the membrane. C99 can be shuttled back to the endoplasmic reticulum (ER) to undergo a second cleavage of this C99 fragment by a γ-secretase to release the Aβ peptide. C99 can also be shuttled back to the plasma membrane where the γ-secretase is also found, or finally, processed by γ-secretase within the endosome itself. The γ-secretase complex is composed of presenilin 1 or 2 (PS1/2), anterior pharynx defective, presenilin enhancer 2 and nicastrin (LaFerla*, et al.* 2007). The amyloidogenic pathway generates Aβ of 40 amino acids ($A\beta_{1-40}$) most frequently however the more toxic peptide of 42 amino acids ($A\beta_{1-42}$) is generated infrequently at a ratio of 10:1 (**Figure 1.3**).

Whilst it is now largely understood how the amyloid peptide is deposited within the brain, there is still much to learn regarding plaque development and deposition. Currently, it is widely understood that amyloid plaques are derived from the extracellular "seeding" of smaller amyloid species (such as the Aβ peptide described above) followed by progressive deposition at this seeding site (Hardy and Higgins 1992). Whilst this hypothesis is adequate for the spread of amyloid pathology throughout the brain, it does not identify differences in morphological features of the plaques. Some amyloid plaques for example, referred to as dense core plaques, are linked with the stages of inflammation and can be distinguished by the presence of activated microglia found within the plaques (Ard*, et al.* 1996). This is different to other plaque types and so presents a problem with characterisation of different plaque staging that occurs with progression of AD. Diffuse and dense amyloid plaques are currently the most predominantly used terminology for different plaque types.

The most popular hypothesis is that amyloid peptide deposits form diffuse plaques that over time evolve into dense core plaques (Mackenzie*, et al.* 1995).

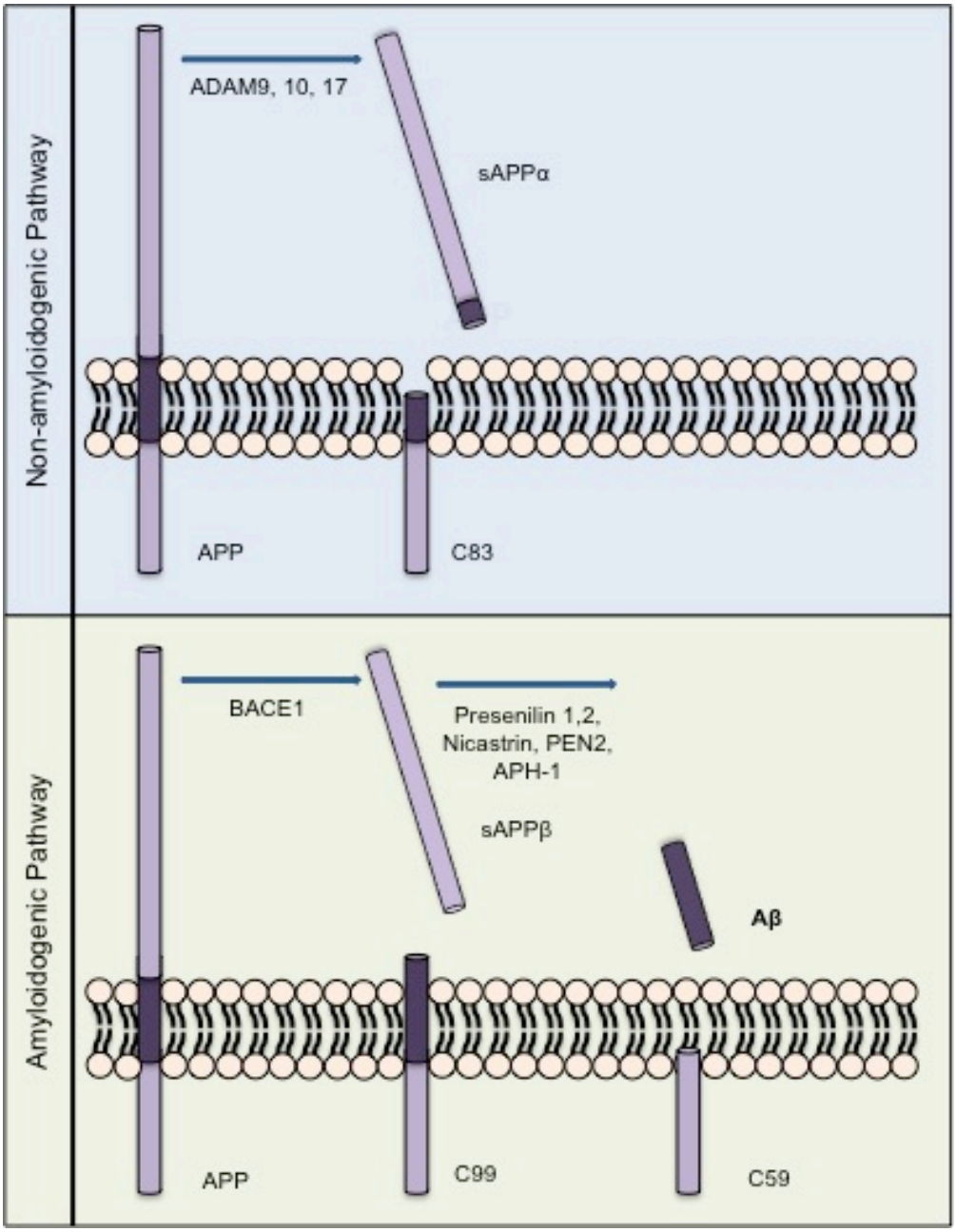

Figure 1.3: APP processing pathways. The Aβ peptide is derived from a large precursor molecule, the amyloid precursor protein (APP), a transmembrane protein that can undergo proteolytic cleavage via two pathways. More often, APP is processed via the non-amyloidogenic pathway whereby the formation of the Aβ peptide is negated as a result of cleavage by an α-secretase (ADAM9, 10 or 17) within the Aβ domain itself. This cleavage generates two fragments, the larger sAPPα domain and the smaller carboxy-terminal c83 domain. APP not cleaved in this manner may become a substrate for a β-secretase enzyme (BACE-1). Cleavage in this way generates two fragments, a sAPPβ ectodomain and a smaller domain consisting of 99 amino acids (C99). C99 may then undergo further cleavage by the γ-secretase complex (Presenilin 1,2, nicastrin, anterior pharynx defective (APH-1) and presenilin enhancer 2 (PEN2)) to generate the Aβ peptide and a C59 domain. This cleavage produces Aβ1-40 and the more amyloidogenic Aβ1-42 at a ratio of 10:1.

Despite this, there are still a great number of unanswered questions concerning why plaques are different sizes and made up of different components and why certain components remain resistant to proteolysis whilst others do not. Recent work by D'Andrea and Nagele (D'Andrea and Nagele 2010) has further elucidated a model for amyloid pathology within the brain of AD patients and predict that the origin of plaques is key in determining the nature of the plaque found there.

This work highlights the problems associated with describing any extracellular aggregate as an amyloid plaque. Understanding distinct morphology differences and localisation may help future treatment strategies with a more targeted approach to removing these insoluble protein buildups. Importantly however, the initial mechanism that initiates the early lay down of toxic Aβ remains the same for all plaques types and arguably is ultimately the starting point for successful therapeutics against AD.

There is also some debate regarding the chain of events that leads to the development of AD pathology whereby the appearance of NFTs, composed of hyperphosphorylated tau protein is not known to either precede or supersede the appearance of amyloid plaque pathology. The amyloid hypothesis asserts that Aβ is the principle driving influence on the development and progression of AD. In support of this theory, mutations in tau-encoding proteins are the primary cause of frontotemporal dementia with Parkinsonism (FTDP-17) (Hutton*, et al.* 1998, Poorkaj*, et al.* 1998). This neurodegenerative condition is characterised by the presence of NFTs within the brain but notably, the absence of any kind of amyloid pathology. In light of this, despite considerable neurodegeneration as induced by robust tau pathology, these effects are not enough to induce the characteristic amyloid pathology unique to AD. By inference, the NFTs composed of wild-type tau, as observed in patients suffering from AD, are more likely to have been deposited as a secondary pathology type after important changes in Aβ metabolism and early amyloid deposition and plaque formation (Hardy*, et al.* 1998). Furthermore, mice transgenic for both mutant human tau and APP present accelerated development of NFTs as compared to mice that are transgenic for mutant tau only. Amyloid burden within the brain interestingly remains unchanged. This provides additional evidence that changes in APP processing occur *prior* to tau pathology (Lewis*, et al.* 2001).

Taken together, this evidence supports the notion that cerebral Aβ accumulation and deposition is the fundamental influence in the driving of AD pathology. Tangle formation is thus deemed a secondary pathological hallmark that results from an imbalance between the production of Aβ and its clearance. Targeting early amyloid peptide generation is an obvious target for potential future therapeutic strategies. One such way this may be achieved is via investigation of the role of GAGs within the amyloid-processing pathway.

1.4 HS and Alzheimer's disease

There are numerous ways in which the role of HS GAGs and their core proteins have been implicated in both the development and persistence of the characteristic hallmarks of AD. Whether they co-localise with, protect, or accelerate the features associated with this disease, the role of HS in AD is both important and varied (Zhang*, et al.* 2014). Further understanding the role of HS in AD in this manner, may prove invaluable in elucidating the mechanisms of the disease as well as potential for novel therapeutic strategies.

1.4.1 HS co-localises with several features of AD

Snow and colleagues were among the first to discover a co-localisation of HSPGs and various different pathological features associated with AD using antibodies directed to HS GAGs and core proteins (Young*, et al.* 1989). This work reported the presence of sulfated HS GAG chains in both neuritic plaques and NFTs, as well as in the presence of cerebral amyloid angiopathy (Snow*, et al.* 1987). Interestingly, the presence of sulfated GAGs has been reported in several other types of amyloidosis, including the amyloid of medullary carcinoma of the thyroid gland, inherited cutaneous amyloid and senile cardiac amyloid. This suggests that sulfated GAGs may have influence over the way in which these proteins fold, such that amyloid displays considerable beta-pleated sheet conformation (Young*, et al.* 1989). A theme in the structure of PGs co-localised with amyloidosis has also been discovered. It has been reported that highly sulfated PGs localise specifically with several types of amyloid aggregates, including amyloid fibrils and PHFs suggesting that the structure of these PGs is of great importance in determining their interaction with the amyloid protein. Such specificity, may indeed infer a functional relationship with PGs and the persistence or function of AD amyloid deposits (Snow*, et al.* 1987).

SDC1-3 and GPC1 are examples of cell surface HSPGs that have been found to be associated with both diffuse and dense cerebral amyloid plaques and NFTs (Verbeek*, et al.* 1999). GPC1 is also associated with cerebellar dense plaques (van Horssen*, et al.* 2002) whilst SDC1-3 do not report co-localisation here. Similarly, HSPG2, an extracellular matrix (ECM) associated HSPG has been shown, in a rat model of AD, to accumulate within the amyloid deposits indicative of Alzheimer's pathology (Castillo*, et al.* 1997). AGRN has more recently been associated with amyloid plaques at all stages also (van Horssen*, et al.* 2002, Verbeek*, et al.* 1999), as well as NFTs composed of hyperphosphorylated tau protein (van Horssen*, et al.* 2003). Interestingly, whilst COL18A1 has also been reported to co-localise with dense amyloid plaques and amyloid-laden vessels, positive immuno-staining for COL18A1 was not detected in NFTs or diffuse plaques (van Horssen*, et al.* 2002). The spatial discrimination of these HSPGs would strengthen a hypothesis for a functional role

of HSPGs in AD, rather than simply a coincidental spatial locality. Intensity of staining of different select HSPGs in different regions of AD pathology as observed in these studies would be suggestive of selective preference of select HSPGs to specific Aβ oligomeric states. COL18A1 for example may well selectively associate with fibrillar Aβ over aggregated Aβ found in mature plaques.

The HS GAG chains, removed from their HSPG core protein, have also been shown to extensively associate with the pathological features of AD in a number of regions in the brain, suggesting it is not only the HSPGs that may hold potential as a modulatory factor in AD pathogenesis. Extensive positive staining for HS GAGs in all types of amyloid plaque and NFTs has been reported and may again point towards a role for accumulation of HS side chains in either response to AD pathology or even as a pre-requisite (Zhan*, et al.* 1995). Indeed, more recent work has shown that human brain pericytes, when cultured in the presence of Aβ protein, display increased mRNA expression of both the genes encoding the AGRN and GPC1 HSPGs. In addition, studies showed that increased sulfates (as labeled with radioactive groups for detection) were incorporated into the GAG chain fraction of the pericytes cultured with Aβ. This work would suggest that not only is the presence of Aβ able to modulate the expression of HSPGs – perhaps in a self-perpetuating cycle, but also that this may contribute to the accumulation and co-localisation of HSPGs observed in AD lesions (Timmer*, et al.* 2009).

The more recent development of more sophisticated antibodies against HS has made understanding the interaction of HS and AD a little clearer. Phage display antibodies including EV3CE and HS4C3 that specifically target N-sulfated motifs along the HS chain, and RB4EA12 and HS4E4 that target partially N-sulfated and N-acetylated residues (Bruinsma*, et al.* 2010, Kurup*, et al.* 2007) can now more easily give an indication of the specific structures of HS co-localised with the features of AD. For example, work has shown that different types of HS are found to co-localise with AB_{1-40} and AB_{1-42} peptides within diffuse plaques (O'Callaghan*, et al.* 2008). In addition, antibodies to detect highly N-sulfated motifs within the HS chain were found in both fibrillar (dense) and non-fibrillar (diffuse) Aβ plaques. In contrast those antibodies used to detect lower degree of N-sulfation displayed signaling only in fibrillar Aβ aggregates (Bruinsma*, et al.* 2010). This would suggest perhaps that variable HS structure is a key determinant in interaction with different AD aggregates.

1.4.2 The role of HS in AD

1.4.2.1 HS and Aβ

It has long been established that HS and amyloidosis specifically in AD are linked in a variety of ways. Furthermore, studies suggest it is not only spatial proximity shared by HSPGs and AD

pathogenesis but rather there is a great deal of evidence to suggest that PGs are potent enhancers of the formation of Aβ fibrils, the precursor of plaques (Castillo*, et al.* 1997). AGRN and HSPG2 have been implicated as PGs that may bind to Aβ with high affinity (Castillo*, et al.* 1997, Cotman*, et al.* 2000). Indeed, immunoassays revealed a correlation between increased binding capacity of Aβ to HSPG2 with increased fibrilisation of $A\beta_{1-40}$ and $A\beta_{1-42}$ species as well as enhanced fibril stability in the presence of HSPG2 (Snow*, et al.* 1994). Traditionally, amyloid plaques are believed to develop from diffuse plaques containing largely non-fibrillar Aβ into classic plaques with a central core of fibrillar Aβ. These classic plaques present reactive astrocytes and glial cells around the densely packed core of fibrillar Aβ (Dickson 1997, Selkoe 1991). AGRN and HSPG2 may thus be implicated in the conversion of non-fibrillar Aβ to fibrillar and in doing so contribute to the development of AD pathogenesis (Snow*, et al.* 1994, Verbeek*, et al.* 1997). Furthermore, both free HS and heparin chains have also been shown to associate with Aβ *in vitro* (Bame*, et al.* 1997, Buee*, et al.* 1993, Leveugle*, et al.* 1994) via the HHQK domain at the N-terminus region of the Aβ peptide (Giulian*, et al.* 1998). Likewise, an N-sulfated hexasaccharide domain within HS containing 2-O sulfated IdoA residues is also known to bind Aβ and has been demonstrated in the human cerebral cortex. This site is also able to bind FGF-2, a neuroprotective growth factor and may suggest a degree of competition between Aβ and FGF-2 for a common HS binding site (Lindahl*, et al.* 1999). As with many other HS ligand binding interactions, the degree of sulfation determines efficacy of interaction with Aβ. Heparin, a highly sulfated variant of HS thus displays a much higher binding affinity to Aβ vs. a de-sulfated form of HS (Lindahl*, et al.* 1999).

Association of HSPGs and Aβ in this manner begs the question as to whether the presence of HS species occurs prior to accumulation of Aβ in the brain, or whether the initial presence of Aβ is enhanced and prolonged via interaction with HSPGs such as HSPG2 and AGRN. To go some way to answer this question, Snow and colleagues have reported the presence of positive HSPG staining in diffuse primitive plaques in the brains of patients with Down's syndrome, indicative of an early role in HSPGs in AD disease pathogenesis (Snow*, et al.* 1990).

1.4.2.2 HS and APP

Other work has more recently reported that both the HS side chain as well as its core protein is able to interact with the brain specific isoform of APP itself, the precursor of Aβ, and as such may be suggestive of a regulatory role in the production of Aβ (Narindrasorasak*, et al.* 1991). The mechanism by which this occurs is still unknown however recent evidence that APP may occur in a CS (Shioi*, et al.* 1992, Shioi*, et al.* 1993), or HS (Schubert*, et al.* 1988) form may indicate a somewhat complex interaction of HSPGs with AD pathology being that it may interact with, mature AD pathology, smaller oligomers and their precursors simultaneously. Furthermore, HS is known to

interact with those enzymes responsible for the processing of APP itself, in particular BACE-1 (discussed later) (Scholefield*, et al.* 2003).

1.4.2.3 HS and Tau

Just as HS chains have been shown to interact directly with the amyloid-based features associated with AD, so has this GAG been implicated in the progression of tau pathology also seen in patients with AD. Goedert and colleagues in 1996 (Goedert*, et al.* 1996), after a much earlier report that sulfated GAGs and NFTs are closely associated (Snow*, et al.* 1987), found that sulfated GAG chains may be able to induce the formation of PHFs and thus induce the fibrilisation of mature tangles within the brain. This work also found that the presence of sulfated GAG chains might also potentiate the phosphorylation of tau causing it to dissociate from the microtubule. In addition, binding of sulfated GAGs chains is believed to occur across the microtubule binding domain itself, preventing the association of tau with microtubules in this manner also (Hasegawa*, et al.* 1997) (Hernandez*, et al.* 2002). In doing so evidence has been put forward that GAG chains not only influence the disassembly of the microtubules, but also potentiate the polymerisation and fibrilisation of the tau and further still, protect tau deposits from proteolytic degradation (Snow and Wight 1989). Taken together, there is a strong case for a role of GAGs in the development of tau-based pathology in AD.

1.4.2.4 Resistance to Aß degradation

Previous studies have suggested that certain HSPGs are able to protect Aβ species from protease degradation both *in vitro* and *in vivo* and that in doing so, may suggest a mechanism by which PGs are able to support the accumulation and persistence of AD pathology within the brain of patients (Gupta-Bansal*, et al.* 1995). It has been suggested that the AGRN PG may be able to do this due to the presence of 9 separate follistatin-like protease inhibitor domains within its structure that may offer a protective mechanism against the degradation of Aβ peptide when co-localised with HSPGs like AGRN (Biroc*, et al.* 1993, Groffen*, et al.* 1998).

Additional research has suggested that HSPGs may also play a role in protection against the degradation of Aβ via indirect pathways, such as phagocytic uptake and degradation by microglia (known to be associated with amyloid plaques). Previous work has found that chondroitin sulfate proteoglycans (CSPGs) are able to inhibit the degradation of Aβ in this manner however it is not yet certain whether HSPGs could play a similar role in inhibition of microglial Aβ uptake and removal (Shaffer*, et al.* 1995). Indirectly, $A\beta_{1\text{-}40}$ has been shown to inhibit the activity of heparanase enzymes, and in doing so may contribute to the persistence of amyloid plaques by blocking the degradation of

the HSPGs themselves (Bame*, et al.* 1997). In light of this, it would seem that the role of HS in this instance is something of a negative one with regard to its ability to enhance formation of toxic senile plaques in Alzheimer's patients.

Despite this evidence for this potentially damaging role of HS in the pathogenesis of AD, one might argue that enhancing the fibrilisation of Aβ peptides may actually prove to be a protective mechanism. The original amyloid cascade hypothesis, as proposed in 1992 (Hardy and Higgins 1992), originally proposed it was the amyloid plaques themselves that were the primary cause of neuronal loss and dementia symptoms. More recently however, this hypothesis has been amended to account for the smaller intermediate Aβ oligomer species that form before mature plaque formation since no real linear correlation was discovered between mature plaque deposition within the brain and the onset and progression of dementia in patients (Verma*, et al.* 2015). Indeed, studies in a novel mouse model presenting a mutation in the presenilin 1 (*PS-1*) gene revealed accumulation of Aβ oligomers within neurons that impeded memory formation and led to synaptic dysfunction, all in the absence of mature amyloid plaques (Zhang*, et al.* 2014). In light of this, mature plaques within the brain may prove to be somewhat "protective" in view of the fact they may actually be basins for the sequestration of more toxic smaller oligomer intermediates (Verma*, et al.* 2015), analogous to that of a granuloma in the context of inflammation. Subsequently, in quickening the turnover of Aβ peptides to oligomers and ultimately plaques densities, it may be hypothesised that this role of HS is indeed protective rather than damaging, depending upon one's view of the relative toxic capacities of the various amyloid entities.

1.4.2.5 HS and the uptake of Aβ into cells

As previously highlighted, HS is able to interact and potentially influence, every feature of pathology associated with AD. Whilst it has already been shown to protect both amyloid and tau from protease degradation, there is also evidence to suggest that it is able to mediate the uptake of Aβ into the cells and in doing so, mediate the effects of cytotoxicity and clearance of this toxic peptide. The pathogenic species Aβ is able to exist both outside and within the cells themselves and internalisation mechanisms allow the transfer of Aβ into the cells to contribute to the intracellular pools present there (LaFerla*, et al.* 2007). Endothelial cells, neurons (Kandimalla*, et al.* 2009), different glial cells including microglia and astrocytes (Nielsen*, et al.* 2010, Paresce*, et al.* 1996) and smooth muscle cells (Kanekiyo*, et al.* 2012) are all able to internalise Aβ into cells via the action of several membrane bound "gateways" including complement receptors (Fu*, et al.* 2012), scavenger receptors (Paresce*, et al.* 1996, Yang*, et al.* 2011), toll-like receptor (Tahara*, et al.* 2006), low density lipoprotein receptor-related protein (LRP-1) (Kanekiyo*, et al.* 2012) and transmembrane protein CD33 (Griciuc*, et al.* 2013). Naturally, due to its inherent abilities to bind a number of different

ligands, HS both as a free GAG and anchored to a core protein (HSPG) is able to regulate uptake of Aβ into the cell by acting as a cell surface receptor. Indeed, previous work has found that Chinese hamster ovary cells (CHO) deficient in HS (CHO pgsD-677) treated with $A\beta_{1-40}$ did not display toxicity due to uptake of the Aβ peptide and survived much better compared to those wild type CHO cells (CHO-WT) expressing HS that was able to facilitate the uptake of Aβ into cells (Sandwall*, et al.* 2010).

There is also evidence to suggest that HS may play a role in the attenuation of appropriate Aβ clearance from the brain via the blood brain barrier (BBB). LRP-1 as an example has been shown to act as a cargo receptor, in which Aβ is able to bind to the cell surface, become internalised and consequently released at the luminal side of the endothelium (Deane*, et al.* 2009). HSPGs have been shown to cooperate with LRP1 to mediate the uptake of Aβ. Indeed knockdown of HSPG expression with heparinase treatment suppressed the uptake of Aβ. Likewise, deletion of the *Ext-1* gene (and ultimately the knockdown of HS biosynthesis) resulted in an accelerated clearance of Aβ into the brain interstitial fluid (Liu*, et al.* 2016). In this way, HSPGs have been shown to play a role in a critical pathway through which Aβ is taken up by surrounding neuronal cells.

1.4.3 HS and BACE-1

In addition, and most importantly in the context of this project, HS has also been shown to have protective affects against the induction of toxic Aβ peptides. Previous studies have discovered a novel interaction between HS and the BACE-1 enzyme implicated in the formation of the Aβ peptide (Scholefield*, et al.* 2003). It has been shown that HS can regulate and block the cleavage of APP via its interaction with BACE-1 and in doing so, reduce processing of Aβ. Co-localisation of endogenous HS and BACE-1 was identified at both the cell surface and the Golgi complex suggesting that endogenous sources of HS may be responsible for restricting the activity of BACE-1. Indeed, chlorate treatment of the cells abolished the production of HS within the cells and resulted in significantly elevated generation of the Aβ peptide within cells, further strengthening the notion that HS and BACE-1 interact (Scholefield*, et al.* 2003).

Work to understand the mechanisms by which this inhibition may be conferred was carried out with fluorescence polarisation studies. Results indicated that HS is able to inhibit BACE-1 by preventing entry of the substrate to the active site of the BACE-1 enzyme. There is also evidence that should the ligand be pre-bound to BACE-1, HS is able to lock this confirmation into the active site to prevent the APP substrate gaining access (Scholefield*, et al.* 2003). In doing so, HS is able to prevent the interaction of APP with BACE-1 and ultimately, attenuate the processing of APP to form the toxic Aβ species (**Figure 1.4).**

Figure 1.4: The roles of HS in Alzheimer's disease. Aβ is produced within the ER and Golgi apparatus and secreted out of the cell. APP is cleaved predominantly via the α-secretase enzyme to form a soluble APPα fragment that is secreted out of the cell and an 83 amino acid fragment (C83) that remains within the membrane. APP that is not cleaved may be internalised into endosomes. Here, APP may be cleaved by the BACE-1 enzyme and results in a C99 fragment that remains within the membrane. C99 can also be shuttled back to membrane, or shuttled back to the ER and be processed into Aβ via action of the γ-secretase. Extracellular Aβ can bind to cell surface receptors such as NMDA and FPRL1 and internalises Aβ into endosomes for degradation. Tau pathology accumulates intracellularly and results from hyperphosphorylation of the tau protein. HS is able to interact with a number of these stages. HS is able to interact directly with APP, the Aβ plaques and the mature amyloid plaques. HS is also able to interact with tau and the mature tau tangles. There is also evidence that HS and HSPGs may protect mature plaques from degradation and aid the persistence of amyloid pathology. HS has also been shown to act with LRP1 to aid clearance of Aβ from the brain.

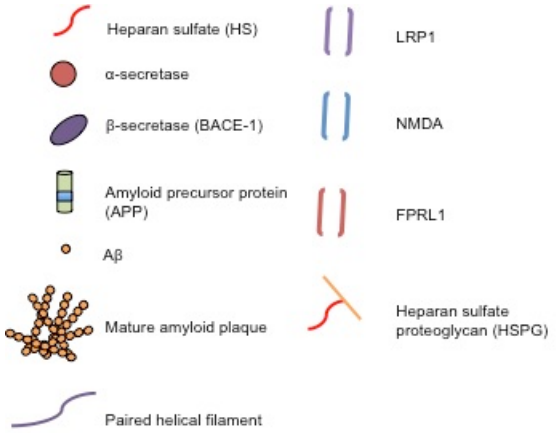

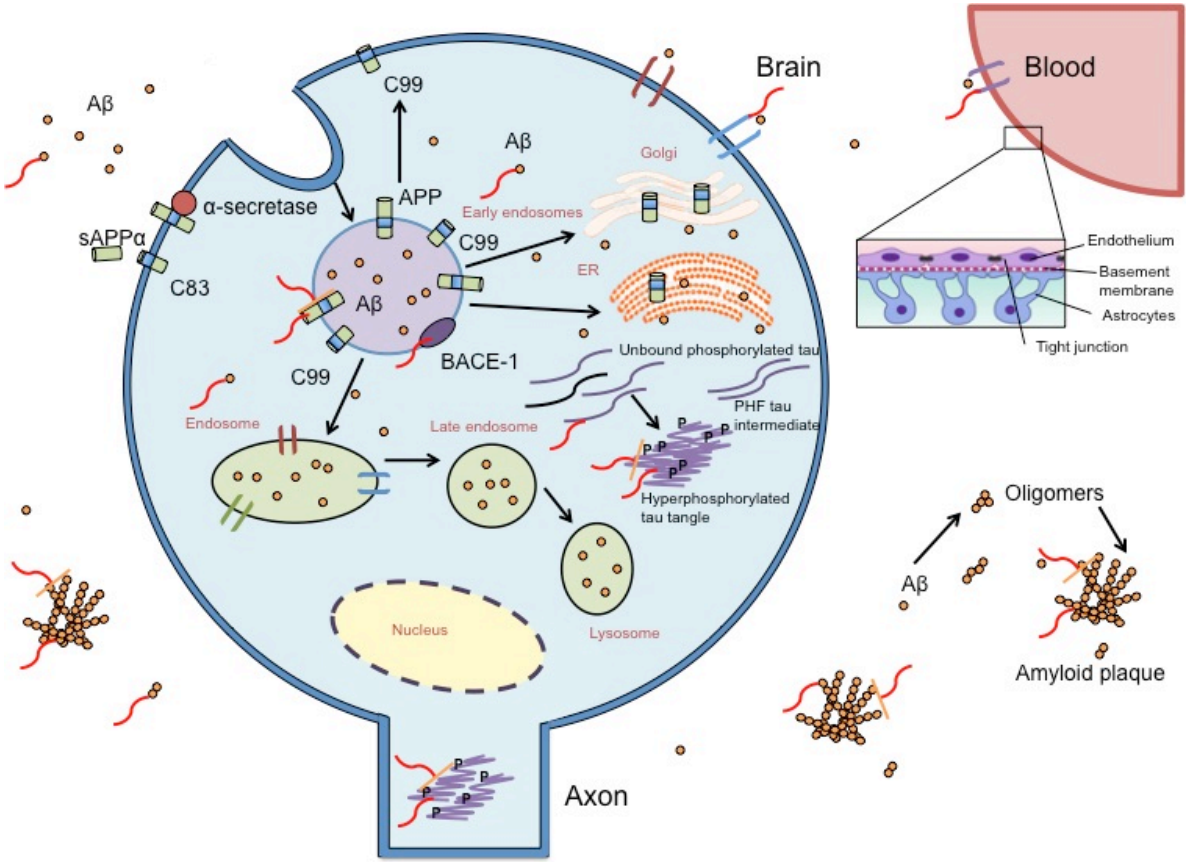

1.4.3.1 BACE-1 inhibition efficacy is dependent upon HS structure

Importantly, the efficacy of BACE-1 inhibition by HS is dependent on the size of the HS saccharide and also the number of sulfated motifs present within the chain (Scholefield*, et al.* 2003). Heparin saccharides of 10 monosaccharide units and higher were able to inhibit BACE-1 whilst their smaller counterparts were unable to successfully inhibit. Similarly, analogues of heparin that were both over-sulfated or missing sulfate groups altogether in the 2-OS and 6-OS position were ineffective inhibitors of BACE-1. Taken together, this evidence suggests that specificity of glycan structures within HS and heparin is key in determining efficacy of BACE-1 inhibition. Additionally, saccharide conformation changes induced by structural modification may also be responsible for changes in BACE-1 inhibition potency. The suggestion that BACE-1 inhibition is dependent upon the structure of HS and heparin sits well with previous work that the structure of HS is dynamically regulated by cells in response to changing cellular environments; for example neurogenesis (Ford-Perriss*, et al.* 2002). This may go some way to explaining the ability of neural cells to modulate and regulate the processing of APP in the appropriate sub-cellular sites and further supports the notion that HS is implicated in the generation of Aβ within the brain in normal physiology and ultimately AD (Scholefield*, et al.* 2003).

Subsequent studies went on to investigate the consequence of structural alterations to the HS chain in an HS analogue; porcine intestinal mucosal heparin (PIMH). Changes to the O-sulfation and N-sulfation/acetylation motif pattern has significant effects on BACE-1 inhibitory activity whereby most potent therapeutic ratios (relative to anticoagulant activity) were achieved in compounds containing NAc and 6-OS groups (Patey*, et al.* 2006). This work again strongly implicates structural specificity of HS to effective inhibition of BACE-1. Furthermore, work in the Tg2576 murine model (a model over expressing a mutant form of APP), revealed that heparin and enoxaparin; a low molecular weight analogue of heparin, were able to reduce levels of Aβ via modulation of APP processing and BACE-1 interaction (Cui*, et al.* 2011).

Chemical synthesis of heparin-like derivatives has proven extremely useful in the subsequent investigation of the consequences of structural changes within the HS saccharide. Schworer and colleagues recently created a library of 16 hexa- to dodecasaccharides that inhibit BACE-1. In line with previous findings, most effective inhibition was achieved in those analogues of larger unit length that contained 6-O sulfated motifs; octosaccharides were found to be the smallest compounds which retained potency (Schworer*, et al.* 2013). Saccharide size is of key importance when we consider their ability to cross the BBB. Should these compounds be of therapeutic viability, size would be a factor in determining their success. Leveugle et al in 1998 (Leveugle*, et al.* 1998) demonstrated that heparin oligosaccharides of 12 units or smaller are able to penetrate the BBB and

may be an effective template for heparin analogue derivatives in the future should this be successfully coupled with appropriate AD therapeutic advantage as described above. Inhibition of BACE-1 has been shown to be most effective with N-acetylated heparin, an analogue of heparin with over 1,000 fold lower anticoagulant activity (Lever and Page 2002). The anticoagulant activity of heparin would usually make its use as an AD therapy impossible however careful design of suitable derivatives in the future could eliminate this side effect and hold potential for the future of BACE-1 inhibitors as a strategy against AD (Lever and Page 2002).

1.5 Changes to the structure of HS occur with ageing

Recent studies suggest that normal ageing (a key risk factor for the development of AD) may initiate changes in the structure of HS and we speculate that this could have implications for the interaction between HS and BACE-1 and its role in the development of AD *in vivo*. Studies have shown that GAGs from aged human hippocampus present altered structural properties compared to their younger counterparts. These structural differences were shown to affect regulation of trophic factors despite having no effect on Aβ peptide toxicity (Huynh*, et al.* 2012). Indeed, altered levels of specific HS biosynthetic enzymes are observed in aged hippocampal samples hinting at an upstream mechanism for the apparent HS structural diversity between these groups. Observed down-regulation of the *GLCE* and *HS2ST* genes and up-regulation of *NDST2* and *HS3ST4* genes may go some way to account for the changes in overall GAG composition as observed in this study (Huynh*, et al.* 2012).

The brain is not the only example where ageing has implications on the structure of HS. One study by Keenan and colleagues has shown an age-dependent decrease in total HS within the human Bruch's membrane – the innermost layer of the choroid, the vascular layer found at the rear of the eye. The Bruch's membrane is known to thicken with age typically and changes in the quantity of HS with age may go some way to explain these changes, particularly in the context of its ligand binding affinity with complement factor H (CFH) – a key inhibitor of complement activation within the ECM (Keenan*, et al.* 2014).

Furthermore, studies in human aorta have found age-dependent changes in the structure of HS such that binding to important ligands are altered including FGF2 and platelet derived growth factor A and B (PDGFA/B). Increased abundance of 6-O sulfation in aged human aorta samples were shown to be a key driver in altered ligand binding in this way and indeed several of the biological properties of the HS that may be found in this part of the cardiovascular system (Feyzi*, et al.* 1998).

Ageing is a naturally occurring process and one that today is still the top risk factor for the development of AD. Understanding therefore the changes HS may undergo in this physiological process may too shed light on changes that may occur in disease scenarios. Altered ligand binding affinity will naturally have huge downstream implications all over the body and understanding the key players that drive these changes will prove invaluable in several fields not limited to dementia. In summary, our hypothesis is that changes in the structure of HS with ageing and in dementia may result in less efficient interaction and inhibition of the BACE-1 enzyme resulting in elevated generation of the toxic Aβ peptide and ultimately the onset of AD. HS may essentially act as a naturally occurring "brake" on BACE-1 activity that is removed if the structure of HS is altered through ageing or in AD. Understanding the *in vivo* relevance of HS in ageing and dementia may thus prove invaluable in elucidating the mechanisms of the disease pathogenesis.

1.6 Current strategies for treatment of Alzheimer's disease

The difficulties with accurate diagnosis of AD that exist currently, coupled with the increasing life expectancy and increasing burden of AD on the medical profession mean that effective treatment strategies are more necessary than ever. Currently, there exists no fully curative treatment for AD. As such, all currently established treatments aim to counterbalance the symptoms of AD, in the hope of managing the side effects associated with this neurodegenerative disorder.

1.6.1 Treatments against behavioral and psychological symptoms of Alzheimer's disease

Current treatment strategies include those that tackle the behavioral and psychological symptoms of AD. Selective serotonin reuptake inhibitors (SSRIs) like fluoxetine, sertraline and citalopram are also clinically proven in the treatment of the depressive symptoms associated with AD (Zec and Burkett 2008). Likewise, mirtazapine and venlafaxine are selective noradrenaline and serotonin inhibitors (SNRIs) that are proven antidepressants that may be used to treat the psychological symptoms of AD. Furthermore, cholinesterase inhibitors and memantine have been proven to improve behavioral symptoms in AD patients (Birks 2006, Farlow 2002). Antipsychotic agents such as risperidone are also favoured in the treatment of psychotic symptoms including aggression and anxiety (Ballard and Corbett 2010). The use of antipsychotics has somewhat been criticised however for worsening some symptoms in AD patients. In particular, benzodiazepines, that may be prescribed to combat psychotic symptoms may actually increase aggression and agitation in older patients, and in some cases a worsening of functionality (Zec and Burkett 2008). Taken together, it is clear that these strategies do go some way to improve daily living for patients. Despite this, timing of treatment is critical as the earlier treatment is initiated the better the outcome.

Furthermore, combinations of certain therapies needs to be carefully considered and the side effects strictly monitored to ensure behavioral therapies do not worsen AD pathogenesis.

1.6.1.1 Cholinesterase Inhibitors

Currently one of the most widely used therapeutic strategies is that of cholinesterase inhibitors. The neuronal cell death that accompanies AD pathogenesis is exacerbated by the loss of acetylcholine neurons, acetylcholine synthesis and degradation resulting in degeneration of cognitive abilities (Bartus*, et al.* 1982). To tackle this, cholinesterase inhibitors are often prescribed to slow the degradation of the acetylcholine neurotransmitter within the synaptic cleft in order to enhance its persistence within synapses. Currently three cholinesterase inhibitors have been approved for the treatment of mild to moderate AD including, donepezil (Pfizer, New York, NY, USA), rivastigmine (Novartis, Basel, Switzerland) and galantamine (Janssen, Beersem Belgium) (Farlow 2002). Research suggests that these drugs are effective in improving cognitive function and activities of daily living (ADL) (Birks 2006). Importantly, early treatment in the development of AD is favoured. Research has shown that a 52 week study of rivastigmine administered to patients with mild to moderate AD was more effective in patients that received their treatment immediately upon diagnosis vs. those who started 6 months later (Farlow*, et al.* 2000). Naturally, the difficulties associated with diagnosis make this somewhat difficult to ensure in some instances. Whilst these drugs do not prevent or slow the progression of AD they have proved modest, and consistent in their symptomatic relief and functional living for those with AD.

1.6.1.2 N-methyl-D-aspartate antagonists

The drug memantine may be another treatment strategy for those suffering from moderate to severe AD (Lundbeck, Vlabeck, Denmark). This drug is an N-methyl-D-aspartate (NMDA) antagonist that has been shown to protect neurons from excitotoxicity. Trials have shown an improvement in cognitive function and ADL in those with severe AD treated for 6 months (McShane*, et al.* 2006). This drug has reported side effects however of headaches and confusion and in some patients, agitation (Alva and Cummings 2008). It must therefore be prescribed with care and caution. Combination of memantine and donepezil however has been shown to improve cognitive function in patients with severe AD and may prove to be an effective combination however this improvement is not observed in those suffering from mild to moderate AD (Tariot*, et al.* 2004) (Farlow*, et al.* 2010) thus strengthening the notion that timing of treatment is particularly important.

1.6.2 Treatments to modify the features of Alzheimer's disease

Directly tackling the pathological features of AD is another way in which research aims to treat this disease. Directly targeting the Aβ and tau components in particular hope to not only prevent the development of AD but also ideally go on to reduce these pathological features and treat AD from its starting point. Additional mechanisms associated with AD may also be targeted including inflammation (Griffin 2006), iron dysregulation (Adlard and Bush 2006), cholesterol metabolism (Stefani and Liguri 2009) and oxidative damage (Reddy*, et al.* 2009).

1.6.2.1 Immunotherapy

There are number of ways in which one might go about treating the features of AD and immunotherapy has proven to be a particularly popular method in which to do so. This may, in part be due to the fact there are a multitude of ways in which immunotherapy can be exploited; either to directly attack and disassemble the aggregated amyloid plaques, induce the activation of microglial cells and in do so induce phagocytosis, neutralise the effects of toxic oligomeric species like Aβ and tau, aid in the clearance of circulating toxic peptides and finally immunoglobulin M (IgM) mediated hydrolysis (Yiannopoulou and Papageorgiou 2013).

Several trials have been undertaken to explore the ways in which amyloid plaque burden in the brain can be reduced. Early treatment of PC 12 cells with anti-Aβ antibodies has been shown to prevent fibrilisation of the Aβ peptide and in doing so prevents the formation of amyloid plaques. In addition this treatment was shown to disaggregate the fibrils already pre-formed *in vitro* (Solomon 2007, Solomon*, et al.* 1997). This data led researchers to prove that full length aggregated $A\beta_{1\text{-}42}$ antibodies was able to reduce plaque burden in a mouse model of AD (Schenk*, et al.* 1999). Success in animals encouraged a human trial in 2002 whereby human $A\beta_{1\text{-}42}$ (AN-1792) was administered to patients with the help of a T-helper adjuvant (QS-21) (adjuvants are necessary to enhance and direct a specific immune response to vaccine antigens; this is normally achieved when adjuvants help to generate depots to trap antigens at the site of injection and in doing so, slow their release to stimulate a full immune response). This trial was prematurely terminated however due to the occurrence of meningoencephalitis in a proportion of the patients (Gilman et al 2005).

The appearance of such a severe side effect prompted significant re-modeling of immunotherapy strategies. Several vaccines underwent modification whereby the amino acid sequence responsible for T-cell response mediated encephalitis was removed in favour of just the small number of residues that are able to bind to Aβ. These new vaccines are largely undergoing

new clinical phases I and II trials in the hope of more successful results without the side affects observed originally (Galimberti and Scarpini 2011).

Passive immunisation over active immunisation (as described above) seems to now be more favorable in light of the adverse reactions observed. One of the most advanced examples of this kind of therapy is the Elan/Wyeth trial of AAB-001 (bapineuzumab). This Aβ N-terminal directed antibody has been shown to have the most considerable effect in apoliporotein E (ApoE) ε4 allele non-carrier patients. This success led to the initiation of a phase III study in this subset of patients only with moderate AD (Wisniewski and Konietzko 2008). Eli Lilly and Co. (Indianapolis, IN, USA) LY2062430 (solanezumab) vaccination against Aβ is also currently under trial (Brody and Holtzman 2008). Immunotherapy strategies including DNA epitope vaccine (Qu*, et al.* 2010), antibodies directed against the BACE-1 cleavage site of APP (Rakover*, et al.* 2007) and mucosal vaccination (Hara*, et al.* 2011) all hold potential as treatments against the pathology of AD.

Passive vaccination in this context requires repeat exposure to the drug that naturally increases the cost of these therapies for patients. Eliminating adverse side effects associated with these therapies are also necessary if this strategy is to be successful in the treatment of AD.

1.6.2.2 Drugs to target tau pathology

A number of compounds have been tested to investigate their ability to modulate tau deposition in patients with AD. Methylene blue (MB) is currently undergoing clinical trials as a therapeutic. The use of this drug however results in blue urine for those who are administered the drug, meaning clinical trials cannot be blinded appropriately. Despite this, cognitive improvement in those patients receiving MB treatment has been reported (Gura 2008). In addition, the pathways by which tau becomes hyperphosphorylated have also been targeted, specifically the role that kinases play as a key inducer of this phosphorylation event. Glycogen synthase kinase 3 (GSK3β) has been found to be a suitable phosphorylation site that could be targeted. Lithium is able to inhibit GSK3 alongside several other compounds including pyrazolopyrazines, amino-thiazole AR-A014418 and sodium valproate (Martinez and Perez 2008). Early research indicates compounds like lithium may have disease modifying potential and may go some way to improve cognitive function in individuals who receive this treatment (Forlenza*, et al.* 2011).

1.6.2.3 Other therapeutic approaches

Other potential approaches to treatment of AD may be with compounds to target the oxidative damage that is associated with AD. Molecules such as Vitamin E, Ginkgo biloba and those

foods containing natural polyphenols such as green tea, wine and blueberries have been suggested to at least slow the rate of cognitive decline. Clinical trials however of high doses of folate, vitamin B6 and B12 have yet to show any improvement in cognitive function or rate of change in patients over an 18-month treatment period despite effective reduction in homocysteine levels – a known inducer of oxidative stress (Aisen*, et al.* 2002). Tumor necrosis factor (TNF) inhibitors have also presented preliminary success in improving cognitive decline in AD patients. Etanercept, an already FDA-approved treatment of rheumatoid arthritis, upon perispinal administration reported a surprisingly rapid improvement in cognitive function in AD patients. This potential treatment still requires much work though (Griffin 2008). Additionally, modulation of cholesterol and other vascular related risk factors may have potential as therapeutics in light of a known link between hypercholesterolemia, cardiovascular disease and AD. Addressing issues of hypertension, stroke, atrial fibrillation and hyperhomocysteinemia may prove beneficial in preventing the onset or progression of AD. Indeed, patients who received statin treatment presented a decreased prevalence of AD (Jick*, et al.* 2000). A recent trial however to assess disease progression in patients with mild to moderate AD who received statin therapy alongside donepezil did not yield satisfying results (Feldman*, et al.* 2006)**.** Combination administration of these prophylactic measures alongside other AD medication may serve to enhance outcomes in patients by controlling known exaggerators of AD such as inflammation, cholesterol etc.

1.6.2.4 Drugs that target Aβ pathology of AD

Several research efforts have attempted to target the aggregation of the toxic Aβ peptide and in doing so slow the progression of AD as a potential therapeutic strategy, One Aβ aggregation inhibitor in particular, a synthetic GAG 3-amino-1-propaneosulfonic acid (tramiprosate) reached a phase III clinical trial and was found to able to interfere with the binding of GAGs to Aβ, and in doing so attenuate the aggregation of Aβ into mature plaques (Gauthier*, et al.* 2009). In doing so however, this drug was found to promote the aggregation of abnormal tau (and so was discontinued) (Santa-Maria*, et al.* 2007) highlighting the complexity of developing inhibitors of this kind, on account of the differing pathological features of AD. A second drug, colostrinin displayed promising improvement in MMSE score of patients with mild AD treated over a 15-month period. This promising early affect however was not maintained over a longer treatment period and the trial was discontinued (Bilikiewicz and Gaus 2004). Finally scyllo-inositol, another Aβ targeting drug was shown to stabilise oligomeric aggregation of Aβ to inhibit the toxicity of the smaller Aβ peptide in mouse hippocampus. This drug however has not proved successful in clinical trials as a decisive benefit of the therapy could not be detected (Salloway*, et al.* 2011). Drugs to target the Aβ pathway have received most attention. To date, much of these efforts have not proved successful at clinical trials, (tarenflurbil,

tramiprosate and semagacestat) and may highlight a difficulty in moving from bench to bedside (Gauthier*, et al.* 2009, Imbimbo and Giardina 2011).

1.6.2.5 Drugs to target gamma-secretase

Another obvious target for potential therapeutic strategies is against the γ-secretase enzyme, the final cleavage enzyme in the APP processing pathway to form the Aβ peptide. Targeting this enzyme could attenuate the formation of amyloid aggregates as a result. The problem with this target however is that γ-secretase is known to have a great deal of functions around the rest of the body, in particular, another γ-secretase substrate is notch receptor 1, inhibition of which has been shown to lead to severe gastrointestinal and hemopoetic side effects making its success negated (Wong*, et al.* 2004). A trial drug, semagacestat (LY-450139) has been shown to reduce levels of Aβ in the CSF of healthy individuals in a dose dependent manner (Siemers*, et al.* 2005). More thorough clinical trials with this drug however have not been successful due to decreased cognitive function in those receiving treatment; a side affect that may well be attributed to unwanted interaction with notch receptor 1. Furthermore inhibition of γ-secretase alone may result in elevated pools of the Aβ precursors, SAPPβ which may have negative implications on cognitive function (Imbimbo and Giardina 2011).

1.6.2.6 Drugs to potentiate alpha-secretase

In contrast to efforts to inhibit the activity of specific secretase enzymes involved in the APP processing pathway, work has also been carried out to potentiate the activity of α-secretase, the secretase key in the driving of non-pathological processing of APP. Enhancing turnover of APP via this pathway will bypass cleavage by BACE-1 and ultimately reduce the formation of toxic Aβ species. One drug currently being trialed, etazolate (EHT 0202; Exon Hit Therapeutics, Paris, France), is able to potentiate the non amyloidogenic pathway and in doing so has been shown to have protective effects against the symptoms of AD, suggesting some kind of disease modifying ability. Encouragingly, there appears to be little toxic side effects associated with administration of this drug however further trials are required to assess if this drug has efficacy against the pathogenesis of AD with prolonged treatment (Vellas*, et al.* 2011).

1.6.2.7 Drugs to target BACE-1

As described previously, targeting BACE-1 in the APP processing pathway is an obvious drug discovery target, as attenuation of this pathway will prevent the generation of the toxic Aβ peptide.

Several efforts have been made to target BACE-1 however none have yet proved successful in completed clinical trials. This may largely be because BACE-1 has several physiological roles all over the body, not limited to the processing of APP (Yiannopoulou and Papageorgiou 2013) that may result in toxicity issues when administering a drug that inhibits BACE-1 activity all over the body. Finally the active site of BACE-1 is known to be reasonably large and as such, effective antagonists may need to be large in size to fully inhibit the action of BACE-1. As a result, this may pose problems for crossing the BBB as larger molecules are difficult to get into the brain (John*, et al.* 2011).

Despite these potential difficulties, the drug MK-8931, a BACE-1 inhibitor has been trialed by Merck. This drug trial reported a reduction in human plasma Aβ in the CSF in a sustained and dose-dependent manner (Vassar*, et al.* 2009). This data is still particularly preliminary and future trials would hope to address whether BACE-1 inhibition with this drug can rescue cognitive function in patients with AD (Ghosh*, et al.* 2012).

The current absence of any curative treatment for AD is testament to the complexity and difficulties associated with designing successful therapeutics against this disease. Largely, this seems to be due to the inherent difficulty in determining an appropriate point in disease progression to initiate treatment. Clinical trials are often carried out in those individuals with severe AD and as such, neuronal dysfunction is both severe and in most cases, largely irreversible (Dubois*, et al.* 2007). Disease modifying compounds as described above may prove more efficacious should they be prescribed earlier. Naturally this new design of trial comes with its own challenges. However, recent trials of aducanumab, an antibody that targets amyloid generation, has shown promising efficacy in a phase I clinical trial in which treatment is given earlier than usual to patients, based on MRI and PET scan screening. Establishing ways to prevent the formation of pathological species such as Aβ within the brain still remains a promising target and understanding the pathways and mechanisms by which we can do this will prove invaluable in generating successful treatments against this disease.

1.7 Conclusions

There seems to be compelling evidence that BACE-1 is still an important drug discovery target to focus on in the context of therapeutic strategies against AD. Finding a way to inhibit BACE-1 will prevent the formation of the toxic Aβ peptides and in doing so, prevent the accumulation of large insoluble mature amyloid plaques. Furthermore, the known interaction of HS with BACE-1 provides the ideal template for further understanding the way in which it can inhibit the activity of the BACE-1 enzyme. With this in mind this project aims to further elucidate the structure of HS in the brains of those patients with AD relative to their healthy age-matched counterparts, and

investigate how these potential changes in structure impact BACE-1 inhibition efficacy. Understanding these changes could lead the way in the future design of chemically synthesised mimetics of these HS compounds as a way of restoring the "ideal" configuration necessary for efficient BACE-1 inhibition. Preliminary unpublished data has shown that small HS based mimetics are able to cross the BBB and can reduce amyloid load within the mouse models of AD without toxic side effects (Turnbull personal communication). The benefit of designing potential therapies based on naturally occurring structures found in the body makes this a promising starting point. Furthermore, this project hoped to further understand the potential changes in expression of those genes encoding HS biosynthetic enzymes, which could ultimately serve as potential diagnostic biomarkers for AD. This information combined with data regarding "optimum" structures of HS necessary for BACE-1 inhibition may provide a solid framework on which to base future drug therapy designs against this disease.

1.8 Project Aims

1. Analyse the structure of purified HS from brain tissue from AD and age-matched control patients, as well as old and young mouse brain tissue. Extraction and purification of HS to determine possible age-related structural changes of HS that may occur within the brain, and potentially identify changes correlated with the onset of AD.
2. Assess the expression of genes encoding HS biosynthetic enzymes to determine possible differences between human AD and age-matched control brain samples, to elucidate possible upstream mechanisms for any observed structural changes to HS with AD.
3. Investigate the ability of HS samples from human AD and age-matched control brain tissue to regulate BACE-1 to identify any possible correlations between structural changes observed in HS and its ability to regulate BACE-1 activity effectively.
4. Study the consequences of HS biosynthetic gene knockdown. Explore whether knockdown of HS biosynthetic genes has any implications on the activity of BACE-1 in cultured cells.
5. Study effects of total gene knockout of selected HS biosynthetic genes in mouse models on both the structure of HS and its ability to regulate BACE-1.
6. Carry out gene expression profiling of specific enzymes involved in the synthesis of HS alongside with the use of bioinformatics to investigate public databases of gene expression data from AD patients. Couple with pathway analysis networks to explore wider role of HS biosynthetic genes in the wider context of AD pathogenesis and development.

Chapter 2: Heparan sulfate disaccharide analysis of brain tissue: AD and age-related differences

2. Chapter 2

2.1 Introduction

2.1.1 Compositional analysis of HS

In recent decades, significant advances have been made in the purification and structural characterisation of both nucleic acids and proteins. Indeed, recent emergence of the genomic and proteomic disciplines highlights the success with which we can now explore these molecules. Despite this, carbohydrate analysis has been less fruitful, perhaps in part due to the inherent complexity of these structures. Much more recently however, glycobiology research has led to the development of novel methods to isolate, purify and characterize these structures and in doing so has revealed the wealth of structural variability and complexity that glycan structures present. Indeed, investigation of the structure and function of the glycome is now made easier with advances in glycoarrays, high performance liquid chromatography (HPLC), mass spectrometry (MS), natural glycan libraries and synthetic chemistry techniques (Turnbull and Field 2007).

The complex nature of HS itself has made its structural determination one of the most challenging in the field of glycomics. The linear polysaccharide chain can be modified in multiple locations and in a number of ways including sulfation at multiple positions within each monosaccharide, and N-acetylation, resulting in a vast degree of variability that in turn confers a huge diversity of protein ligand binding affinities (Skidmore*, et al.* 2006). For this reason, elucidating the structural motifs that underlie specific protein interaction properties has become particularly important. As such, finding ways to isolate HS without altering its native structure has proved somewhat challenging.

2.1.1.1 Extraction and purification of HS

Historically chaotropic agents such as guanidium salts in an appropriate buffer (that can disrupt the hydrogen bonds between water molecules) were used prior to protease digestion to purify HS from cells or tissues of interest. This was carried out alongside addition of a suitable detergent to facilitate the extraction of PGs from within membrane bound organelles (Esko 2001). Whilst this method has no doubt proved very useful for large-scale purification of HS/HSPGs, it has several drawbacks, one of which is the lengthy nature of the protocol. Not least however, is also the fact that the chemicals used can remove sulfate groups at the N- position along the HS chain (Drummond*, et al.* 2001, Rej*, et al.* 1989). Recent work has therefore identified a more streamlined

method of HS extraction from tissue that reduces product loss and ensures efficient purification of the native structure for comparative analysis. Use of TRIzol®, a well known phenol/guanidine/chloroform reagent used more commonly in the purification of DNA and RNA from tissue (Chomczynski and Sacchi 1987), has been found to successfully separate PGs to the aqueous phase making it a suitable candidate for a more streamlined method of extraction (Guimond*, et al.* 2009).

Most commonly, structural composition is assessed following disaccharide compositional analysis to obtain a profile of the structural motifs present within HS (Guimond*, et al.* 2009). This is then followed by a series of steps to allow analysis of GAG structural motifs with either UV or fluorescence detection methods (**Figure 2.1**). The specificities by which this may be carried out vary somewhat, however the fundamental protocol steps remain the same.

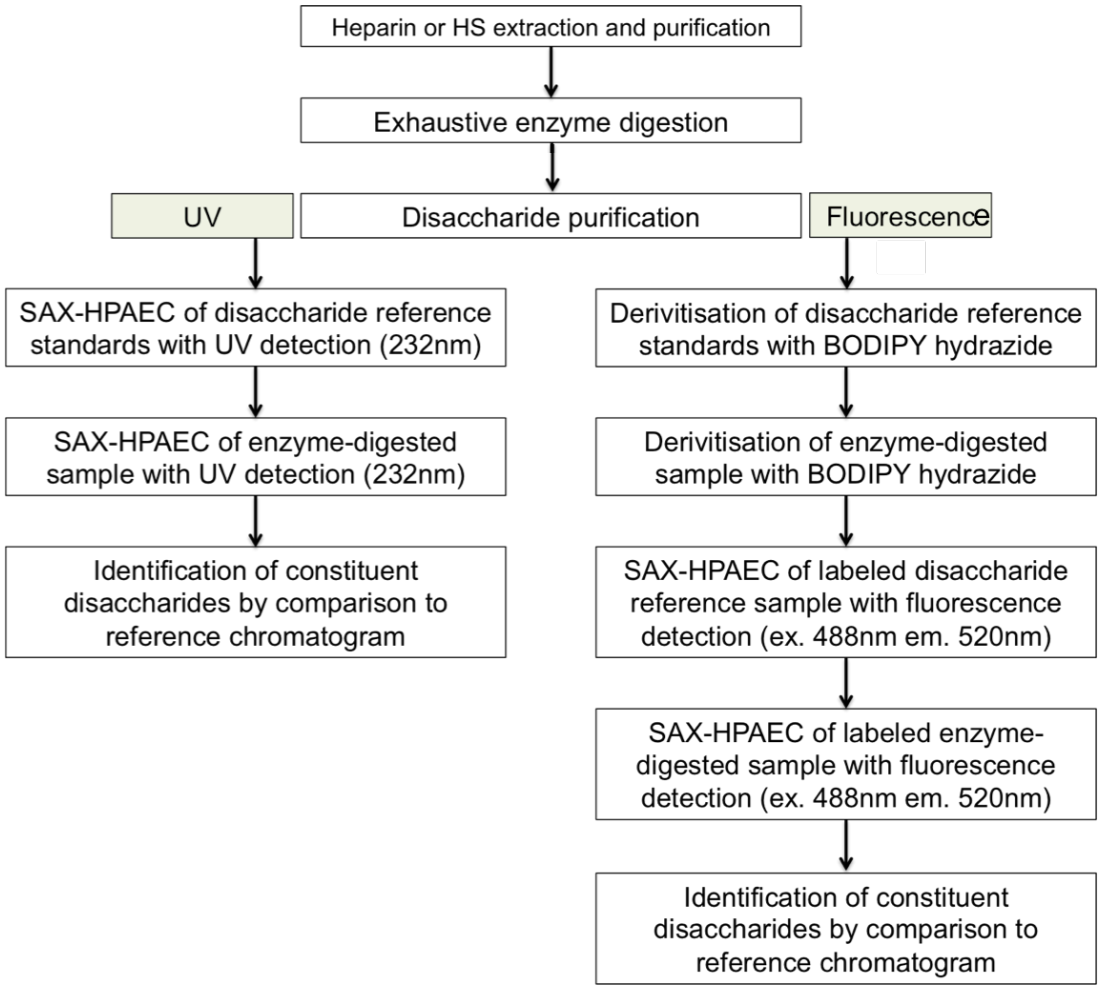

Figure 2.1: Flow diagram to outline the key steps involved in compositional analysis of GAG disaccharides. Exhaustive enzyme digestion of the GAG chain and appropriate purification steps followed by either UV or fluorescent detection methods may be employed to carry out compositional analysis. Taken and adapted from (Skidmore et al., 2010). Abbreviation: SAX-HPAEC: Strong Anion Exchange- High Performance Anion Exchange Chromatography, UV: Ultraviolet.

2.1.1.2 Depolymerisation of the glycosaminoglycan chain

2.1.1.2.1 Enzymatic digestion

The disaccharide constituents of HS/heparin may be better thought of as their "building blocks" and understanding the profile of these units may provide valuable insights into the overall structural heterogeneity of this GAG. Digestion of long chain GAGs is most often achieved via exhaustive digestion with bacterial lyase enzymes, heparinase I, heparinase II and heparinase III (also referred to as heparitinases III, II and I respectively). Addition of these enzymes digests the polysaccharide chain and introduces a 4,5, unsaturated double bond at the non-reducing end of the uronic acid residues, one of the units of the newly generated disaccharides (the delta symbol Δ is used to identify these disaccharides, "Δ-disaccharides"). A cocktail of these three enzymes ensures efficient digestion owing to the fact that each of the heparinase enzymes has its own cleavage site specificity as shown in **Table 2.1**. Largely, heparinase I cleaves the GAG chain at regions of high levels of sulfation whilst heparinase III conversely favors regions of low sulfation for cleavage (Linhardt*, et al.* 1990).

Table 2.1: Enzymes used for digestion of heparin and HS into constituent disaccharides. Taken from (Skidmore et al., 2010; Lindhart et al., 1990).

Enzyme (Lyase)	Sequence specificity
Heparinase I (Heparitinase III)	-GlcNS (±6S)-α (1-4) IdoA (2S)-
Heparinase II (Heparitinase II)	-GlcNR (±6S)-α (1-4) GlcA/IdoA-
Heparinase III (Heparitinase I)	GlcNR (±6S)-α (1-4) GlcA-

It is important to note that the action of these heparinase enzymes on the HS/heparin chains ultimately makes it impossible to identify the nature of the original uronic acid epimer within the disaccharide, i.e. it is not possible to distinguish between GlcA and IdoA residues. This is a result of the introduction of the C4-C5 carbon-carbon double bond at the non-reducing end of the disaccharide. This feature is unavoidable in the digestion of HS/heparin, but should be noted as a shortcoming of this method since epimer identity may prove crucial in understanding GAG structure heterogeneity in tissues/cells of interest.

2.1.1.2.2 Chemical degradation

There are several other means by which GAG chains like HS/heparin may be digested into their smaller constituents. Chemical digestion is also a common method for this. For several years nitrous acid digestion was a common choice for the depolymerisation of GAG chains. Nitrous acid at

pH 1.5 is able to rapidly cleave at N-sulfated GlcN residues of HS/heparin to remove N-sulfate groups and yield de-N-sulfated oligosaccharides. As such, this is still largely the cheapest and easiest method for generating unsulfated oligosaccharides of varying lengths (Conrad 2001). N-acetylated amino sugar residues of these chains however do not react with nitrous acid and as a result, digestion by this method will not touch any part of the chain with an acetyl group. This hurdle can be overcome via N-deacetylation of these residues followed by further nitrous acid treatment at pH 4 to finally digest the remaining de-N-acetylated chains. The process of N-deacetylation was initially carried out via a process termed hydrazonolysis (Shaklee and Conrad 1984). This was achieved using either hydrazine or hydrazine hydrate, however was found to initiate only partial N-deacetylation and caused degeneration of the GAG chain – an unfavorable outcome for a protocol used to assess structural characteristics. Later, it was discovered that full de-N-acetylation and degradation could be afforded by the use of a mixture of hydrazine and hydrazine sulfate instead (Yosizawa*, et al.* 1966) which released a free amino in place of the acetyl group that could then be attacked by nitrous acid treatment for degradation (Shaklee and Conrad 1984). Despite the ease and speed with which this method can be carried out, nitrous acid and hydrazonolysis are limited to lack of production of disaccharides with a carbon-carbon double bond that can be easily detected by UV (232nm), as is the result with enzymatic degradation. These do however maintain the uronic acids in their original configuration allowing identification of differences in GlcA and IdoA content.

UV can be used to detect other parts of the disaccharide at different wavelengths (e.g. 210nm) however these are not as sensitive as the signal afforded by exploiting the carbon-carbon double bond. Secondly, the use of hydrazide in this process makes the C-5 uronic acid more susceptible to epimerisation. Compositional analysis of polysaccharides containing only one type of uronic acid is not hindered by this, however the presence of both GlcA and IdoA acid residues within both HS/heparin means that recovery of the relative proportions of these uronic acid residues may not be a true reflection of the native structure (Shaklee and Conrad 1984).

2.1.1.2.3 Free radical degradation

Digestion of GAG chains by free radicals is another available method. Reactive oxygen species (ROS) may be described as chemically active molecules that are generated as a result of the partial reduction of oxygen. These products are very similar to reactive nitrogen species (RNS) that are identical except derived from nitric oxide (NO) based reactions (Winterbourn 2008). The generation of free radicals may be both due to exogenous (UV radiation and ionisation) and endogenous (mitochondrial respiration, enzymes that produce ROS/RNS) means within the body (Kohen and Nyska 2002) and can be both beneficial and detrimental to cells. Free radical exposure may play a role in pathways such as signal transduction and transcriptional regulation, but may also expose the cell to intense oxidative stress that can be damaging (Fialkow*, et al.* 2007).

ROS and RNS species may be thought of as free radicals that contain one unpaired electron. This family of active chemicals may include superoxide ion radicals (O_2^-), peroxyl (ROO^-), hydroxyl (OH^-), alkoxyl (Ogishima*, et al.*) and NO radicals (NO^-) (Kohen and Nyska 2002). These species are able to interact with polysaccharides such that they cause breakage of the sugar backbone and generate smaller fragments (Duan and Kasper 2011). One species in particular, the hydroxyl radical is the most reactive of all the reactive oxygen species. It is able to abstract hydrogen atoms from the substrate in a number of positions along the polysaccharide chain. Most importantly, previous work has found that a free radical reaction initiated by a mixture of Cu^{2+}, hydrogen peroxide and ascorbate dramatically reduces the molecular weight of heparin by approximately a third and also attenuates its anti Xa activity by nearly a half. These results suggest a regional selectivity of the Cu^{2+} ion and heparin that can be exploited for depolymerisation of the GAG chain (Liu and Perlin 1994).

Furthermore, research shows that the degree of depolymerisation via the action of free radicals is dependent upon the levels of sulfation to the GAG chain. For example hyaluronan (HA), lacking sulfate groups, is the most susceptible to free radical attack. HS however, is much less susceptible due to the highly sulfated nature of this sugar (Kennett and Davies 2007). This discrimination of efficacy for free radical degradation for different GAGs does not make it the most suitable method of depolymerisation, particularly in this instance for the compositional analysis of HS.

2.2 Heparin/HS disaccharide standards

Within both heparin and HS structures, there exist 8 “most common” disaccharide motifs that are often used as standards. These 8 disaccharides are consistently observed within HS and heparin GAGs and may therefore be used as a commercially available comparison for identification of those disaccharides present within the HS/heparin sample of interest. The 8-disaccharide standards range from those with no or very low levels of sulfation to those with a much greater degree of sulfation. In its simplest form, there are 3 positions (R1, R2 and R3) onto which modifications to the HS/heparin chain may be made (**Figure 2.2**). A sulfate or hydroxyl group may be found at position 2 of the iduronate residue (R1) or position 6 of the glucosamine (R2), and finally a N-sulfate or N-acetyl group may be added at position 2 of the glucosamine (R3) (Yates*, et al.* 2004).

Modifications at these positions may occur together or in isolation and as such, these modifications open up a great variety of possible combinations of sulfation/acetylation that ultimately confer a wide binding capacity of HS/heparin and other protein ligands. The disaccharide standards used as authentic comparisons in this instance consist of the most commonly occurring varieties of these three modification patterns (**Table 2.2**). One can make use of strong anion

exchange high performance chromatography (SAX-HPAEC) to separate these standards using an increasing linear salt gradient to dissociate each standard from the column.

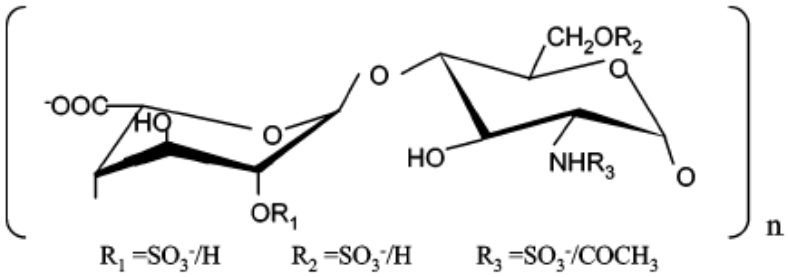

Figure 2.2: Simplified diagram of the repeating disaccharide unit that make up the HS/heparin polysaccharide. Modification of these units may occur at 3 positions, R1, R2 and/or R3. A sulfate or hydroxyl group may be present at both the 2 position of iduronate or glucosamine residue and a N-sulfate or N-acetyl group may be substituted at the 6 position of the glucosamine residue. Taken from (Yates*, et al.* 2004)

Table 2.2: Structures of the 8 most commonly occurring disaccharide components within HS/heparin following exhaustive enzymatic digestion with heparinase I,II and III enzymes. The delta symbol represents the presence of the 4,5 unsaturated carbon-carbon double bond. Abbreviations: UA, uronic acid residue; Ac, acetyl; GlcNAc, N-acetyl glucosamine; GlcNS, glucosamine-N-sulfate; H, hydrogen; 2S, 2-O-sulfate; 6S, 6-O-sulfate; Sulf, Sulfate. Taken and adapted from (Skidmore*, et al.* 2010)

Unit formula	R1	R2	R3
Δ-UA-GlcNAc	Ac	H	H
Δ-UA-GlcNAc(6S)	Ac	Sulf	H
Δ-UA(2S)-GlcNAc	Ac	H	Sulf
Δ-UA(2S)-GlcNAc(6S)	Ac	Sulf	Sulf
Δ-UA-GlcNS	Sulf	H	H
Δ-UA-GlcNS(6S)	Sulf	Sulf	H
Δ-UA(2S)-GlcNS	Sulf	H	Sulf
Δ-UA(2S)-GlcNS(6S)	Sulf	Sulf	Sulf

2.3 Detection methods of heparin/HS disaccharides for analysis by strong anion exchange chromatography

2.3.1 Detection by UV absorbance or fluorescence

The chromophore of the unsaturated double bond that is introduced via heparinase digestion can be detected optimally with UV absorbance at 232nm, making analysis of disaccharide composition relatively simple. A major drawback of this protocol however is that the detection limit

of this method is limited to the low nanomolar range whereby approximately 1-5µg of starting material is used for HS/heparin analysis (Turnbull*, et al.* 1999). Practically however, extraction of HS cannot be achieved often in such large quantities and a much more sensitive detection method may be needed for many applications.

Labeling samples of interest with an appropriate fluorophore has been widely used as a method to enhance sensitivity and reduce detection limits for disaccharide analysis without the risk of contaminant signal as is common with UV detection (Skidmore*, et al.* 2006). Indeed work has been carried out more recently to improve sensitivity without the need for additional chromatography hardware that usually accompanies improved detection. In common practice, a fluorophore may be added to the reducing end of the disaccharide unit via a Schiff's base reaction between a nitrogen containing functional group on the fluorophore (such as an amino or hydrazide) and the carbonyl group of the reducing end of the sugar.

Examples of this type of detection include addition of 2-aminoacridone, a small amine-containing fluorophore, to the reducing end of the disaccharide followed by detection with reverse-phase high performance liquid chromatography (RP-HPLC). This fluorophore is widely used to label any carbonyl containing biomolecule and has reportedly improved sensitivity for disaccharide analysis of as little as 10ng of the original GAG (Deakin and Lyon 2008). Other fluorescent-based methods for glycan sequencing include the use of another fluorescent label, anthranilic acid, followed by gel electrophoresis to detect nmol levels of disaccharide for analysis. This was improved further by an alternative label, 7-aminonapthalene-1,3-disulfonic acid to improve sensitivity an additional ten fold to confer detection with starting material quantities in just the pmol range (Drummond*, et al.* 2001).

Despite the undoubted improvement in sensitivity and detection limits that these new methodologies have afforded, there is literature to suggest that they may lack the ability to successfully resolve all 8 of the most common disaccharide standards within HS/heparin. In particular, RP-HPLC has more recently been used to enhance separation of the disaccharide standards present within HS/heparin and also other GAGs such as CS, DS and HA. In this protocol, the GAG disaccharides may be derivitised with a fluorophore called AMAC and separated via reverse phase HPLC. As such, this method became the first of its kind to facilitate the successful separation of the disaccharide standards in one step with appropriate efficiency, accuracy and stability (Ambrosius*, et al.* 2008).

2.3.2.Detection of BODIPY-tagged disaccharides by fluorescence

Advances in methodology for disaccharide compositional analysis have proved invaluable for further understanding and characterising the structure and function of GAG chains. Much more recently however, the use of a fluorophore, BODIPY FL hydrazide (λ_{ex} 488nm, λ_{em} 520nm) has become a popular choice for detection of HS/heparin disaccharides. Most notably, this is due to its ability to label disaccharides that may be only in the fmol (10^{-15} mol) range in terms of quantity available. As such this is an ideal method for the compositional analysis of HS from tissues such as AD patient and healthy aged-matched control samples as obtained for this project. Only small amounts of tissue can be sampled at any one time and high sensitivity means only 30-80mg of starting material is required for successful analysis of the disaccharides present.

The BODIPY protocol, as first described by Skidmore and colleagues in 2006 (Skidmore*, et al.* 2006), utilises reductive amination (a process in which a carbonyl group is converted to an amine via the action of an intermediate imine) to label the disaccharide of interest. In this instance the carbonyl group present on the reducing end of the disaccharide undergoes reductive amination with the hydrazide group present on the fluorophore (the BODIPY tag). In some cases, the resulting conjugate may be stabilised by reducing the intermediate imine to an amine using sodium borohydride. When the disaccharides have been labeled they may be separated through the use of strong anion exchange chromatography (as with other labeling methods). A linear sodium chloride gradient can successfully dissociate each disaccharide from the column and each peak can be compared to a chromatogram generated with authentic disaccharide standards for comparative analysis. As mentioned previously, the identity of the uronic acid residue within each disaccharide remains unsolved with this method, as with other detection systems; however the use of the BODIPY fluorophore undoubtedly improves the speed, efficiency and accuracy of disaccharide compositional analysis.

For this project, the use of BODIPY was ideal due to limited sources of starting material. Being able to detect and analyse disaccharide composition at low levels meant precious human tissue could be used for other experiments/assays without waste. Additional clean up steps were added before and after the addition of the fluorescent label to ensure clean chromatograms with no contaminating peaks. By understanding the potential differences/similarities in disaccharide composition between the HS from AD patients and age-matched controls, this project aimed to further elucidate and understand the consequences and functionality of altered HS structures within the brains of AD patients and its role in the onset of this disease.

2.4 Changes in the structure of glycosaminoglycans like HS

There are several examples whereby the study of GAG structure has demonstrated changes in the presence of a disease or ageing phenotype. Specifically in the context of this project, recent studies have suggested that normal ageing may initiate changes in the structure of HS. Studies in aged rat myocardium have recorded an age-dependent increase in the quantity of HS in the myocardium. In addition, this change was accompanied by significantly increased 6-O sulfation and some changes in N- and 2-O sulfation also (Huynh*, et al.* 2012). In addition, studies have shown that GAGs from aged human hippocampus present altered structural properties vs. their younger counterparts. These structural differences were shown to affect regulation of trophic factors despite having no effect on Aβ peptide toxicity (Huynh*, et al.* 2012). In light of this, we can conclude there are significant structural alterations that take place with ageing and we might postulate that these changes could contribute to the AD phenotype.

Indeed, other studies to look at brain tissue have also recorded changes in the structure of another PG, KS in AD patients vs. age-matched controls. Lindahl and colleagues reported a significant decrease in levels of highly sulfated KS within the cerebral cortex of patients with AD vs. age-matched controls and have suggested this may reflect a specific deficit in the function of those cells affected by Alzheimer's pathology. Whether this change in the structure of KS is a secondary effect of the disease pathology or indeed an upstream cause of the deficits observed with this disorder is unknown; however understanding the structure of PGs in this way is key in elucidating links between this complex sugar and disease pathology (Lindahl*, et al.* 1996).

Likewise, Lindahl and colleagues have also observed a slight increase in the level of N-sulfation along the HS chain in AD patients vs. age-matched controls. This was observed despite a relative uniformity of HS profiling between all patient samples studied; however more work is needed to determine whether this is a cause of AD pathology or a secondary consequence. Whilst work has already shown an interaction between HS and BACE-1 (Scholefield, 2003) indicative of a causative role of HS in AD, there is a great deal of evidence to suggest it also has secondary roles in disease progression. With this in mind, we must also be aware of the changes in structure of HS and how this may alter interaction with the Aβ protein itself and the exacerbation of AD pathology after it has been initiated (Lindahl*, et al.* 1995).

HS displays the highest level of structural complexity of all the GAGs, which may explain its diverse role in so many physiological and pathological functions. Such interactions will be dependent upon the distribution of charges along the polysaccharide chain that confers specificity in the way in which the sugar is able to interact with its ligands (Lindahl*, et al.* 1995). With this in mind, understanding the changes in the structure of HS will be of key importance in determining more about its role in disease. Even the subtlest of changes in the structure of this GAG may be instrumental in affecting a number of downstream processes associated with a particular disease.

This project aimed to study potential changes in the structure of HS in the brains of AD patients and their healthy age-matched control counterparts.

2.5 Aims of this chapter

1. Determine if there are differences in the disaccharide compositional profile of HS from the middle temporal gyrus tissue from human AD and age-matched control patients.
2. Determine whether there are global changes in the degree of sulfated motifs found within the HS from the middle temporal gyrus tissue from human AD and age-matched control patients.
3. Investigate the quantity of total HS found within middle temporal gyrus brain tissue from human AD and age-matched control patients.
4. Determine whether there are any gender-based differences in the overall composition of HS within human AD and age-matched control patients.
5. Explore potential changes in the structure of brain HS as above but from young (3 month) and old (18month) old mice to explore age as a variable for HS structure.

2.6 Methods

2.6.1 Sample selection

2.6.1.1 Ethical approval

Human brain samples were received from the Oxford Brain Bank, supported by the MRC, BDR and the NIHR Oxford Biomedical Research Centre. All human tissue work was carried out under ethical approval from the Oxford Brain Bank (ref number: 07/0606/85). Furthermore, all human tissue was acquired, used and disposed of appropriately, according to all environmental, healthy and safety laws as described by the Human Tissue Act 2004. For mouse samples, all animals were used in accordance with the Animal (Scientific Procedures) Act 1986 and the EU Directive 2010/63/EU. All procedures were performed in accordance with the UK Home Office Regulation of Animal Experimentation.

2.6.1.2 Selection of human samples

Brain samples were received from the Oxford Brain Bank, supported by the MRC, BDR and the NIHR Oxford Biomedical Research Centre. Brain sampling was performed according to the

Consortium to Establish a Registry of AD (CERAD). Two experimental groups were established; an AD group (n=20) of 10 females and 10 males with subject ages ranging from 71- 91 (mean ±S.E.M = 78.85 ± 2.11), and a healthy control group (n=15) of 9 females and 6 males with subject ages ranging from 75-101 (mean ±S.E.M = 86.3±1.6) (**Table 2.3**). Post-mortem delay intervals varied from 19.0-107.0 and 22.0-120.0hr for AD patients and healthy controls respectively. Brains were frozen and 200mg/sample of the middle temporal gyrus (BA21) dissected. Tissues were immediately frozen after dissection in dry ice.

AD samples were selected based on both a clinical and neuropathological diagnosis of the disease. Difficulties with diagnosing AD with 100% accuracy until post-mortem made it necessary to confirm pathology after death with the histologically identified presence of AD pathology. CERAD criteria for disease progression were used as a primary target for sampling and those patients with "definite AD" were selected for sampling with priority. Availability of samples meant this was not possible in all cases; however "classical" AD pathology was confirmed in all AD patients selected for this study. Braak staging was the only confirmed measure of AD in some patients and were selected for when CERAD staging could not be confirmed. Post mortem delay was challenging to control for; however sex of the patient, age and diagnosis were all carefully selected for. For the control group, age-matched samples were selected with a similar sex distribution. All patients within this group were deemed neuropathologically normal at post mortem and in all but 2 exceptions, no neurological or psychiatric symptoms of any kind were reported (**Table 2.4**). Again, post-mortem delay times varied somewhat for this cohort however no significant statistical difference ($p<0.08$, Student's t-test)) was found for post mortem delay between the two groups (**Figure 2.3**). Fortunately, the structure of HS is relatively resistant to this variable, as it does not suffer degradation or instability as readily as RNA, DNA or protein.

Brodmann's area 21, or the middle temporal gyrus, was selected as a sample region in this instance. The middle temporal gyrus is part of the temporal cortex and is a well-documented area to show neuropathological and neurochemical changes in AD (Scheff and Price 1993). This made selection of the middle temporal gyrus a suitable candidate for this study, as it was desirable to select a region that was vulnerable to the onset of AD pathology (**Figure 2.4**). Furthermore, bioinformatics analysis of publically available microarray gene expression profiling databases highlighted key changes in the expression of HS-related genes with AD within the middle temporal gyrus which supported the decision to sample this area of the brain. Data collected from this work is described in detail in **chapter 5**. It is important to note, previous work including 3D magnetic resonance imaging (MRI) studies have identified the hippocampus as the first area known to be affected in the onset of AD (Zhang*, et al.* 2015). In particular, hippocampal atrophy has been observed in patients before the onset of symptoms (Fox*, et al.* 1996). However due to the small nature of this brain region, and its primary role in memory formation is a highly sought- after sample

for studies like this and was unavailable for this early work. The middle temporal gyrus is implicated in AD pathology and is available in relative abundance making it an ideal choice for sampling in this study.

Table 2.3: Samples selected from the Oxford Brain Bank for analysis. AD and age-matched control samples were selected and sex, age and post-mortem delay recorded as shown below. Abbreviations: PMD, Post-mortem delay.

Sex	Age (yrs.)	PMD (hrs.)	Group	Sex	Age (yrs.)	PMD (hrs.)	Group
F	72	85.0	AD	F	79	31.0	Ctrl
F	83	19.0	AD	F	89	59.0	Ctrl
F	71	22.0	AD	F	85	40.0	Ctrl
F	86	72.0	AD	F	87	52.0	Ctrl
F	89	30.0	AD	F	88	27.0	Ctrl
F	67	107.0	AD	F	101	37.0	Ctrl
F	68	49.0	AD	F	88	62.0	Ctrl
F	91	49.0	AD	F	83	52.0	Ctrl
F	70	84.0	AD	F	84	31.0	Ctrl
F	93	80.0	AD	M	93	120.0	Ctrl
M	78	77.0	AD	M	75	45.0	Ctrl
M	86	50.0	AD	M	86	31.0	Ctrl
M	85	65.0	AD	M	82	22.0	Ctrl
M	88	24.0	AD	M	88	31.0	Ctrl
M	88	72.0	AD	M	86	28.0	Ctrl
M	70	79.0	AD				
M	71	85.0	AD				
M	84	96.0	AD				
M	66	42.0	AD				
M	71	20.0	AD				

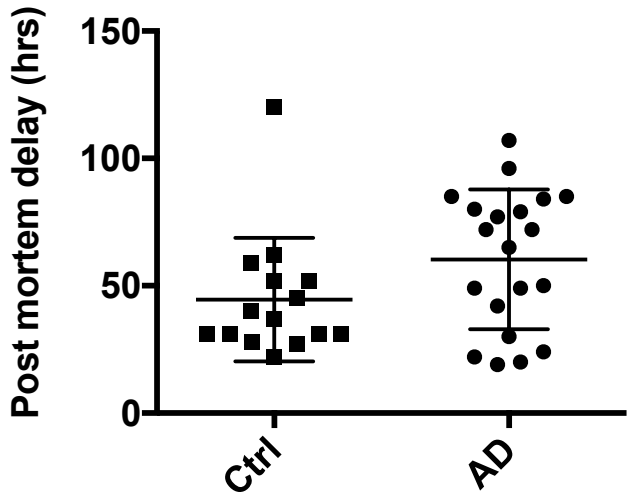

Figure 2.3: Post mortem delay in AD and control samples. Post mortem delay was reasonably varied between AD and age-matched control brain samples however no significant difference was found between the two groups ($p<0.08$, Student's t-test). Post-mortem delay intervals varied from 19.0-107.0hr and 22.0-120.0hr for AD patients and healthy controls respectively.

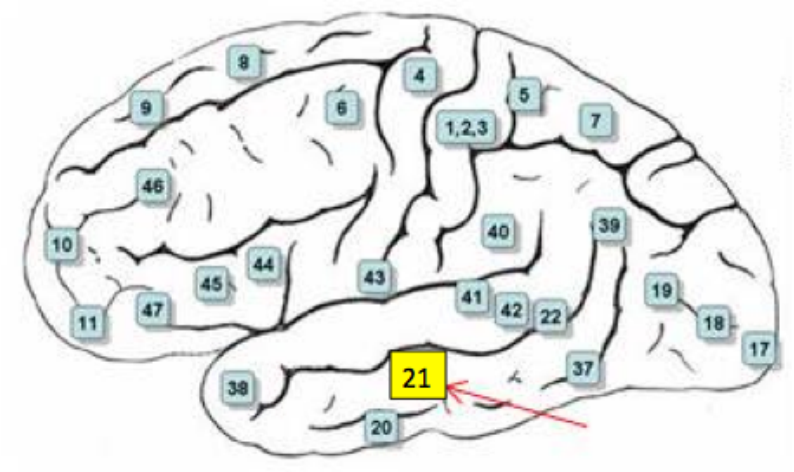

Figure 2.4: Brodmann's areas of the brain labeled in lateral view. Brodmann's area 21 (BA21), or the middle temporal gyrus is located within the temporal cortex in the human brain. The middle temporal gyrus comprises most of the lateral temporal cortex, a region most associated with language and auditory processing. Previous work has implicated this area in AD pathogenesis. The BA21 region is found superior to BA20 and inferior to BA40 and BA41.

Table 2.4: Details of clinical and neuropathological diagnosis of AD and age-matched control samples selected for this study as recorded by the Oxford Brain Bank. Abbreviations: AD: Alzheimer's disease; Ctrl: Control; VD: Vascular dementia; CERAD: Consortium to Establish a Registry of AD.

Group	Clinical Diagnosis	Neuropathological Diagnosis	Group	Clinical Diagnosis	Neuropathological Diagnosis
AD	AD	AD, Braak + Braak stage VI / AD, CERAD definite AD	Ctrl	No neurological or psychiatric symptoms	No neuropathological or normal ageing changes
AD	AD	AD, Braak + Braak stage VI / AD, CERAD definite AD	Ctrl	No neurological or psychiatric symptoms	No neuropathological or normal ageing changes
AD	AD	AD, Braak + Braak stage VI / AD, CERAD definite AD	Ctrl	No neurological or psychiatric symptoms	No neuropathological or normal ageing changes
AD	AD	AD, Braak + Braak stage VI / AD, CERAD definite AD	Ctrl	Depression	No neuropathological or normal ageing changes
AD	AD / vascular dementia	AD, Braak + Braak stage VI/ AD, CERAD definite AD / vascular disease	Ctrl	No neurological or psychiatric symptoms	No neuropathological or normal ageing changes
AD	AD	AD, Braak + Braak stage VI / AD, CERAD definite AD / infarction, ischaemic	Ctrl	Depression	No neuropathological or normal ageing changes
AD	AD, hypertension	AD, Braak + Braak stage VI / AD, CERAD definite AD / hippocampal sclerosis	Ctrl	No neurological or psychiatric symptoms	No neuropathological or normal ageing changes
AD	AD / depression, vascular dementia	AD, Braak + Braak stage VI / AD, CERAD definite AD	Ctrl	No neurological or psychiatric symptoms	No neuropathological or normal ageing changes
AD	n/a	AD, Braak + Braak stage VI / AD, CERAD definite AD	Ctrl	No neurological or psychiatric symptoms	No neuropathological or normal ageing changes
AD	n/a	AD, Braak + Braak stage VI / AD, CERAD definite AD	Ctrl	No neurological or psychiatric symptoms	No neuropathological or normal ageing changes
AD	AD	AD, Braak tangle stage VI	Ctrl	No abnormality detected	Cerebrovascular arteriolosclerosis
AD	AD	AD, Braak tangle stage VI	Ctrl	No abnormality detected	Cerebrovascular disease / mild cerebrovascular atherosclerosis, moderate non-amyloid SVD
AD	Brain atrophy / vascular dementia / AD	Mild non amyloid SVD/ Mild cerebrovascular atherosclerosis/ Mild arteriolar AB-CAA/ AD, CERAD high density of neuritic plaques	Ctrl	No abnormality detected	No abnormality detected
AD	AD, brain atrophy / depressive episodes	AD, Braak tangle stage VI	Ctrl	Malignant neoplasm of bronchus and lung / no abnormality detected	Cerebrovascular disease / no abnormality detected / moderate non-amyloid SVD / microinfarcts, cerebral white matter / microinfarcts, basal ganglia
AD	AD	Mild arteriolar AB-CAA/ AD, Braak tangle stage VI / CERAD high density of neuritic plaques	Ctrl	No abnormality detected	Infarcts >10mm in diameter
AD	AD / epilepsy	AD, Braak tangle stage VI			
AD	AD / depression	AD, Braak tangle stage VI			
AD	AD	AD, Braak tangle stage IV			
AD	AD	AD, Braak tangle stage VI			
AD	AD	AD, Braak tangle stage VI			

2.6.1.3 Selection of old and young mouse brain samples

Young (3 months, n=5) and old (18 months, n=5) C57Bl/6J (female) mice were obtained from Charles River (France), housed (4 per cage) in a pathogen free facility at the University of Oxford, UK under a 12hr day-night cycle and fed with standard chow and water as libitum. In the final two weeks of experiment, old mice were housed one per cage. At appropriate ages, mice were culled and the brains dissected and immediately snap frozen before sending to the University of Liverpool for analysis. Whole brain HS was isolated.

2.6.2 Compositional analysis of HS

Compositional analysis of HS was carried out in the same manner for both human and mouse brain samples. 30mg of starting wet tissue was used in both instances for HS extraction and purification and protocols were identical for both species. Optimisation of this protocol is detailed in **Appendix A**.

2.6.2.1 HS extraction and purification

Extraction of HS from tissue was achieved using a previously established protocol in the lab and labeled with BODIPY hydrazide for HPLC analysis with fluorescence detection. Briefly, wet tissue (30mg) was homogenised with a tissue grinder in 1ml of TRIzol™ (Life Technologies) reagent/100mg of tissue to break down the cell membranes and aid the release of HS. The tissue was then incubated for 5 minutes at room temperature and transferred to Eppendorf tubes and 0.2ml chloroform (Sigma)/1ml of TRIzol™ added before shaking vigorously for 15s. Samples were centrifuged at 8000 x g for 15 mins at 4°C. HSPGs were collected in the upper aqueous phase and the pellet discarded. The aqueous phase was applied to a diethylaminoethanol (DEAE) Sephacel weak-anion exchange resin (GE Healthcare, UK) (bead storage ethanol pre washed off with 3x washes with phosphate buffered saline (PBS), for 30mg sample 400µl of PBS and beads, assuming a 1:1 ratio of PBS to beads overnight and then washed with 10ml of PBS, 10ml of PBS (0.25M NaCl), pH 7.4 (x2) and eluted with 2ml of PBS (2M NaCl), pH 7.4. PBS (2M NaCl) fractions were then desalted on a HiTrap desalting column (GE Healthcare, UK) and freeze-dried.

Samples were suspended in 100mM sodium acetate, 0.1mM calcium acetate, pH 7.0 and digested by sequential addition of 1.25 mU of heparinase 1 (2hr), heparinase III (2hr) and finally heparinase II (Ibex, Canada) (2hr) at 37°C. This was followed by addition of a further 1.25 mU of each enzyme for incubation at 37°C overnight (Ibex, Canada). Samples were brought to a 0.5M salt

concentration and heated for 5 minutes at 95°C before being run over Pierce C18 spin columns (Thermo Scientific). Columns were prepped and run according to manufacturer's instructions with the exception that flow through (containing HS disaccharides) was kept rather than discarded. Samples were then run over graphite spin columns (Thermo Scientific) to remove salt according to manufacturer's preparation and run instructions.

2.6.2.2 BODIPY labeling and HPLC analysis with fluorescence detection

Disaccharides were labeled with BODIPY hydrazide, as described previously (Skidmore*, et al.* 2006). In addition HS disaccharide standards were also labeled for analysis by HPLC as a comparison. Samples were suspended in BODIPY fluorescent label hydrazide (5mg/ml in methanol) and the methanol removed by centrifugation under vacuum. Samples were then re-suspended in dimethyl sulfoxide (DMSO): acetic acid (17:3 v/v: 10µl) and incubated in the dark for 4hr. Excess BODIPY tag was removed using aluminium-silica thin-layer chromatography (TLC) plates (Sigma) using butanol as a mobile phase.

Finally samples underwent ethanol precipitation to remove any unwanted chemical species that may have co-purified with the HS. A saturated ethanol solution was made with sodium acetate (Sigma) and incubated on ice with the samples for 15 minutes before being centrifuged and the supernatant collected. Samples were then freeze-dried ready for HPLC analysis. Labeled disaccharides were re-suspended in water (<1ml) and loaded onto a Propac PA-1 strong-anion exchange column (4.6x250mm; Dionex, Leeds, UK). This was followed by elution with a linear gradient of 0-1M sodium chloride and isocratic sodium hydroxide (150mM) over 30 min at a flow rate of 1ml/min on a Shimadzu HPLC system. Peaks were detected with an inline fluorimeter with an excitation wavelength of λ = 488nm and an emission wavelength of λ = 520nm using a Shimadzu RF-10AXL detector. The column was reconditioned with a 2M NaCl wash (in 300mM NaOH) before finally equilibrating it in 150mM NaOH.

2.6.2.3 Quantification of total HS within brain samples

Quantification of HS from tissue was carried out after a very similar extraction and preparation process as described above for the disaccharide compositional analysis (Section 2.6.2.1). Following desalting however, samples underwent exhaustive enzymatic clean up steps to remove any impurities and other GAG chains that could contaminate the sample of HS. This was achieved with sequential addition of DNAse, RNAse, chondroitin ABC lyase, neuraminidase, keratanase (Sigma Aldrich, UK) and Pronase® (Roche, UK) enzymes to remove DNA, RNA, chondroitin, N-linked sugars, sialic acids, KS and proteins respectively. Enzymes were added in appropriate buffers, as detailed in

Table 2.5, for various periods of time at 37°C, and after addition of Pronase, underwent a final incubation overnight at 37°C.

Following digestion, samples underwent DEAE and desalting treatment for a second time (as outlined in section 2.6.2.1), to remove the enzymes and salt that were introduced during this purification process. Samples were then digested with multiple heparinases as described above. This was followed by addition of a further 1.25 mU of each enzyme for incubation at 37'C overnight (Ibex, Canada). Pure digested HS was then quantified using the Nano Drop (Thermo Scientific), a spectrophotometer set for UV absorbance at 232nm to detect the presence of the glycosidic double bond within the HS disaccharides. HS quantification was calculated as a total concentration and then μg/100mg of starting "wet" tissue. The concentration of HS was calculated with the following equation.

$$\mathbf{A = \varepsilon l c}$$

(Where **A** = absorbance (at 232nm), **ε** = molar absorption, (5500 for HS) **l** = length of solution the light passes through (0.1) and **c** = concentration.

Table 2.5: Enzymatic purification protocol of HS samples for total HS quanitfication as described. Sequential addition of DNase, RNase, chondroitin ABC lyase, neuraminidase, keratanase and Pronase® enzymes were added in their respective buffers in the quantities described below.

Enzyme	Enzyme Buffer	Aliquot	Incubation
DNase	40mM Tris-acetate pH 8.0, 6mM magnesium chloride, 10mM calcium chloride.	1μg/ml	4hr
RNase	10mM Tris-acetate pH 8.0, 5mM EDTA, 8mM sodium acetate,	0.5mg/ml	1hr
chondroitin ABC lyase	100mM Tris-acetate pH 8.0	1.25U	4hr
neuraminidase	50mM Tris-acetate pH 7.5	2.5mU	4hr
keratanase	50mM Tris-acetate pH 7.5	100mU	4hr
Pronase®	100mM Tris-acetate, 10mM calcium acetate pH 8.0	10mg/ml	Overnight

2.6.3 Statistical analysis

All data was tested for normal distribution and differences between study groups assessed with a student's t- test. Compositional analysis of HS structures from both human and mouse brain samples are expressed as bar graphs showing peak areas as a percentage of total HS analysed. Error bars represent standard error of the mean (S.E.M).

2.7 Results

2.7.1 Human HS samples - Alzheimer's disease vs. healthy age-matched controls

2.7.1.1 Disaccharide peak analysis

HS from all brain samples (middle temporal gyrus, BA21); (20 AD patients and 15 healthy age-matched controls) was extracted and underwent exhaustive heparinase digestion in preparation for disaccharide compositional analysis. Disaccharides were labeled with BODIPY hydrazide and run over a strong anion exchange (SAX) Propac PA-1 column. This method allowed compositional analysis of the structure of the HS within the samples with reference to chromatogram of authentic standards (**Figure 2.5**).

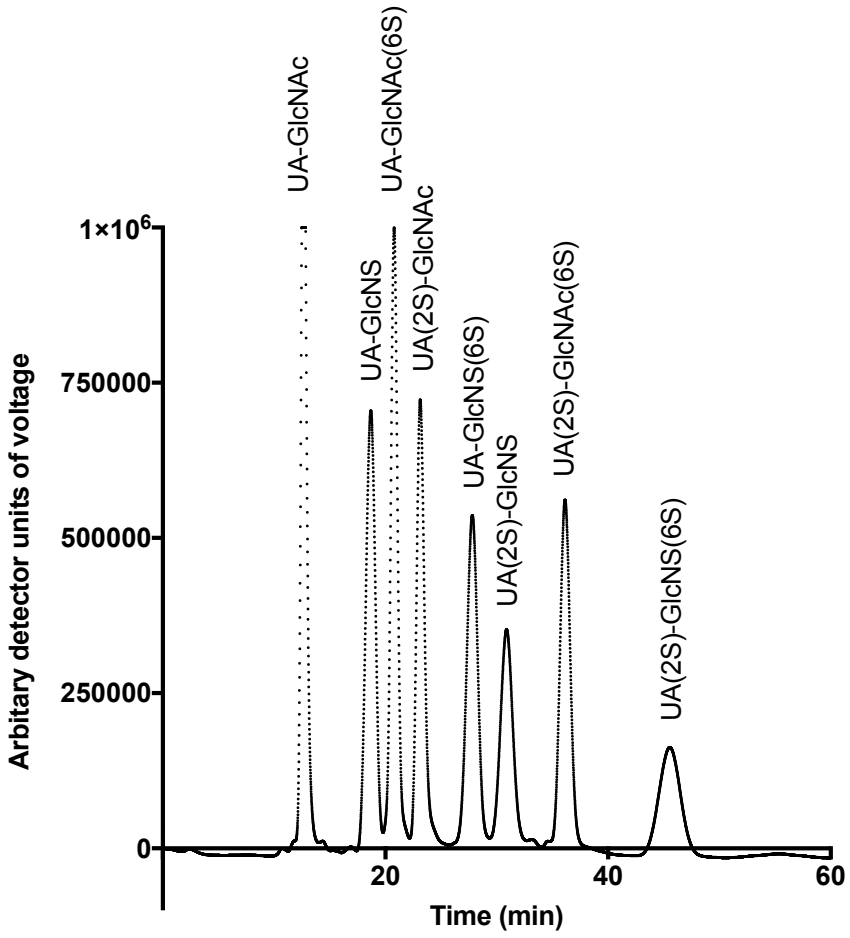

Figure 2.5: Fluorescence strong anion exchange (SAX) HPLC of the 8 most common Δ-disaccharides within HS and heparin after heparinase digestion and labeling with BODIPY hydrazide. Commercially available Δ-disaccharide HS standards (80ng) were labeled with the BODIPY fluorescent tag and run over TLC plates before undergoing ethanol precipitation. Labeled standards were then injected over a Propac PA1 column and eluted with a linear gradient of sodium chloride (0-1M over 30 min) and isocratic sodium hydroxide (150mM). Peaks were detected using an inline fluorimeter, λ_{ex} = 488nm and λ_{em} = 520nm. From left to right disaccharides present a progressively greater level of sulfation.

These standards were used to identify changes in disaccharide ratios in the AD and healthy age-matched control groups. Previous studies have found that the efficiency with which sugars are labeled via Schiff's base formation is influenced heavily by the structure of the reducing end unit (Drummond*, et al.* 2001). The different disaccharide standards are not all labeled with identical efficiency and as a result, appropriate correction factors were applied to standardise the disparity between the different disaccharide labeling affinities as previously published (Skidmore*, et al.* 2006) (**Table 2.6**).

Table 2.6: Correction factors for quantification of the Δ-disaccharides observed in human brain tissue with BODIPY labeling. Abbreviations: UA, uronic acid residue; Ac, acetyl; GlcNAc, N-acetyl glucosamine; GlcNS, glucosamine-N-sulfate; H, hydrogen; 2S, 2-O-sulfate; 6S, 6-O-sulfate; Sulf, Sulfate. *not detected. The Δ represents the presence of an unsaturated double bond (Skidmore*, et al.* 2006).

Standard	Relative efficiency (%)	Correction factor
Δ-UA-GlcNAc	n.d*	1.3
Δ-UA-GlcNAc(6S)	2.5	1.2
Δ-UA(2S)-GlcNAc	n.d*	1.7
Δ-UA(2S)-GlcNAc(6S)	0.9	1.4
Δ-UA-GlcNS	12.6	1.2
Δ-UA-GlcNS(6S)	28.4	1.0
Δ-UA(2S)-GlcNS	11.6	1.1
Δ-UA(2S)-GlcNS(6S)	43.9	1.1

For each of the samples analysed, a chromatogram was generated (**Figure 2.6**) and the area of each disaccharide peak was calculated as a percentage of the total sample to more easily compare changes in the ratio of disaccharides within HS. Extraction and purification of HS from human middle temporal gyrus (BA21) samples revealed the presence of 7 of the 8 most commonly occurring disaccharides, with the exception of the Δ-UA(2S)-GlcNAc(6S) disaccharide, which was found to be present in only very small quantities in all of the samples observed, 1.74% and 3.53% on average in AD and control groups respectively. Largely, the least sulfated disaccharides were found in greatest abundance vs. their more highly sulfated counterparts. For easier comparative analysis, the area of each peak was calculated as a percentage of the total sample to more efficiently compare changes in the ratio of disaccharides within HS (**Figure 2.7**). Overlaying standard disaccharide chromatograms over sample chromatograms made it possible to accurately identify those disaccharides present within tissue samples. This was done for each individual sample and the distribution of disaccharides noted. **Figure 2.6** represents one AD sample chromatogram overlaid with reference standards.

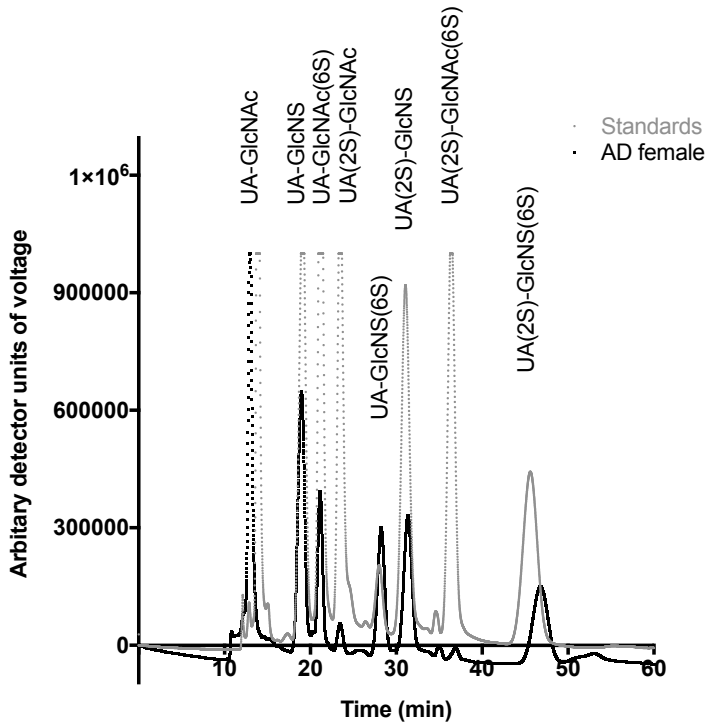

Figure 2.6: SAX HPLC of one AD female sample (black) overlaid with commercially available disaccharide standards after exhaustive heparinase digestion and labeling with BODIPY hydrazide. HS was isolated from one AD female middle temporal gyrus (BA21) brain sample (black line) and digested with a mixture of heparin lyases (heparinase I, II, and III). The resultant disaccharides alongside commercially available HS standards (grey line) were then labeled with BODIPY hydrazide. Samples were then subjected to strong anion exchange chromatography on a Propac PA-1 column and eluted with a linear gradient of sodium chloride (0-1M over 30 min) and isocratic sodium hydroxide (150mM). Peaks were detected using an inline fluorimeter, λex = 488nm and λem = 520nm.

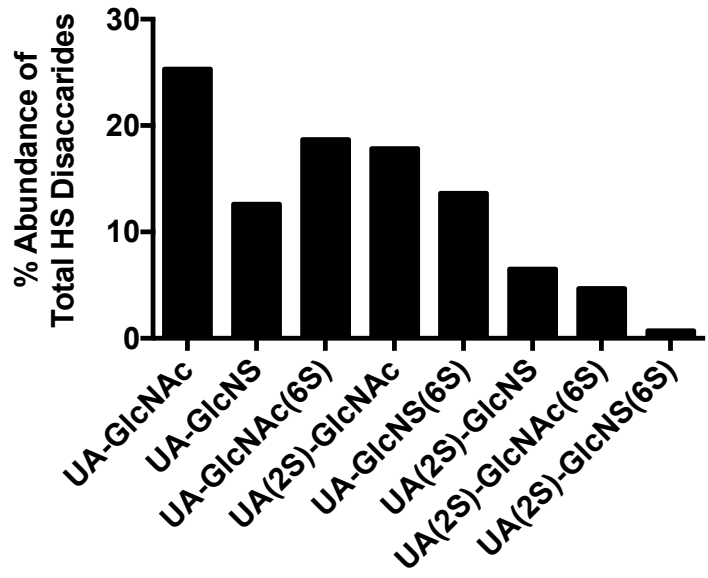

Figure 2.7: Chromatogram peaks from one AD female sample presented in Figure 2.6 depicted as peak areas as a % of total HS. Chromatogram peaks as observed in Figure 2.6 were best analysed by presentation of the area of each peak as a % peak area of the total HS sample. Bar graphs for each sample could then be more easily compared. This figure represents an example of just one human AD patient HS sample. Variability between constituent disaccharide ratios was reasonable within samples. Across all samples in both AD and control groups, the Δ-UA(2S)-GlcNAc(6S) disaccharide was present at very low quantities. In this sample, the least sulfated, Δ-UA-GlcNAc disaccharide was present in the highest abundance. This was not true of all AD samples.

2.7.1.2 Quantification of total heparan sulfate levels

2.7.1.2.1 There are significantly higher levels of total HS within healthy age-matched control samples vs. their AD counterparts

The HS extracted and purified from AD and age-matched control brain tissue for disaccharide composition analysis was quantified and normalised to µg/100mg of wet starting material to look for potential changes in overall levels of HS in AD and control brain samples. Quantification was achieved by measuring UV absorbance at 232nm, to detect the presence of the glycosidic double bond within disaccharides. Results showed that healthy control HS was present at significantly higher levels when compared to their AD counterparts. A mean (±S.E.M) of 122.3 (±12.40) µg/100mg of HS was extracted from Ctrl (n=15) brain tissue and 78.61 (±9.81) µg/100mg from AD (n=20) brain tissue. This increase in the quantity of HS extracted and purified from control tissue vs. AD samples was found to be significant (p=0.009, Student's t-test) (**Figure 2.8**). Quantification of this type did not discriminate between individual disaccharides present within each of the brain samples studied. This quantification allowed a basic evaluation of differences in total HS GAGs within brain samples of AD and age-matched control patients. Despite this, the trend towards slightly lower average sulfation of HS from AD patients (**Figure 2.9**) would in any case suggest slightly lower average disaccharide weight per disaccharide.

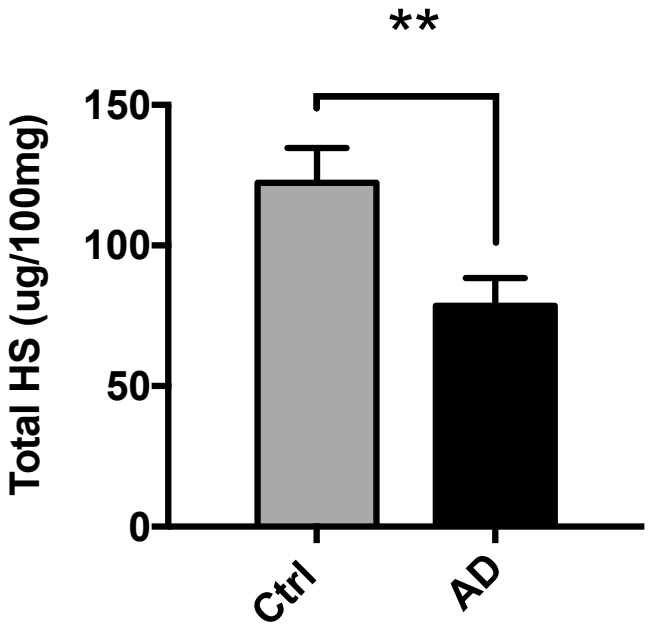

Figure 2.8. Total HS levels in AD and healthy age-matched control middle temporal gyrus (BA21) human brain samples are significantly different. HS was extracted from AD (black) and healthy age-matched control (grey) and digested with a mixture of heparin lyases (heparinase I, II and III mixture) followed by exhaustive clean up enzymatic digestion to remove other GAGs, DNA, RNA and protein. Resultant disaccharides were finally quantified and total HS levels were normalised to µg /100mg of wet tissue starting material. Error bars represent mean (±S.E.M). $p<0.05$ *, $p<0.01$ **, Student's t-test.

2.7.1.3 Compositional profiling of Alzheimer's disease and healthy age-matched control samples

2.7.1.3.1 The number of sulfs/disaccharide within HS from Alzheimer's disease and healthy age-matched control samples does not differ between study groups

Compositional data obtained from 20 AD HS brain samples and 15 control HS brain samples were combined and mean (±S.E.M) abundance of differing sulfated moieties was calculated. First, the degree of sulfation of HS extracted and purified from AD and healthy age-matched control samples. This was studied by calculating the number of sulfate groups present per individual disaccharide of the HS chain. No significant differences in the number of sulfs/disaccharide (±S.E.M) was observed between AD and age-matched control samples (0.87 (±0.07) and 0.91 (±0.10) respectively) (p=0.734 Student's t-test) suggesting that overall average sulfation levels might not be changing but rather altered levels of individual disaccharides (**Figure 2.9**).

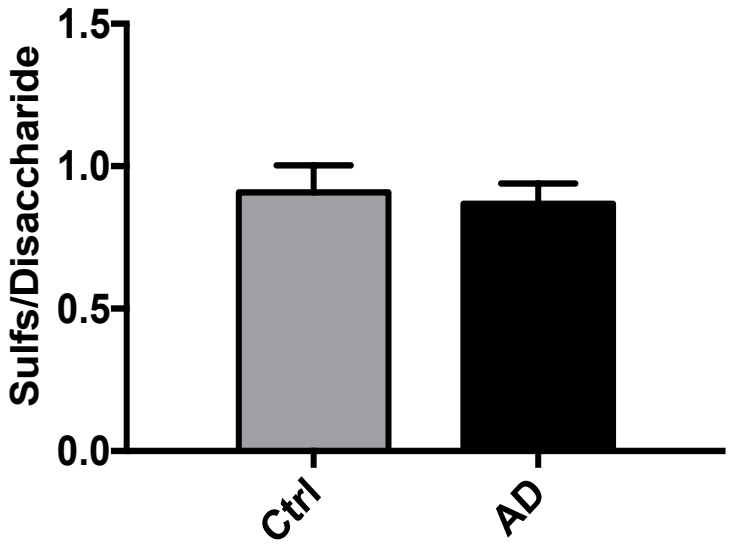

Figure 2.9. Total sulfs/disaccharide levels in AD and age-matched Ctrl BA21 brain samples are not altered between groups. HS was extracted from both AD (n=20) (black) and age-matched controls (n=15) (grey) and purified as previously described and the total number of sulfs/disaccharide calculated. No change in the number of sulfs/disaccharide was observed between Ctrl and AD patient samples of HS. Error bars represent mean (±S.E.M).

2.7.1.3.2 There are no significant differences in the relative abundance of N-, 6-O and 2-O sulfated moieties in HS from Alzheimer's disease and healthy age-matched control samples

Since no changes in the level of sulfs/disaccharide were recorded between AD and control samples, the % abundance of NS-, 6-OS and 2-OS groups within the HS samples from AD and healthy age-matched control patients were also calculated to explore possible changes in the location of

sulfate groups along the HS chain. This did not distinguish between composition of individual disaccharides but rather the overall content of sulfates of specific types in the HS chain.

No significant changes were observed in mean % abundance (±S.E.M) of N-, 6-O and 2-O sulfated disaccharides in HS from AD and healthy age-matched control samples (**Figure 2.10**). Distribution of disaccharides exhibiting sulfation at the N-, 6-O and 2-O position was largely equal across both groups. Mean % abundance (±S.E.M) of N-sulfated disaccharides for AD and control groups respectively were 28.81% (±3.42) and 35.35% (±3.02) (p=0.177, Student's t-test). Mean abundance of 6-O sulfated disaccharides in both AD and control groups were similar to that of N-sulfated units however were also found to not differ between AD and control groups (29.56 (±3.27) and 33.21 (±3.43) respectively) (p=0.453). Finally, abundance of 2-O sulfated disaccharides within both AD and control HS brain samples (19.70% (±2.53) and 22.29 (±3.77) respectively) (p=0.558) indicated no significant change in sulfation at this position in the AD phenotype. HS from AD patient samples did reveal a trend for decreased levels of N-, 6-O and 2-O sulfated disaccharides vs. controls, perhaps indicative of a less sulfated HS.

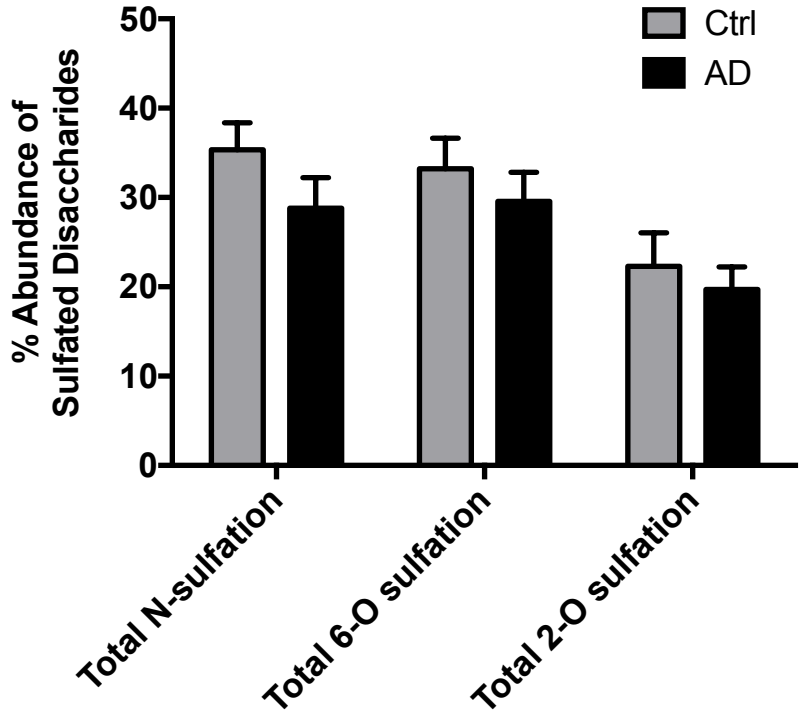

Figure 2.10: Average levels of specific sulfation types do not change with AD. HS isolated from AD (black) and age-matched control (grey) middle temporal gyrus (BA21) samples were digested with a mixture of heparin lyases (heparinase I, II and III mixture) and resultant disaccharides were labeled with BODIPY hydrazide and subjected to strong anion exchange chromatography on a Propac PA-1 column and eluted with a linear gradient of sodium chloride (0-1M over 30 min) and isocratic sodium hydroxide (150mM). Peaks were detected using an inline fluorimeter, λex = 488nm and λem = 520nm. Peak areas for each disaccharide were measured and disaccharide analysis is expressed as a % of N- 6-O and 2-O sulfated motifs within the HS analysed. Data shown are from AD (n=20) and control (n=15) patient samples and error bars represent mean (±SEM).

2.7.1.3.3 HS from Alzheimer's disease brain samples displays significantly altered levels of di-sulfated disaccharides vs. their healthy age-matched control counterparts

Compositional data obtained from 20 AD HS brain samples and 15 Ctrl HS brain samples were combined and also grouped based on sulfation levels (unsulfated, mono-, di- and tri-sulfated patterns) within HS samples of AD and age-matched control patients. Structural motifs were grouped in this manner to assess gross potential changes across samples. Unsulfated (36.40% (±5.08) and 38.26% (±5.79) in AD and age-matched control samples respectively) and mono-sulfated (46.02% (±3.73) and 36.24% (±3.62) respectively) disaccharides were found to represent the largest proportion of all disaccharides analysed. Mean abundance (±S.E.M) of the di- sulfated (14.71% (±1.74) and 21.9% (±3.21) for AD and control samples respectively) and tri- sulfated (2.87% (±0.77) and 3.61% (±1.14) for AD and control samples respectively) units was found to be considerably lower. No significant differences in the abundance of unsulfated disaccharides, between AD and healthy control samples were observed. However, AD HS samples displayed a strong trend towards greater levels of mono-sulfated disaccharides vs. their control counterparts, though this was observed to be just below statistical significance (Student's t-test p=0.074) (**Figure 2.11**).

In contrast, the difference in abundance of di-sulfated disaccharides between AD HS samples and healthy age-matched control samples was found to be statistically significant. AD samples were found to display significantly less of the di-sulfated disaccharides vs. controls (14.71% (±1.74) and 21.9% (±3.21) for AD and control samples respectively; p=0.045, Student's t-test). Increased levels of mono-sulfated disaccharides and decreased levels of di-sulfated disaccharides may be indicative of an overall lesser-sulfated HS displayed in AD patients vs. their healthy age-matched counterparts. No significant differences in mean abundance (±S.E.M) of tri-sulfated disaccharides were recorded (2.87% (±0.77) and 3.61% (±1.14) for AD and control samples respectively) (p=0.585) (**Figure 2.11**).

2.7.1.3.4 Alzheimer's disease patient HS samples display altered levels of some HS disaccharides when compared to their healthy age-matched control counterparts

Compositional analysis data from AD and age-matched control samples revealed significant differences in levels of some individual disaccharides in AD vs. age-matched control samples. The least sulfated disaccharide, Δ-UA-GlcNAc, was present in highest abundance in both groups with mean (±S.E.M) peak areas across the group of 34.64% (±5.04) and 38.26% (±5.79) for AD and age-matched control groups respectively (**Figure 2.12**). Conversely, the more highly sulfated disaccharides were present in much lower quantities. Most noticeably, the di-sulfated disaccharide Δ-UA(2S)-GlcNAc(6S) was observed in the lowest abundance of all the disaccharides in both AD and

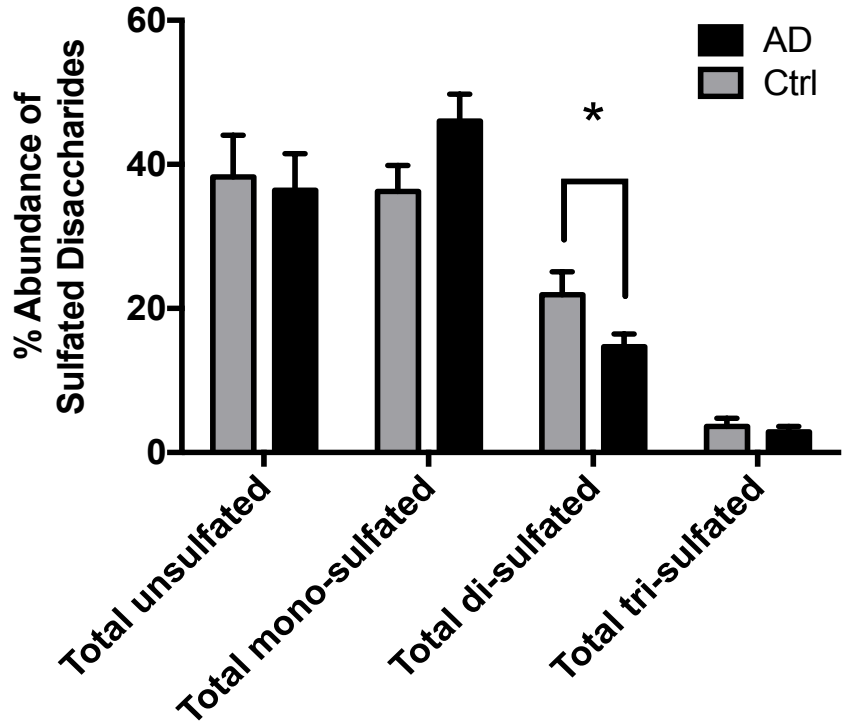

Figure 2.11: Composition of HS disaccharides displaying different numbers of sulfate groups change with AD. HS isolated from AD (black) and age-matched control (grey) middle temporal gyrus (BA21) samples were digested with a mixture of heparin lyases (heparinase I, II and III mixture) and resultant disaccharides were labeled with BODIPY fluorescent hydrazide and subjected to strong anion exchange chromatography on a Propac PA-1 column and eluted with a linear gradient of sodium chloride (0-1M over 30 min) and isocratic sodium hydroxide (150mM). Peaks were detected using an inline fluorimeter, λexc = 488nm and λemm = 520nm. Peak areas for each disaccharide were measured and disaccharide analysis is expressed as a % of mono- di and tri- sulfated motifs within the HS analysed. Data shown are from AD (n=20) and Ctrl (n=15). Error bars represent mean (±S.E.M). $p<0.05$ *, Student's t-test.

age-matched control samples with observed mean (±S.E.M) peak areas of 1.74% (±0.36) and 3.53% (±1.36) for the AD and age-matched control groups respectively – perhaps indicative of a structural characteristic of human brain HS. The analysis also revealed that AD and age-matched control samples display significantly altered HS compositional profiles, suggestive of HS structural changes in the presence of AD pathogenesis. AD samples (n=20) displayed significantly more of the mono-sulfated Δ-UAGlcNAc(6S) disaccharide vs. healthy age-matched control samples with recorded mean (±S.E.M) peak % abundances of 20.94% (±2.30) and 12.83% (±1.83) respectively (Student's t-test p=0.012). Conversely, HS from AD patients displayed significantly less of the Δ-UA-GlcNS(6S) disaccharide, a di-sulfated disaccharide common in HS chain structure. Mean (±S.E.M) % abundances of 7.18% (±0.86) and 13.25% (±1.75) in AD and age-matched control samples respectively (Student's t-test p=0.003) were recorded in this instance.

Of the other HS disaccharide standards analysed, less significant differences in profiles of AD and control patients samples were recorded. A trend for a decreased abundance of the di-sulfated Δ -UA(2S)-GlcNAc(6S) disaccharide in AD patients vs. healthy controls was observed with

mean (±S.E.M) % abundances of 1.74% (±0.36) and 3.53% (±1.36) observed in samples respectively (p=0.177) (**Figure 2.12**).

Due to technical issues over variability in the recovery of the unsulfated, N-acetylated Δ-UA-GlcNAc disaccharide (note the larger error bars for this disaccharide), data analysis of HS from the AD and control samples was also conducted with exclusion of the non-sulfated disaccharide (calculated based on relative abundance of the sulfated units only). This was done to remove potential bias in the calculated proportions of disaccharides of interest. Overall ratios were very similar to those observed above. The same significant alterations in compositional profiles across AD and control groups were observed. The Δ-UA-GlcNS(6S) disaccharide was consistently observed at significantly lower abundance in the AD groups vs. their healthy age-matched control counterparts (p=0.002 Student's t-test) whilst the UA-GlcNAc(6S) disaccharide was significantly more abundant in AD patient HS samples vs. healthy controls and reached a greater degree of statistical significance in the absence of the UA-GlcNAc disaccharide (p=0.003 Student's t-test) (**Figure 2.13**).

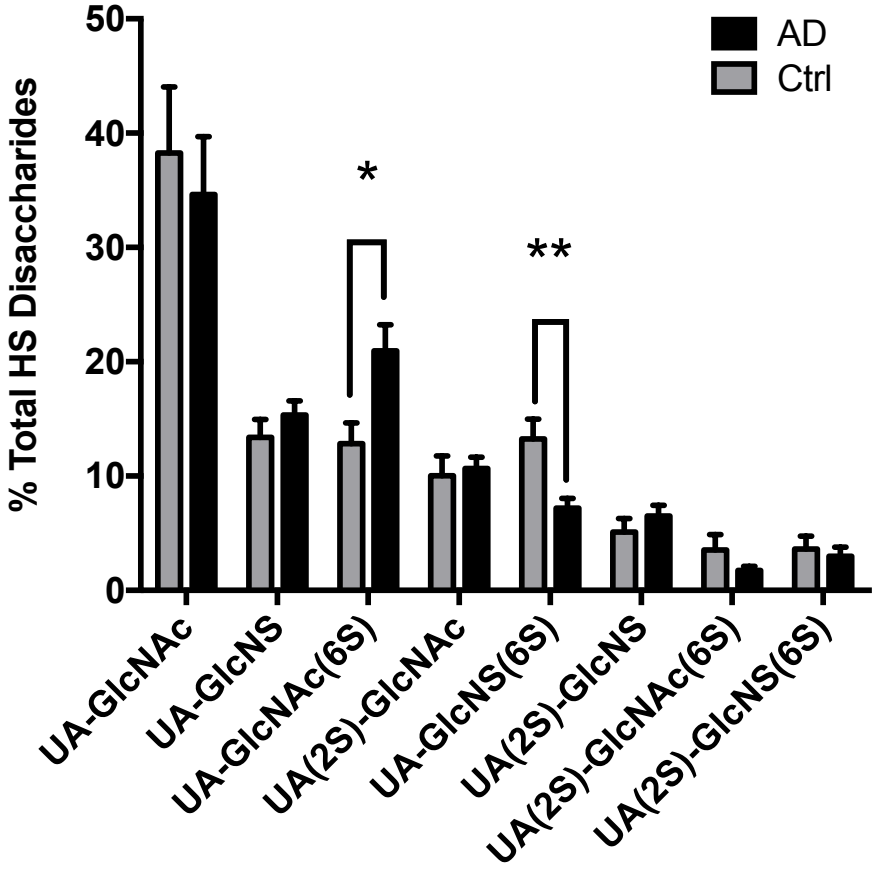

Figure 2.12: Brain HS composition changes with AD. HS isolated from AD (black) and age-matched control (grey) middle temporal gyrus (BA21) samples were digested with a mixture of heparin lyases (heparinase I, II and III mixture) and resultant disaccharides were labeled with BODIPY hydrazide and subjected to strong anion exchange chromatography on a Propac PA-1 column and eluted with a linear gradient of sodium chloride (0-1M over 30 min) and isocratic sodium hydroxide (150mM). Peaks were detected using an inline fluorimeter, λex = 488nm and λem = 520nm. Peak areas for each disaccharide were measured and disaccharide analysis is expressed as a % of total HS analysed. Data shown are from 35 patients; AD (n=20) and Ctrl (n=15) Error bars represent mean (±S.E.M). p<0.05 *, p<0.01 **, Student's t-test.

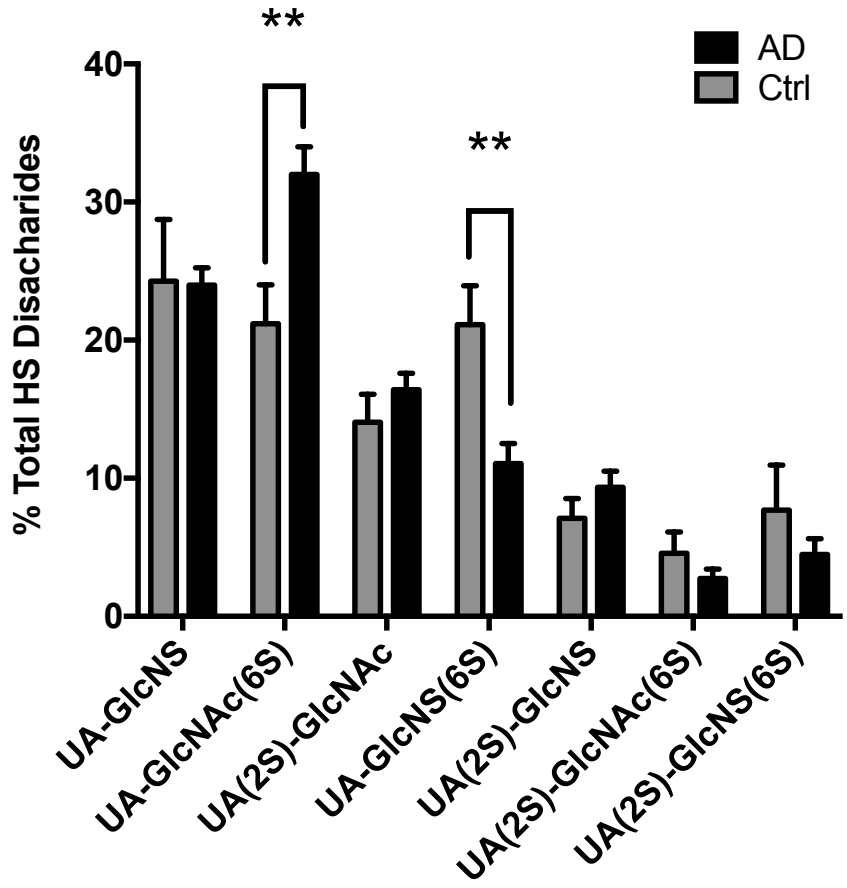

Figure 2.13: Brain HS composition of sulfated disaccharides changes with AD. HS isolated from AD (black) and age-matched control (grey) middle temporal gyrus (BA21) samples were digested with a mixture of heparin lyases (heparinase I, II and III mixture) and resultant disaccharides were labeled with BODIPY hydrazide and subjected to strong anion exchange chromatography on a Propac PA-1 column and eluted with a linear gradient of sodium chloride (0-1M over 30 min) and isocratic sodium hydroxide (150mM). Peaks were detected using an inline fluorimeter, λex = 488nm and λem = 520nm. Peak areas for each sulfated disaccharide were measured and disaccharide analysis is expressed as a % of total HS analysed. Peak areas for each disaccharide were measured and disaccharide analysis is expressed as a % of total HS analysed. Data shown are from 35 patients; AD (n=20) and Ctrl (n=15) Error bars represent mean (±S.E.M). $p<0.05$ *, $p<0.01$ **, Student's t-test.

2.7.1.3.5 There are no gender differences in the structure of HS in either AD or healthy age-matched control patients

Analysis as described previously but with respect to gender revealed no significant differences between male and female AD patients. Despite a slight trend for reduced N- 6-O and 2-O sulfation in males vs. their female counterparts, no significant gender factor was observed in these samples (**Figure 2.14**). Likewise distribution of unsulfated, mono-, di- and tri-sulfated motifs within HS samples from male and female AD patients were not significantly different. These results indicate that structural changes in HS as observed in AD patient brain samples were not driven by gender-specific factors (data not shown). Gender differences were also not apparent within the age-matched control set of samples analysed in this study (data not shown).

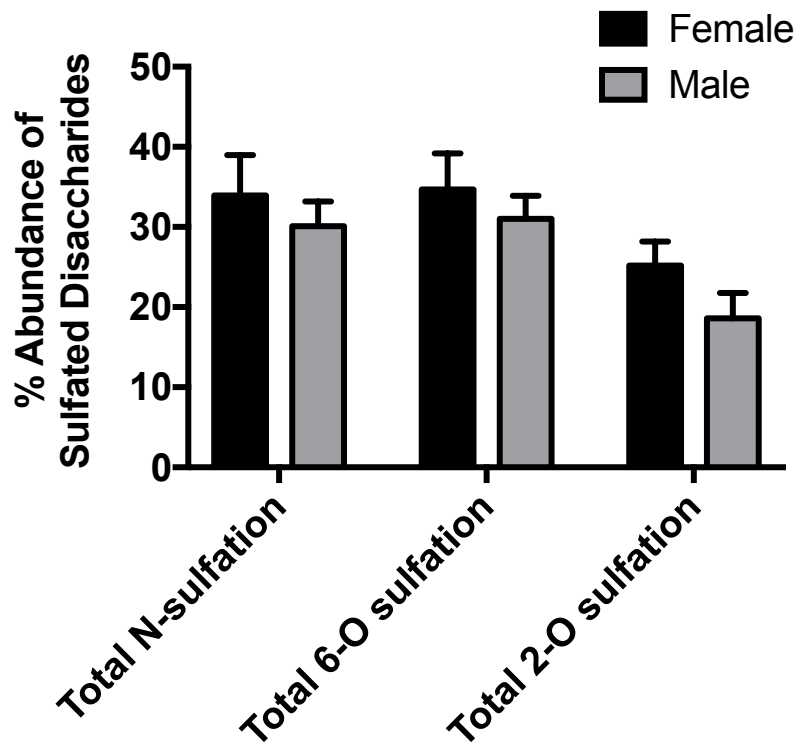

Figure 2.14: Composition of human AD brain HS disaccharides sulfated at different positions do not display gender differences. HS isolated from AD middle temporal gyrus (BA21) samples were digested with a mixture of heparin lyases (heparinase I, II and III mixture) and resultant disaccharides were labeled with BODIPY hydrazide and subjected to strong anion exchange chromatography on a Propac PA-1 column. Peaks were eluted with a linear gradient of sodium chloride (0-1M over 30 min) and isocratic sodium hydroxide (150mM). Peaks were detected using an inline fluorimeter, λex = 488nm and λem = 520nm. Peak areas for each disaccharide were measured and disaccharide analysis is expressed as a %NS-, %6-OS and %2-OS within the HS analysed. Data shown are from 10 female (n=10) and 10 male samples (n=10) Error bars represent mean (±S.E.M).

2.7.2 Mouse samples (old vs. young)

Compositional profiling of disaccharides within HS extracted from old (18 month) and young (3 month) mice was carried out in an identical manner to those methods employed for analysis of AD human patient samples. All disaccharide peak analysis was carried out as previously described in section 2.7.1.1. Overall levels of sulfation were analysed, including total HS quantification and individual disaccharide composition within HS samples.

2.7.2.1 Quantification of total HS levels in aged and young mouse brain

2.7.2.1.1 Aged mice display significantly increased levels of total HS (µg/100mg tissue) vs. their younger counterparts

The HS extracted and purified from aged and young brain tissue samples for compositional analysis was also quantified and normalized to µg/100mg of wet starting material to look for any potential changes in the overall levels of HS that may occur in the ageing phenotype. Quantification of total HS levels from mouse brain samples revealed significantly higher levels of HS in aged mice vs. their younger counterparts with mean (±S.E.M) total levels of 67.39 (±10.16) and 29.33 (±9.81) µg/100mg respectively (Student's t-test p=0.027) (**Figure 2.15**).

2.7.2.2 Compositional profiling of old and young mouse brain samples

2.7.2.2.1 There is no significant difference in the number of sulfs/disaccharide in HS extracted from the brains of old and young mice

Next the average degree of sulfation of disaccharides within the HS purified from aged and young mice brain samples were studied to explore potential global changes in overall sulfation with age. The average number of sulfate groups present per individual disaccharide was calculated for each sample. On this occasion, aged mice displayed a strong trend for an increase in the number of sulfs per disaccharide vs. their younger control counterparts with mean (±S.E.M) values of 0.58 (±0.14) and 0.23 (±0.08) respectively; however, this difference was not statistically significant (p=0.084). This trend would suggest that overall sulfation might be changing in addition to more subtle changes at the individual disaccharide level (**Figure 2.16**).

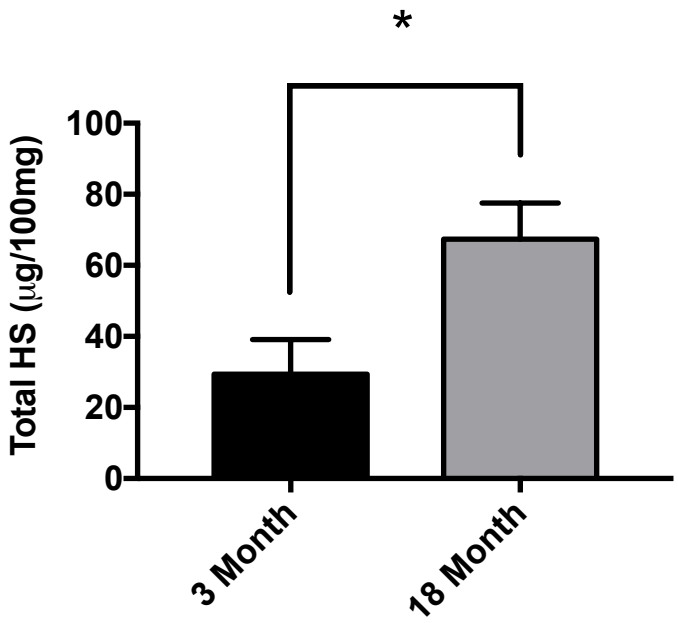

Figure 2.15: Aged (18 month) mouse brain samples display significantly greater levels of total HS vs. their younger (3 month) counterparts. HS was extracted from young (3 month) (black) and aged (18 month) (grey) and digested with a mixture of heparin lyases (heparinase I, II and III mixture) followed by exhaustive clean up by enzymatic digestion to remove other glycosaminoglycans, DNA, RNA and protein. Resultant disaccharides were finally quantified and total HS levels were normalized to µg /100mg of wet tissue starting material. Data is representative of 10 mouse brain HS samples, young (n=5) and aged (n=5). Error bars represent mean (±S.E.M). p<0.05 *, Student's t-test.

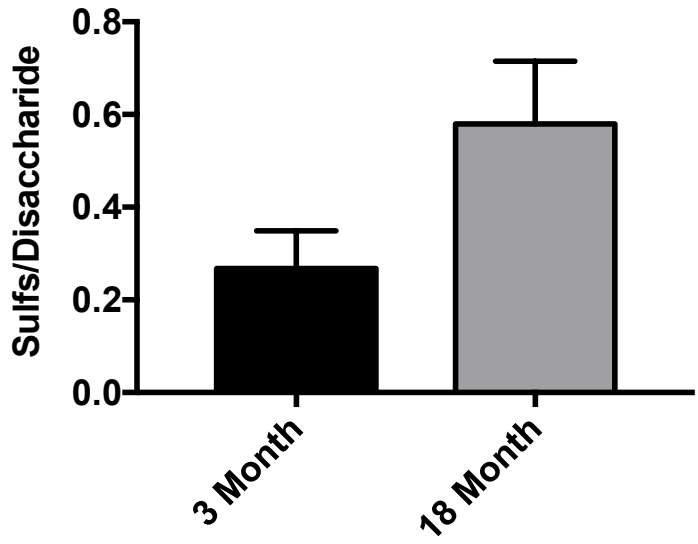

Figure 2.16. Total sulfs/disaccharide levels in aged (18 month) and young (3 month) mouse brain HS samples are not altered between groups. HS was extracted from both young (black) and aged (grey) mice and purified as previously described and the total number of sulfs/disaccharide calculated. No change in the number of sulfs/disaccharide was observed between aged and young samples of HS. Data is representative of 10 mouse brain HS samples, young (n=5) and aged (n=5). Error bars represent mean (±S.E.M).

2.7.2.2.2 Aged mice display significantly higher levels of 2-O sulfated disaccharides vs. their younger counterparts

Total % abundance of N-, 6-O and 2-O groups within HS samples from aged and young mice brain samples was also calculated to explore possible changes in the levels of specific sulfate groups in the HS chain. In this instance, aged mice were found to display significantly higher mean (± S.E.M) abundance of 2-O sulfated moieties vs. their younger counterparts with mean (±S.E.M) % abundance levels of 11.37% (±2.61) and 2.77% (±0.44) respectively (Student's t-test; p=0.012). Aged mice brain HS samples were also found to contain more of the N- sulfated disaccharides vs. their younger control counterparts with mean (±S.E.M) recorded % abundance levels of 27.05% (±6.57) and 13.62% (±4.22) respectively. Furthermore, aged mice also displayed increased abundance of levels of 6-O sulfation with recorded mean (±S.E.M) % levels of 19.54 (±5.27) and 10.41% (±3.89) respectively. However, these differences were not found to be statistically significant on this occasion (p=0.124 and p=0.200 respectively, Student's t-test) with significantly large error bars noted for these measurements (**Figure 2.17**).

2.7.2.2.3 There are no significant differences between the % abundance of mono-, di- or tri-sulfated disaccharides in HS extracted from old and young mouse brain samples

Compositional data obtained from 5 aged (18months) and 5 young (3 months) HS mouse brain samples were combined and the mean (±S.E.M) % abundance of differing sulfated moieties

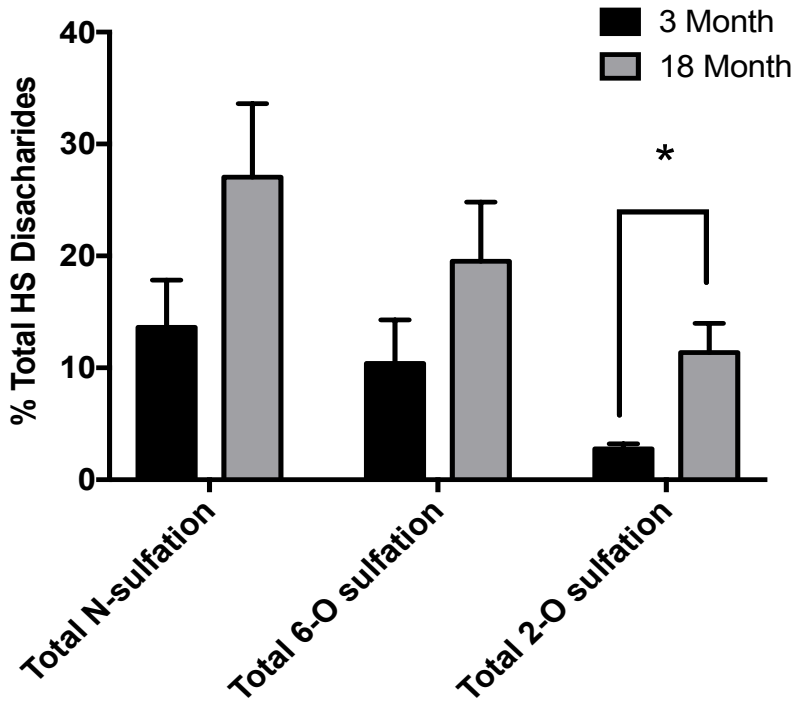

Figure 2.17: Composition of mouse brain HS disaccharides sulfated in different positions change with ageing. HS isolated from young (3 month) (black) and aged (18 month) (grey) total mouse brain samples were digested with a mixture of heparin lyases (heparinase I, II and III mixture) and resultant disaccharides were labeled with BODIPY hydrazide and subjected to strong anion exchange chromatography on a Propac PA-1 column and eluted with a linear gradient of sodium chloride (0-1M over 30 min) and isocratic sodium hydroxide (150mM). Peaks were detected using an inline fluorimeter, λex = 488nm and λem = 520nm. Peak areas for each disaccharide were measured and disaccharide analysis is expressed as a % of NS- 6-OS and 2-OS disaccharides within the HS analysed. Data shown are from aged (n=5) and young (n=5) in each group. Error bars represent mean (±S.E.M). $p<0.05$ *, Student's t-test.

was calculated. Samples were first analysed based on total % abundance of unsulfated, mono-, di- and tri- sulfated disaccharides within HS samples of young and old mice. Structural motifs were grouped in this manner to assess gross potential changes that may occur with age. Analysis revealed no significant changes in the patterning of sulfation between old and young mice groups. Overall % abundance of unsulfated and mono-sulfated disaccharides were found to represent the largest proportion of all disaccharides across both the aged and young mice groups with mean (±S.E.M) % abundance of unsulfated disaccharides recorded of 75.74% (±8.70) and 50.71% (±11.6) for young and aged groups respectively. Presence of tri-sulfated disaccharides within mouse HS brain samples, in both groups, was virtually absent. Indeed, overall compositional profiles were considerably different to that observed in human tissue. Aged mice did display a trend for increased levels of di-sulfated disaccharides vs. their younger control counterparts with respective mean (±S.E.M) % abundance levels of 7.87% (±3.14) and 1.14% (±0.35) that was close to reaching significance in this instance ($p=0.065$).

In addition, levels of the mono-sulfated disaccharides were also found to be higher in aged mice vs. younger counterparts with respective mean (±S.E.M) % abundance levels of 41.02%

(±10.12) and 22.42% (±9.17). Again, this did not reach significance in this instance (p=0.212). Conversely, unsulfated and tri-sulfated disaccharides were present at lower levels in younger mice vs. aged mice, though these changes only displayed a trend and did not reach significance in this instance (p=0.123 and 0.458 respectively) (**Figure 2.18**).

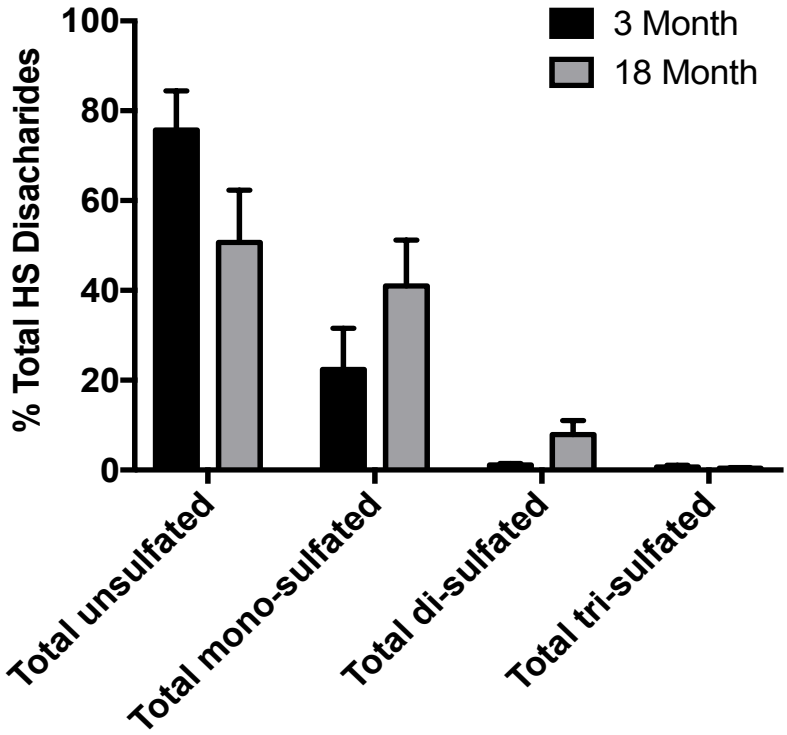

Figure 2.18: Composition of mouse HS disaccharides displaying different numbers of sulfate groups does not change with age. HS isolated from young (3 month) (black) and aged (18 month) (grey) total mouse brain samples were digested with a mixture of heparin lyases (heparinase I, II and III mixture) and resultant disaccharides were labeled with BODIPY hydrazide and subjected to strong anion exchange chromatography on a Propac PA-1 column and eluted with a linear gradient of sodium chloride (0-1M over 30 min) and isocratic sodium hydroxide (150mM). Peaks were detected using an inline fluorimeter, λex = 488nm and λem = 520nm.. Peak areas for each disaccharide were measured and disaccharide analysis is expressed as a % of mono- di and tri- sulfated motifs within the HS analysed. Error bars represent mean (±S.E.M) in aged (n=5) and young (n=5).

2.7.2.2.4 Aged mouse brain samples display significantly altered levels of specific HS disaccharides when compared to their younger counterparts

Analysis of HS disaccharide composition data from aged and young mouse brain samples revealed significant differences in the relative abundance of disaccharides. The least sulfated disaccharide Δ-UA-GlcNAc, was present in highest abundance in both groups with mean (±S.E.M) % abundances of 75.74% (±8.70) and 50.73% (±11.61) in young and aged groups respectively (**Figure 2.19**). Conversely, the more highly sulfated Δ-UA(2S)-GlcNS, Δ-UA(2S)-GlcNAc(6S) and Δ-UA(2S)-GlcNS(6S) disaccharides represented a much smaller proportion in both groups. Indeed, these three disaccharides were found to represent less than 1% total HS in both the aged and young control mice groups.

Compositional analysis also revealed that aged and young mouse brain HS samples display significantly altered profiles suggestive of HS structural changes with the ageing phenotype. Aged samples displayed significantly higher levels of the Δ-UA(2S)-GlcNAc disaccharide vs. their younger counterparts with mean (±S.E.M) recorded % abundances of 9.56% (±2.29) and 1.97% (±0.30) respectively (Student's t-test p=0.011). Likewise, aged mice also display significantly higher levels of the Δ-UA(2S)-GlcNS disaccharide with mean (±S.E.M) % abundance levels of 0.70% (±0.19) and 0.08% (±0.04) respectively (Student's t-test p=0.014). There was also a strong trend to suggest that aged mice display increased abundance of the Δ-UA-GlcNS(6S) disaccharide (6.45% (±2.58) and 1.04% (±0.36) for aged and young respectively), though this was just short of reaching statistical significance (Student's t-test p=0.071) (**Figure 2.19**). The Δ-UA-GlcNAc and Δ-UA(2S)-GlcNS(6S) disaccharides were found to be present in increased abundance in younger mice vs. their aged counterparts. This data suggests considerable alterations in specific sulfation of mouse brain HS with ageing.

2.8 Discussion

2.8.1 Human samples - Alzheimer's disease vs. healthy age-matched controls

2.8.1.1 Disaccharide peak analysis and total HS quantification

2.8.1.1.1 AD HS samples contain altered HS disaccharide sulfated moieties when compared to their age-matched counterparts

Analysis of the composition of HS from samples with respect to sulfation level within constituent disaccharides revealed significant changes in the patterning of sulfation between AD and control groups. Overall abundance across both study groups of the less modified, unsulfated and mono-sulfated disaccharides was found to be greater than the di- and tri-sulfated units as is typical for tissue HS. No significant differences in the abundance of unsulfated disaccharides between AD and healthy control samples were recorded. AD HS samples were found to display greater levels of mono-sulfated disaccharides vs. their control counterparts, though this trend was not found to be statistically significant. However, AD HS samples also displayed significantly less of the di-sulfated disaccharides vs. controls respectively. Increased levels of mono-sulfated disaccharides and decreased levels of di-sulfated disaccharides may be indicative of an overall lesser-sulfated HS displayed in AD patients vs. their healthy age-matched counterparts (**Figure 2.11**).

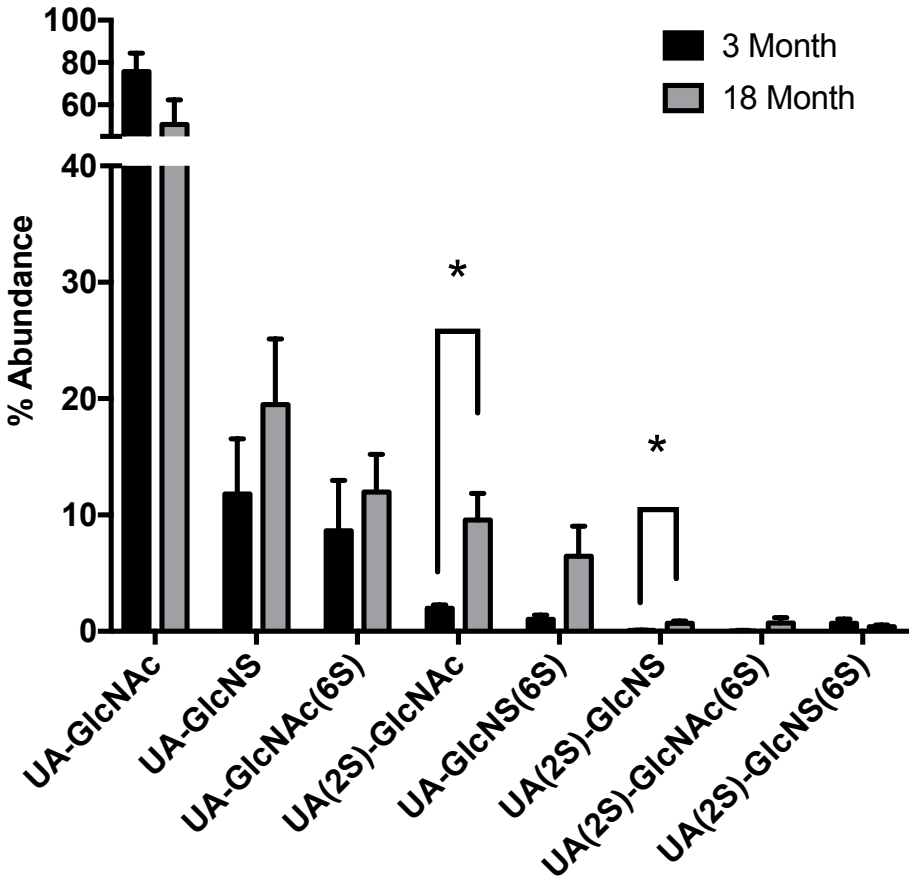

Figure 2.19: Mouse brain HS composition changes with ageing. HS isolated from young (3 month) (black) and aged (18 month) (grey) total mouse brain samples were digested with a mixture of heparin lyases (heparinase I, II and III mixture) and resultant disaccharides were labeled with BODIPY hydrazide and subjected to strong anion exchange chromatography on a Propac PA-1 and eluted with a linear gradient of sodium chloride (0-1M over 30 min) and isocratic sodium hydroxide (150mM). Peaks were detected using an inline fluorimeter, λexc = 488nm and λemm = 520nm. Peak areas for each disaccharide were measured and disaccharide analysis is expressed as a % of total HS analysed. Data shown are from 10 mouse brain samples; young (n=5) and aged (n=5) Error bars represent mean (±S.E.M). $p<0.05$ *, Student's t-test.

This is consistent with the hypothesis that a less sulfated HS is present in those suffering with AD could lead to less efficient inhibition of the BACE-1 enzyme, and ultimately the elevated production of the toxic Aβ peptide. As Patey and colleagues observed, efficacy of BACE-1 inhibition is largely determined by degree of sulfation (Patey*, et al.* 2006), and hence we might expect to observe differences in sulfation pattern between AD and control groups. Changes observed here in the number of sulfate groups present on specific disaccharides would suggest that sulfate moiety patterning could be key in determining BACE-1 inhibition efficacy, though this data alone does not allow a conclusion on whether the average number of sulfate groups is key or whether sulfate location plays a role in determining HS mediated BACE-1 inhibition.

Following recorded changes of reduced % abundance of di-sulfated disaccharides in AD HS brain samples, total % abundance of N- 6-OS and 2-OS groups within the HS samples from AD and healthy age-matched control patients was also calculated to explore possible changes in the location

of sulfate groups along the HS chain. Relative abundance of the 2-O sulfated moiety was lower than that of N- and 6-O sulfation in both the AD and healthy age-matched control samples, suggestive of differential functional roles of sulfation at each position of the disaccharide. The presence of just one 2-O sulfotransferase enzyme may go some way to explain this reduced abundance of 2-O sulfated disaccharides relative to those patterned with sulfate groups at the 6-O and 3-O positions (Esko and Selleck 2002).

Analysis of HS from AD patient samples did reveal a trend for decreased levels of N-, 6-O and 2-O sulfated disaccharides vs. their healthy age-matched control counterparts; however this did not reach statistical significance, perhaps due to patient-patient variability (**Figure 2.10**). Lindahl and colleagues have also previously reported a differential distribution of NS- groups within HS extracted from AD and control human cerebral cortex brain samples (Lindahl*, et al.* 1995), although they did not report any significant differences between overall HS composition from AD and control brain tissue. As such, the trends observed here, in the absence of statistically significant changes, may support a notion of high variability between samples that make it challenging to determine significant average changes across a population. That being said, this work by Lindahl and colleagues also sampled only relatively small sample groups. Moreover, the work by Lindahl and colleagues analysed the disaccharide composition of HS samples digested with nitrous acid. The digestion products of this method are somewhat more limited to that afforded by heparinase digestion (nitrous acid cleaves at the site of free amino groups only) as carried out in this project hence we might expect differences in the final analysis of HS structural changes with AD. 6-O sulfation is already known to be key for the efficacy of BACE-1 inhibition such that removal of 6-O sulfate groups greatly reduces potency of inhibition (Scholefield*, et al.* 2003). A trend for reduced abundance of 6-O sulfated disaccharides observed here in AD patient brain samples would thus be consistent with our hypothesis that HS from these patients in less able to inhibit the BACE-1 enzyme and ultimately result in elevated generation of the Aβ peptide. Reduction in 2-O sulfation however has not been shown to impact BACE-1 inhibition significantly relative to heparin, indicating changes in this region would not be particularly rate-limiting in the context of BACE-1 inhibition (Scholefield*, et al.* 2003).

Changes in sulfation patterning as observed here, may be accounted for by changes in expression of HS-related genes that modulate sulfation of HS chains. Indeed, HS in different tissues has been shown to present variable sulfation patterns suggesting regulation of HS biosynthetic enzymes varies between tissue type (Guimond*, et al.* 2009). With this in mind, variability between tissue types and indeed regional differences in the brain specifically may be something to investigate in the future. The hippocampus is the first area of the brain to be affected by Alzheimer's pathology and extraction and analysis of the HS from this region may reveal different changes in the structure of HS to those already studied. Anti-HS phage-display antibodies (Smits*, et al.* 2006, van Kuppevelt*,*

et al. 1998) could also be used to identify region variability in the degree and/or pattern of sulfation of the HS present in different brain regions.

No significant difference in the number of sulfs/disaccharide was observed between AD and age-matched control samples (**Figure 2.9**). The lack of difference between the two groups in this instance would suggest that sulfation patterning in HS is not inherently changing in terms of abundance (as indicated by sulfs/disaccharide) but rather that the configuration of sulfation is altered in the presence of AD. Position of sulfation of disaccharides exhibiting specific sulfated features may be the key driver in downstream BACE-1 inhibition efficacy. Promisingly, Toida and colleagues in 1997 confirmed that the average HS chain sulfation isolated from porcine brain samples is 1.01sulfate group per disaccharide (Toida*, et al.* 1997). The HS extracted and purified from AD and healthy age-matched control brain samples in this instance was found to contain disaccharides with 0.87 (±0.07) and 0.91 (±0.10) sulfs/disaccharide for AD and control groups respectively. This data is therefore consistent with previous findings and indicates that the extraction process used for this analysis has not resulted in loss of any sulfate groups.

2.8.1.1.2 AD HS samples present altered levels of specific HS disaccharides when compared to their age-matched control counterparts

Extraction and purification of HS from human cortex samples revealed the presence of 7 of the 8 most commonly occurring disaccharides in AD and age-matched control groups. Most noticeably, the di-sulfated disaccharide, Δ-UA(2S)-GlcNAc(6S) was observed in the lowest abundance of all the disaccharides in both AD and age-matched control samples. This finding is supported by that of Huynh and colleagues who did not observe this disaccharide in rat myocardial muscle samples, perhaps indicative of this HS disaccharide being very rare in occurrence (Huynh*, et al.* 2012). The Δ-UA-GlcNAc disaccharide was found in highest abundance in both treatment groups. This standard is the non-sulfated disaccharide constituent of the HS chain and hence we would expect it to be present within all of our samples in significant quantities as it is the common non-modified unit in all HS species. This finding is also consistent with the work of Huynh and colleagues who investigated changes in HS disaccharide composition with ageing. They also found that the Δ-UA-GlcNAc disaccharide unit was present in highest abundance within their HS samples analysed (Huynh*, et al.* 2012). Conversely, abundance of the most highly sulfated disaccharide, the Δ-UA(2S)-GlcNS(6S) unit, was considerably lower in both groups of samples observed. This disaccharide is sulfated at the 2-O, N- and 6-O position and hence has undergone the most extensive modification of the whole HS chain (excluding consideration of the rare 3-O sulfation modification).

Compositional profiling found significantly greater quantities of the UA-GlcNAc(6S) disaccharides in AD brain samples compared to their control counterparts. These mono-sulfated disaccharides have undergone only moderate modification and carry only one sulfate group. In contrast, data analysis revealed significantly decreased levels of the UA-GlcNS(6S) disaccharide in AD samples vs. controls. This disaccharide is sulfated in 2 locations and is therefore modified to a greater degree than the mono-sulfated units found to be in higher abundance in this group. In keeping with our hypothesis, lower levels of this disaccharide in AD patients would be indicative of HS composed of disaccharides containing fewer sulfated disaccharides (**Figure 2.12**).

It is clear that we can conclude that changes do occur in the overall composition of HS with the AD phenotype vs. healthy age-matched controls. Somewhat surprisingly, these structural changes are occurring at an individual disaccharide level rather than just a global one. In light of this, the argument for consideration of the overall configuration of sulfate patterning along the HS chain when elucidating ligand-binding functionality may be stronger than ever. Patient variability is naturally a likely contributor to variation and increasing the number of patient samples analysed in future studies may help smooth out the observed variability in HS composition and aid a more conclusive picture of the changes that are occurring. Furthermore, the variability observed here might be due to upstream changes that contribute to a change in the order in which these disaccharides appear rather than their relative amounts, something that SAX chromatography cannot distinguish. Similarly, whilst we can conclude that there are significant if subtle changes in the structure of HS with AD, overall population differences may be harder to observe. Matching altered expression levels of enzymes in specific samples to their individual disaccharide profile may therefore prove more beneficial in understanding how very subtle changes are occurring.

Finally, quantification of the total HS found within brain AD and age-matched control samples revealed significantly greater quantities of HS within control samples v. their AD counterparts. Interestingly, this finding is not in agreement with previous work that found that levels of HS were increased in ageing individuals (Huynh*, et al.* 2012). Despite ageing and dementia being different conditions, dementia is commonly associated with ageing and we would have thus perhaps expected to observe a similar trend in the amount of HS found within AD samples. Having said that, we cannot at this point rule out that altered expression of those genes responsible for synthesising HS are responsible for this change with the AD phenotype and that these expression patterns are distinct from these in general ageing. Finally, this finding that HS is present in lower abundance in AD patients compared to healthy age-matched controls is consistent with our hypothesis of reduced BACE-1 inhibition efficacy in AD patients. Less total HS will naturally be less able to block the activity of BACE-1 effectively. Indeed, reduced BACE-1 inhibition may not only be a result of altered HS structure but also simply reduced levels of total HS present.

No significant variation in disaccharide profiles between male and female AD patients were observed (**Figure 2.14**), and likewise for the age-matched control study group. Previously, research has found Alzheimer's pathology to be accelerated in females vs. their male counterparts and studies in transgenic murine models over expressing the *APP* and *PS1* genes have recorded a heavier amyloid burden and increased plaque number within the brain of female compared to male mice of the same age. Likewise, increased levels of the plaque precursor peptides, Aβ40 and Aβ42 were also observed at greater levels in female mice (Wang*, et al.* 2003). Furthermore, more complex mouse models expressing both *TAU* and *APP* genes have been shown to have greater spatial learning deficits in females over their male littermates (Ribe*, et al.* 2005). Likewise, differences in the severity of neuropathology in the limbic system and olfactory cortex has been reported in a second APP/tau model whereby females appear more severely affected than their male counterparts (Lewis*, et al.* 2001). In the human condition, females have also been shown to be more susceptible to Alzheimer's diseases than males. It is still unknown why females present an accelerated form of pathology; however it has been speculated that estrogenic action in younger females might have a protective role against mitochondrial toxicity caused by amyloid-beta that is lost after menopause. Indeed, it has been reported that mitochondria, when in the presence of amyloid beta increase the production of reactive oxygen species that lead to a series of reactions that ultimately induce neuronal apoptosis by increasing intracellular toxicity (Vina and Lloret 2010). Whether hormonal interactions with mitochondria are important with regards to Alzheimer's pathology still remains to be elucidated however it is something to consider when studying Alzheimer study groups composed of both female and male donors.

In light of this research, we might have expected to observe variation in the disaccharide composition of HS in female and male AD patients, such that, in line with our hypothesis, a greater proportion of Aβ peptides were generated as a result of altered BACE-1 activity and APP processing. As we did not observe gender differences in either of our study groups, we can infer that structural alterations to HS chains are not vulnerable to gender determined risk factors. Furthermore, larger samples sizes may reveal these seemingly subtle differences between males and females. The inherent variability between patient samples as discussed previously may make these differences less transparent than one might expect to observe in murine models. Likewise of course, the mechanisms for gender differences in observed Alzheimer's pathology may simply not be intrinsically linked with the BACE-1 processing pathway as focused on in this project.

2.8.2 Mouse samples (Aged vs. Young)

2.8.2.1 Disaccharide peak analysis and total HS quantification

2.8.2.1.1 Aged (18 month) HS samples display altered HS disaccharide sulfated moieties when compared to their young (3 months) counterparts

Analysis of the composition of HS from mouse brain samples with respect to the level of sulfation within constituent disaccharides revealed no significant changes in the patterning of sulfation between young and aged mice. As with the human samples, the observed large representation of the unsulfated, or mono-sulfated disaccharides vs. the more modified, di- and tri-sulfated disaccharides would be expected across both groups as a product of the typical modification process that occurs during the biosynthesis of HS.

Analysis was undertaken to explore whether the location of sulfate groups within HS was vulnerable to change with ageing. Aged mice were found to display significantly elevated levels of 2-O sulfated disaccharides vs. their younger control counterparts. Furthermore a trend for elevated levels of N- and 6-O sulfated disaccharides was also observed in aged mice vs. young controls, suggestive of an overall, globally more sulfated HS with the ageing phenotype (**Figure 2.17**).

The connection between ageing and AD is well established; however the effect normal physiology may have on BACE-1 inhibition is unknown and has not been fully elucidated. Likewise, the interaction between age as a risk factor and the onset and development of AD is likely a very complex one and thus we might not expect to observe identical changes in the structure of HS due simply to ageing and compared with AD. Here, our ageing variable has only been investigated in mice. Similarities between mice and humans, whilst they do exist, cannot be assumed in every instance. Hence we must not be surprised to see different changes in the structure of HS with ageing in our mouse system vs. those changes observed in human AD patients.

Interestingly, changes in levels of sulfation have been observed in HS with ageing in other tissues. Muscle from mice has been reported to display an age dependent increase in levels of 6-O sulfation (Ghadiali*, et al.* 2016), indicating that dynamic changes in the structure of HS do occur with ageing. Whilst this study did not report changes in the level of 2-O sulfation as observed here, we may attribute this difference to the fact that we have studied HS from a different tissue and HS is known to present organ/tissue specific differences (Kreuger and Kjellen 2012). In addition, the known efficacy of BACE-1 inhibition as afforded by sulfated HS might suggest aged mice might thus be better able to block the action of BACE-1 due to their enhanced sulfation. Conversely, the increased 2-O sulfation observed alongside an increase in 6-O sulfation with age may also enhance BACE-1 inhibition as 2-O sulfation has been shown to impact BACE-1 inhibition, though to a lesser degree than 6-O sulfation (Scholefield*, et al.* 2003, Schworer*, et al.* 2013). However; the HS-BACE-1 interaction is complex and currently poorly understood. The consequences of HS structural changes,

and the compensation mechanisms these may induce, will surely further complicate what determines efficacious BACE-1 inhibition/regulation.

Moreover, as discussed previously, regional variability in HS structure across the brain cannot be distinguished on this occasion due to total mouse brain HS sampling. Only those more gross changes in brain HS may be detected at this level of analysis. In the future, anatomical dissection of specific regions of the brain should be explored to allow more subtle region-specific differences in HS structure to be determined.

No significant changes in the number of sulfs/disaccharide were observed between young and aged mice (**Figure 2.16**). There was however a strong trend to indicate that aged mice do display elevated levels of sulfs/disaccharide vs. their younger control counterparts. This lack of change with ageing may also be due to combinations of disaccharides being observed resulting in masking of specific or average changes. This idea may be supported by the observation that there was no change in the abundance of sulfs/disaccharide in the human brain samples also. Configuration of sulfated disaccharides in combinations (sequences) may be more important in determining BACE-1 inhibition efficacy over changes in the level of specific disaccharides themselves.

2.8.2.1.2 Aged mouse samples display significantly altered levels of some HS disaccharides when compared to their younger control counterparts

Purification of HS from aged and young control mouse brain tissue revealed changes to the compositional profile of the 8 most common disaccharides one would expect to see within HS. Most noticeably, the three sulfated disaccharides, Δ-UA(2S)-GlcNS, Δ-UA(2S)-GlcNAc(6S) and Δ-UAGlcNAc(6S), were found to be under represented with respect to the other disaccharides. Whether this is a feature of mouse HS or whether more samples are needed to confirm this result remains to be determined. Should the very low abundance of di- and tri- sulfated disaccharides in mouse brain HS be a characteristic of this species and organ, one might question whether much more subtle changes in disaccharide composition are occurring to drive potential changes in ligand binding interactions.

Furthermore, aged mice were found to display significantly increased levels of the Δ-UA(2S)-GlcNAc disaccharide, a mono-sulfated unit with a sulfate group at the 2-O position, when compared to their younger control counterparts. Increased levels of this sulfated disaccharide may be indicative of changes that occur with ageing that may go some way to alter HS' ability to interact with its ligands. Similarly, aged mice also were found to display significantly higher levels of the Δ-UA(2S)-GlcNS disaccharide, a di-sulfated disaccharide, sulfated at both the 2-O and N- positions.

Observed abundance of this disaccharide, in combination of the Δ-UA(2S)-GlcNAc disaccharide not only indicates that 2-O sulfation is altered in the presence of ageing but also that HS from aged mice may be becoming overall, more sulfated. The consequence of enhanced 2-O sulfation may be unknown; however we might hypothesise that this could have implications on efficacy of BACE-1 inhibition (**Figure 2.19**).

These observed changes in the abundance of a disaccharide sulfated at the 2-O position also strengthen the finding that 2-O sulfation is significantly enhanced in aged mice compared to other sulfate positions. One might expect to observe global changes in patterning of sulfation, whereas differences at the individual disaccharide level as reported here also might be suggestive of very subtle changes that could have big implications on ligand binding affinity and HS functions. Interestingly, abundance of disaccharide units sulfated at the 2-O position was not found to change at all in the human patient brain samples discussed previously. In light of this, it might be postulated that ligand binding is mediated via different pathways/mechanisms in mice vs. humans. More work is needed to confirm/deny this hypothesis.

As was the case with the human tissue, the Δ-UA-GlcNAc disaccharide was found in highest abundance in both treatment groups. This standard is the least sulfated disaccharide constituent of the HS chain. This finding is consistent with the work of Huynh and colleagues who investigated changes in HS disaccharide composition with ageing in humans. They also found that the Δ-UA-GlcNAc disaccharide unit was present in highest abundance within their HS samples analysed (Huynh*, et al.* 2012).

From this data, we can conclude that changes occur in the overall composition of HS with ageing vs. young controls. The observation that these changes do not only occur globally but also at the individual disaccharide level, would suggest that the overall configuration of sulfate moieties within HS maybe key in determining ligand binding efficiency. Changes in the structure of HS are known to occur with ageing and understanding these changes may prove useful in further elucidating the role that ageing may play as a risk factor of AD. Linking ageing and AD together may shed light on processes that may be initiated very early before full onset of brain pathology and as such may offer new potential drug discovery targets.

As with human tissue, variability between individuals is naturally a likely contributor to the variation observed between samples observed here, and increasing sample size may not only smooth out the observed variability but also offer a more conclusive picture of structural changes of HS that may be occurring. Similarly, and as highlighted previously, changes with ageing may contribute to changes in the specific order of disaccharides rather than just their relative ratios; disaccharide compositional analysis by SAX chromatography cannot determine this. In future

studies, sequence determination may prove invaluable in identifying HS saccharide sequences that underpin its interaction with protein ligands, and the changes in those sequences that may occur with ageing.

Extraction, purification and quantification of the total HS found within aged and young control mouse brain samples revealed a significantly increased level of total HS within aged samples compare to their younger control counterparts (**Figure 2.15**). This observation may suggest that either some kind of upstream mechanism is altering the total level of HS being synthesised, or, that the turnover and degradation of HS is altered such that levels are accumulating within the tissue. The synthetic enzymes responsible for the polymerisation of the HS chain, or the core proteins onto which HS may be attached, may be a pathway by which total levels of HS are controlled. This finding sits well with previous studies that found that levels of HS were increased in ageing individuals (albeit humans) (Huynh*, et al.* 2012).

2.9 General conclusions

Overall, compositional analysis of the constituent disaccharides from AD and age-matched control samples revealed that changes in the structure of HS do occur in the presence of the AD phenotype. AD samples display significantly less di-sulfated disaccharides and more mono-sulfated disaccharides. This data is consistent with our hypothesis that HS from AD patient samples is less sulfated, and may be less able to inhibit the BACE-1 enzyme and thus implicated in the elevated generation of the Aβ peptide. These changes are not seemingly occurring at a global level but rather at a much more subtle, individual disaccharide level. Absolute abundance of sulfation along the full HS chain is not altered with AD but rather perhaps the specific configuration of aforementioned sulfate groups in combination along the HS chain.

Furthermore, we observed a significant decrease in the total amount of HS in AD vs. their age-matched control counterparts, indicative of an upstream change in the expression of those enzymes that generate the HS chain (**Figure 2.8**). Further analysis of potential changes in the expression of these enzymes may help to elucidate the upstream causes of these changes in the structure of HS and begin to further elucidate the consequences of these changes on BACE-1 inhibition and generation of the toxic Aβ peptide as observed in AD patients.

As with any study of this nature, larger sample group sizes in the future may more effectively reveal global changes between groups. Variability between individuals is naturally impossible to control for and ultimately will make detection of seemingly very subtle changes

difficult. Gender differences may too be too subtle to pick out easily and accurately with these sample group sizes.

With respect to the ageing variable of this study, as explored with mouse brain HS samples, ageing alone appears to induce an increase in overall sulfation to the HS chain, alongside an increase in total HS levels. This is contrary to that observed in the AD samples and might suggest that perhaps ageing and AD pathogenesis in the context of HS may be mediated by separate mutually exclusive mechanisms. Naturally of course we cannot make conclusions based on data from human and mice as the two species may behave differently; however this data certainly hints at separate means by which HS may be involved in normal ageing and in disease development. Further studies on changes in HS with ageing of healthy brains is warranted.

Ultimately, full sequencing of full-length HS chains would allow elucidation of the specific patterning of sulfate groups. However despite recent advances in NMR analysis and MS to study the fine structure of HS oligosaccharides, information of full-length intact HS chains is still elusive. Composition analysis of digested chains as employed in this project has proved to be successful, and are most suitable for determining changes in the relative ratios of individual disaccharides as well as global changes in sulfated moieties along the chain. They are thus highly useful in understanding structural changes to HS with AD or ageing (and indeed in other diseases). One must however be aware of the limitations of this technique and the need to understand more detailed structural information on HS in the future, perhaps initially by using MS profiling methods (Shao*, et al.* 2013, Shi and Zaia 2009).

Chapter 3: Analysis of the expression of HS-related genes in AD

3. Chapter 3

3.1 Introduction

3.1.1 Gene expression of HS biosynthetic genes

Exploring the gene expression of the biosynthetic enzymes that produce HS has proved particularly useful in further elucidating the upstream events that may account for the changes in its structure of this GAG as observed in conditions like ageing and dementia. There are several different strategies that may be employed to study the function of HS and in particular specific biosynthetic genes have been targeted and can be knocked down and the consequences observed. Understanding the wider function of these enzymes and their baseline expression patterns will aid the study of their expression in the context of disease and help us in understanding the implications of altered expression patterns. Having shown changes in the overall disaccharide compositional profiles of brain HS in AD patients, this project aimed to investigate the potential upstream causes for these structural differences. As described previously, there are three main phases of HS biosynthesis; chain initiation, chain polymerisation and chain modification. Different biosynthetic enzymes are involved in each of these phases and their knockdown will lead to very different alterations in the final structure of HS. Knock down for example of those enzymes responsible for the elongation of the HS chain will result in truncated and/or lower levels of HS chain, whilst alteration in the expression of modification enzymes may have a more subtle outcome on the level and positions of sulfation along the HS chain. All of these could have downstream implications for the HS chain's ligand binding capacity. In addition, interruption in the expression of those core proteins onto which HS chains may be attached, will have considerable effects on the location of HS on the cell surface and in the ECM, and may prove useful in understanding function and roles within the cell (Forsberg and Kjellen 2001). There is added complexity when we consider the various isoforms of each biosynthetic gene that exist. For example, there are 4 *NDST* genes that have been identified and knock down of individual members have different consequences. With that in mind, the detailed outcome of gene knockdown is somewhat complex.

3.1.1.1 Knockdown mouse models to study function of HS biosynthetic genes

3.1.1.1.1 Knockdown of Ext genes

Knockout mouse modes are perhaps the clearest way to study the roles of specific genes in physiological pathways and to that effect, there are several knock out models that currently exist

that have explored the consequences of knocking out some key HS biosynthetic enzymes. The EXT1 and EXT2 proteins both share glucuronyl- and N-acetylglucosaminyl-transferase activity (McCormick*, et al.* 2000). *In vivo*, these two proteins form a heterodimer to achieve efficient transferase activity to initiate the polymerisation of the HS chain. Patients who inherit a single mutation in one of the *EXT* genes develop several benign bone tumours. Furthermore, homozygous mutant mouse models for this gene do not reach full term due to death at gastrulation, presumably as a result of an absent organised mesoderm. Similarly, human homozygous mutants have not been identified for (assumed) similar reasons of early developmental abnormality (Lin*, et al.* 2000). These studies combined highlight the key role of EXTs in the synthesis of HS and importantly, the vast consequences it can have on the GAG's formation and function.

3.1.1.1.2 Knockdown of Ndst genes

Modification of the HS chain follows polymerisation. The NDSTs are the first group of enzymes to initiate this modification and are ultimately the gateway to addition of sulfate groups along the HS chain. With this in mind, the *Ndst* genes in mice are a strong candidate for knock down. Knockout of the *Ndst1* gene in previous studies revealed dramatic loss of N-sulfation of the HS chain in most parts of the body, as well as considerable reduction in the levels of O-sulfation and epimerisation of GlcA to IdoA residues in organs such as the liver, suggesting that alterations in the expression of this enzyme has significant implications in the degree of sulfation at not only the N-position. Lung abnormality proved to be the most significant phenotype in this model and ultimately resulted in neonatal lethality (Ringvall*, et al.* 2000).

In contrast, Humphries and colleagues observed that knockdown of the *Ndst2* gene in mice, was not as catastrophic as predicted but rather only manifested as a deficit in the connective tissue type mast cells – those cells that release heparin upon inflammatory stimulation (Humphries*, et al.* 1999). Indeed, the little heparin that was observed in those few remaining mast cells was found to be largely un-sulfated. Most notably, the lack of phenotype in the *Ndst2* $^{-/-}$ model in other parts of the body, would suggest that other NDST enzymes are able to compensate for the loss of NDST2 and may also hint at a flexible model of enzyme activity whereby other isoforms of this family are in fact more important functionally in the synthesis of HS (Grobe*, et al.* 2002). This idea is strengthened in view of *Ndst1* and *Ndst2* gene double knockouts. The absence of both of these enzymes causes embryonic lethality in mice (Holmborn et al; unpublished results) suggesting the role of NDST3 and NDST4 enzymes is not sufficient to compensate for the lack of NDST1 and 2.

Ndst3 gene knockout mice have been shown to display normal development and fertility and might suggest some kind of redundancy in its function relative to its other family members (Pallerla*, et al.* 2008). The action of the NDST enzymes is arguably the driver of all further HS

modification as it determines the location of the NA- and NS- domains (Lindahl*, et al.* 1998). Indeed the formation of these NS- domains suggest a substrate specificity for the NDST enzymes and may hint at a self-fulfilling influence over its own substrate.

3.1.1.1.3 Knockdown of the Glce and Hs2st1 genes

Final steps in the modification of the HS chain include the epimerisation of GlcA to IdoA residues by C5-epimerase, followed by sulfation at the 2-O position. Previous work has identified that the epimerisation reaction is totally reversible however the action of the HS2ST1 enzyme is intrinsically linked in light of the fact it is able to lock the GlcA or IdoA epimerized configuration. Lack of 2-O sulfation therefore will drive the epimerisation reaction back to the GlcA configuration (Feyerabend*, et al.* 2006). Furthermore, loss of the C5 epimerase (GLCE) in mast cells lead them to display distorted heparin O-sulfation patterning as a result of inhibited epimerisation of GlcA to IdoA residues.

Total knockout of the *Glce* gene in mice has been found to result in death immediately after birth and also display agenesis of the kidney alongside stunted body growth and defects within the lungs (Jia*, et al.* 2009, Li*, et al.* 2003). Mice lacking IdoA decorated HS chains (as a result of knockout of the *Glce* gene) also display attenuated morphogenesis of the thymus via binding with FGF2 and 10 (Reijmers*, et al.* 2010), suggesting this moiety within HS is responsible for some key physiological events.

HS2ST1 has also previously been shown to play a key role in binding ligand specificity, such as FGF-2 (Maccarana*, et al.* 1993). Mutations in the *Hs2st1* gene in mice result in death at birth on account of significant renal agenesis and abnormalities of the CNS (Bullock*, et al.* 1998). It should be noted that loss of HS2ST1 activity in this way is compensated for with a concomitant increase in the abundance of N- and 6-O sulfation. In addition, FGF-2 signaling is not attenuated in mice lacking *Hs2st1* gene expression, further strengthening an idea of a degree of flexibility for other sulfate positions to maintain a similar ligand-binding efficacy (Merry*, et al.* 2001) whether that be replaced with 6-O sulfation rather than 2-O (Kamimura*, et al.* 2006). As with *Ndst* gene expression, knockout of both the *Hs2st1* and *Hs6st* genes results in HS that cannot play a role in FGF-2 signaling, suggesting the level of sulfation along the HS chain is of greater importance to its positioning (Kreuger*, et al.* 2006). Loss of sulfation may result in a significantly altered final confirmation of the resultant HS chain and in doing so drastically alter the ligand binging motif necessary for efficient ligand binding (Powell*, et al.* 2004).

3.1.1.1.4 Knockdown of the Hs6st genes

The 3 members of the HS6ST enzyme family share 50% homology however show very similar patterns of substrate specificity suggesting they can "share" each other's roles of adding sulfate groups at the 6-O position along the HS chain. HS6ST1 has been previously shown to display minimal preference for binding sites lacking 2-O sulfation suggesting the presence of absence of this modification may regulate in some way the addition of sulfation at the 6-O position (Habuchi*, et al.* 2003).

Hs6st1 null mice do not survive past late embryonic stage (Pratt*, et al.* 2006). These mice are also smaller in size vs. their wild type counterparts and also display deficits in retinal axon guidance due to perturbed Slit-Robo signaling (Conway*, et al.* 2011, Pratt*, et al.* 2006). In contrast however, *Hs6st2* null mice survive normally, despite exacerbated thyroid hormone levels (Nagai*, et al.* 2013) and abnormal muscle formation (Bink*, et al.* 2003). Fatality with knockout of the *Hs6st1* gene but not the *Hs6st2* gene may suggest functional preference of these isoforms and hint at the "key players" in HS modification. Despite this, the specific role of the HS6ST isoforms is still yet to be fully determined. Furthermore, differential expression of the *Hs6st* genes during different stages of development and in specific tissue regions would suggest tight regulation of 6-O sulfation – a key feature of several ligand-binding partnerships (Habuchi*, et al.* 2000). Double knockout of both *Hs6st1* and the *Hs6st2* genes resulted in defected storage of mast cell proteases as well as hindered FGF signaling in embryonic fibroblasts (Sugaya*, et al.* 2008).

3.1.1.1.5 Knockdown of the Hs3st genes

The 3-O sulfotransferase enzymes are a group of enzymes that catalyse the addition of a sulfate group in the 3-O position. The presence of the 3-O sulfate group has been shown to be instrumental in the interaction between the unique pentasaccharide sequences of HS and antithrombin (Lindahl*, et al.* 1980). Mouse models lacking the *Hs3st1* gene however have been found to display normal development and anticoagulant activity (HajMohammadi*, et al.* 2003). As such, it cannot be ruled out that other members of the HS3ST family are able to compensate for the loss of the *Hs3st1* gene (HajMohammadi*, et al.* 2003). Indeed this may go some way to explain the large number of HS3ST enzyme isoforms that exist despite relatively low abundance of 3-O sulfated moieties within HS.

The seven isoforms of HS3ST are known to have selective substrate specificities and as a result, HS may be endowed with a number of distinct biological functions by different 3-O sulfate substitutions. HS3ST5 is also implicated in the key 3-O sulfation required for anticoagulant activity (Liu and Pedersen 2007). The activity of other isoforms including HS3ST2, 3,4,5 and 6 are believed to promote the infection of the herpes simplex virus type 1 (HSV-1) (Shukla*, et al.* 1999, Xu*, et al.*

2005). As such, knockdown of the genes that encode these enzymes may have considerable consequences on physiological function.

3.1.1.1.6 Knockdown of the Sulf genes

The action of the SULFs, HS sulfatase enzymes that remove sulfate groups at the 6-O position have been shown previously to fine tune final HS structure and in doing so play an important role in determining ligand binging configurations of HS. Both the SULF1 and SULF2 enzymes have shown preference for binding to tri-sulfated disaccharide units (Hossain*, et al.* 2010) however their activity might not be only restricted to these sites giving the SULFs a great deal of functionality in the modification of HS. Indeed, analysis of *in vivo* cerebellum HS from knockout mice has demonstrated that there are non-redundant actions of the 2 forms although they do display some overlap in substrate preferences (Kalus*, et al.* 2015).

Previous work on *Sulf* gene knockout mouse models found the mice deficient in the SULF1 enzyme (*Sulf1* $^{-/-}$) are seemingly unaffected (Lamanna*, et al.* 2006) whilst knockout of the *Sulf2* gene results in a smaller body size and mass and would suggest stunted growth (Lamanna*, et al.* 2006, Lum*, et al.* 2007). Furthermore, mice lacking both the *Sulf1* and *Sulf2* gene display considerable malformations of both the skeleton and renal function and as a result, die before birth (Holst*, et al.* 2007). 6-O sulfation is known to be a key modulator of several ligand-binding interactions and as such knockout of the *Sulf* genes may go some way to interfere with this functionality. The SULF enzymes have long been shown to be important in maintenance of cartilage (Otsuki*, et al.* 2010), dentinogensis via Wnt signaling (Hayano*, et al.* 2012), muscle regeneration (Langsdorf*, et al.* 2007), brain development (Kalus*, et al.* 2009) and neurite outgrowth (Ai*, et al.* 2007). Furthermore, the SULFs have also been shown to promote the migration of corneal epithelial cells during wound repair (Maltseva*, et al.* 2013). Key roles such as this during morphogenesis implicate the SULF enzymes heavily in modulating HS function.

Knockdown of genes in this manner offers a great deal of insight into the pathways by which important physiological mechanisms may be regulated. Seemingly very subtle changes in HS structure could have very significant down stream functional consequences.

3.1.1.2 Complexities of HS chain synthesis and modification

The roles these enzymes play is seemingly not independent of one another. Studies suggest that action of the NDST enzymes is a determinant for the actions of other modification enzymes downstream. C5 epimerase has been shown to occur after N-sulfation (Esko and Selleck 2002) and 2-

O sulfated moieties are more abundant within the NS- domains of HS, indicative of a functional tie between the NDSTs and HS2ST1 (Rong*, et al.* 2001). Conversely, knockdown of *Hs2st1* and *Glce* genes in mouse models display increased N- and 6-O sulfation further interlinking the role of HS biosynthetic enzymes and presenting a rather more complex mechanism to elucidate.

It is also important to note that there is evidence that suggests that the baseline expression of HS biosynthetic genes, particularly between members of the individual gene families is particularly varied. Differential baseline expression of these key enzymes suggests some kind of regulation; however exactly how this occurs is still largely unknown. It is already well established that HS from different tissues differs in composition significantly (Lindahl*, et al.* 1995). Furthermore, immunohistochemistry has demonstrated that antibodies for different HS epitopes reveal markedly different staining patterns when applied to different tissue sections, even sections of the same tissue, perhaps as a result of altered cell types (Kapp*, et al.* 1995). Changes of this kind are indicative of altered enzyme expression and previous work has proved that heparin-producing mast cells express the NDST2 enzyme in preference to other members of the NDST family (consistent with the *Ndst2* gene mouse knockout phenotype described above), despite a trend for the opposite in other tissue types (Hansebo*, et al.* 1998). The amounts and proportions of different HS biosynthetic enzyme isoforms are seemingly therefore largely regulated to some extent and may be controlled by gene expression predominantly but also post translational degradation. Indeed further elucidation of the ways in which this may occur and the ways in which these enzymes interact with each other in the context of their cellular localisation is also of key importance (Lindahl*, et al.* 1998). Patterns of action of these enzymes and substrate interaction is largely dependent on previous reactions and modification steps and these factors may all play a role in determining baseline expression of these genes (Lindahl*, et al.* 1998). Furthermore, observed changes in baseline expression of these genes encoding HS biosynthetic enzymes may hint at explanations for differential vulnerability to AD pathogenesis as exhibited by different regions of the brain. Spatial accumulation of AD pathology in distinct regions of the brain may result in part from variable expression of HS biosynthetic genes and may offer insights into disease spread. Altered baseline expression of these enzymes may make identifying changes with AD in the context of this project, trickier to identify as a result.

Taken together, the work with knock out models of HS biosynthetic genes, and studies to investigate substrate specificities highlight the importance of these enzymes and their role in the synthesis and modification of the HS chain. Importantly, whilst knockdown of these genes of interest is expected to produce a somewhat exaggerated phenotype, in doing so, this highlights the significance that altered expression of these genes may play. Changes in expression of these genes may go some way to explain changes in the structure of HS and potential compensatory mechanisms employed by cells to re-equilibrate to the norm. Furthermore, understanding these potential changes in the context of disease, such as AD in this instance, will prove invaluable in understanding

what it causing the downstream changes in the structure of HS and ultimately, its efficacy as a ligand binding GAG.

3.1.2 Methods available to explore gene expression

There are a number of methods available for the analysis of global gene expression in a particular sample of interest. As with all techniques, there are merits and disadvantages of each method and each one may prove the "best' depending on the samples to be analysed, the number of genes and the resources available. Investigating the levels of relative mRNA expression may be achieved via northern blots, Real Time-Polymerase Chain Reaction (RT-PCR), macroarrays, microarrays, differential display RT-PCR, Serial Analysis of Gene Expression (SAGE), comparative Expressed Sequence Tag (EST) analysis, and Massively Parallel Signature Sequence tag (MPSS) analysis (Fryer*, et al.* 2002).

In general, those methods that work via sequence analysis to identify the transcript of the gene of interest, like SAGE, EST analysis and MPSS analysis often prove expensive and require specialised equipment that may not be available. Other methods, such as RT-PCR often prove the most popular and allow analysis of more than one gene at a time at a relative low cost. The most traditional method of gene expression analysis is the Northern blot (Sabelli and Shewry 1995). The northern blot technique can be used to analyse the expression of one gene at a time. It uses gel electrophoresis to separate samples of RNA based on their size, which can then be detected with various hybridised probes. This technique is largely criticised for being only a single gene analysis method and blot-to-blot variation may introduce error in large-scale gene level comparisons. By the same token, scaling this method up for large numbers of genes makes this technique costly and time-consuming.

Development in the 1980s went on to create the use of microarrays via dot-blots initially that aided analysis of multiple RNA samples that could be detected and quantified with radioactivity (Fryer*, et al.* 2002). This technique was and still is largely a popular method as it can be carried out easily and the arrays can be manufactured by individual research groups to suit their specific needs very easily. Despite this there are issues with comparisons between multiple dot-blot arrays and they are reportedly tricky to use for analysis of very low-abundance transcripts (Fryer*, et al.* 2002).

Following this, in the 1990s, the process of RT-PCR was developed and has become arguably the most prominent gene analysis technique (Cale*, et al.* 1998, Freeman*, et al.* 1999). This technique allows the researcher to use a 96-well plate format to design an experiment in which to analyse the relative expression of several genes at one time, and allows detection with even only a

very small amount of the target template. More recent development of this method has allowed relatively affordable techniques for the real-time quantification of genes of interest within multiple samples in a timely and non-labour intensive manner. Naturally, each reaction volume (well) is restricted to a single gene so generating data for hundreds of thousands of genes would prove very expensive (Freeman*, et al.* 1999). As such, RT-PCR is largely regarded as a reliable validation method for confirming the expression levels of target genes of interest. More sophisticated PCR techniques have been developed to assess expression differences by using primers to amplify arbitrary subsets of genes that be quantified and then sequenced to identify specific genes (Shimkets*, et al.* 1999). This method is beneficial in that it requires no earlier knowledge of specific genes or their sequence; however this is largely a much more technical procedure and requires expertise so as to avoid the wrong identification of target sequences (Adams*, et al.* 1993).

Other newer methodologies have since been able to generate high throughput expression data, based on large libraries of cDNA that may represent all of the expressed mRNA within a tissue or cell type. From this a database can be generated that quantifies all of the genes that are expressed within that sample and are referred to as expressed sequence tags (ESTs) (Fryer*, et al.* 2002). SAGE is a similar method that creates a library of short DNA fragments derived from single mRNA molecule in a sample of interest. These shorter fragments, or SAGE tags, can then be linked together linearly to form larger fragments for sequencing, as like EST analysis. Whilst both of these methods are highly specific and accurate in the identification of gene transcript levels, they both require expertise and are fairly technically challenging and can be both highly costly and time-consuming (Fryer*, et al.* 2002). MPSS is similar in that it is able to deduce the identity of thousands of transcripts at any one time and is most often employed in conjunction with a pre-existing EST database or existing mapped genome (Brenner*, et al.* 2000, Tyagi 2000).

For larger projects to explore global gene expression changes, microarrays or “gene chips” have become the most popular choice for research scientists. Microarrays have become a great deal more cost effective in recent years and have proved relatively simple and reproducible to carry out and can be used to investigate the expression levels of thousands of genes at any one time (Hsiao*, et al.* 2000, Kurella*, et al.* 2001). Greater fluorescence intensity will be recorded with those probes that bind more abundantly to a specific spot on the microarray and hence indicate a greater abundance of a specific gene. Whilst microarrays are now widely available from a number of different manufacturers and can be engineered in house by researchers, they still remain relatively expensive. Similarly, disadvantages with this method include varying degrees of unspecific binding that must be corrected for.

Meta-analysis of large expression profiling data is also a useful tool in this field of research as it allows investigation of large numbers of genes in the context of different phenotype

perturbations. Software is now readily available with large datasets to make these comparisons, making these resources a useful tool for target finding strategies.

For the purposes of this project, it was most appropriate to use a combination of RT-PCR and meta-analysis of microarray expression data, to investigate the expression of HS biosynthetic enzymes in the brains of AD and age-matched control patients. This method allowed high sensitivity detection of the gene transcripts of interest, from relatively very small quantities of wet starting material. Indeed, this method is relatively cheap and does not require hugely challenging technical informatics processing. As a target finding endeavor, RT-PCR was by far the most appropriate and practical method to employ.

3.1.3 Changes in HS biosynthetic enzyme expression observed in disease

The extensive variability in structure afforded by HS alongside its ubiquity all over the body, makes it a prominent member of several key signaling pathways and cellular functionalities, that if disturbed could prove detrimental in the context of several diseases. In particular, the EXT1 and EXT2 enzymes are central in initiating the polymerisation of the HS chain. Should the expression of these genes be altered in any way, the resulting HS chains will absent or truncated and consequently prove unable to function effectively (Sugahara and Kitagawa 2000). Likewise, the variety of biosynthetic enzymes involved in the synthesis and modification of the HS chain make it vulnerable to potentially significant alteration should these enzymatic pathways be disrupted. Altering the structure of HS, as described previously will have dramatic effects on the ligand binding affinities the HS chain can participate in. As such, HS is implicated in a number of diseases including bone disorders (Shimo*, et al.* 2004) and tumor growth; EXT1 has been shown to present tumor suppressing activity (Ropero*, et al.* 2004). Analysis of the causes of these disorders and the role of HS and its biosynthetic enzymes may play offer an obvious drug discovery target for modification and treatment of these diseases (Nadanaka and Kitagawa 2008).

More recently, the *HS6ST1* gene has been identified as a new genomic locus associated with albuminuria in diabetes. Genome Wide Association Studies (GWAS) revealed single nucleotide polymorphisms (SNPs) at this gene locus that was associated with those with but not without diabetes. Not only could variants of the *HS6ST1* gene thus provide potential as a novel biomarker for susceptibility to albuminuria in diabetes but offers insight into ways in which HS biosynthetic gene expression may have significant implications for normal physiology and the development of disease (Teumer*, et al.* 2016).

In addition, as described previously, HS is implicated in the pathogenesis of AD in a number of ways. Its role in BACE-1 inhibition (Scholefield*, et al.* 2003), alongside its ability to sequester Aβ peptides and induce fibrilisation into fibrils and eventually mature plaques (McLaurin*, et al.* 1999), make it a key target for further investigation and drug discovery. Importantly, the structure of HS is key in these interactions and as such, understanding the upstream causes of these structural changes will prove invaluable in further elucidating the *in vivo* role of HS. The relative expression of the various HS biosynthetic enzymes is an obvious upstream cause of the structural changes observed in HS. The structural differences as observed in the previous chapter would indicate that those biosynthetic enzymes responsible for sulfation modification events are expressed differently in those patients suffering from AD vs. their age-matched counterparts and may offer a mechanism by which HS is altered between these two study groups.

3.2 Aims of this chapter

1. Determine whether there is altered expression of HS-related genes in middle temporal gyrus tissue from AD patients vs. age-matched controls.
2. Determine whether there is any correlation between expressions of HS metabolic enzymes and prevalence of specific HS disaccharides.

3.3 Methods

3.3.1 Quantitative real time polymerase chain reaction

Due to limited supplies of each of the AD and age-matched control samples, optimisation of qRT-PCR protocol was carried out with RNA from HEK293T cells (ATCC). Optimisation of primer concentrations, protocol measures and analyses were practiced with this cell line before carried out on the tissue samples to assess potential changes in the expression of key genes. HEK293T cells were grown in DMEM media (Gibco, UK) supplemented with foetal bovine serum (FBS), 1mM L-glutamine (Gibco, UK) and 1% of penicillin/streptomycin (Gibco, UK). Cells were grown to ~90% confluence and harvested ready for RNA extraction. Following optimisation, RNA extraction and qRT-PCR was carried out on human AD and age-matched control sample brain tissue.

3.3.1.1 Manual real time polymerase chain reaction

3.3.1.1.1 RNA extraction

To minimise the risk of RNase contamination, vessels and pipette tips used in the reaction were autoclaved and RNase Zap (Thermo Fisher Scientific, UK) was used to clean experimental workspace. For the brain samples to be analysed, an RNeasy® (Qiagen Cat no: 74134) RNA extraction kit was used according to manufacturer's instructions. Briefly, 20mg of brain tissue from each patient was homogenised in 350µl of lysis buffer RLT Plus. Homogenisation was achieved with a hand-held automatic homogeniser (VWR, UK) in a sterile RNase-free ependorf tube. The lysate was then centrifuged for 3min at 13,000 x g before removing the supernatant and transferring to a gDNA Eliminator spin column and collection tube. The spin column was centrifuged for a further 30s at 8,000 x g and the flow through kept for the next step. 350µl of 70% ethanol was then added to the flow-through and mixed well by pipetting. Samples were next transferred to an RNeasy spin column and centrifuged for 15s at 8,000 x g and the flow-through discarded. 700µl of buffer RW1 was added and centrifuged for 15s at 8,000 x g and the flow-through discarded again. This was followed by 500µl of buffer RPE and a further spin for 15s at 8,000 x g. A second 500µl aliquot of buffer RPE ensured complete washing of the column before adding 30µl of RNase-free water to the spin column membrane. Samples were spun for a further min at 8,000 x g to elute the purified RNA. Extracted RNA was immediately used to synthesise cDNA in preparation for qRT-PCR steps. A NanoDrop™ 2000 spectrophotometer (Thermo Fisher Scientific, UK) was used to assess the concentration and purity of the RNA extracted from samples. A A260/A230 ratio of ≥1.8 and a A260/A280 ratio between 1.8 and 2.1 was used as a threshold for RNA to be taken forward for use in qRT-PCR reactions.

3.3.1.1.2 cDNA synthesis

cDNA synthesis was carried out using Reverse Transcriptase Transcriptor™ (Roche, UK Cat no: 03531317001) according to manufacturer's instructions. This step allowed synthesis of first strand cDNA for qRT-PCR steps to follow. Into a 0.2ml microfuge PCR tube, according to manufacturer's protocol, 11µl of the newly synthesised template RNA was added, followed by 6µl of random $p(dN)^{6}$ * 50 A_{260} units (Roche, UK Cat no: 11034731001) to a final concentration of 0.08 A260 units (3.2µg). This mixture was then incubated at 65°C for 10min before being immediately placed on ice. This incubation step ensured the denaturation of RNA secondary structures.

Following this, 4µl of Transcriptor RT reaction buffer 5x (Roche, UK) was added to the microfuge tube, followed by 0.5µl (20U) of Protector RNase inhibitor (Roche, UK). Next, 2µl of 10mM dNTP-Mix was added followed by 0.5µl (10U) of the Transcriptor Reverse Transcriptase™ (Roche, UK). The microfuge tube was mixed and centrifuged briefly before being put in a Thermo Scientific Hybrid PX2 thermal cycler (Thermo Fisher Scientific, UK) and a two-step incubation carried out to allow efficient annealing. Samples were first incubated for 10min at 25°C followed by 30min at 55°C.

The reverse transcriptase was then inactivated by heating to 85°C for 5min. The tube was immediately placed on ice and stored at -25°C ready for the qRT-PCR reaction.

3.3.1.1.3 Design of PCR primers and probes

Primers were purchased, pre-validated from GeneCopoeia in Maryland, USA. All in one mixes were purchased containing a mixture of the upstream and downstream detection primers for qRT-PCR. All primers were dissolved in TE (10mM Tris-Cl, 1mM EDTA) and used at a final concentration of 0.2 µM per well. Full sequences were undisclosed however primer identification and IDs are included in **Table 3.1**.

Table 3.1: Primers used for qRT-PCR study of gene expression of HS-related metabolic enzymes and core proteins. Primers were purchased pre-validated from GeneCopoeia in Maryland USA. * The *GAPDH* reference gene was selected as a control. Specific sequences are undisclosed however Primer ID's are listed above.

Gene name	Primer ID	Final conc. per well
HS6ST1 - Heparan sulfate 6-O sulfotransferase 1	HQP022653	0.2µM
HS6ST2 – Heparan sulfate 6-O sulfotransferase 2	HQP021871	0.2 µM
HS6ST3 – Heparan sulfate 6-O sulfotransferase 3	HQP007336	0.2 µM
HS2ST1 – Heparan sulfate 2-O sulfotransferase 1	HQP064242	0.2 µM
HS3ST1 – Heparan sulfate 3-O sulfotransferase 1	HQP023407	0.2 µM
HS3ST2 – Heparan sulfate 3-O sulfotransferase 2	HQP023406	0.2 µM
HS3ST4 – Heparan sulfate 3-O sulfotransferase 4	HQP023403	0.2 µM
HS3ST5 - Heparan sulfate 3-O sulfotransferase 5	HQP005363	0.2µM
NDST1 – N-deacetylase/N-sulfotransferase 1	HQP071495	0.2µM
NDST2 – N-deacetylase/N-sulfotransferase 2	HQP021133	0.2µM
NDST3 – N-deacetylase/N-sulfotransferase 3	HQP022574	0.2µM
NDST4 – N-deacetylase/N-sulfotransferase 4	HQP017045	0.2µM
SULF1 – Sulfatase 1	HQP058565	0.2µM
SULF2 – Sulfatase 2	HQP064803	0.2µM
GLCE – C5 epimerase	HQP006988	0.2µM
AGRN – Agrin	HQP067787	0.2µM
*GAPDH** - Glyceraldehyde-3-Phosphate Dehydrogenase	HQP064347	0.2µM

3.3.1.1.4 Protocol design

qRT-PCR reactions were carried out in a final volume of 20µl per well, according to the manufacturer's specifications, using 20ng (in 5µl) of the cDNA template, with 2µl of primer (0.2µM final concentration), 10µl of LightCycler® 480 SYBR Green I Master mix (Roche, UK Cat no: 04707516001) and 3µl of PCR-grade water (Roche, UK). Reaction volumes were assembled into white, 96 well plates (Roche, UK) with triplicate wells for each primer and each sample. The plates were sealed with optical film and centrifuged at 2,000 x g for 5min before being placed in a LightCycler 480® system (Roche, UK). The following cycling conditions were maintained as described in **Table 3.2a and b**. qRT-PCR was performed using the LightCycler® 480 Roche machine (Roche, UK).

3.3.1.1.5 Statistical analysis

Expression levels were normalised to Glyceraldehyde 3-Phosphate Dehydrogenase (*GAPDH*) levels and the delta-delta Ct method was used to calculate the relative change in expression of the HS-related genes of interest from AD and age-matched control brain samples, assuming primer efficiency. In this instance, the relative change in gene expression compared to normal conditions was calculated as:

Table 3.2a: List of programs used for qRT-PCR on the LightCycler 480 machine. Each sample underwent 45 amplification cycles.

Program name	Cycles	Analysis mode
Pre-incubation	1	None
Amplification	45	Quantification
Melting Curve	1	Melting Curve
Cooling	1	None

Table 3.2b: Breakdown of incubation steps used for qRT-PCR.

Step	Target °C	Acquisition	Hold hh:mm:ss	Ramp °C
Pre-Incubation	95	None	00:05:00	4.4
Amplification	95	None	00:00:10	4.4
	60	None	00:00:10	2.2
	72	Single	00:00:10	4.4
Melting Curve	95	None	00:00:10	4.4
	70	None	00:01:00	2.2
	95	Continuous	-	
Cooling	40	None	00:00:30	1.5

Fold change = $2^{-\Delta\Delta Ct}$ = [(Ct gene of interest – Ct internal control) sample A – (Ct gene of interest – Ct internal control) sample B)]

- Internal control = *GAPDH* (reference housekeeping genes)
- Sample A = Alzheimer's patients (diseased state)
- Sample B = Age-matched controls ("normal" state)

All analyses were expressed as the fold change of expression of the gene of interest relative to the internal control in the diseased samples as compared with the age-matched controls. Using the Ct method of analysis allowed fold changes of expression to be calculated for each gene of interest with respect to the disease state (AD samples).

All PCR reactions were carried out in triplicate. Experimental triplicates were combined and the mean calculated and data for individual sample groups were also averaged (4 AD patients and 8 age-matched control patients). Values of $2^{-\Delta\Delta Ct}$ were logged to generate positive and negative values indicative of up and down regulated expression of target genes.

3.3.1.2 TaqMan® low density array microfluidic cards

***All TaqMan® array analysis was carried out at the Kennedy Institute of Rheumatology at the University of Oxford in the Troeberg Lab, with the help of Dr. Anastasios Chanalaris and Dr. Linda Troeberg. ***

The TaqMan® array cards are 384-well microfluidic cards that allow 384 simultaneous real time PCR reactions in a high throughput manner that utilise a small volume design to minimise sample and reagent consumption and to avoid labour intensive steps. These array cards were custom designed to probe for selected HS biosynthetic target genes. A total of 8 samples could be run per card allowing the analysis of 48 genes (36 of which were HS-related gene specific) including endogenous housekeeping controls. This technique was done to both validate the findings of the manual qRT-PCR and to also screen a larger number of gene targets with much smaller quantities of cDNA, something of a premium in the small sample sizes obtained from the Oxford Brain Bank.

3.3.1.2.1 RNA extraction

RNA from AD and age-matched control brain samples was extracted in the same manner (at the University of Liverpool before transport to Oxford) as described previously in section 3.3.1.1.1.

3.3.1.2.2 cDNA synthesis

For the conversion of RNA to cDNA for TaqMan® array expression profiling, a High Capacity cDNA Reverse Transcription Kit (cat no: 4368814) (Thermo Fisher, UK) was used, according to the manufacturer's instructions to convert extracted RNA to cDNA. Briefly, using the kit component reagents, a 2x reverse transcription master mix was prepared (10µl per reaction volume) with 2µl of 10x RT buffer, 0.8µl of 25 x dNTP mix (100mM), 2.0µl of 10x RT random primers, 1.0µl of MultiScribe™ Reverse Transcriptase, 1.0µl of RNase Inhibitor and 3.2µl of nuclease free H_2O.

Following preparation of the master mix, 10µl was transferred to thin walled PCR tubes and 10µl of sample RNA (prepared to 500ng and the total volume made up with nuclease free H_2O) added before mixing gently and centrifuging briefly. Samples were then placed in a thermo cycler and heated to 25°C for 10min, 37°C for 120min and finally 85°C for 5min before cooling at 4°C. Once complete, the newly synthesised cDNA was stored at -20°C until ready for use in the TaqMan® array.

3.3.1.2.3 PCR primers and probes

The TaqMan® array card was custom made by Applied Biosystems for the Troeberg lab in Oxford and contained 48 genes of interest including 36 of the HS metabolic genes and the core proteins onto which they are able to bind. Details of these gene probes and their IDs are outlined in **Table 3.3.**

3.3.1.2.4 TaqMan® Array-card protocol

The TaqMan® Array Micro Fluidic Card (Applied Biosystems, USA) was prepared and run according to manufacturer's instructions. Briefly, following RNA extraction and cDNA synthesis, in a 1.5ml ependorf tube, per sample, 100µl of total reaction mixture was made, containing 50µl of cDNA template (200ng starting RNA) in nuclease free water and 50µl of 2X Universal PCR mix (Applied Biosystems, USA). Each sample was then vortexed and briefly centrifuged before loading onto the card. Following loading, the card was centrifuged twice (1 minute at 12,000 rpm and repeated, Sorvall centrifuge with custom buckets) before being sealed with the microfluidic card sealer. Each TaqMan® card was run on the ViiA7 thermocycler (Applied Biosystems, USA). The conditions for the reaction was as follows; held for 2 min at 50°C, denatured at 10min at 94.5°C, followed by 40 cycles of denaturing at 97°C for 30 sec and finally annealing/extending for 1 min at 60°C.

Table 3.3: Details of gene probes printed on custom TaqMan® array card.

Gene name on TaqMan® array card	Gene ID	Gene Function
18S	Hs99999901_s1	Housekeeping/Reference gene*
AGRN	Hs00394748_m1	HS core protein
EXT1	Hs00609162_m1	HS biosynthetic enzyme
EXT2	Hs00181158_m1	HS biosynthetic enzyme
EXTL1	Hs00184929_m1	HS biosynthetic enzyme
EXTL2	Hs01018237_m1	HS biosynthetic enzyme
EXTL3	Hs00918601_m1	HS biosynthetic enzyme
GLCE	Hs00392011_m1	HS biosynthetic enzyme
GPC1	Hs00892476_m1	HS core protein
GPC2	Hs00415099_m1	HS core protein
GPC3	Hs01018936_m1	HS core protein
GPC4	Hs00155059_m1	HS core protein
GPC5	Hs00270114_m1	HS core protein
GPC6	Hs00170677_m1	HS core protein
HPSE2	Hs00222435_m1	HS biosynthetic enzyme
HPSE	Hs00935036_m1	HS biosynthetic enzyme
HS2ST1	Hs00202138_m1	HS biosynthetic enzyme
HS3ST1	Hs00245421_s1	HS biosynthetic enzyme
HS3ST2	Hs00428644_m1	HS biosynthetic enzyme
HS3ST3A1	Hs00925624_s1	HS biosynthetic enzyme
HS3ST3B1	Hs00797512_s1	HS biosynthetic enzyme
HS3ST4	Hs00901124_s1	HS biosynthetic enzyme
HS3ST5	Hs00999394_m1	HS biosynthetic enzyme
HS3ST6	Hs03007244_m1	HS biosynthetic enzyme
HS6ST1	Hs00757137_m1	HS biosynthetic enzyme
HS6ST2	Hs02925656_m1	HS biosynthetic enzyme
HS6ST3	Hs00542178_m1	HS biosynthetic enzyme
HSPG2	Hs00194179_m1	HS core protein
NDST1	Hs00925442_m1	HS biosynthetic enzyme
NDST2	Hs00234335_m1	HS biosynthetic enzyme
NDST3	Hs01128584_m1	HS biosynthetic enzyme
NDST4	Hs00224024_m1	HS biosynthetic enzyme
RPLP0	Hs99999902_m1	Housekeeping/Reference gene*
SDC1	Hs00896423_m1	HS core protein
SDC2	Hs00299807_m1	HS core protein
SDC3	Hs01568665_m1	HS core protein
SULF1	Hs00290918_m1	HS remodelling enzyme
SULF2	Hs01016476_m1	HS remodelling enzyme

3.3.1.2.5 Statistical analysis

Expression levels were normalised to the housekeeping 60S ribosomal protein P0 (*RPLP0*) and ribosomal RNA (*18S*) levels and the delta delta Ct method was used to calculate the relative change in expression of the HS biosynthetic genes of interest from AD and age-matched control brain samples, assuming primer efficiency. In this instance, the relative change in gene expression of HS biosynthetic enzymes compared to normal conditions was calculated as:

Fold change = $2^{-\Delta\Delta Ct}$ = [(Ct gene of interest – Ct internal control) sample A – (Ct gene of interest – Ct internal control) sample B)]

- Internal control = *RPLP0* and *18S* (reference housekeeping genes)
- Sample A = Alzheimer's patients (diseased state)
- Sample B = Age-matched controls ("normal" state)

All analyses were expressed as the fold change of expression of the gene of interest relative to the internal control in the diseased samples as compared with the age-matched controls.

The Ct method of analysis allowed fold changes of expression to be calculated for each target gene with respect to the diseased state. All reactions were carried out in triplicate. The mean of experimental triplicates was calculated and data for individual samples were also averaged (11 AD patients and 11 healthy controls in each group). Values of $2^{-\Delta\Delta Ct}$ were logged to generate positive and negative values indicative of up and down regulated expression of target genes.

3.4 Results

3.4.1 Quantitative real time PCR of HS-related genes

3.4.1.1 Manual real time polymerase chain reaction

Analysis of the expression of HS-related genes by manual qRT-PCR was carried out on AD (n=4) and healthy age-matched controls (n=8). Expression of HS-related genes were calculated with manual qRT-PCR and normalised with respect to *GAPDH* gene levels and the delta delta Ct method use to calculate the relative change in expression of these genes, assuming pre-optimised primer efficiency (data not shown). Mean (±S.E.M) fold changes of the expression of HS-related genes as recorded in AD and healthy age-matched control patients are displayed in **Table 3.4**. No statistically

Table 3.4: Data collected from manual qRT-PCR studies. HS biosynthetic and core protein genes were profiled in AD (n=4) and healthy age-matched control patients (n=8) brain samples using qRT-PCR. RNA was purified from samples and converted to cDNA followed by qRT-PCR. All changes presented are relative to healthy controls and normalised to the *GAPDH* housekeeping gene. The delta delta CT method was used for analysis and are the $\log_2$ fold changes presented below.

Gene Name	Gene ID (GeneCopoeia ref)	Mean log (fold change) in AD ±S.E.M (n=4)	Mean log (fold change) in Ctrl ±S.E.M (n=8)	Up/Down reg. in AD vs. Ctrl	T-test p-value p<0.05*
NDST1	HQP071495	1.304 ± 1.62	1.25e-010 ± 0.45	UP	0.3265
NDST2	HQP021133	0.4501 ± 1.88	1.25e-010 ± 0.76	UP	0.7927
NDST3	HQP022574	11.21 ± 8.45	-1.25e-010 ± 0.756	UP	0.0809
NDST4	HQP017045	-2.249 ± 9.64	-1.875e-009 ± 5.94	DOWN	0.8388
HS6ST1	HQP022653	1.07 ± 1.64	1.25e-010 ± 0.72	UP	0.4972
HS6ST2	HQP021871	-2.142 ± 9.52	-1e-009 ± 5.70	DOWN	0.8416
HS6ST3	HQP007336	4.794 ± 5.12	1.25e-010 ± 0.82	UP	0.2165
HS2ST1	HQP064242	9.898 ± 7.68	0.00 ± 0.63	UP	0.0878
GLCE	HQP006988	10.26 ± 8.49	1.25e-010 ± 1.30	UP	0.1181
AGRN	HQP067787	9.966 ± 8.55	-1.25e-010 ± 0.58	UP	0.1161
SULF1	HQP058565	1.89 ± 3.18	2.5e-010 ± 0.45	UP	0.4165
SULF2	HQP064803	2.022 ± 2.23	0.00 ± 0.57	UP	0.2640
HS3ST1	HQP023407	-5e-010 ± 4.32	-5.081 ± 8.52	UP	0.5642
HS3ST2	HQP023406	6.341 ± 8.49	0 ± 4.44	UP	0.4774
HS3ST4	HQP023403	8.405 ± 8.14	-6.25e-010 ± 4.10	UP	0.3224
HS3ST5	HQP005363	1.152 ± 9.19	-2.5e-010 ± 5.82	UP	0.9144

significant changes were detected by manual qRT-PCR, though some strong trends for altered expression were noted for *NDST3*, *HS2ST1*, *SULF2*, *HS6ST2*, *AGRN* and *GLCE* genes. This absence of statistical significance may be due to a combination of patient variability and small sample size.

Analysis of expression of the *NDST* genes (which code for NDST enzymes that catalyse the removal of an acetyl group and the addition of a sulfate group along the HS chain) revealed variable changes in expression in the presence of the AD phenotype. The *NDST1, NDST2 and NDST3* genes were found to be up-regulated with AD relative to age-matched controls with mean (±S.E.M) fold changes of 1.30 (±1.62), 0.45 (±1.88) and 11.21 (±8.45) recorded respectively. *NDST3* expression exhibited the strongest trend of this family however fell just short of statistical significance (p=0.081). Conversely, the *NDST4* gene was down regulated with a mean (±S.E.M) fold change of -2.25 (±9.64).

Expression of the *HS2ST1* gene (which codes for the HS2ST enzyme that catalyses the addition of a sulfate group to the 2-O position of the HS chain) exhibited the next strongest trend

with a recorded increase in expression with AD with respect to the *GAPDH* housekeeping gene and healthy age-matched control samples. A mean (±S.E.M) fold change of 9.90 (±7.68) was observed in this instance and may be indicative of an increase in the sulfation at the 2-O position of the HS chain. Despite a strong trend, this did not quite reach statistical significance (p=0.088).

Quantitative analysis of the expression of the *HS6ST* family of genes (which code for the HS6ST enzymes that catalyse the addition of a sulfate group to the 6-O position of the HS chain) revealed variable regulation with the AD phenotype. The *HS6ST1* gene displayed a trend towards up-regulation with a mean (±S.E.M) fold change of 1.07 (±1.64) in AD patients relative to healthy controls alongside the *HS6ST3* gene that also displayed increased expression with a mean (± S.E.M) fold change of 4.79 (±5.12). Despite the strong trend for increased expression of *HS6ST3* with AD, larger error bars meant this change fell short of statistical significance (p=0.217). In contrast, the *HS6ST2* gene displayed decreased expression in those patients with AD with a mean (±S.E.M) fold change in expression of -2.14 (±9.52).

Expression of the *SULF2* gene (that codes for the SULF2 enzyme that catalyse the removal of a sulfate group at the 6-O position along the HS chain) displayed the next strongest trend for change in expression with the AD phenotype with a recorded mean (±S.E.M) fold change of 2.02 (±2.23) (p=0.264). Expression of the *SULF1* gene followed a similar, however less strong trend for up regulation with the AD phenotype with mean (±S.E.M) fold change of 1.89 (±3.18) (p=0.417).

Finally, strong trends for changes in expression with the AD phenotype were recorded for the *GLCE* gene (responsible for the epimerisation of GlcA to IdoA) with a mean (±S.E.M) fold change in expression of 10.26 (±8.49) relative to healthy age-matched controls. This change fell short of statistical significance despite a strong trend for up-regulation (p=0.118). In addition, expression of the core protein gene *AGRN*, displayed a strong trend for up-regulation with the AD phenotype with a recorded mean (±S.E.M) fold change of 9.97 (±8.55) (p=0.116).

Changes in the expression of the *HS3ST* gene family did not reveal any strong trends for changes in expression with the AD phenotype. The *HS3ST4* gene presented the biggest mean (±S.E.M) fold change in expression of 8.41 (±8.14) whilst the *HS3ST2* and *HS3ST1* genes displayed mean (±S.E.M) fold changes of 6.34 (±8.49) and 5.08 (±8.62) respectively. The *HS3ST5* gene displayed the most modest increase in expression with a mean (±S.E.M) fold change of 1.15 (±9.19) observed. The large variation between samples is likely the reason why these fold changes did not reach statistical significance on this occasion.

Overall, manual qRT-PCR as carried out here, suggested the possibility of significant alterations in HS related-gene expression profiles in AD, but was not conclusive. It was hypothesised

that larger numbers of samples would need to be analysed to observe significant changes. Strong trends to indicate changes in the expression of *the SULF2*, *NDST3*, *HS6ST3*, *HS2ST1*, *GLCE* and *AGRN* genes may go some way to account for the structural changes in HS as observed in chapter 2 and may offer an upstream mechanism by which some of these changes may be mediated.

3.4.1.2 TaqMan® low density array microfluidic cards

Analysis of gene expression using TaqMan® array fluidic cards revealed changes in the expression of HS biosynthetic enzyme genes and core protein genes. AD (n=11) and Ctrl (n=11) patient HS samples were screened for the expression of 36 HS-related genes. Results were compared to the relative expression of the *RPLP0* and *18S* housekeeper genes whilst also relative to the expression of the healthy controls. The delta delta CT method was used for analysis as described previously. Results, for the most part, matched those found with manual qRT-PCR, but also allowed for a much more extensive profiling of HS-related genes. Details of $\log_2$ fold changes (±S.E.M) in expression are detailed in **Table 3.5.**

Significant changes in expression were observed in AD (relative to housekeeper genes and healthy controls) in the *AGRN*, *HS3ST2*, *HS6ST1*, *HSPG2* and *NDST1* genes. The *AGRN* and *HSPG2* genes code for core proteins onto which HS may be covalently bound. Both of these genes were found to be up-regulated in the presence of the AD phenotype with mean (±S.E.M) fold changes of 1.19 (±0.28) (p=0.003, Student's t-test) and 1.40 (±0.51) (p=0.041, Student's t-test) recorded respectively (**Figure 3.1A-B**). Up-regulation of these core proteins may be indicative of mechanisms to regulate quantity of total HS within cells and its location. The observed increase in expression of the *AGRN* gene here also matched that found with manual qRT-PCR as described previously in section 3.4.1.1.

Furthermore, the *HS6ST1* gene, coding for a 6-O sulfotransferase 1 was also found to be significantly up-regulated with a mean (±S.E.M) fold change of 1.30 (±0.34) (p=0.012, Student's t-test), also matching the results generated with manual qRT-PCR. This was in contrast to the 3-O sulfotransferase 2, *HS3ST2* gene that was significantly down regulated with a mean (±S.E.M) fold change of -1.10 (±0.35) (p=0.029, Student's t-test) (**Figure 3.2A-B**). Here, TaqMan® analysis contradicted that of manual qRT-PCR that had reported a trend for up-regulation of the *HS3ST2* gene (but was not statistically significant).

A significant up-regulation was also observed for the *NDST1* gene, coding for the N-deacetylase/N-sulfotransferase 1 enzyme. A mean (±S.E.M) fold change of 1.23 (±0.40) (p=0.011, Student's t-test) was recorded (**Figure 3.3**). Again, this change matched the trend reported with

Table 3.5: Data from TaqMan array card. HS-related genes were profiled in AD (n=11) and healthy age-matched control patients (n=11) brain samples using a custom made TaqMan array card. All changes presented below are relative to healthy age-matched controls and normalized to the *Rplp0* and *18s* housekeeping genes. The delta delta CT method was used for analysis and the log2 fold changes presented below. Those genes found to be expressed significantly altered in AD are displayed in bold.

Gene Name	Gene ID	Mean log (fold change) in Ctrl ± S.E.M (n=11)	Mean log (fold change) in AD ± S.E.M (n=11)	Up/Down reg. in AD vs. Ctrl	t-test p-value P<0.05*
AGRN	Hs00394748_m1	-1.45E-15 ± 0.24	1.19 ± 0.29	UP	**0.003****
EXT1	Hs00609162_m1	2.67E-16 ± 0.29	0.51 ± 0.43	UP	0.313
EXT2	Hs00181158_m1	4.74E-16 ± 0.29	0.50 ± 0.48	UP	0.359
EXTL1	Hs00184929_m1	1.07E-15 ± 0.21	-0.15 ± 0.40	UP	0.726
EXTL2	Hs01018237_m1	9.84E-16 ± 0.42	0.10 ± 0.67	UP	0.900
EXTL3	Hs00918601_m1	-5.12E-16 ± 0.22	0.87 ± 0.40	UP	0.062
GLCE	Hs00392011_m1	-7.78E-16 ± 0.28	1.43 ± 0.81	UP	0.093
GPC1	Hs00892476_m1	3.13E-16 ± 0.14	0.53 ± 0.33	UP	0.140
GPC2	Hs00415099_m1	-7.11E-16 ± 0.27	0.81 ± 0.33	UP	0.069
GPC3	Hs01018936_m1	9.69E-16 ± 1.39	1.49 ± 2.08	UP	0.538
GPC4	Hs00155059_m1	1.61E-16 ± 0.23	0.70 ± 0.51	UP	0.203
GPC5	Hs00270114_m1	1.08E-15 ± 0.40	0.97 ± 0.49	UP	0.125
GPC6	Hs00170677_m1	-3.53E-16 ± 0.41	1.47 ± 0.72	UP	0.086
HPSE	Hs00935036_m1	1.49E-15 ± 0.34	0.99 ± 0.39	UP	0.059
HPSE2	Hs00222435_m1	-4.64E-16 ± 0.37	1.11 ± 0.45	UP	0.056
HS2ST1	Hs00202138_m1	1.91E-15 ± 0.25	0.61 ± 0.25	UP	0.243
HS3ST1	Hs00245421_s1	3.40E-15 ± 0.37	1.15 ± 0.77	UP	0.175
HS3ST2	Hs00428644_m1	9.49E-16 ± 0.32	-1.10 ± 0.35	DOWN	**0.029***
HS3ST3A1	Hs00925624_s1	-1.33E-15 ± 0.72	2.00 ± 0.70	UP	0.091
HS3ST3B1	Hs00797512_s1	0.00 ± 0.34	1.28 ± 0.66	UP	0.085
HS3ST4	Hs00901124_s1	-1.01E-15 ± 0.25	0.82 ± 0.47	UP	0.122
HS3ST5	Hs00999394_m1	5.15E-16 ± 0.32	0.47 ± 0.48	UP	0.405
HS6ST1	Hs00757137_m1	-6.66E-16 ± 0.34	1.30 ± 0.36	UP	**0.012***
HS6ST2	Hs02925656_m1	-3.57E-15 ± 0.76	-0.13 ± 0.65	DOWN	0.899
HS6ST3	Hs00542178_m1	1.81E-16 ± 0.29	-0.53 ± 0.39	DOWN	0.261
HSPG2	Hs00194179_m1	-9.69E-16 ± 0.41	1.40 ± 0.54	UP	**0.041***
NDST1	Hs00925442_m1	0.00 ± 0.18	1.23 ± 0.42	UP	**0.011***
NDST2	Hs00234335_m1	-7.87E-16 ± 0.31	1.20 ± 0.62	UP	0.085
NDST3	Hs01128584_m1	-2.93E-16 ± 0.29	-0.10 ± 0.51	UP	0.854
NDST4	Hs00224024_m1	3.55E-16 ± 0.87	1.05 ± 0.85	UP	0.467

SDC1	Hs00896423_m1	-1.08E-15 ± 0.26	0.59 ± 0.83	UP	0.507
SDC2	Hs00299807_m1	8.07E-16 ± 0.28	0.30 ± 0.49	UP	0.589
SDC3	Hs01568665_m1	-2.52E-17 ± 0.20	0.16 ± 0.26	UP	0.617
SDC4	Hs00161617_m1	1.76E-15 ± 0.39	-0.17 ± 0.29	DOWN	0.712
SULF1	Hs00290918_m1	-1.44E-15 ± 0.27	0.99 ± 0.52	UP	0.097
SULF2	Hs01016476_m1	-6.46E-16 ± 0.34	0.02 ± 0.39	UP	0.966

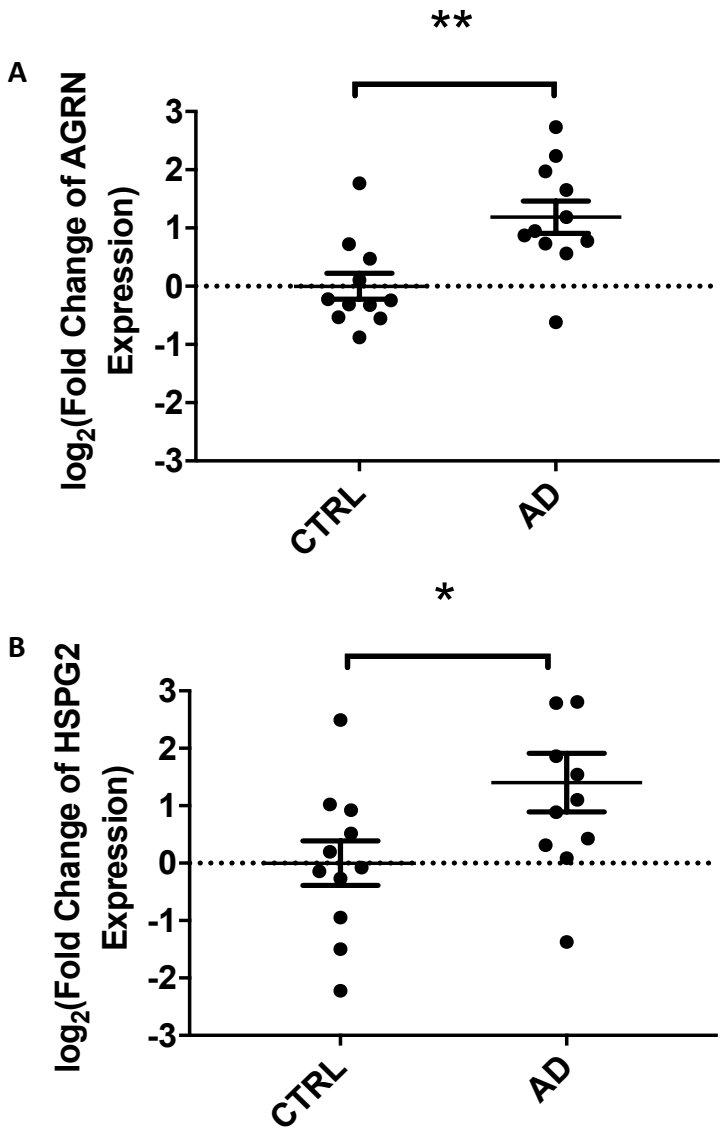

Figure 3.1A – B. TaqMan® array profiling of *AGRN* and *HSPG2* core protein gene expression is altered in AD. Expression of HS genes from AD (n=11) and healthy age-matched controls (n=11) brain samples were analysed on a custom made TaqMan® array card and the delta delta CT method used for analysis. All expression changes were normalised to healthy controls and the *RPLP0* and *18S* housekeeper genes. Of the core proteins, Agrin (*AGRN*) (**A**) and Perlecan (*HSPG2*) (**B**) were found to be up-regulated with significant mean (±S.E.M) $\log_2$ fold changes of 1.19 (±0.29) and 1.40 (±0.54) respectively. $p<0.05$*; $p<0.01$ **, Student's t-test.

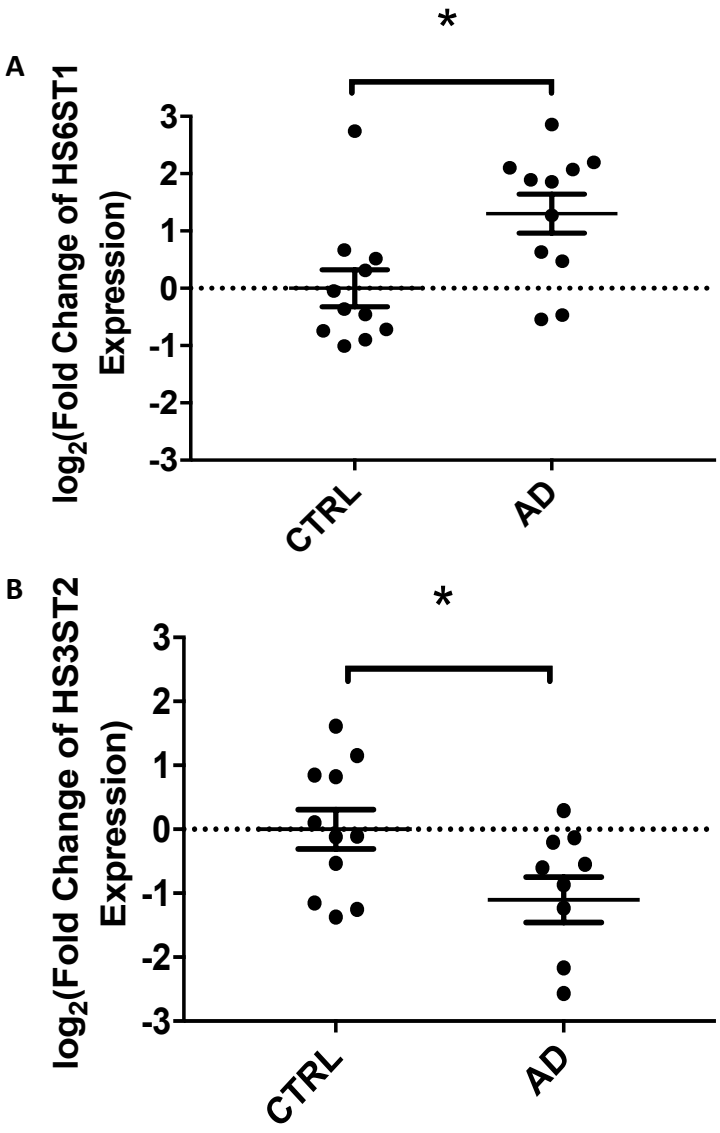

Figure 3.2A – B. **TaqMan® array profiling of *HS6ST1* and *HS3ST2* sulfotransferase gene expression is altered in AD**. Expression of HS genes from AD (n=11) and healthy age-matched controls (n=11) brain samples were analysed on a custom made TaqMan® array card and the delta delta CT method used for analysis. All expression changes were normalized to healthy controls and the *RPLP0* and *18S* housekeeper genes. Of the sulfotransferases, heparan-sulfate 6-O-sulfotransferase 1 (*HS6ST1*) (**A**) and heparan-sulfate 3-O-sulfotrasnferase 2 (*HS3ST2*) (**B**) were found to be up- and down-regulated respectively with significant mean (±S.E.M) $\log_2$ fold changes of 1.30 (± 0.36) and -1.10 (± 0.35) respectively. $p<0.05$ * Student's t-test.

with manual qRT-PCR, however, perhaps due to larger sample sizes; this result reached statistical significance here.

Other genes studied were not found to be altered significantly in AD; this was consistent with findings from the manual qRT-PCR despite smaller sample sizes in the manual method. Likewise, trends in expression levels suggested that other key sulfotransferases such as the genes for the *HS6ST2* and *HS6ST3* enzymes were down regulated in the presence of the AD phenotype with

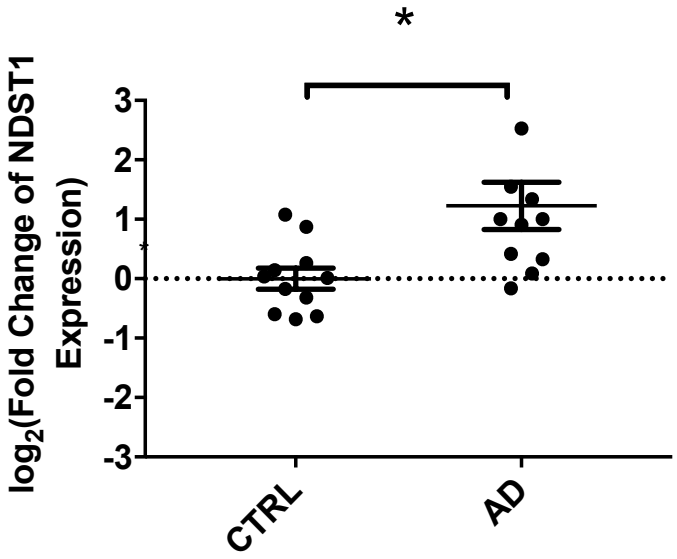

Figure 3.3. **TaqMan array profiling of *NDST1* N-deacetylase/N-sulfotransferase gene expression is altered in AD**. Expression of HS genes from AD (n=11) and healthy age-matched controls (n=11) brain samples were analysed on a custom made TaqMan® array card and the delta delta CT method used for analysis. All expression changes were normalized to healthy controls and the *RPLP0* and *18S* housekeeper genes. N-deacetylase/N-sulfotransferase 1 (*NDST1*) was up regulated with a significant mean (±S.E.M) $\log_2$ fold change of 1.23 (±0.42). $p<0.05$ *, Student's t-test.

mean (±S.E.M) fold changes of -0.13 (±0.65) (p=0.899, Student's t-test) and -0.54 (±0.37) (p=0.261, Student's t-test) respectively, implicating these too as being altered and potentially affecting sulfate patterning along HS chains found in the brains of these patients. In addition, trends for the up-regulation of the *SULF1* gene, coding for the HS 6-O sulfatase 1 enzyme, was found to show a strong trend to be increased with AD, with a recorded mean (±S.E.M) fold change of 0.99 (±0.52) (p=0.097, Student's t-test). This data also corroborated data collected from manual qRT-PCR work. TaqMan® did however report an absence of any change in the expression of the *SULF2* gene with mean (±S.E.M) fold change of 0.02 (±0.39) (p=0.966, Student's t-test). Furthermore, the *HPSE* and *HPSE2* genes that encode the heparanase enzymes that digest the HS chain, displayed strong trends for up-regulation with AD with recorded mean (±S.E.M) fold changes of 0.99 (±0.37) (p=0.059, Student's t-test) and 1.12 (±0.43) (p=0.056, Student's t-test) respectively.

In addition, trends for an increase in other HS core proteins such as the *GPC1-6* family of genes were observed in AD patient brain samples vs. their healthy age-matched control counterparts. This was also true of the SDC1-4 family, with the exception of *SDC4* that displayed a trend for a decrease in expression with AD. Furthermore, the *EXT* and *EXTL* genes, that encode the EXT and EXTL enzymes required for HS chain polymerisation and extension, also displayed elevated expression relative to healthy age-matched controls. All details of recorded mean (±S.E.M) fold changes in expression of HS-related genes are detailed in **Table 3.5**.

3.5 Discussion

3.5.1 Relative expression of the HS-related genes are altered in Alzheimer's disease compared to their healthy age-matched counterparts

Having established some strong trends for changes in expression of these genes in the presence of the AD phenotype with manual qRT-PCR, the use of the TaqMan® technology to explore this further could be justified, with both a larger number of samples, and across a broader spectrum of HS-related genes. TaqMan® microfluidic arrays were thus carried out to confirm the findings and also to overcome some of the shortcomings experienced with this earlier technique. As described previously, post-mortem delay proved to be a significant limiting factor with human tissue as this unavoidable feature dramatically affects RNA quality. TaqMan® array analysis, as employed on this occasion, overcame some of these difficulties in that it conferred a much broader analysis of HS-related genes, but also, with significantly less RNA material than required for manual qRT-PCR.

Promisingly, in the majority of cases, the data reported with TaqMan® analysis supported that found using manual qRT-PCR. In addition, perhaps due to the larger sample numbers that could be analysed with this technique, some of these changes were found to be significant. This study revealed a significant up-regulation of the *HS6ST1* gene in the presence of the AD phenotype relative to healthy controls. This was coupled with a trend for decreased expression of the *HS6ST2* and *HS6ST3* genes. Furthermore, whilst a decrease in the expression of the *HS6ST2* and *HS6ST3* genes is consistent with the notion that HS from AD patients is less sulfated and less able to block the activity of BACE-1 (Scholefield*, et al.* 2003), the significant increase in *HS6ST1* expression reported here may represent compensation to counter the loss of sulfotransferase activity induced by other isoforms.

There seems to be a strong argument for distinct substrate specificities of the HS6ST enzymes whose activities may be somewhat distinct from their isoforms (Esko and Selleck 2002). Previous research has indeed indicated that each HS6ST isoform does appear to display varied substrate specificity whereby, HS6ST1 shows preferences for IdoA-GlcNS units, HS6ST2 acts on both GlcA-GlcNS and IdoA-GlcNS units and HS6ST3 displays preferences for any substrate independently of substrate concentration. In light of this, it may be plausible that HS6ST isoforms are able to target enzymatic reactions in regions of HS different to their usual preferences in their absence of other family members (Habuchi*, et al.* 2000). Understanding the mechanisms by which enzyme isoforms are able to re-establish equilibrium via compensatory mechanisms may prove invaluable in deciphering the upstream causes for the observed structural changes of HS with AD. Regulation of HS biosynthesis is known to be complex and as such it is highly unlikely that there are not regulatory pathways in place to counteract disturbances that may be induced by disease conditions like AD.

Manual qRT-PCR also reported a trend for up-regulation of the *HS6ST1* gene and a down regulation of *HS6ST2* to support this finding. In contrast, manual qRT-PCR did report a trend for an up-regulation of the *HS6ST3* gene, however large error bars would suggest great variability and this result was not statistically significant. This coupled with a small sample group may explain this alternate observation.

A significant decrease in the expression of the *HS3ST2* gene was observed following TaqMan® array analysis. Previous research did not explore whether BACE-1 inhibition efficacy is directly affected by 3-O sulfation (Patey*, et al.* 2006), so we cannot know how decreased expression of the *HS3ST2* gene as noted here may have implications for HS structure and its ability to interact with, and potentially modulate BACE-1. There is some evidence to suggest that HS modification enzymes exhibit preferences with regard to location of action dependent upon the motifs that surround their active site. Specifically, 6-O sulfation is reported to be favoured on GlcNS residues flanked by 2-O sulfated IdoA units (Liu*, et al.* 2014). As such, we cannot rule out the possibility that changes in 3-O sulfation may impact the activity of other biosynthetic enzymes such as the binding preferences of other sulfotransferases. In reference to 2-O sulfation in this context, a reported up-regulation of expression of the *HS2ST1* gene in this study, as well as the *GLCE* gene (encoding the C5-epimerase responsible for epimerisation of the GlcA unit to IdoA units) (Hagner-McWhirter*, et al.* 2004) may again prove to act as compensation mechanisms to indirectly enhance 6-OS sulfation in response to its decline in AD patients.

Elevated expression of the *GLCE* gene observed here would suggest the potential for increased levels of the GLCE enzyme and ultimately, an enhanced turnover of GlcA residues to IdoA residues along the HS chain. As discussed previously, SAX chromatography as employed in chapter 2 to investigate structural changes in HS with AD, was unable to distinguish the original uronic acid identities. As such, changes in the expression of this gene as noted here cannot be attributed to any structural changes that may or may not be occurring with respect to uronic acid unit abundance within the AD and control samples under investigation. The increase in the expression of this gene however may indicate some gross structural changes that may be occurring that could have implications on the activity of HS and its ability to interact with and inhibit BACE-1. Up-regulation of the *HS3ST2* gene with TaqMan® array analysis was not supported by findings with manual qRT-PCR, however this disparity may be explained by the lack of a large enough sample population in the manual qRT-PCR experiments. Trends for an up-regulation of the *HS2ST1* and *GLCE* genes however were consistent across both sets of PCR data. In addition structural analysis as described in chapter 2, did not reveal any significant changes in levels of 2-O sulfation; however there was a reported trend for AD patient brain HS to display elevated abundance of the UA(2S)-GlcNS disaccharide, vs. healthy controls. This might be consistent with the increased levels of *HS2ST1* gene expression

The reported significant increase in *NDST1* gene expression noted here with TaqMan® array analysis could be indicative of enhanced N-deacetylase/N-sulfotransferase activity along the HS chain. It has already been established that NDST enzymes exhibit variable sulfotransferase activity and NDST1 is known to display a much-reduced N-acetylase/N-sulfotransferase activity vs. NDST2, and even less activity vs. the NDST4 enzyme (Aikawa*, et al.* 2001). Assuming the NDST1 enzyme does indeed display the lowest degree of sulfotransferase activity, the observed increased in expression of the *NDST1* gene in this manner may indicate an enhanced NDST activity that actually confers reduced NS sulfation levels. Indeed, Patey and colleagues found that, after unmodified PIMH, de-N-sulfated and re-N-acetylated heparin was the best inhibitor of BACE-1 (Patey*, et al.* 2006). This indicated that when coupled with 6-O sulfation, N- sulfation is not essential for efficacious BACE-1 inhibition, but can modulate activity. As such, enhanced *NDST1* gene expression as noted here may serve to attempt to restore BACE-1 inhibition efficacy, assuming there is a combinatorial effect between 6-O sulfation and N- sulfation patterns. It should also be noted that loss of N- sulfation only has minor effects on BACE-1 inhibitory activity compared to the loss of 6-O sulfation (Patey*, et al.* 2006, Scholefield*, et al.* 2003). We might therefore expect that changes in *NDST* gene expression might act in combination with other modification enzymes, rather than in isolation to modulate efficacy of BACE-1 inhibition. Indeed, changes in the expression of all of the *NDST* genes was largely consistent with the findings of manual qRT-PCR, with the exception of the *NDST4* gene, which reported both up and down regulatory trends with manual and TaqMan® analysis respectively.

The *HSPG2* and *AGRN* core protein genes were also significantly regulated in AD. AD patient brain samples displayed significantly increased expression of both the *HSPG2* (encoding the perlecan core protein) and *AGRN* (encoding the agrin core protein) genes, suggesting enhanced levels of these core proteins as a result. This data is somewhat contradictory to compositional analysis data (chapter 2) that revealed significantly decreased levels of HS within AD patient brain samples relative to their age-matched healthy controls. Enhanced levels of core proteins might be indicative of elevated levels of HS, rather than decreased levels, as we reported. This discrepancy may however be reconciled with the notion that these core proteins, whilst expressed at greater levels, may not actually carry more HS chains thus explaining the reduced levels in AD as reported in chapter 2. Indeed, a trend for increased levels of *HPSE* and *HPSE2* genes in AD vs. healthy controls as reported here following TaqMan® array analysis supports the finding of decreased levels of total HS as these genes encode the HPSE enzymes, responsible for degradation of the HS chain (Tao*, et al.* 2013).

There may also be a shift in the balance of HS modification of different alternative core proteins. Interestingly, HSPG2 and AGRN are both extracellular HSPGs, and these may be less efficient at regulating BACE-1 at the cell surface compared to the SDCs and GPCs for example. Furthermore, the HSPG2 and AGRN proteins are both known to associate with the features of AD

including NFTs and amyloid plaques (Snow*, et al.* 1994, Verbeek*, et al.* 1999) and as such, we might expect their gene transcript levels to be elevated. It is therefore encouraging that we observed a an increase in the expression of *AGRN* and *HSPG2* genes in this instance as we might expect this to translate to enhanced levels of the core proteins that co-localise with the pathological features of AD. It has been hypothesised that the presence of nine follistatin-like protease inhibitor domains (Groffen*, et al.* 1998) in AGRN may drive the persistence of the plaque and tangle features of AD by protecting them from degradation. This interaction between AGRN and AD pathology may thus explain the disparity between enhanced levels of the *AGRN* gene expression vs. lowered total HS levels within the cell, as their abundance may be driven by separate pathways. Moreover, if we accept the hypothesis that these core proteins might drive the pathogenesis of AD, the elevated expression of these proteins may not be attributed to changes in HS levels at all, but rather, their context in AD pathology interactions. This hypothesis may also go some way to explain the observed trend for increase in expression of other HS core protein genes, including the *GPC* and *SDC* family (with the exception of the *SDC4* gene).

Reasonably little work has been done to assess the potential changes in the expression of HS-related genes that may occur with disease despite the known importance of these enzymes as established by knockout models as described previously. That being said, there is increasing evidence to suggest that changes in the expression of specific HS-related genes may be occurring alongside a variety of different pathologies. Of note, up-regulation of *HPSE*, particularly in a number of cancers has been reported recently (Vlodavsky*, et al.* 2012). Indeed, this post synthetic modulator of HS has also been associated with the pathogenesis of a number of inflammatory disorders including inflammatory lung injury, rheumatoid arthritis and chronic colitis (Goldberg*, et al.* 2013, Meirovitz*, et al.* 2013). A great deal of work has now been done to further elucidate the role of heparanase in a number of neuroinflammatory disorders (Massena*, et al.* 2010, Wang*, et al.* 2005). Furthermore, extensive work in a transgenic murine model for the over expression of the *HPSE* gene (Hpa-tg), has reported enhanced sulfation and fragmentation of the HS chain (Zcharia*, et al.* 2004) and has also been utilised as a model by which to explore the role of HS and heparanases in amyloidosis. In 2005, Li and colleagues reported direct *in vivo* evidence that over-expression of human heparanase in the Hpa-tg mouse model resulted in dramatic fragmentation of HS and consequentially attenuated amyloidosis (Li*, et al.* 2005). This work naturally confirmed the key role of HS in amyloid disorders such as AD, but also raises the question as to whether the observed trend for up-regulation of *HPSE* and *HPSE2* genes as reported here, is a compensatory mechanism by which to protect cells from the accumulation of amyloid.

In addition, work by Huynh and colleagues in 2012, reported changes in the expression of some HS-related genes in the context of an ageing phenotype. Expression analysis of HS-related genes from aged and adult hippocampus samples revealed a decreased expression of *GLCE*, *HS2ST1*

and *HS3ST5* genes and an increase in the expression of *NDST2* and *HS3ST4* in aged individuals vs. their younger counterparts (Huynh*, et al.* 2012). Interestingly, some of the genes found to be significantly down-regulated in this study displayed a trend for an increase in expression in the TaqMan® array profiling carried out here. In contrast, the *NDST2* and *HS3ST4* genes reported to be up-regulated with ageing, were similarly observed to be up-regulated in the work as described in this chapter. Naturally, this study looked at an ageing phenotype rather than AD and as such differential regulation of HS structure might not be surprising particularly in light of the altered structural changes described with ageing and with AD in chapter 2. Changes in the expression of HS-related genes as reported by Huynh and colleagues however, not only support the notion of an upstream mechanism by which HS structure may be modulated, but also go some way to confirm the hypothesis of separate and distinct mechanisms by which HS may mediate normal physiological ageing and dementia.

Conditional deletion of the *Ext-1* gene in postnatal neurons of the amyloid mouse model APP-PS1 has also been reported to attenuate both the oligomerisation of the Aβ peptide as well as its deposition into more mature plaques (Liu*, et al.* 2016). This work by Liu and colleagues in 2016 also goes some way to support the notion that changes in the expression of HS-related genes may be key in underpinning key functionality of HS both physiologically and in a disease context. The strong association between HS and a number of features of AD, not least its interaction with the BACE-1 enzyme, immediately implicates the expression of those enzymes responsible for its modification as the main upstream coordinators of the functionality of HS in AD.

Finally, there has been a great deal of research to investigate the ways in which the roles of PGs may be important in psychiatric disorders and intellectual disabilities (Maeda 2015). Functional mutations of the *XYLT1* gene has been shown to result in short stature syndrome linked with intellectual disability (Schreml*, et al.* 2014). The *EXT1* gene has also been shown to be associated with autism (Li*, et al.* 2002). Finally, mutations within the *NDST1* gene have been shown to cause intellectual disability, epilepsy and muscular hypotonia implicating in HS in key developmental functionality of neuronal circuits (Reuter*, et al.* 2014). These studies together all strongly implicate not only HS in a number of pathological pathways but also the biosynthetic machinery that generates heterogeneous HS species. The changes observed here in the expression of a number of HS-related genes in AD confirm the notion of an upstream mechanism by which the final structure of HS is altered such that it becomes unable to efficiently deliver its normal functionality. This could include its ability to modulate BACE-1 activity.

3.6 General conclusions

It is important to note here, that qRT-PCR, whether via manual qRT-PCR methods or the TaqMan® microfluidic card arrays, was only able to quantify the levels of RNA transcripts of target biosynthetic genes and core proteins, and not the actual protein levels. We cannot therefore be certain that altered RNA levels as detected in these experiments truly represent changes in inherent levels and activity of the HS biosynthetic enzymes. This may be due to regulation of translation of the mRNA, or a low turnover rate (half life) of the proteins themselves. As such, we must be careful in making conclusions about protein activity based on RNA levels alone. Antibodies for these enzymes may prove useful in western blot studies to more conclusively determine the levels of these proteins within brain samples. Availability of specific antibodies however is limited; furthermore determining the specific activity of these enzymes (in addition to their abundance within brain tissue samples) is another challenge in itself and is not currently technically feasible. qRT-PCR was the best methodology to employ at this time for identifying possible up stream causes of the observed structural alterations to HS. It is, however important to recognise the limitations of this approach and the conclusions from the data collected here.

The changes in expression of the genes encoding some of the HS-related enzymes as observed here may go some way to explain the observed changes in the structure of HS as described in chapter 2. Expression of the enzymes responsible for the elongation and modification of the HS chain is an obvious upstream target for understanding how structural changes are occurring and this data supports our hypothesis of altered HS structure in AD. Whilst we cannot attribute enzyme expression directly to enzyme activity, changes in the expression of the *HS6ST* and *SULF* genes as described in this chapter are consistent with our findings of altered sulfation patterns as determined directly by compositional analysis. The mechanisms by which HS structure is modulated and refined is still largely undiscovered and there are undoubtedly compensation mechanisms that occur that may counter loss of gene expression of specific HS biosynthetic machinery. More work is needed to fully understand changes in HS biosynthesis that may occur in disease conditions. Indeed, a recent GWAS study has identified a SNP of the *HS6ST1* gene that may cause genetic predisposition to albuminuria associated with diabetes (Teumer*, et al.* 2016). This work strengthens the notion that changes in HS biosynthetic machinery gene expression could have significant affects on downstream functionality of HS and may even prove useful as diagnostic biomarkers should these genes be altered in early disease pathogenesis. This work, albeit preliminary, offers a pathway by which HS structure, and ultimately its effect on BACE-1 activity, may be determined within the AD phenotype.

Chapter 4: Changes in endogenous HS structure affect BACE-1 inhibition and have downstream consequences on Aβ peptide generation

4. Chapter 4

4.1 Introduction

4.1.1 More about BACE-1

The BACE-1 enzyme is a key transmembrane aspartic protease with important roles in the processing of APP and ultimately, the onset and development of AD. BACE-1 is related to the pepsin family of aspartyle proteases and works best at low pH. As a result, BACE-1 is predominantly found in more acidic regions of the cell, in particular the endosomes and trans-golgi regions. With respect to locality of action, the highest expression of BACE-1 has been reported in the neurons of the brain (most likely explaining its large contribution to AD pathogenesis, a disorder of the brain). BACE-2, a homolog of BACE-1 was discovered shortly after and the two isoforms share 64% structural homology. It has however since been ruled out that BACE-2 shares functionality as a β-secretase. BACE-2 is expressed only at very low levels within neurons and does not process APP as BACE-1 does, suggesting it is not a strong candidate as a β-secretase (Vassar*, et al.* 2009).

4.1.2 Pro-BACE-1 and mature BACE-1

Upon synthesis, BACE-1 is initially formed as an immature, pro-peptide (pro-BACE-1) (Benjannet*, et al.* 2001), where it is then cleaved into mature BACE-1 in the Golgi (Haniu*, et al.* 2000). Pro-BACE-1 may exist in two different conformations, open and closed. The open conformation of BACE-1 displays a small degree of enzymatic activity however, in the closed conformation, the pro-domain of BACE-1 physically blocks the active site of BACE-1 thus precluding any enzymatic activity (Shi*, et al.* 2001). Naturally therefore, cleavage of the pro-domain of BACE-1 removes inhibition of the active site and results in full enzymatic potential of BACE-1 (Ermolieff*, et al.* 2000). There exist N-glycosylation sites at four potential locations within BACE-1 alongside six cysteine residues that are able to form three disulfide bonds (Huse*, et al.* 2000). The folding and final confirmation of mature BACE-1 is dependent upon these disulfide bonds, specifically Cys 330/Cys380 is located within the active site of BACE-1 and as such, is responsible for maintenance of the stability of the active site of this enzyme (Fischer*, et al.* 2002). In addition, a dileucine motif within the cytoplasmic domain of BACE-1 is responsible for the localisation of this enzyme to the endosomes (Huse*, et al.* 2000).

Variations in conformation are not limited to just pro-BACE-1, mature BACE-1 may also exist in either a flap open or flap closed confirmation. BACE-1 not bound to its substrates exists in a flap open confirmation, an energetically stable confirmation secured via hydrogen bonding (Hong

and Tang 2004). If bound to its substrate however, BACE-1 displays a flap-closed confirmation. The hydrogen bonds that once stabilised the flap open confirmation are broken and a new interaction established to allow substrates of BACE-1 to interact via a cleft in BACE-1 (Hong and Tang 2004). There is evidence that a small degree of substrate flexibility is required for effective interaction of substrate and BACE-1 via this cleft and it has been hypothesised that this apparent selectivity of BACE-1 may confer a substrate specificity mechanism (Hong and Tang 2004).

4.1.3 Physiological roles of BACE-1

Whilst BACE-1 may be most commonly known for its role in the processing of APP in AD, there are several other substrates that BACE-1 may also act upon. Understanding these binding partners is particularly important when we consider side effects to new therapeutic strategies that may block the action of BACE-1. Furthermore, understanding the ways in which BACE-1 is able to interact with these binding ligands may also shed light into the ways in which novel therapeutics can be designed to effectively interact whilst sparing these alternative targets (Vassar*, et al.* 2009). Previous work to confirm that soluble BACE-1 is unable to process APP led to the notion that all BACE-1 substrates must be membrane bound proteins. There are a number of substrates that have been confirmed in recent years, all of which are indeed transmembrane proteins. BACE-1 substrates include; APP homolog proteins APLP1 and APLP2 (Eggert*, et al.* 2004), voltage gated sodium channel (Na_v1) β2 subunit ($Na_v\beta2$) (Kim*, et al.* 2005), neuregulin-1 (NRG1) (Hu*, et al.* 2006), neuregulin-3 (NRG3) (Hu*, et al.* 2008), P-selectin glycoprotein ligand-1 (PSLG-1) (Lichtenthaler*, et al.* 2003), low-density lipoprotein receptor related protein (LRP) (von Arnim*, et al.* 2005) and Golgi-localised membrane bound α2, 6-sialytransferase (Kitazume*, et al.* 2001). Total inhibition of BACE-1 may therefore have the potential to also block several critical physiological processes. NRG1 and NRG3 for example is key in synaptic plasticity and have been shown to balance excitatory and inhibitory connections within the brain. In essence, NRG isoforms are essential for the development and maintenance of the CNS (Talmage 2008). Attenuation therefore of NRG1 binding for example and NRG3 may result in reduced myelin sheath thickness of axons, and could have significant consequences on synaptic plasticity and cognitive function in patients. Finally, BACE-1 is known to regulate voltage-gated sodium channels. Strong inhibition of BACE-1 therefore may well lead to substantial behavioral phenotypes as a result of altered neuronal excitability and must be considered when considering the effects of BACE-1 inhibition (Vassar*, et al.* 2009). Understanding the implications of these physiological binding partners of BACE-1 is key if successful therapeutics against BACE-1 are to be generated.

4.1.4 Inhibitors of BACE-1

Extensive research has been carried out to further understand the mechanisms by which the activity of BACE-1 can be inhibited effectively and use of 3D crystallography and X-ray has offered a great deal of insight into the ways in which substrates are able to bind to BACE-1 and the ways to best design potent inhibitors. The creation of substrate-based pseudo peptide inhibitors and elucidation of BACE-1 structure upon substrate binding provided substantial aid in the design of drug inhibitor templates. Despite this advance in our understanding of BACE-1 inhibition, there are still several complexities to overcome with regard to successful design of therapeutics to block the activity of this enzyme. Not least of all, is molecular size; drugs to target BACE-1, an enzyme predominantly expressed within the brain, will need to be small enough to efficiently cross the BBB. Likewise, the expression of several other aspartic acid proteases such as pepsin, renin, cathepsin E and D alongside BACE-1 all over the body may result in significant off target effects unless a high degree of BACE-1 specificity is achieved. Aspartic acid residues are conserved across the whole family of proteases, hence much more subtle specificity, perhaps via exploitation of the non-native side chains (Turner*, et al.* 2002), needs to be achieved in any successful BACE-1 inhibitor (Ghosh and Osswald 2014). Targeting other substrates such as cathepsin D (CatD) may prove particularly detrimental in terms of toxic adverse effects in light of CatD's role in protein degradation, apoptosis and hydrolysis of cholesterol (Benes*, et al.* 2008). In addition, P-glycoprotein (Pgp) efflux is another key hurdle to be overcome in effective drug design of BACE-1 inhibitors. The P-gp protein is an ATP-dependent efflux pump that coordinates the removal of xenobiotics such as toxins or drugs out of the brain and back into the capillaries. This efflux is essentially a defense mechanism to protect the brain against harmful, unknown substances and as such, offers a significant barrier against the administrations of BACE-1 inhibitors into the brain (Ghosh*, et al.* 2012).

Despite the potential benefits of inhibition of BACE-1 in the treatment of AD, currently there exists no FDA approved inhibitors on the market despite some candidates showing some potential within the clinic. Currently, efforts to design BACE-1 inhibitors may be classified under two categories, peptidomimetic and nonpeptidic. Some natural products including epigallacatechin gallate from green tea have also shown efficacy as a non-competitive inhibitor of BACE-1 (Jeon*, et al.* 2003). Combination of understanding the interaction between substrate and BACE-1, alongside recognition of the hurdles associated with designing new therapeutics has led to a high throughput screening effort to generate lead molecules as BACE-1 inhibitors. Inhibitors developed by AstraZeneca and Eli Lilly have reached phase II clinical trials and have suggested preliminary evidence for efficacy as drugs to reduce Aβ burden within the brain. Merck also has a compound currently in phase III clinical trials that is showing promise (Kennedy*, et al.* 2016). These drugs are yet to reach FDA approval and a great deal more work is necessary to generate suitable treatment of AD via BACE-1 inhibition (Ghosh and Osswald 2014). There are number of ways to regulate the activity of BACE-1, as described in the following sections.

4.2 BACE-1 and the treatment of AD: how can it be targeted?

As previously discussed in chapter 1, the role of BACE-1 is fundamental in the generation of the toxic Aβ species associated with the onset and development of AD pathogenesis. As such, finding ways to target BACE-1 may be crucial in successfully generating an appropriate therapeutic strategy to this disease. Indeed, a great deal of research effort has been focused on finding ways to most effectively inhibit the action of BACE-1. Early work has concluded that inhibition of BACE-1 should directly reduce accumulation of the toxic Aβ amyloid species; siRNA to disrupt the expression of the *Bace-1* gene resulted in the decreased build up of Aβ species and ultimately improved cognitive deficits in APP transgenic mice (Laird*, et al.* 2005, Singer*, et al.* 2005). Furthermore, rescue of memory deficits in mice totally void of BACE-1 (*Bace-1*$^{-/-}$) confirm the notion that BACE-1 inhibitors could be very effective as treatment for AD (Ghosh and Osswald 2014).

BACE-1 is known to play several key roles in normal physiological function (as described above) and as such robust inhibition of BACE-1 with AD therapeutics may have major toxic side effects within the brain. Research has gone on to assess the effects of only a moderate reduction in the activity of BACE-1. 12-month-old transgenic *APPswe*; *Ps1de9*; *Bace-1*$^{+/-}$ mice display a significant reduction in Aβ deposition within the brain vs. BACE-1 double knockout counterparts. Interestingly, this improvement was not observed in 20-month-old mice, perhaps indicative of an effect of age on the efficacy of BACE-1 knockdown (Laird*, et al.* 2005). Partial reduction in BACE-1 activity in this manner may prove more beneficial overall vs. total block. In the same vein, γ-secretase is a cleavage event that follows that of BACE-1. Indeed, reduction of γ -secretase has not displayed adverse side effects (Li*, et al.* 2007) and as such may implicate a combination of BACE-1 and γ-secretase reduction as a worthy therapeutic strategy against AD to preclude the formation of the Aβ peptide.

4.2.1 Regulation of trafficking of BACE-1

BACE-1 is synthesised as a zymogen that contains a pro-domain, within the endoplasmic reticulum (ER) before transport to the Golgi complex and early endosomes where it can process APP. The low pH found within the Golgi and early endosomes is strongly favoured by BACE-1 and greatly enhances its activity. Phosphorylation of BACE-1 at the Ser^{498} residue alongside a C-terminal dileucine motif are together responsible for regulating the movement of BACE-1 between the cell surface and endosomes (Huse*, et al.* 2000, Walter*, et al.* 2001). Additionally, BACE-1 is S-palmitoylated on 4 Cys residues found between the cytosolic and transmembrane domains (Benjannet*, et al.* 2001). It is this post-translational modification that sequesters BACE-1 into lipid rafts. Research has indicated that targeting of BACE-1 to the lipid raft increases the processing of APP and as such, the turnover of Aβ is increased (Tun*, et al.* 2002). With this in mind, regulation of

the specific localisation of BACE-1 within the cell may prove a useful target for AD therapeutics. In particular, various regulatory factors may play a role in this such, increased expression of reticulon (RTN) proteins (found predominantly within the ER), for example, known BACE-1 binders (He*, et al.* 2004, Murayama*, et al.* 2006), have been shown to increase the retention of BACE-1 within the ER, and in doing so reduce its activity due to the sub optimal pH in this region of the cell (Shi*, et al.* 2009). Transgenic mice expressing RTN3 display reduced levels of C99 fragments (the product of BACE-1 cleavage). Therapeutic targets to enhance levels of these proteins may go some way therefore to regulate the production of Aβ within cells. In addition, physical interaction between BACE-1 and RTN proteins obstructs the ability of BACE-1 to interact with, and process APP to further reduce the formation of the Aβ peptide (Vassar*, et al.* 2009). Finally, expression of neuronal reticulon protein is significantly reduced in the brains of those with AD, implicating this protein perhaps in an abnormal increase of BACE-1 activity (Hu*, et al.* 2007).

Conversely, targeted trafficking of BACE-1 to sites of optimal pH such as the endosomes will enhance the processing of APP (He*, et al.* 2005). Studies have shown that depletion of specific GGA proteins (Golgi-localised γ-ear–containing ARF-binding proteins) with RNAi modulates BACE-1 in such a way that it is targeted to early endosomes (He*, et al.* 2002), an acidic environment that promotes processing of APP. AD patients have been shown to display significantly decreased levels of GGA3 (Tesco*, et al.* 2007) such that finding ways to enhance the brain levels of both RTN3 and GGA3 may also be effective therapeutics against AD.

4.2.2 Enhancing shedding of BACE-1

An alternative method by which BACE-1 may be targeted as a potential therapeutic in AD is to enhance the level it is shed. A fragment of BACE-1 found within cells is regularly shed between Ala^{429} and Val^{430} via the action of an ADAM-like sheddase (Hussain*, et al.* 2003). Interestingly, this fragment is able to act like other proteases to process their substrate (β-secretase cleavage site containing) peptides. However, the effects of these fragments have only been shown *in vitro*. As such, finding ways to enhance the shedding of BACE-1 may be successful in reducing the generation of the Aβ peptide. Indeed, soluble BACE-1 is unable to successfully interact with APP in cells thus precluding its processing (Yan*, et al.* 2001). It is also noteworthy that, ADAM activity, if elevated, may drive the processing of BACE-1 towards the non-amyloidogenic pathway such that APP is processed by α-secretases instead thus precluding formation of the Aβ peptide (Vassar*, et al.* 2009).

4.2.3 Targeting BACE-1 indirectly

Expression levels of BACE-1 are significantly increased in those with AD (Fukumoto*, et al.* 2002). In light of this, one might postulate that BACE-1 in some way is the main driver of AD development within the brain. Furthermore, reports have suggested that oxidative stress, a known associate of AD pathology, may enhance the levels of BACE-1 found within the brain (Tamagno*, et al.* 2002). Indeed, other factors including, ischemia (Wen*, et al.* 2004), apoptosis (Tesco et al 2007), hypoxia (Zhang*, et al.* 2007) and traumatic brain injury (Blasko*, et al.* 2004) may also elevate the levels of BACE-1 detected in the brain. Finding ways to treat and/or prevent these risk factors may thus prove effective as indirect strategies to target BACE-1. Combination of this method alongside direct targets of BACE-1 may prove particularly useful in combating the processing of APP and ultimately the generation of the Aβ peptide. Glucose metabolism is another inducer of cellular stress that may also elevate BACE-1 levels in the brain. Indeed, work in APP mouse models of AD treated to disrupt energy metabolisms pathways were found to display increased levels of BACE-1 and also Aβ (Velliquette*, et al.* 2005). In addition, mRNA expression levels of BACE-1 remained unaltered indicating enhanced levels as observed here were not a result of elevated gene expression per se (Velliquette*, et al.* 2005). Further research went on to confirm that energy deprivation may induce phosphorylation events that result in elevation of mRNA translation (O'Connor*, et al.* 2008) (Lammich*, et al.* 2004). These findings would suggest that appropriate management of cellular homoeostasis may be a key regulator in BACE-1 levels and therapeutics to maintain this equilibrium may prove efficacious in AD patients.

4.3 HS and BACE-1

The role of HS and its interaction and inhibition of BACE-1 is naturally, a very attractive target for the design of AD therapies in light of the challenges discussed earlier. Following the discovery that HS was able to effectively inhibit BACE-1 and ultimately the processing of APP to generate Aβ, work was done to investigate how chemically modified analogues of HS might vary in their ability to block BACE-1, as a potential template for therapeutics in the future (Patey*, et al.* 2006). As discussed previously, administration of unmodified heparins would have serious side affects, most specifically in the context of their anticoagulant activities. Unmodified derivatives may therefore increase the risk of internal bleeding and disrupt blood-clotting mechanisms all around the body. On the other side of the coin, utilising a naturally occurring structure like HS may also be key in avoiding rejection via Pgp efflux (HS is largely expressed within the brain) and toxic side effects that may result from unnatural type structures as represented by typical small molecule organic drugs. To compromise, finding ways to subtly alter the structure of HS so as to create derivatives that still exert BACE-1 inhibitory activity whilst negating their anti-coagulant effects may prove effective as AD therapeutics, without adverse effects that would otherwise make them unsuitable in the clinic. Work by Patey and colleagues investigated the activities of several HS analogues with

respect to their BACE-1 activity and anti-coagulant activity. Results suggested that strong BACE-1 inhibition efficacy could still be maintained alongside reduced anti-coagulant activity (Patey*, et al.* 2006). The most simple and effective inhibitor of BACE-1 was achieved with a de-N-sulfated, re-N-acetylated porcine intestinal mucosal heparin (PIMH). 2-O de-sulfated and 2-O de-sulfated/N-acetylated PIMH also exhibited good BACE-1 inhibitory action suggesting that neither 2-O sulfation nor N-sulfation is the key motif in effective inhibition of BACE-1, particularly when levels of 6-O sulfation is maintained. Removal of 2-O and 6-O sulfate groups dramatically reduced BACE-1 inhibitory activity whilst total de-sulfation totally abolished activity altogether, thus implicating 6-O sulfation as key determinants in BACE-1 inhibition efficacy (Patey*, et al.* 2006).

The presence of some correlations between sulfation pattern (especially 6-O sulfation) and BACE-1 inhibition would indicate that the interaction between HS and BACE-1 is not simply dependent upon charge density. Understanding the ways in which HS is able to block the activity of BACE-1 is key to further "fine tune" HS derivatives.

Most interestingly, the use of HS analogues as inhibitors of BACE-1 may also avoid adverse affects as early work indicates they do not interact significantly with other protease family members, a significant downfall of other similar compounds that have been identified in the past. Activities of a number of the HS analogues tested by Patey and colleagues revealed that modified HS derivatives exhibiting substantial BACE-1 inhibitory activity were not able to significantly inhibit renin, pepsin or cathepsin D (Patey*, et al.* 2006). Overcoming adverse interactions and potential side effects in this manner, makes the interaction of HS and BACE-1 even more attractive as a target to design templates for AD therapeutics in the future.

4.3.1 How does HS inhibit BACE-1?

The exact mechanism by which HS is able to inhibit the activity of BACE-1 has not been widely studied as yet. However initial research upon the discovery of the interaction between HS and BACE-1 went some way to elucidate this mechanism. Fluorescence polarisation was used to examine the effects of binding of a rhomadime-labeled non-cleavable peptide substrate (R110) to BACE-1. Research found that R110 ligand is able to bind to free BACE-1 at the substrate-binding site. In doing so, the polarisation of light relative to an unbound ligand was increased. In addition, a known competitive ligand of the binding site of the BACE-1 (GW642976A) produced a detected decrease in the polarisation of light, due to dose-dependent displacement of the R110 ligand as would be expected for a competitive inhibitor. This effect was observed independently of whether the antagonist was added before, or after the pre-equilibrium of BACE-1 and R110. Furthermore, incubation of R110 and BACE-1 before addition of N-acetylated heparin negated its inhibitory

effects. From this data, it was concluded that HS is able to prevent the entry of the substrate to the active site but is not a competitive inhibitor. In addition, this research suggested that if the ligand is pre-bound to BACE-1, HS is able to lock the ligand into the active site (Scholefield*, et al.* 2003).

This study, coupled with the research to determine how differing structures of HS are able to inhibit BACE-1, led to conclusions that the principal means by which HS in able to inhibit the activity of BACE-1 is via binding to the secretase enzyme at, or near to the active site and in doing so either physically blocks the binding of the substrate to BACE-1, or possibly exerts a conformational change in BACE-1 that precludes substrate access. Previous research into the co-crystal structure of BACE-1 with a peptide isoster analogue (OM99-2) has previously revealed the presence of a hairpin loop that covers the active site of BACE-1 when not actively bound to its ligand (Hong*, et al.* 2000). The data collected in this study sits well with the notion of the binding of HS when BACE-1 is in its closed conformation. NMR and X-ray crystallography however would be required to fully confirm this notion (Scholefield*, et al.* 2003), though preliminary evidence from small angle X-ray scattering (SAXS) has identified a change in BACE-1 conformation that would be consistent with a conformational effect model (Turnbull, personal communication).

Alongside the observed interaction of HS and BACE-1, it has also been established that HS can interact with its substrate, APP. As such, the role of HS in BACE-1 cleavage pathways is somewhat of a complex one and suggests a further potential mechanism of inhibition of BACE-1 in that HS may be able to bind to APP and sequester it away from the BACE-1 active site, thus blocking its processing. Indeed, in light of the many interactions HS is able to make with the components of the amyloid processing pathway, it has been suggested that perhaps binding of HS to BACE-1 alone is not enough to achieve maximum inhibition but rather interaction with the native protein substrate is also an important factor to consider in this pathway (Scholefield*, et al.* 2003).

Now that research has identified the potential mechanisms by which HS is able to inhibit BACE-1 specifically, further work is needed to clarify the HS binding site in the BACE-1 enzyme. The structural characterisation of HS from AD and healthy age-matched control patients as described in chapter 2 may go some way to elucidate some of the structures that are responsible for this interaction between HS and BACE-1. Changes in the structure of HS as we have observed here may account for possible changes in the way in which HS is able to interact with BACE-1. Furthermore, previous research into the surface charge modeling of the known crystal structure of BACE-1 (Hong*, et al.* 2000) identified strongly basic regions that may serve as binding sites with which HS can interact. Changes in charge density of the HS chain as a result of changes in the pattern of sulfation along the chain for example may also go some way to provide a mechanism by which elevated BACE-1 activity is observed in AD patients. Finally, the conformational shape that HS may exhibit as a

result of specific structural features along its chain may too provide a physical mechanism by which it is able to interact with BACE-1 in an allosteric fashion.

4.4 Conclusions

In light of the advances made in this manner towards understanding the interaction of HS and BACE-1, as well as ways in which inhibitors may be used to target processing of APP, this project aimed to determine whether HS purified from AD patient brain samples was able to inhibit BACE-1 compared to the HS purified from age-matched control healthy counterparts. Now that it has been established that structural alterations in HS do occur with AD, we might hypothesise that this could have downstream consequences on the ability of HS to interact with and regulate BACE-1. Should the reported structural changes in HS in AD patient brain samples have consequences for BACE-1 inhibition efficacy, the notion of appropriately designed inhibitors of BACE-1 based on these changes will be strengthened. This chapter aimed to determine the BACE-1 inhibitory activity of HS from AD and healthy-age-matched control patients. In addition, the purified HS from aged and young mouse brain samples as analysed in chapter 2 were also assayed for BACE-1 inhibitory activity to determine whether the structural changes that occur with age have implications for BACE-1 activity.

4.5 Chapter Aims

- Investigate the BACE-1 inhibitory activity of HS purified from AD patient and healthy age-matched control human brain samples.
- Explore how manipulation of HS structure via knockdown of HS6ST and SULF enzymes in a cell-based system *in vitro* can regulate the activity of BACE-1 and ultimately the generation of Aβ by cells.
- Investigate how age may be implicated in BACE-1 inhibition efficacy by testing the BACE-1 inhibitory activity of HS purified from old and young mouse brains.
- Determine whether total knockdown of *Sulf* gene expression in a mouse model has consequences for BACE-1 inhibition efficacy.

4.6 Methods

4.6.1 Exploring the relationship between changes in endogenous HS structure and BACE-1 inhibition efficacy

4.6.1.1 Sample selection

The ability of HS to inhibit BACE-1 at differing concentrations was assessed from human AD (n=20) and healthy age-matched control (n=15) samples as described previously in chapter 2, as well as HS purified from old (n=5) and young (n=5) mice as detailed in chapter 2. In addition, mouse brain samples from *Sulf* KO mouse models (n=3) for each of *Sulf1* KO, *Sulf2* KO, Double KO and controls were analysed for their ability to block the activity of the BACE-1 enzyme. Having highlighted the importance of sulfation, in particular 6-O sulfation in BACE-1 inhibition, a mouse model that ablated all SULF activity was utilised to capitulate a scenario whereby HS is "highly" sulfated due to the absence of sulfatase activity at the 6-O position. *Sulf* KO mice were donated from Bielefeld University, Germany and were raised on a C57BL6/JRccHsd background. Mice were fed ad libitum and sacrificed at embryonic stage 18.5 (E18.5). Brains were removed immediately and snap frozen before being sent to the University of Liverpool.

4.6.1.2 FRET BACE-1 activity assay

FRET is a method employed to measure the transfer of energy from a donor fluorophore in an excited state to an appropriate acceptor fluorophore. The donor fluorophore, in an excited electronic state is able to transfer its energy to a nearby (this technique is distance dependent) acceptor chromophore and in doing so significantly reduces the fluorescence intensity. Disturbances in this intramolecular resonance energy transfer to the acceptor chromophore will disrupt fluorescence intensity and enhance the fluorescent signal emitted by the donor. The BACE-1 activity assay exploits the features of FRET by incubating the BACE-1 enzyme with its substrate, a peptide with a fluorescent tag linked to one end and a second, quencher tag on the other. When in its full-length form, the distance between the donor chromophore and quencher is small enough for energy transfer to occur, thus quenching the fluorescence intensity of the donor tag. Cleavage of the peptide by the BACE-1 enzyme however, separates the tag and quencher thus disrupting the resonance energy transfer and consequently enhances the fluorescent signal that can be measured. As such, Fluorescence intensity is a signal for the efficacy of BACE-1 cleavage activity. Addition of the heparan sulfate inhibitors will modulate this activity and alter these intensities accordingly.

This assay was carried out in a 96 well format and measured the fluorescence intensity of the cleaved BACE-1 substrate peptide after incubation in the presence of a selected HS (inhibitor) sample. 10µl of the substrate peptide (N-terminus: 5-FAM, C-terminus: Amide and Sequence: EVNLDAEFK) (Pepceuticals Limited, Leicestershire, UK) was added to 265µl assay buffer (20mM sodium acetate with 0.1% Triton X-100 pH 4.5. 0.2µm filtered). Followed by a further 1:8 dilution in assay buffer for addition of 10µl of peptide to each well to be assayed. The BACE-1 enzyme (R+D systems 931-AS 50mg – reconstituted to 500µg/ml in sterile deionised water) was diluted 1:500 in

assay buffer for addition of 25µl per test well and kept on ice until needed. For the heparin inhibition curve, samples were prepared at 5.0µg/ml and diluted 1:2 sequentially to a final concentration of 0.16µg/ml. To note, addition of 20µl of heparin samples in a final well volume of 100µl, resulted in a 1:5 dilution of all samples so final working concentrations of heparin samples ranged from 1.0µg/ml to 0.03µg/ml. Finally, HS samples purified from mouse samples was prepared at either 10.0, 5.0, 2.5 or 1.25 µg/ml with a final working concentration of 2.0, 1.0, 0.5 or 0.25 µg/ml and human samples to a final working concentrations of 2.0, 1.0, 0.2 or 0.02 µg/ml.

To each well, 45µl of assay buffer was added, followed by 20µl of inhibitor (heparin standards or HS purified from tissue), 25µl of enzyme, and 10µl of peptide. All samples were assayed in triplicate. A no inhibitor control (65µl of assay buffer, 25µl of enzyme and 10µl of peptide) and substrate control (90µl assay buffer and 10µl of substrate) were also set up in triplicate. The plate was sealed with a cover, protected from the dark and incubated for 2hr at 37°C. Following incubation, 100µl of stop solution (2.5M sodium acetate, 0.2µm filtered) was added to each well to stop the reaction. The plate was then read using a FRET endpoint 488/520nm protocol (**Figure 4.1**).

4.6.1.3 Statistical Analysis

BACE-1 activity was calculated as a percentage relative to a no-inhibitor control (100%). All test cases were carried out in triplicate. For human AD (n=10) and healthy age-matched control samples (n=10), mean (±S.E.M) % BACE-1 activity was plotted as a bar graph and Two-Way ANOVA with multiple comparisons used to calculate the statistical difference between mean BACE-1 % activity of AD and control samples at each concentration of HS. This was true also for the old and young mice derived HS studied. For the *Sulf* KO mice, *Sulf1* KO (n=3), *Sulf2* KO (n=3), Double KO (n=3) and control mice (n=3) were tested for mean (±S.E.M) % BACE-1 activity in the presence of purified HS in the same manner, however a One-Way ANOVA with multiple comparisons was used to assess changes in BACE-1 activity between control mice and knockout models at each concentration of HS assayed.

4.6.2 Exploring whether modulation of HS structure *in cellulo* is able to regulate generation of the toxic Aβ peptide

4.6.2.1 Transfection

All transfection experiments were carried out using human embryonic kidney cells modified to expression the Swedish APP mutation (overexpression of APP). HEKSweAPP cells were kindly donated by the Hooper Lab at the University of Manchester. Cells were maintained in Dulbecco's

Modified Eagled Medium (DMEM) (Gibco, Thermo Fisher, UK) supplemented with fetal bovine serum (FBS), 1mM L-glutamine (Gibco, UK) and 1% penicillin G/streptomycin (Gibco, UK).

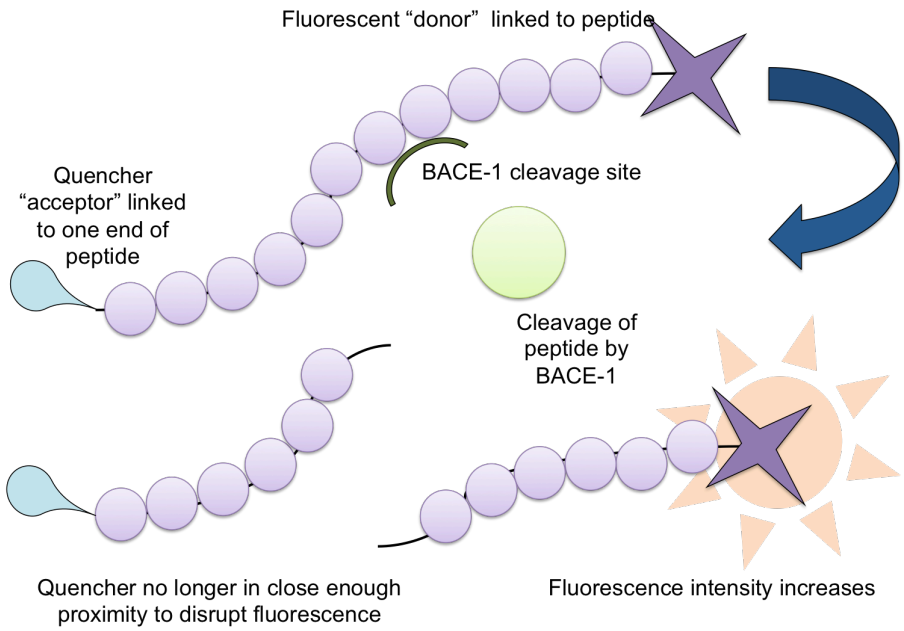

Figure 4.1: FRET based assay to assess BACE-1 inhibition efficacy by HS samples. The BACE-1 substrate peptide is tagged at both ends. On one, a fluorescent tag and at the other, a quencher. Due to a intramolecular resonance energy transfer phenomenon, so long as the quencher is in close proximity (i.e. the peptide remains intact), the intensity of the fluorescent tag is significantly reduced. Upon cleavage, the spatial proximity of the quencher and fluorescent tag is disrupted and the fluorescence intensity of the tag is enhanced for detection. Incubation of the BACE-1 enzyme and peptide substrate with HS inhibitors will attenuate this fluorescent signal.

24hr before transfection, $6x10^4$ HEKSweAPP cells were plated in 400µl of (DMEM) (Gibco, Thermo Fisher, UK) growth medium and FBS *without* antibiotics per well (all experiments were carried out in 24 well plates). Cells were ~90% confluent at the time of transfection. For each of the sample wells to undergo transfection RNAi-Lipofectamine™ 2000 (Thermo Fisher, UK) complexes were prepared as follows. Per well, 100pmol of RNAi (Silencer Select RNAi, Ambion, Thermo Fisher, UK) (**Table 4.1**) was diluted in 50µl of Opti-MEM® reduced serum medium (Gibco, Thermo Fisher, UK) and mixed gently. Additionally, per well, 1µl of Lipofectamine™ 2000 was diluted in 50µl of Opti-MEM® reduced serum medium, mixed gently and incubated at room temperature for 15min. "Scrambled" RNAi (Stealth™ RNAi Negative Control Duplexes, Invitrogen, Cat no: 12935-100) was used as an internal control for the transfection and was selected based on the GC content of the gene to be knocked down (**Table 4.2**).

Following incubation, the diluted RNAi (or scrambled RNAi for the control wells) and the diluted Lipofectamine™ 2000 were combined and mixed gently before a further 15min incubation at room temperature to allow complexes to form. After incubation, 106µl of the RNAi-Lipofectamine™ 2000 complexes were added to each well containing cells and medium and the plate gently mixed.

Plates were incubated at 37°C in a humidified CO_2 incubator for 6hr to allow transfection to take place. At this time, medium was removed and discarded and replaced with fresh DMEM (Gibco, Thermo Fisher, UK) growth medium and antibiotics as described previously. Transfection studies were carried out over a 72hr time period with 24hr timepoints. At designated timepoints (24, 48 and 72hr), cells and media were collected, as described below and prepared in preparation for qRT-PCR to confirm knock down and ELISA to quantify the concentration of Aβ present within the media.

4.6.2.2 Extraction of cells and RNA

Cells at appropriate timepoints were collected according to manufacturer's instruction for Roche High Pure RNA Isolation kit (Roche, UK Cat no: 11 828 665 001). Briefly, 200µl of PBS was added to each well to be collected followed by 400µl of lysis-binding buffer. A cell scraper was used to remove cells from the well and collected in an Eppendorf before vortexing for 15s. Samples were then transferred to a high pure filter tube and centrifuge for 15s at 8,000 x g. After centrifugation, the flow-through liquid was discarded and the filter tube and collection tube re-assembled. Following this, 10µl of DNase I was added to 90µl of DNase incubation buffer and added to the glass filter fleece in the upper reservoir of the filter tube and incubated for 15min at room temperature. Following incubation, 500µl of washer buffer I was added and centrifuged for 15s at 8,000 x g. The flow through was discarded and 500µl of wash buffer II added and centrifuged again for 15s at 8,000 x g. The flow through was discarded again and was followed by 200µl of washer buffer II and centrifuged at maximum speed for 2min. Finally, the RNA was eluted by adding 50µl of elution buffer to the upper reservoir and the assembly centrifuged for 1min at 8,000 x g. The RNA was quantified using the Nano Drop™ 2000c (Thermo Fisher Scientific, UK) and stored at -80°C until needed for qRT-PCR.

Table 4.1: Details of silencer RNAi used for transfection experiments. 5 genes were studied individually, *HS6ST1*, *HS6ST2*, *HS6ST3, SULF1* and *SULF2*. All RNAi was purchased from Ambion, Life Technologies; product codes are outlined below.

Gene	Type of RNAi	Ambion Cat no:	Concentration per well in 50µl media	GC content
HS6ST1	Silencer	AM51331	100pmol	48%
HS6ST2	Silencer	AM16708	100pmol	14%
HS6ST3	Silencer	AM16708	100pmol	9%
SULF1	Silencer	AM16708	100pmol	43%
SULF2	Silencer	AM16708	100pmol	43%

Table 4.2: Details of "scrambled" RNAi duplexes used as internal controls for each transfection experiment. Appropriate control RNAi was selected based on the GC content of the target gene RNAi used in each instance. RNAi duplexes were purchased from Invitrogen.

RNAi Negative Control Duplex	%GC	Suitable for use with RNAi duplexes containing %GC	Suitable as control for target genes
Low GC	36	35-45%	SULF1, SULF2, HS6ST2, HS6ST3
Medium GC	48	45-55%	HS6ST1
High GC	68	55-70%	n/a

4.6.2.3 Extraction of media

Total media was collected at time points as outlined above and frozen at -80°C until required for analysis by ELISA. All media samples were diluted 1:10 for all ELISA protocol steps.

4.6.2.4 Manual quantitative real time polymerase chain reaction (qRT-PCR)

All qRT-PCR steps were carried out as described earlier in chapter 3, section 3.3.1.1. Only expression analysis of the gene knocked down in each experiment (**Table 4.1**) was carried out. All primers used and protocol design was identical to that used in chapter 3, section 3.3.1.1 also.

qRT-PCR was performed using the LightCycler® 480 Roche machine (Roche, UK). Expression levels were normalised to Glyceraldehyde 3-Phosphate Dehydrogenase (*GAPDH*) levels and the delta delta Ct method was used to calculate the relative change in expression of the HS biosynthetic genes of interest from samples, assuming primer efficiency. All analyses were expressed as the fold change of expression of the gene of interest relative to the internal control in the treated samples as compared with the controls. Using the Ct method of analysis allowed fold changes of expression to be calculated for each gene of interest at each time point with respect to the treated state normalised to internal controls. All qRT-PCR reactions were carried out in triplicate. Experimental triplicates were combined and the mean (±S.E.M) calculated and data for individual samples were also averaged. Values of $2^{-\Delta\Delta Ct}$ were logged to generate positive and negative values indicative of up- and down-regulated expression of target genes.

4.6.2.5 ELISA protocol

$A\beta_{1-42}$ peptide was quantified from media following transfection to identify possible regulation of the generation of this toxic species. An amyloid beta 42 ELISA kit for Human samples (Cat no: KHB3441, Thermo Fisher, UK) was used to quantify levels of this peptide in media samples

collected during transfection experiments. The kit was used according to manufacturer's instructions.

Briefly, human beta-amyloid standards 1-42 were reconstituted with 1ml of peptide standard reconstitution buffer to 1000mg/ml final concentration and hydrated for 10min. Standards were then aliquoted in 100µl per vial and stored at -80°C until needed. The mouse monoclonal anti-beta-amyloid 1-42 coated plate was then assembled according to sample number and a standard curve of 9 serial dilutions of the amyloid beta standards set up from 1000pg/ml to 15.63pg/ml. Dilutions were prepared with standard dilution buffer as provided by the ELISA kit. Media samples collected from each timepoint were diluted 1:10 in standard dilution buffer also. 50µl of either $A\beta_{1-42}$ standards (as part of the concentration curve) or media samples were pipetted (in duplicate) into test wells of the plate.

Following preparation of the standard curve and test samples, 50µl of detection antibody solution was then added to all wells to be assayed and the plate tapped gently to mix. The plate was then covered with an adhesive plate cover, and incubated for 3hr at room temp with gentle shaking throughout.

Following incubation, assay wells were aspirated and washed 4x with a 1x wash buffer (as diluted from the 25x stock included in kit). Next, an anti-rabbit IgG HRP solution was prepared. Per 8 well strip of the assay plate used, 10µl of the 100X Anti-Rabbit IgG HRP solution was added to 1ml of HRP diluent. 100µl of the diluted anti-rabbit IgG HRP solution was then added to each assay well before recovering the plate with a plate cover and incubating for 30min at room temp. After 30min, wells were aspirated and washed again 4x as previously before addition of 100µl of stabilized chromagen to each well, causing a colour changes from clear to blue. The plate was then covered with a plate cover and incubated in the dark for 30 min at room temp. Following incubation, 100µl of stop solution was added to each well and the plate tapped gently to mix. This mixing causes a colour change from blue to yellow. The absorbance (OD) of the plate was then measured at 450nm using a microplate absorbance reader (Multiskan EX, Thermo Fisher Scientific, UK) within 30 min of adding the stop solution.

4.6.2.5.1 Analysis of ELISA data

Mean absorbance values for the Aβ peptide standard curve were calculated and a calibration curve plotted using linear regression curve fit and a threshold value for R2 of 0.98 used for accuracy. The straight-line equation was determined and used to calculate average concentrations of each of the test media samples and multiplied by 10 to account for dilution factor. Concentrations of Aβ standards from the media were then plotted as bar graphs over the time

course of the transfection experiment to observe changes in its regulation over time. Transfection experiments were carried out in triplicate and assayed with ELISA as duplicates. Mean (±S.E.M) differences between timepoints were determined using a Student's t-test.

4.7 Results

4.7.1 Exploring the relationship between changes in endogenous HS structure and BACE-1 inhibition efficacy

Varying concentrations of purified HS from AD and age-matched control samples, aged and young mouse brain samples and mouse *Sulf* KO brain samples, were incubated in the presence of a fluorescently labeled peptide to assess inhibition of the BACE-1 enzyme. Previous work has already established that HS is able to interact with and inhibit BACE-1, and so this part of the project aimed to determine how known changes in the structure of HS (as already identified in chapter 2), may be implicated in the ability of HS to regulate BACE-1.

4.7.1.1 AD and age-matched control healthy human brain sample HS

HS extracted and purified from human AD (n=10) and age-matched control samples (n=10) was incubated at varying concentrations, 0.02, 0.2, 1.0 and 2.0µg/ml with the BACE-1 enzyme and fluorescently tagged peptide. Each HS sample was assayed in triplicate and mean (±S.E.M) % BACE-1 activity was calculated relative to a no inhibitor control (100%). Potent inhibitory activity of a positive control, heparin, was noted at 1.0µg/ml (~35% of no inhibitor control; **Figure 4.2**). A dose dependent decrease in % BACE-1 activity in the presence of healthy age-matched control HS was observed (**Figure 4.2**).

In contrast, HS purified from human AD (n=10) samples displayed a reduced ability to block the activity of the BACE-1 enzyme particularly at higher concentrations. No significant inhibition of BACE-1 by HS from AD patient brain samples was observed at any dose (**Figure 4.2**). At the highest dose tested, 2.0µg/ml, HS from AD patient brain samples incubated with BACE-1 and substrate peptide displayed mean (±S.E.M) % BACE-1 activity of 90.02% (±7.81). This differed significantly to that of age-matched control HS samples at this concentration (55.30% (±4.00)) (p=0.004, Two-Way ANOVA with multiple comparisons), indicating reduced inhibitory activity of BACE-1 of HS from AD patients. At all concentrations assayed, inhibition of BACE-1 by HS was found to be less than in the presence of heparin (data not shown).

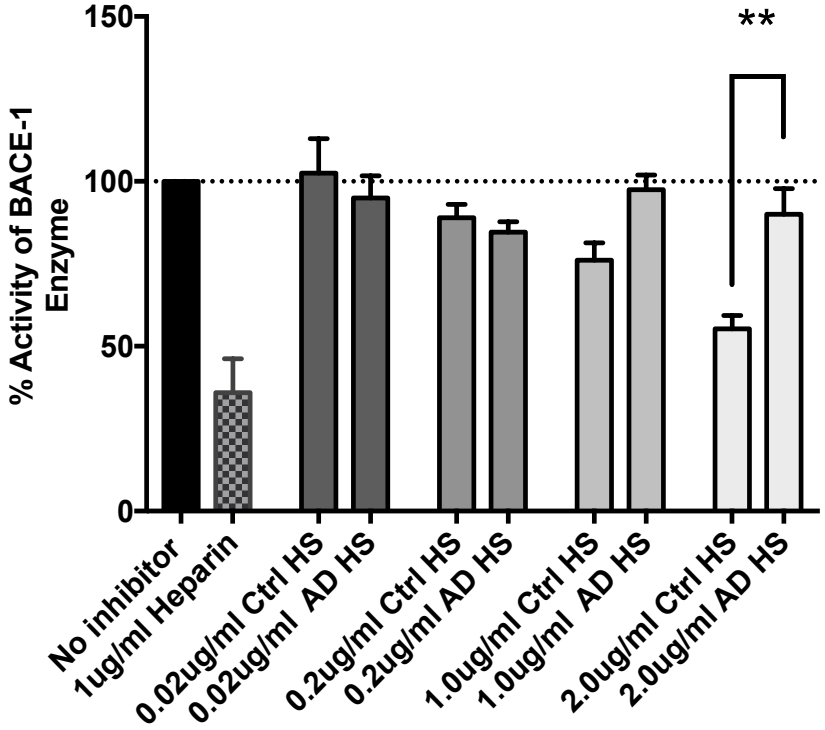

Figure 4.2: BACE-1 inhibition efficacy by HS is reduced in AD. HS extracted and purified from AD (n=10) and age-matched healthy controls (n=10) was incubated at varying concentrations with the BACE-1 enzyme and the fluorescently tagged substrate peptide. At higher concentrations of 1.0µg/ml and 2.0µg/ml, HS from AD patient brain samples was less able to inhibit the BACE-1 enzyme, as evidenced by elevated mean (±S.E.M) % BACE-1 activity. At 2.0µg/ml, the difference in BACE-1 inhibition efficacy was significantly different between AD and healthy age-matched control samples. All samples were assayed in triplicate and mean (±S.E.M) % BACE-1 activity calculated relative to an internal no inhibitor control (100%). $p<0.05$ *, $p<0.01$ **, Two-Way ANOVA with multiple comparisons.

4.7.1.2 Aged vs. young mouse brain samples

HS extracted from aged (18 month) (n=5) and young (3 month) (n=5) mouse brain samples was incubated with the BACE-1 enzyme and fluorescently tagged peptide at varying concentrations, identical to that of the AD and control HS samples. Each HS sample was assayed in triplicate and mean (±S.E.M) % BACE-1 activity was calculated relative to a no inhibitor control (100%). HS from aged and young brain samples was compared at each concentration for its ability to block the action of the BACE-1 enzyme. Unexpectedly, the lowest concentration of HS tested, 0.25µg/ml, elicited the most potent inhibition of BACE-1 with recorded mean (±S.E.M) % BACE-1 activity for young and aged HS of 57.20% (±4.39) and 18.04% (±2.28) respectively. Aged HS at this concentration was notably more able to inhibit BACE-1 as highlighted by the considerably reduced BACE-1 % activity. This change was found to be statistically significant ($p=0.0004$, Two-Way ANOVA with multiple comparisons). At 0.5µg/ml, HS from young mouse brain samples (n=5) reduced % BACE-1 activity to 74.48% (±4.86) and to, 72.68% (±5.58) from aged samples; this difference was not found to be statistically significant ($p=0.999$). No significant inhibition of BACE-1 was observed at higher

concentrations. Overall lower concentrations of HS in this instance were found to be most effective at inhibiting BACE-1 activity. Indeed, aged mouse brain HS samples at these concentrations proved more efficacious as a BACE-1 inhibitor compared to younger mouse brain HS samples (**Figure 4.3**).

4.7.1.3 Sulf KO mouse model brain samples

Following the finding that AD patient HS was functionally less able to inhibit the action of the BACE-1 enzyme and aged mouse HS was more able to block BACE-1 activity it was hypothesised that alterations in 6-O sulfation may be implicated in these effects. Studies were thus carried out to evaluate how mouse models exhibiting knockout of either (or both) *Sulf1* or *Sulf2* genes (compositional profiling detailed in **Appendix B**) were able to regulate BACE-1 activity (since these mice do not express the SULF enzymes, they express HS that is more highly 6-O sulfated). HS was purified from d18.5 embryonic mice (as described in methods) and tested in BACE-1 inhibitory assays. In control mice and all of the *Sulf* KO groups (*Sulf1* KO, *Sulf2* KO and Double KO mice), a dose dependent increase in mean (±S.E.M) % BACE-1 activity was recorded indicating a reduction in inhibition efficacy by these embryonic HS samples with increasing concentration. In addition, at the

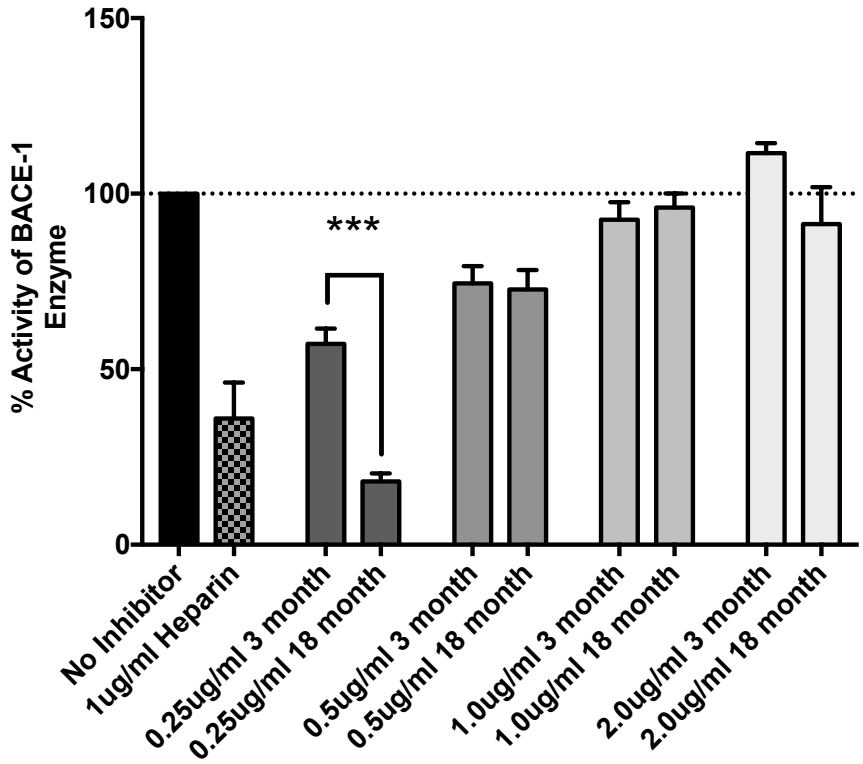

Figure 4.3: BACE-1 inhibition efficacy by HS is increased with age at low concentrations. HS extracted and purified from aged (n=5) and young (n=5) mice brain samples was incubated at varying concentrations with the BACE-1 enzyme and the fluorescently tagged substrate peptide. At 0.25µg/ml, HS from aged mouse brain samples was more able to inhibit the BACE-1 enzyme, as evidenced by reduced mean (±S.E.M) % BACE-1 activity. These differences were less apparent at higher concentrations, whereby BACE-1 activity was not reduced in the presence of HS from either aged or young mouse brain samples. All samples were assayed in triplicate and mean (±S.E.M) % BACE-1 activity calculated relative to an internal no inhibitor control (100%). $p<0.05$ *, $p<0.01$ **, $p<0.001$ *** , Two-Way ANOVA with multiple comparisons.

highest concentrations, 1.0 and 2.0µg/ml, HS extracted from the *Sulf* KO mouse model brain samples appeared to activate the BACE-1 enzyme by ~20% with mean (±S.E.M) % BACE-1 activity values greater than 100%. At all concentrations assayed (apart from 0.25 µg/ml), HS from *Sulf1* KO mice did not reveal any inhibitory activity but rather activation.

In contrast, the *Sulf2* KO mice, at lower concentrations of 0.25µg/ml and 0.5µg/ml, displayed strong inhibition of the BACE-1 enzyme with recorded mean (±S.E.M) % BACE-1 activity values of 54.66% (±3.46) and 68.62% (±8.34) at each respective concentration. Indeed, at this concentration, the HS from *Sulf2* KO mouse model brain samples exhibited the highest BACE-1 inhibition efficacy with the lowest mean (±S.E.M) % BACE-1 activity values recorded. When compared to HS from control mouse brain samples at 0.5µg/ml, % BACE-1 activity in the presence of 0.5µg/ml HS from *Sulf2* KO mouse samples were significantly decreased (p=0.035 One-Way ANOVA with multiple comparisons). This difference was not found to be significant between control and *Sulf2* KO mice at 0.25µg/ml.

Double KO mouse model HS at 0.25µg/ml also displayed strong inhibitory action against the BACE-1 enzyme, similar to that of heparin (a known potent inhibitor of HS) with mean (±S.E.M) % BACE-1 activity of 40.84% (±3.44). This was greatly reduced vs. control mouse HS tested at this concentration (71.35% (±10.09) however did not reach statistical significance on this occasion (p=0.763). HS extracted from Double KO mice brain samples exhibited the greatest degree of sulfation as a consequence of knockout of both the *Sulf1* and *Sulf2* genes, indicative of a highly sulfated HS with greater ability to inhibit BACE-1. The *Sulf2* KO mice displayed a similar profile of HS inhibition suggesting HS from these mice is, at the right concentration, an effective BACE-1 inhibitor.

The *Sulf1* KO mouse model derived HS samples did not display BACE-1 inhibition efficacy. At all concentrations of HS from these mice assayed, mean (± S.E.M) % BACE-1 activity was greater than 100%, indicating possible activation of the BACE-1 enzyme in the presence of HS extracted and purified from these samples. However, none of these differences were statistically significant. This data indicates that SULF1 has less or no impact on the BACE-1 inhibitory activity of HS. Similarly, at 0.5, 1.0 and 2.0µg/ml concentrations, the activity of BACE-1 in the presence of HS purified from control mice samples was potentially slightly raised through these differences were not statistically significant (**Figure 4.4**).

4.7.2 Exploring whether modulation of heparan sulfate structure *in cellulo* is able to regulate generation of the toxic Aβ peptide.

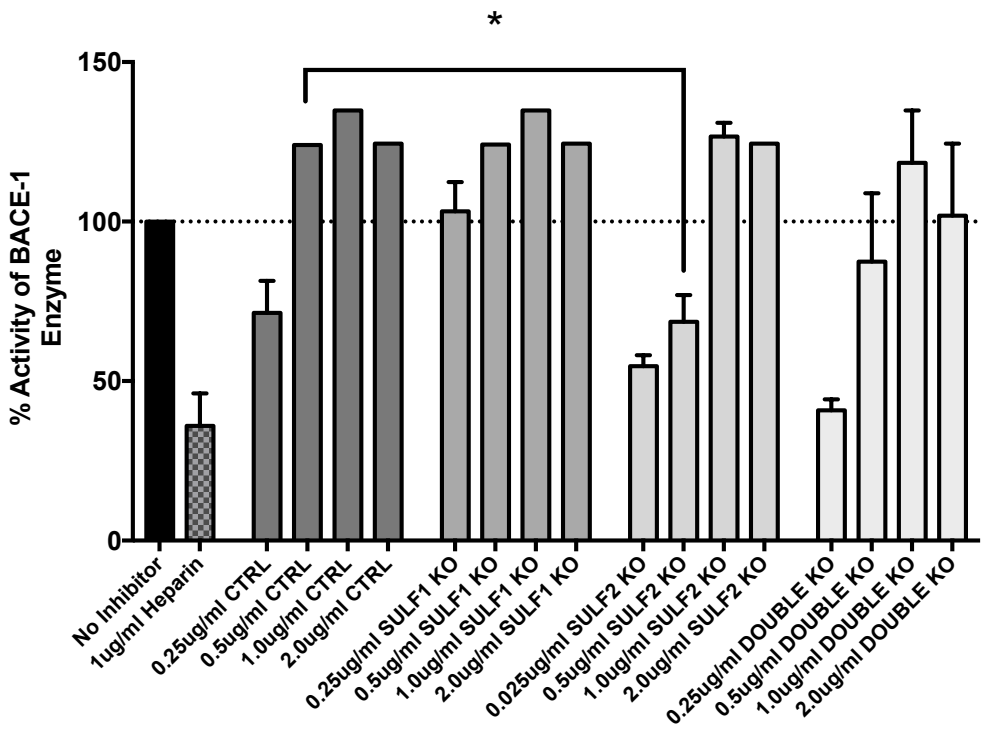

Figure 4.4: BACE-1 inhibition efficacy by HS is increased in *Sulf2* and Double *Sulf* KO mice brain samples at low concentrations. HS extracted and purified from *Sulf1* KO (n=3), *Sulf2* KO (n=3), Double *Sulf* KO (n=3) and control (n=3) mice brain samples was incubated at varying concentrations with the BACE-1 enzyme and the fluorescently tagged substrate peptide. At lower concentrations of 0.25 and 0.5ug/ml, HS from *Sulf2* and DOUBLE *Sulf* KO mouse brain samples was more able to inhibit the BACE-1 enzyme, as evidence by decreased mean % BACE-1 activity. All samples were assayed in triplicate and mean (± S.E.M) % BACE-1 activity calculated relative to an internal no inhibitor control (100%). p>0.05*, One-Way ANOVA with multiple comparisons.

The above data provided evidence that endogenous *in vivo* HS from AD patient brain samples has altered structure and reduced ability to inhibit BACE-1 *in vitro*. To explore this mechanism further cell culture models were employed, using human embryonic kidney cells expressing the Swedish mutant form of APP. The focus was knockdown of genes involved in controlling 6-O sulfation in HS.

4.7.2.1. Aβ$_{1-42}$ peptides accumulate in a time-dependent manner in cultured HEKSweAPP cells.

Before knockdown of selected genes, a time course of the Aβ$_{1-42}$ peptide accumulation was recorded to assess rising levels of this oligomer within the media of culture HEKSweAPP cells with time without any experimental knockdown of genes. Cultured cells displayed a time dependent accumulation of Aβ$_{1-42}$ peptide within the media up to 72hr with mean (±S.E.M) peptide levels rising from 496.50 (±9.92) pg/ml at 24hr to 1141.00 (±65.63) pg/ml over the full course of the experiment. Accumulation of the toxic Aβ species in this manner would be expected over time and set a baseline to compare the effects of gene knockdown upon these levels (**Figure 4.5**).

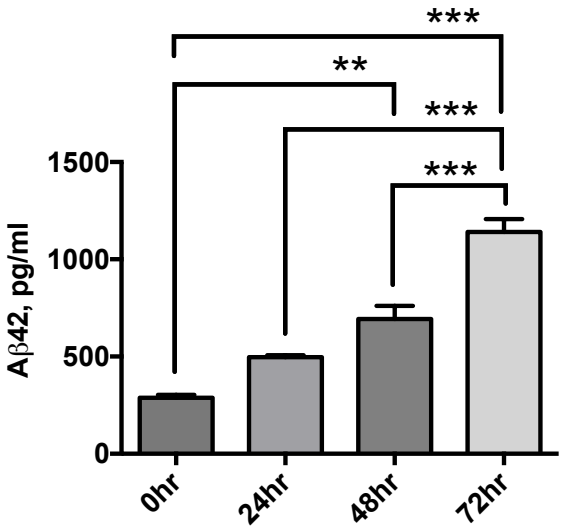

Figure 4.5: Time course of $A\beta_{1-42}$ accumulation in HEKSweAPP cells. Before knockdown of target genes, a time course was carried out to investigate baseline accumulation of toxic $A\beta_{1-42}$ species within the media of cultured HEKSweAPP cells. Cultured cells displayed a time dependent increase in the accumulation of $A\beta_{1-42}$ with significant (One-way ANOVA) differences in the quantity (pg/ml) of Aβ at specified time points. All data points are representative of triplicate experiments tested in triplicate with ELISA. Error bars represent mean ± S.E.M.

4.7.2.2 Knockdown of the HS6ST1 gene in cultured HEKSweAPP cells does not affect generation of the toxic $A\beta_{1-42}$ peptide.

Cultured HEKSweAPP cells were incubated with Lipofectamine 2000 and *HS6ST1* pre-validated RNAi complexes, and media and cells collected at specified time points. Cells were collected and the RNA extracted for qRT-PCR analysis to assess success of knockdown of the *HS6ST1* gene with transfection. Following this, media samples were analysed by ELISA to quantify total levels of the $A\beta_{1-42}$ generated by the HEKSweAPP cells. Expression of the *HS6ST1* gene was calculated by normalising the change in expression with both the housekeeping *GAPDH* gene and relative to untreated controls using the delta delta Ct method.

Analysis revealed a decreased expression of the *HS6ST1* gene across a 72hr time period with mean (±S.E.M) $\log_2$ fold change of expression of -1.607 (±0.25), -1.72 (±0.66) and -1.54 (±0.66) at 24, 48 and 72hr respectively. Decreased expression as reported here was indicative of successful transfection whereby the expression of the *HS6ST1* gene had been knocked down appropriately (**Figure 4.6A**). ELISA analysis to quantify total levels of $A\beta_{1-42}$ within media collected at each timepoint revealed no statistically significant changes in the abundance of the $A\beta_{1-42}$ peptide, with similar levels of Aβ generated at each timepoint (**Figure 4.6B**). These results indicate that decreased expression of the *HS6ST1* gene does not result in elevated levels of the $A\beta_{1-42}$ peptide. At 48hr, the

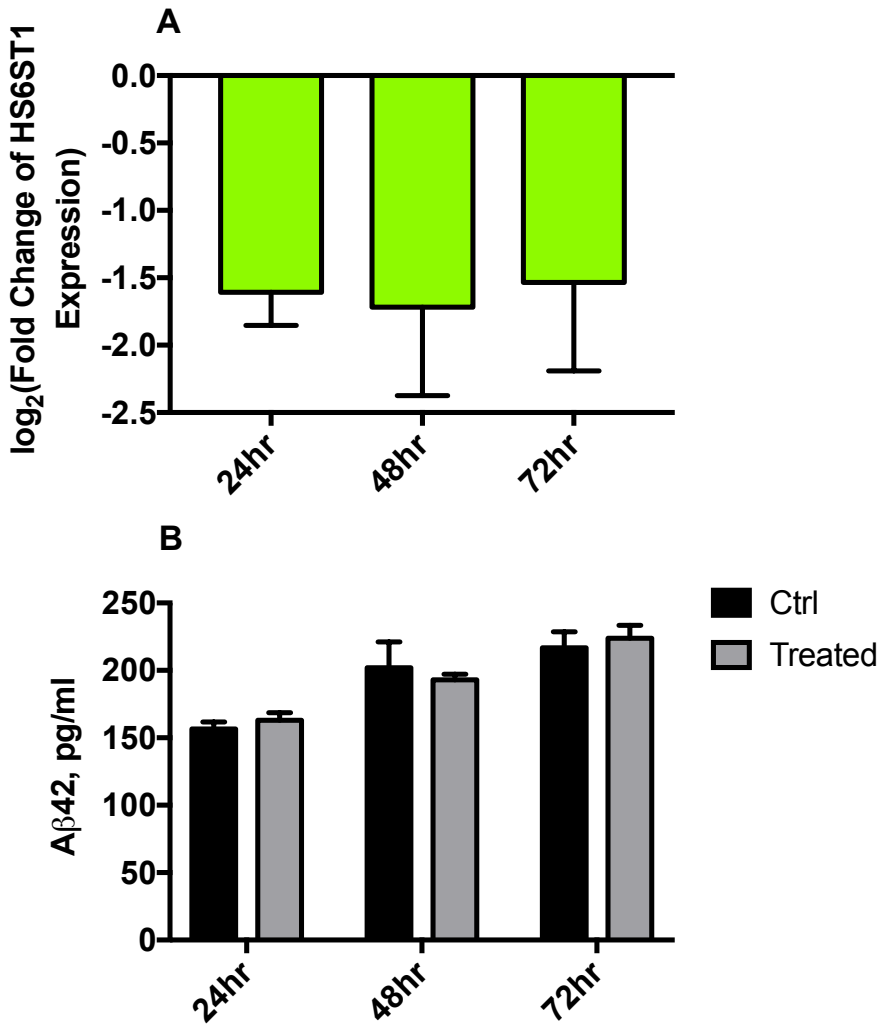

Figure 4.6: Knockdown of the *HS6ST1* gene in cultured HEKSweAPP cells results in no effect on the generation of the toxic $A\beta_{1-42}$ peptide. 6A: Cultured HEKSweAPP cells were incubated with *HS6ST1* RNAi and Lipofectamine 2000 complexes to knockdown the expression of the *HS6ST1* gene. Cells and media samples were collected for analysis over a 72hr time period at 24hr time points. qRT-PCR was used to confirm success of transfection. Fold changes in expression of the *HS6ST1* gene were calculated relative to the housekeeper *GAPDH* gene and relative to untreated controls. **6B**: ELISA was used to quantify total levels (pg/ml) of the $A\beta_{1-42}$ peptide within the media samples collected at each timepoint. Changes in relative abundance of the $A\beta_{1-42}$ peptide were recorded between treated and untreated cells following knockdown of the *HS6ST1* gene. All qRT-PCR data points are representative of n=3 assayed in triplicated and all ELISA data points are representative of n=3 assayed in duplicate. All data points represent mean (±S.E.M).

opposite trend was recorded whereby treated wells displayed higher levels of $A\beta_{1-42}$ vs. their untreated counterparts (**Figure 4.6B**).

4.7.2.3 Knockdown of the HS6ST2 gene in cultured HEKSweAPP cells results in significantly reduced generation of the toxic $A\beta_{1-42}$ peptide

Cultured HEKSweAPP cells were incubated with Lipofectamine 2000 and *HS6ST2* pre-validated RNAi complexes, and media and cells collected at specified time points. Analysis of qRT-

PCR data to assess success of transfection revealed a decrease in the expression of the *HS6ST2* gene over the 72hr time period with mean (±S.E.M) $\log_2$ fold change of expression of -1.77 (±0.41), -1.80 (±0.35) and -0.87 (±0.98) at 24, 48 and 72hr respectively. Decreased expression of the *HS6ST2* gene as reported here was indicative of successful transfection whereby the expression of the *HS6ST2* gene had been knocked down appropriately (**Figure 4.7A**).

ELISA analysis to quantify total levels of $A\beta_{1-42}$ within media collected at each timepoint revealed changes in the abundance of the $A\beta_{1-42}$ peptide following knockdown of the *HS6ST2* gene. At all timepoints, cells treated with *HS6ST2* gene knockdown were found to produce reduced mean (±S.E.M) levels of the $A\beta_{1-42}$ peptide vs. their untreated cell counterparts. At the 24hr timepoint, treated cells had generated a 166.39 (±0.41) pg/ml $A\beta_{1-42}$ whilst untreated cells at this timepoint had generated 172.51 (±2.16) pg/ml $A\beta_{1-42}$. This difference was found to be statistically significant (p=0.050, Student's t-test). At 48hr, this difference was still evident whereby treated cells displayed decreased levels of the $A\beta_{1-42}$ peptide vs. their untreated counterparts with mean (±S.E.M) levels of $A\beta_{1-42}$ of 186.37 (±5.09) pg/ml and 227.56 (±15.64) pg/ml respectively; however, this difference was just short of statistical significance (p=0.066, Student's t-test). No difference was observed at the 72hr timepoint (**Figure 4.7B**).

4.7.2.4 Knockdown of the HS6ST3 gene in cultured HEKSweAPP cells results in significantly reduced generation of the toxic Aϐ$_{1-42}$ peptide

Cultured HEKSweAPP cells were incubated with Lipofectamine 2000 and *HS6ST3* pre-validated RNAi complexes, and media and cells collected at specified time points. Analysis of qRT-PCR data to assess success of transfection revealed a decrease in the expression of the *HS6ST3* gene over the 72hr time period with mean (±S.E.M) $\log_2$ fold change of expression of -3.15 (±2.50), -0.84 (±0.39) and -0.55 (±0.89) at 24, 48 and 72hr respectively. Decreased expression of the *HS6ST3* gene as reported here was indicative of successful transfection whereby the expression of the *HS6ST3* gene has been knocked down appropriately at 24 and 48hr (**Figure 4.8A**).

Using quantification by ELISA, all timepoints displayed a reduction in levels of the $A\beta_{1-42}$ peptide in treated cells vs. their untreated counterparts at respective time points (**Figure 4.8B**). At 24hr, treated cells had generated mean (±S.E.M) 286.94 (±2.32) pg/ml of the $A\beta_{1-42}$ whilst untreated cells recorded 303.50 (±5.38) pg/ml. This difference was found to be statistically significant (p=0.048 Student's t-test). At 48hr, knockdown of the *HS6ST3* gene generated reduced levels of the $A\beta_{1-42}$ peptide in treated cells vs. untreated controls with mean (±S.E.M) recorded levels of $A\beta_{1-42}$ of 379.00 (±8.37) pg/ml and 502.72 (±27.07) pg/ml in treated and untreated control cells respectively (p=0.012, Student's t-test). Finally, at 72hrs, cells treated with *HS6ST3* RNAi complexes were still found to generate reduced levels of the $A\beta_{1-42}$ peptide with respective mean (±S.E.M) levels in

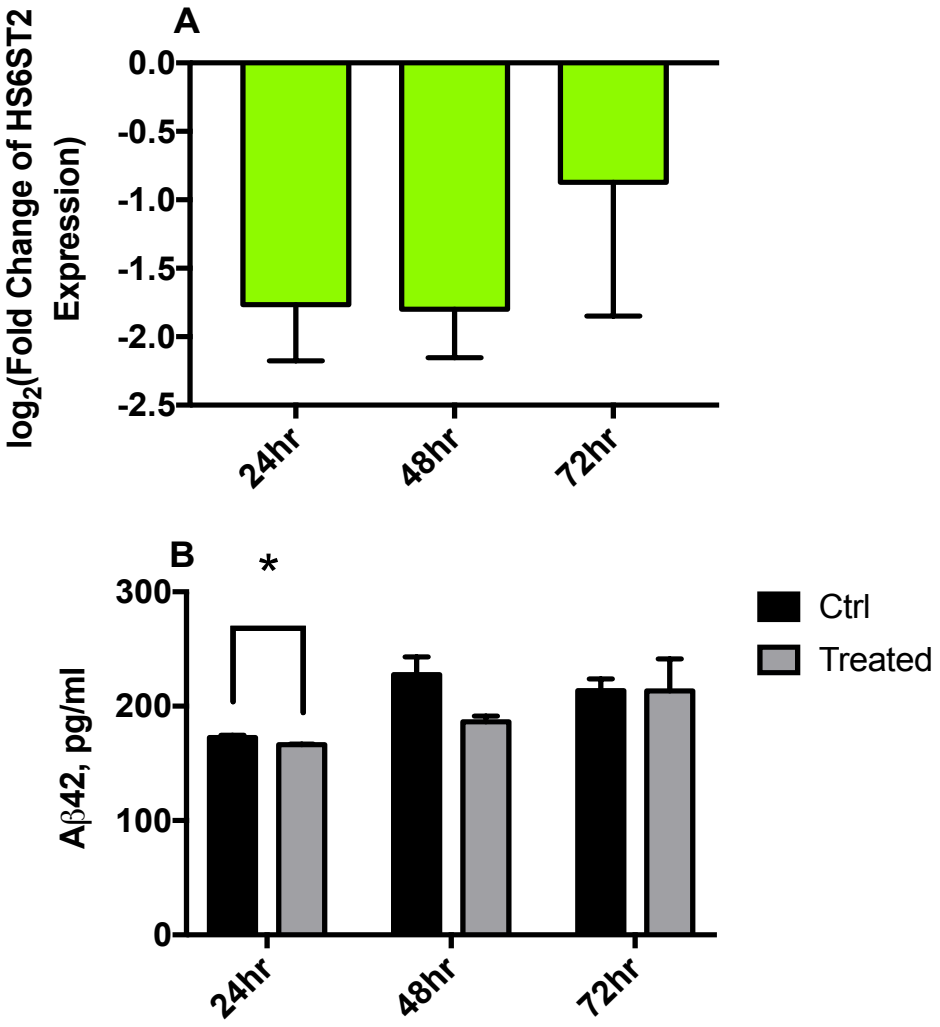

Figure 4.7: Knockdown of the *HS6ST2* gene in cultured HEKSweAPP cells results in reduced generation of the toxic $A\beta_{1-42}$ peptide. 7A: Cultured HEKSweAPP cells were incubated with *HS6ST2* RNAi and Lipofectamine 2000 complexes to knockdown the expression of the *HS6ST2* gene. Cells and media samples were collected for analysis over a 72hr time period at 24hr time points. qRT-PCR was used to confirm success of transfection. Fold changes in expression of the *HS6ST2* gene were calculated relative to the housekeeper *GAPDH* gene and relative to untreated controls. **7B**: ELISA was used to quantify total levels (pg/ml) of the $A\beta_{1-42}$ peptide within the media samples collected at each timepoint. Changes in relative abundance of the $A\beta_{1-42}$ peptide were recorded between treated and untreated cells following knockdown of the *HS6ST2* gene. All qRT-PCR data points are representative of n=3 assayed in triplicate and all ELISA data points are representative of n=3 assayed in duplicate. All data points represent mean (±S.E.M). $p<0.05$ *, Student's t-test.

treated and untreated cells of 559.35 (±20.66) pg/ml and 638.92 (±82.89) pg/ml, though this difference was not found to be statistically significant (p=0.404, Student's t-test) (**Figure 4.8B**).

4.7.2.5 Knockdown of the SULF1 gene in cultured HEKSweAPP cells results in significantly reduced generation of the $A\beta_{1-42}$ peptide

Analysis of qRT-PCR confirmed an initial decrease in the expression of the *SULF1* gene over

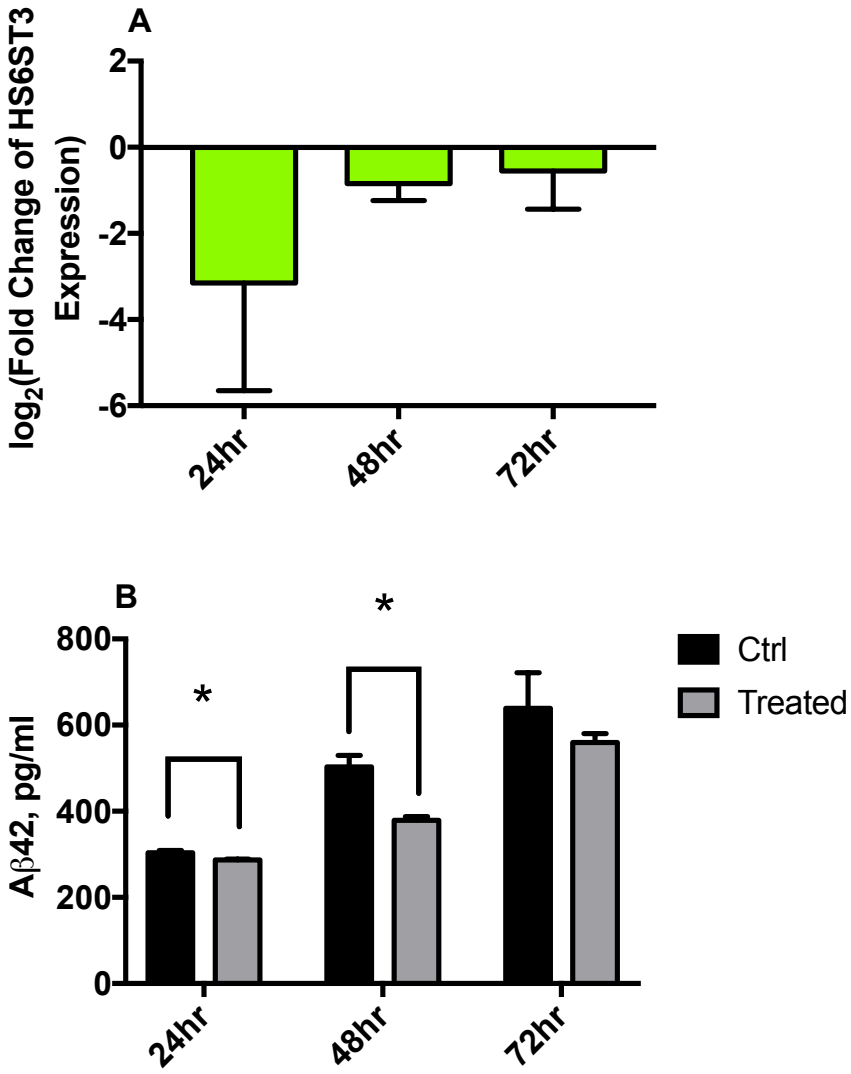

Figure 4.8: Knockdown of the *HS6ST3* gene in cultured HEKSweAPP cells results in reduced generation of the toxic $A\beta_{1-42}$ peptide. 8A: Cultured HEKSweAPP cells were incubated with *HS6ST3* RNAi and Lipofectamine 2000 complexes to knockdown the expression of the *HS6ST3* gene. Cells and media samples were collected for analysis over a 72hr time period at 24hr time points. qRT-PCR was used to confirm success of transfection. Fold changes in expression of the *HS6ST3* gene were calculated relative to the housekeeper *GAPDH* gene and relative to untreated controls. **8B**: ELISA was used to quantify total levels (pg/ml) of the $A\beta_{1-42}$ peptide within the media samples collected at each timepoint. Changes in relative abundance of the $A\beta_{1-42}$ peptide were recorded between treated and untreated cells following knockdown of the *Hs6st3* gene. All qRT-PCR data points are representative of n=3 assayed in triplicate and all ELISA data points are representative of n=3 assayed in duplicate. All data points represent mean (±S.E.M). $p<0.05$ *, Student's t-test.

a 48hr time period, followed by an increase by 72hr (perhaps indicative of the transfection effects lessening) with mean (± S.E.M) $\log_2$ fold change of expression of -9.66 (±5.61), -10.85 (±9.09) and 10.26 (±1.35) at 24, 48 and 72hr respectively (**Figure 4.9A**).

ELISA analysis to quantify total levels $A\beta_{1-42}$ within media collected at each timepoint revealed changes in the abundance of the $A\beta_{1-42}$ peptide following knockdown of the *SULF1* gene. At 24hr, treated cells were found to display similar levels of the $A\beta_{1-42}$ peptide vs. untreated cells at

this timepoint with mean (±S.E.M) abundance values of 248.93 pg/ml (±32.06) and 234.96 pg/ml (±12.10) in treated and untreated cells respectively. At 48 and 72hr timepoints however, treated cells displayed reduced levels of the $A\beta 1_{-42}$ peptide indicative of decreased processing of the APP protein as a consequence of knockdown of the *SULF1* gene. At 48hr, media collected from treated and untreated cells displayed mean (±S.E.M) levels of $A\beta_{1-42}$ of 267.55 pg/ml (±13.11) and 360.66 pg/ml (±8.68) respectively, (p=0.011, Student's t-test). At the 72hr timepoint, there were no statistically significant difference (mean (±S.E.M) levels of $A\beta_{1-42}$ of 259.09 pg/ml (±37.77) and 293.79 pg/ml (±59.75) in treated and untreated cells respectively, (p=0.649, Student's t-test) perhaps reflecting the lack of knockdown of the *SULF1* gene at 72hrs (**Figure 4.9B**).

4.7.2.6 Knockdown of the SULF2 gene in cultured HEKSweAPP cells results in reduced generation of the $A\beta_{1-42}$ peptide

Finally, cultured HEKSweAPP cells were treated to knockdown the expression of the *SULF2* gene over a 72hr time period. Cells and media were collected as with other gene knockdown studies at 24hr timepoints to assess transfection success and the consequences of gene knockdown on the generation of the $A\beta_{1-42}$ peptide. Analysis by qRT-PCR confirmed a decreased in the expression of the *Sulf2* gene over a 72hr time period with mean $\log_2$ fold change of expression of -0.17 (± 0.83), -2.01 (± 0.71) and -1.90 (± 0.26) at 24, 48 and 72hr respectively. Reported decrease in expression as reported here confirmed that transfection had been successful and expression of the *SULF2* gene had been knocked down appropriately (**Figure 4.10A**).

ELISA analysis to quantify total levels of the $A\beta_{1-42}$ peptide within media collected at each timepoints revealed changes in the abundance of the $A\beta_{1-42}$ peptide following knockdown of the *SULF2* gene. At 24hr, the levels of $A\beta_{1-42}$ recorded in treated vs. untreated cells were not statistically significant, with mean (±S.E.M) levels of 205.99 (±1.70) pg/ml and 194.66 (±6.47) pg/ml respectively, (p=0.084, Student's t-test). At 48hr, media collected from treated and untreated cells displayed similar mean (±S.E.M) levels of $A\beta_{1-42}$ of 243.74 (±15.45) pg/ml and 256.48 (±4.93) pg/ml respectively, (p=0.476, Student's t-test). Similarly, at 72hr, levels of the $A\beta_{1-42}$ peptide vs. untreated cells had similar recorded levels of 276.77 pg/ml (± 3. 69) and 294.70 pg/ml (± 7.59) respectively, (p=0.101, Student's t-test) (**Figure 4.10B).**

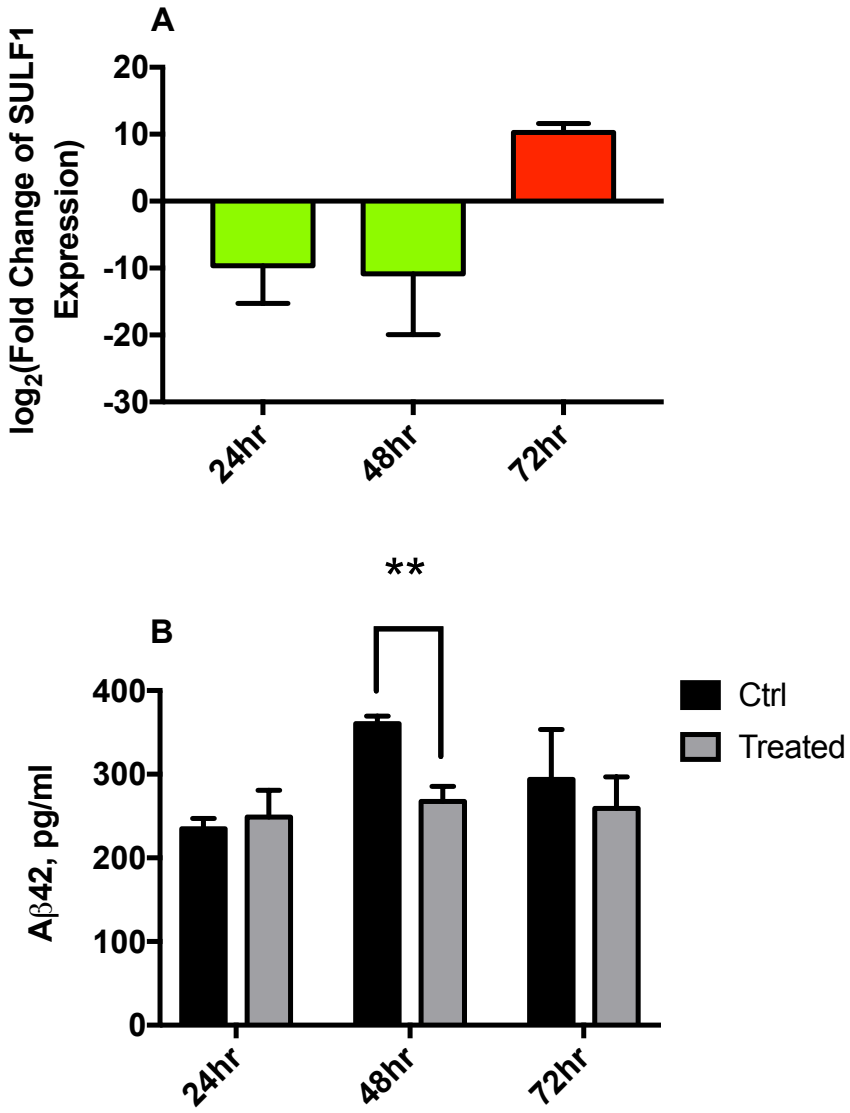

Figure 4.9. Knockdown of the *SULF1* gene in cultured HEKSweAPP cells results in reduced generation of the toxic $A\beta_{1-42}$ peptide at 48hrs. 9A: Cultured HEKSweAPP cells were incubated with *SULF1* RNAi and Lipofectamine 2000 complexes to knockdown the expression of the *SULF1* gene. Cells and media samples were collected for analysis over a 72hr time period at 24hr time points. qRT-PCR was used to confirm success of transfection. Fold changes in expression of the *SULF1* gene were calculated relative to the housekeeper *GAPDH* gene and relative to untreated controls. **9B**: ELISA was used to quantify total levels (pg/ml) of the $A\beta_{1-42}$ peptide within the media samples collected at each timepoint. Changes in relative abundance of the $A\beta_{1-42}$ peptide were recorded between treated and untreated cells following knockdown of the *SULF1* gene. All qRT-PCR data points are representative of n=3 assayed in triplicate and all ELISA data points are representative of n=3 assayed in duplicate. All data points represent mean (± S.E.M). $p<0.05$ * **,** $P<0.01$ **, Student's t-test.

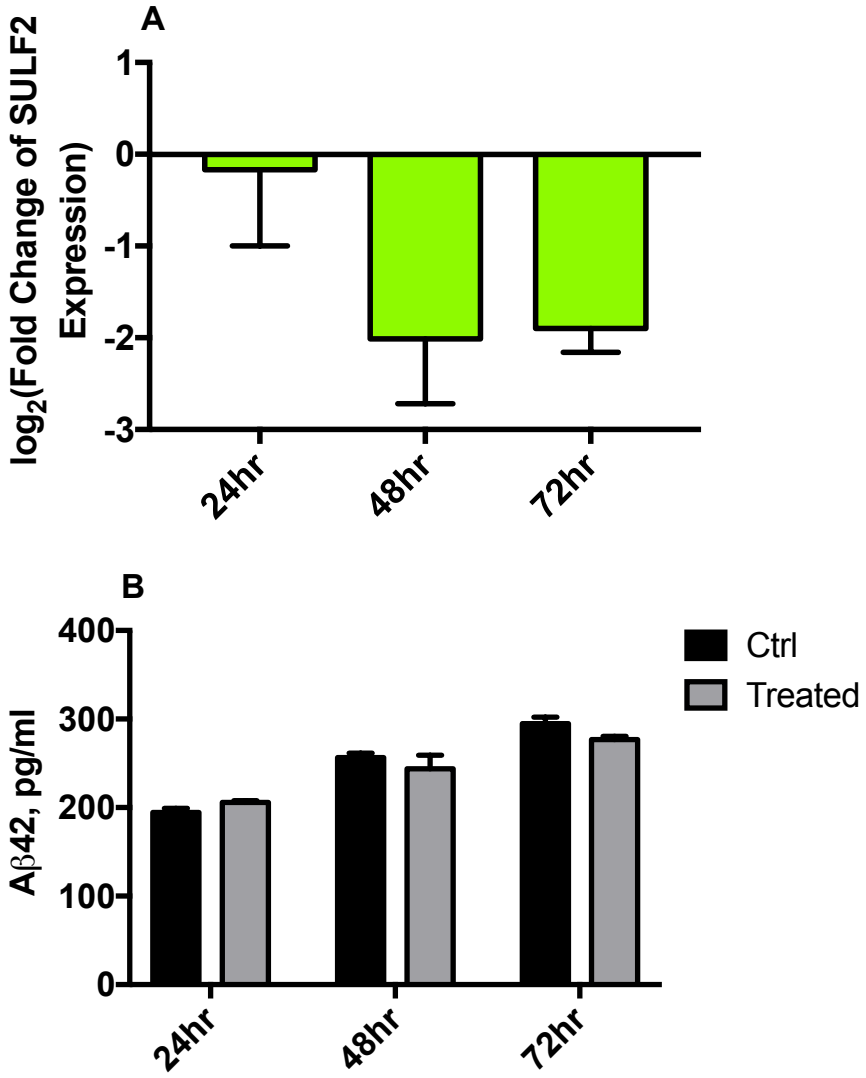

Figure 4.10: Knockdown of the *SULF2* gene in cultured HEKSweAPP cells results in reduced generation of the toxic $A\beta_{1-42}$ peptide. 10A: Cultured HEKSweAPP cells were incubated with *SULF2* RNAi and Lipofectamine 2000 complexes to knockdown the expression of the *SULF2* gene. Cells and media samples were collected for analysis over a 72hr time period at 24hr time points. qRT-PCR was used to confirm success of transfection. Fold changes in expression of the *SULF2* gene were calculated relative to the housekeeper *GAPDH* gene and relative to untreated controls. **10B**: ELISA was used to quantify total levels (pg/ml) of the $A\beta_{1-42}$ peptide within the media samples collected at each timepoint. Changes in relative abundance of the $A\beta_{1-42}$ peptide were recorded between treated and untreated cells following knockdown of the *SULF2* gene. All qRT-PCR data points are representative of n=3 assayed in triplicate and all ELISA data points are representative of n=3 assayed in duplicate. All data points represent mean (±S.E.M).

4.8 Discussion

4.8.1 Exploring the relationship between changes in endogenous heparan sulfate structure and BACE-1 inhibition efficacy

4.8.1.1 AD and age-matched control healthy human samples

HS extracted and purified from human AD (n=10) and age-matched control samples (n=10) was incubated with the BACE-1 enzyme and fluorescently tagged peptide at varying concentrations. A dose dependent decrease in % BACE-1 activity in the presence of healthy age-matched control HS was observed. A dose dependent decrease in BACE-1 activity is consistent with previous findings that HS is able to interact with, and inhibit BACE-1 (Scholefield, 2003). In contrast, HS purified from human AD samples displayed a greatly reduced ability to block the activity of the BACE-1. In particular, at the higher concentrations of 1.0 and 2.0µg/ml, HS from AD patient brain samples did not inhibit the BACE-1 enzyme whereas control HS was strongly inhibitory at these doses (**Figure 4.2**) and possibly is interesting in the context of the findings of chapter 2 that found that changes in the structure of HS with AD result in reduced sulfation vs. age-matched healthy counterparts. Reduced sulfation as observed would be indicative of HS that may be less able to inhibit BACE-1 (Patey*, et al.* 2006, Scholefield*, et al.* 2003). This hypothesis was confirmed here supporting the notion that structural changes in HS associated with AD have downstream implications on the efficacy of BACE-1 inhibition, and thus process most APP to form the toxic Aβ peptide. Loss of sulfate groups at various positions along the HS chain may affect the final structure of the HS chain and affect the way it is able to interact with the BACE-1 enzyme.

Previous research by Cui and colleagues (Cui*, et al.* 2016) found that AD Swe*App*Tg2576 mice, treated with enoxaparin, a low molecular weight heparin, displayed elevated levels of amyloid plaques compared to untreated controls. This data contrasted previous work that found that enoxaparin could reduce BACE-1 levels and Aβ peptide generation (Bergamaschini*, et al.* 2004, Cui*, et al.* 2011). The increased deposition of amyloid plaques in Tg2576 mice as reported here was not found to result from elevated BACE-1 expression or APP processing as one might expect. It may be that the heterogeneous molecular weights of the heparins that make up enoxaparin may account for diminished concentrations within the brain (larger chains will not effectively cross the BBB (Leveugle*, et al.* 1997)) that were too low to regulate APP processing fully. It may be also, that increased amyloid plaque burden as noted, may reflect decreased toxic Aβ species (arguably the most potent species linked to AD-related cognitive decline) and a shift in the relative ratios of Aβ42 and Aβ40. The conflicting results reported in these studies confirm the complexities of understanding AD pathogenesis and the mechanisms that underpin it. Creating a heparin derivative

that can be administered without anti-coagulant side effects, cross the BBB, inhibit BACE-1 and preclude fibrilisation of Aβ species is undoubtedly a challenge however currently unpublished work by Turnbull and colleagues (personal communication) have identified promising heparin derivatives (particularly N-acetylated chains) that upon administration, can cross the BBB and reduce plaque burden within AD mouse brain tissue. The challenges associated with standard heparins may account for some of the disparity reported here.

Interestingly, as observed in chapter 2, AD patient brain samples displayed significantly less total HS vs. their healthy age-matched control counterparts. The known role of HS in a number of different features of AD pathology, including its potential role in BACE-1 regulation and also amyloidogenesis, may all be affected by these overall reduced total levels of HS as described in chapter 2. As such, understanding the implications of changes in endogenous levels in this manner may help further elucidate the mechanisms by which HS is able to play important roles in AD pathogenesis.

4.8.1.2 Aged vs. young mouse brain samples

In contrast to the lack of inhibition of BACE-1 by HS from AD patient brain, low concentrations of HS from both aged and young mouse brain samples elicited the most potent inhibition of BACE-1. This result contrasts that observed with AD patient HS samples at low concentrations whereby incubation with HS at these concentrations did not result in any BACE-1 inhibitory action. This disparity may partly reflect the variability between HS from human and from mouse species samples, although control HS samples from healthy age-matched patients did inhibit BACE-1 (**Figure 4.3**). To study the effect of age on HS structure and its interaction with BACE-1, a young control was necessary, something difficult to obtain with human tissue samples. As such, a mouse model was most suitable to study this variable. Of course, there are therefore drawbacks with respect to alternate tissue sources. It has not previously been established whether HS derived from mouse brain is able to inhibit the BACE-1 enzyme so the observation here that thy can be potent inhibitors of the enzyme are entirely novel and warrant further studies. HS has been shown to be differentially regulated with respect to structure in different tissue regions (Warda*, et al.* 2006) hence one might expect HS structure to vary even more considerably across different species.

Having previously observed that AD HS (at 0.25µg/ml) is unable to block the action of BACE-1, one might have expected to observe a similar response in the case of aged HS compared to young HS, in light of the fact that age remains the greatest risk factor for the development of AD. In contrast, aged HS was better able to inhibit BACE-1 (**Figure 4.3**) Recent research has reported decreased levels of the microRNA-186 gene, *miR-186,* in ageing mouse cortices, and was also shown

to suppress the expression of BACE-1. It was concluded that miR-186 is a potent negative regulator of BACE-1 and as such, decreased expression of miR-186 with ageing, may induce up-regulation of BACE-1 within the brain and provide a molecular link between ageing and the onset and development of AD (Kim*, et al.* 2016). Our findings suggest the possibility that aged HS, even at low concentrations, is able to decrease BACE-1 activity. The role of HS as an inhibitor of BACE-1 may well sit entirely independently of changing BACE-1 levels with ageing and in AD; indeed the potential changes in HS with ageing may provide a protective "balancing" effect to control excessive BACE-1 activity. The observed increase in BACE-1 expression with ageing however further strengthens the notion that this is an important and potentially very potent target to block in efforts to treat AD.

In addition, a previous study by Fukumoto et al in 2004, reported increased activity of the BACE-1 enzyme in humans, monkeys and mice brain samples with ageing that correlated with enhanced levels of the $A\beta_{1-42}$ peptide in these brain samples (Fukumoto*, et al.* 2004). Based on our finding, it is possible that aged brain HS at high concentrations could enhance the activity of BACE-1 leading to elevated Aβ levels. The overall role HS may play in regulating activity of BACE-1 in aged samples has not yet been studied and as such our study's findings are novel; more studies will be necessary to full understand the mechanisms involved.

4.8.1.3 SULF KO mouse model brain samples

Surprisingly in all of the *Sulf* KO groups, a reciprocal relationship between % BACE-1 activity was noted. Indeed, at the highest concentrations, (1.0 and 2.0µg/ml), HS extracted from the *Sulf* KO mouse model brain samples appeared to activate the BACE-1 enzyme with activity values slightly greater than 100%. Furthermore, HS from *Sulf1* KO mice did not demonstrate inhibitory activity at any of the doses tested but rather activation. Activation of the BACE-1 enzyme as recorded here indicates a potential balance between both inhibition and activation of BACE-1 and may suggest some kind of biphasic relationship between HS and BACE-1. Research in 1997 reported the role of heparin as a promoter of BACE-1 activity and subsequently the processing of APP (Leveugle*, et al.* 1997). Other findings indicated that heparin at similar high doses can activate the pro-enzyme form of BACE-1 (Beckman*, et al.* 2009). These findings coupled with more recent work that reported the role of HS in the inhibition of BACE-1 (Scholefield*, et al.* 2003) may suggest that abundance of HS within the cells is important in determining the effects it has on the BACE-1 activity component of AD pathology.

In contrast, the *Sulf2* KO mice, at lower concentrations (0.25µg/ml and 0.5µg/ml), displayed strong inhibition of the BACE-1 enzyme. Indeed, at these concentrations, the HS from *Sulf2* KO mouse model brain samples exhibited the highest BACE-1 inhibition efficacy recorded in the experiments here. When compared to HS from control mouse brain samples at 0.5µg/ml, % BACE-1

activity in the presence of 0.5µg/ml HS from *Sulf2* KO mouse samples were significantly decreased. The strong inhibitory effect as exhibited by *Sulf2* KO mice in this manner indicates that the influence of the SULF2 enzyme is the more prominent of the two enzyme isoforms. Indeed, *Sulf1* KO mice do not display any major abnormality whilst mice deficient in both the *Sulf1* and *Sulf2* gene display significant renal and skeletal deficits (Lamanna*, et al.* 2006) suggesting the action of SULF2 is key in HS modification and resultant functionality. Deficiencies in brain HS have also been noted as being different between *SULF1* and *SULF2* indicating that these genes are not redundant and may only partially overlap (Kalus*, et al.* 2015).

Double KO mouse model HS at 0.25µg/ml also displayed strong inhibitory activity against the BACE-1 enzyme, similar to that of heparin (a known potent inhibitor of HS). Consistent with this, HS extracted from Double KO mice brain samples exhibited the highest degree of sulfation as was expected due to knockout of both the *Sulf1* and *Sulf2* genes. Double knockout of both the *Sulf1* and *Sulf2* genes in this manner would totally negate post-biosynthetic removal of sulfate groups at the 6-O position hence we would expect it to exhibit strong inhibitory action as described here. However, at high concentrations activation of BACE-1 activity was again observed and is suggestive of a biphasic regulation of BACE-1 activity (Leveugle*, et al.* 1997, Scholefield*, et al.* 2003). It will clearly be important to undertake further studies on lower doses of these HS species to examine more complete dose response relationships.

4.8.2 Exploring whether modulation of heparan sulfate structure *in cellulo* is able to regulate generation of the toxic Aβ peptide

ELISA revealed no statistically significant changes in the abundance of the $A\beta_{1\text{-}42}$ peptide following knockdown of the *HS6ST1* gene however; there was a recorded trend at the 24 and 72hr timepoints for an increase in the $A\beta_{1\text{-}42}$ peptide with respect to untreated controls. A trend for enhanced levels of this peptide would be consistent with the notion that knockdown of the *HS6ST1* gene may result in reduced inhibition of BACE-1 and thus elevated processing of the APP precursor to generate the $A\beta_{1\text{-}42}$ peptide. Reduction of the expression of the *HS6ST1* gene as induced via knockdown in this instance may result in decreased translation of the HS6ST1 enzyme though this was not confirmed at the protein level. This in turn may have implications for the addition of sulfate groups at the 6-O position and as such, generate a lesser sulfated HS less able to inhibit the BACE-1 enzyme (Patey*, et al.* 2006). The absence of statistically significant changes in the BACE-1 inhibitory activity of this HS may however be confounded by altered expression of other HS6ST enzymes, compensating for decreased expression of the *HS6ST1* gene. The HS6ST3 enzyme is known to display variable substrate specificity (Esko and Selleck 2002) and this could go some way to explain why more dramatic effects on processing of APP were not observed. Further studies to examine whether

compensatory increases in HS6ST2 or HS6ST3, or other sulfation enzymes are occurring, alongside changes in their protein levels, are clearly warranted, along with analysis of the HS structures produced in those cells.

Interestingly, TaqMan® analysis of the expression of genes that encode HS biosynthetic enzymes (as detailed in chapter 3), revealed a significant up-regulation of the expression of the *HS6ST1* gene. Elevated expression of this gene, we would hypothesise, would elicit enhanced sulfation of HS causing increased inhibition efficacy for the BACE-1 enzyme. Despite this, we observed decreased sulfation of actual HS products (chapter 2) and reduced ability for this HS to inhibit the BACE-1 enzyme. In light of this, one might question how much of a role HS6ST1 may play in the changes to HS observed with AD. Perhaps its isoform, HS6ST2 and HS6ST3 play more central roles in the changes associated with this disease. Knockdown of this gene alone therefore, may not be sufficient to elicit significant effects on the processing of APP and the generation of the $A\beta_{1-42}$ peptide. Furthermore, the situation may be more complex depending on the interplay of multiple enzymes to alter the functional capacity of HS.

ELISA analysis to quantify total levels of $A\beta_{1-42}$ within media following knockdown of the *HS6ST2* reduced levels of the $A\beta_{1-42}$ peptide vs. their untreated controls at respective timepoints. At the 24hr timepoint, this difference was found to be statistically significant, perhaps indicative of early, more pronounced effects of the transfection. Knockdown of the *HS6ST2* gene, we hypothesised, would result in reduced 6-O sulfation of the HS chain that would ultimately confer reduced inhibition of BACE-1 and enhanced levels of the $A\beta_{1-42}$ peptide. This result therefore contradicted our hypothesis. Again, knockdown of this gene in isolation may be insufficient to elicit a consistent or expected response. Total knockout of the *Hs6st2* gene in mice in previous studies reported normal development with no significant abnormality and raises the question of the potency this enzyme exhibits with respect to HS modification and its resultant functionality (Nagai*, et al.* 2013). Again, there may well be compensatory changes in other HS6STs and the broader biosynthetic machinery that confound over-simplistic interpretation of this data.

TaqMan® array analysis as detailed in chapter 3, reported a decrease in expression of the *HS6ST2* gene. This finding partially mimics the knockdown as established in this experiment and so we might expect the results observed in the HEKSweAPP cells to infer what might occur in the body. Our findings suggest that HS modification is more complex than originally thought and that knockdown of individual genes in isolation may not be suitable to test for modulation of the processing of APP and production of the $A\beta_{1-42}$ peptide. Naturally, we cannot know for certain the enzyme turnover rates with respect to knockdown of gene expression, and how this translates into changes in protein levels and ultimately enzyme activity. It is possible that at the timepoints studied,

knockdown may have not efficiently negated presence of the HS6ST2 enzyme and its activity with respect to modification of the HS chain.

Finally, knockdown of expression of the *HS6ST3* gene revealed reduced levels of the $A\beta_{1-42}$ peptide vs. their untreated controls at respective timepoints. As with the *HS6ST2* gene, knockdown of the *HS6ST3* gene, would, we hypothesised, reduce the translation of the HS6ST3 enzyme, and as such, reduce the sulfation of the HS chain at the 6-O position. As a consequence, we hypothesised that a lesser-sulfated HS as generated in this scenario would be less able to block the action of BACE-1, and ultimately result in elevated levels of the $A\beta_{1-42}$ peptide. Observation therefore of reduced levels of the $A\beta_{1-42}$ peptide, suggests that knockdown of *HS6ST3* alone is not sufficient to modify HS and $A\beta_{1-42}$ production.

In addition, whilst it has been reported previously that 6-O sulfation is necessary for potent BACE-1 inhibition efficacy, it may be that the overall structure and conformation of HS, i.e. the combination of 6-O sulfated motifs and other features of the HS chain together, may be necessary to elicit the appropriate structures to regulate BACE-1 activity. Single gene knockdown as carried out in these initial studies may not be sufficient to mimic the changes that occur with AD to modulate the production of the $A\beta_{1-42}$ peptide. Detection of very subtle changes as induced by knockdown of only single genes may not be possible in this context. Knockdown for example of the *HS6ST3* gene alongside full expression of the NDST enzymes may negate the consequences of knockdown, due to currently unknown compensation mechanisms to re-establish a functional HS chain following disruption in expression of genes encoding HS biosynthetic machinery.

Analysis of the consequences of the HS modification enzymes, SULF1 and SULF2 was carried out to investigate other means by which 6-O sulfation of HS may be important for BACE-1 inhibition. Knockdown of both the *SULF1* and *SULF2* genes resulted in a reduction (or at least a trend for reduction) in levels of the $A\beta_{1-42}$ peptide suggesting knockdown of these genes was sufficient to modulate the structure of HS and its interaction with the BACE-1 enzyme. The sulfatase enzymes are responsible for the removal of sulfate groups at the 6-O position. Knockdown of the *SULF1* and *SULF2* genes, we hypothesised, would enhance the overall sulfation of the HS chain, making it more able to inhibit BACE-1 and thus reduce the formation of the toxic $A\beta_{1-42}$ peptide. Therefore the reduced levels of $A\beta_{1-42}$ supported our hypothesis and are consistent with 6-O sulfation as a key determinant in BACE-1 inhibition efficacy. The action of SULF enzymes is known to fine tune the final structure of HS after all biosynthetic modification events are complete; as such, they can confer very subtle changes in functionality with big consequences on HS ligand binding affinity (Morimoto-Tomita*, et al.* 2002). Knockdown of these genes therefore may elicit more substantial effects on HS structure compared to knockdown of other genes. Further studies to confirm expected changes in HS structure in the SULF knockdown cells are clearly warranted.

4.9 General conclusions

In conclusion, this work has established that changes in the structure of HS (as determined in chapter 2), resulting from changes in expression of the genes encoding the HS biosynthetic machinery (as described in chapter 3) have direct implications on the ability of HS to interact with and inhibit the activity of the BACE-1 enzyme. AD sample HS was shown to be less able to inhibit BACE-1, confirming the notion that changes in the structure of HS are implicated in APP processing by BACE-1 and production of the $A\beta_{1-42}$ peptide *in vivo*. Furthermore, the observation that changes in the structure of HS with ageing linked with enhanced BACE-1 inhibition in aged mouse brain samples may also indicate separate pathways by which BACE-1 activity is regulated in ageing and in AD. Understanding the mechanisms by which HS is able to interact with BACE-1 and the implications this has for development of AD pathogenesis and in ageing is undoubtedly complex, but this data strengthens the connection between HS and roles in AD pathogenesis.

Furthermore, this chapter has identified that controlled modulation of the endogenous structure of HS in cultured HEKSweAPP cells can regulate the production of the $A\beta_{1-42}$ peptide. Knockdown of the *SULF* genes were found to decrease levels of $A\beta_{1-42}$, supporting our hypothesis that modulation of HS can alter its BACE-1 inhibitory activity, and result in altered accumulation of the toxic oligomers that pre-dispose the development of mature amyloid plaques in AD patient brains. Naturally, we cannot assume a direct correlation between gene expression and protein translation, or indeed enzyme activity of the final protein; however, changes in HS may have significant implications for its ability to interact with BACE-1. Moreover, knockdown of genes as described in this chapter may also have consequences for the functions of HS and in other pathogenic features of AD such as amyloid aggregation. Decreased sulfation of HS induced by knockdown of the *HS6ST* genes, whilst not necessarily directly regulating production of $A\beta_{1-42}$, may have other implications on how HS induces fibrilisation of toxic oligomers into mature plaques (van Horssen*, et al.* 2003) for example. It is also important to note that these experiments were only focused on determining changes in the abundance of the $A\beta_{1-42}$ peptide. It may be that changes in endogenous HS structure as induced by gene knockdown may not effect levels of the $A\beta_{1-42}$ but rather $A\beta_{1-40}$ peptides that also result from processing of the APP precursor (LaFerla*, et al.* 2007). Future studies to assess changes in this peptide may also help to elucidate the role of HS in APP processing. Likewise, the sAPPβ and C99 fragment, the first products of APP processing before final cleavage by γ-secretase, may also change with alteration to endogenous HS structure. As such further work may be needed to explore the mechanisms by which HS is able to modulate BACE-1 activity and how structural changes may affect this interaction.

Finally, these preliminary experiments naturally did not look into the potentially very complex interactions between specific HS-related gene isoforms and the ways in which disturbances

to one gene may be compensated for by another. Detecting very small changes may be made even harder by the masking effects that compensation of this nature may have. Future studies to determine combinatorial roles of HS-related genes, especially the 3 HS6ST isoforms, will prove particularly useful in further understanding the ways in which modulation of endogenous HS can be exploited to regulate production of amyloid species. Despite these added complexities, this work has confirmed not only a role for HS in modulating the activity of BACE-1 and the formation of the Aβ peptide in AD, but also establishes an argument for the fine tuning of HS structure that may significantly modulate the APP processing pathways and amyloid accumulation within the brains of AD patients. Finding ways to exploit these structural motifs may be key in developing effective AD therapies in the future.

Chapter 5: Bioinformatics and pathway analysis to explore the wider role of heparan sulfate in Alzheimer's disease

5. Chapter 5

5.1 Introduction

5.1.1 The use of bioinformatics in research

With the huge growth and speed of technological advances in scientific research, the output of data has grown also with large throughput data sets becoming the norm. With this growth come new challenges in the ways in which this data can be stored and analysed. Bioinformatics, including large-scale data analysis, has now become common practice in all fields of scientific research from structural biology to gene expression studies. As early as 2000, SWISS-PROT databases of protein sequences were reported to be doubling in size approximately every 15 months (Benson*, et al.* 2000). Furthermore, as of 2011, The Genomes On Line Database (GOLD) has reported information for 11,472 sequencing projects, of which 2,907 have been completed and published for public consumption (Pagani*, et al.* 2012). Similarly, genome-sequencing projects are often accompanied by studies to investigate gene expression, elucidate protein structure and study protein network interactions and in combination, result in complex data sets that must be appropriately digested and analysed. Large datasets as described here are best suited to computer based analytical techniques and software has been developed to aid the processing of large datasets. Furthermore, data of this kind is largely becoming publically available allowing a number of projects to assess gene expression changes in multiple diseases, sequencing data for a number of organisms and structural information for a variety of target proteins.

5.2 The aims of bioinformatics

Ultimately, the aim of bioinformatics as a research tool is to allow comparison, classification and systematic storage of complex and often large data sets. Types of data may include biological structures, functions and correlations discovered via experimental or computational studies. The Protein Data Bank (PDB) is an example of this, the database for the 3D structures of selected proteins (Bernstein*, et al.* 1977) (Berman*, et al.* 2000). Furthermore, meta-analysis of existing data can largely complement a focused experimental research project and the data that may be generated from this work. In essence, the world of the classified and stored biological meta-data can be, and is, constantly validated, updated and refined. Queries that may originate from the specific need of a research project may be able to utilise existing data in a novel way such that these datasets may help answer questions which they were not previously originally intended to address.

There is a large variety of data that may be mined and analysed with the use of various tools and software. These include raw DNA sequence data sets, protein sequences, macromolecular structures, genome sequences and gene expression data. The ways in which this data may be mined with bioinformatics is many-fold and are highlighted in **Table 5.1**.

Table 5.1: Bioinformatics tools. Table to highlight the variety of datasets more commonly available in biological research and the bioinformatics projects that may be employed to utilise these datasets. Information taken and adapted from table in (Luscombe*, et al.* 2001).

Dataset	Uses for dataset with bioinformatics
Raw DNA sequence	• Separation of coding and non-coding regions • Identification of introns and exons • Gene product prediction • Forensic analysis
Protein sequence	• Sequence comparison algorithms • Multiple sequence alignment algorithms • Identification of conserved sequence motifs
Macromolecular structure	• Secondary and tertiary structure prediction of proteins • 3D structural alignment algorithms • Protein geometry measurements • Surface and volume shape calculations • Intermolecular interactions • Molecular simulations (force-field calculations, molecular movements and docking predictions)
Genome sequence	• Characterisation of repeats • Structural assignments to genes • Phylogenetic analysis • Genomic-scale censuses (characterisation of protein content, metabolic pathways and prediction of functional interactions) • Linkage analysis relating specific genes to diseases, anatomical and structural features and experimental conditions
Gene expression	• Correlating expression patterns to validate potential of interactions between proteins and to suggest possible regulators • Mapping expression data to sequence structural and biochemical data

5.3 Types of datasets that may be mined with bioinformatics

5.3.1 Raw DNA and genome sequences

The advent of the availability of genome sequences has proved one of the most exciting advances in scientific research. Databases such as GenBank (Benson*, et al.* 2000), EMBL (Baker*, et al.* 2000) and DDBJ (Okayama*, et al.* 1998) are all examples of databases that contain DNA sequences for the genes that encode a variety of proteins. In a similar fashion, the Entrez database (Tatusova*, et al.* 1999) is a repository for all of the complete and partially complete genomes that have been elucidated so far and allows users to investigate sequencing at a number of different levels of detail including, chromosomes, non-coding and coding regions all the way down to the sequences for single genes. Detailed annotations are also available within these datasets regarding sequence alignments between proteins and genes as well as information regarding functionality of specific proteins, whether that be lab-validated or hypothesised. GeneCensus (Tatusova*, et al.* 1999) is a resource for studies at a higher level whereby reference between individual genomes may be made in order to gain insight from an evolutionary standpoint (Luscombe*, et al.* 2001).

5.3.2 Protein sequences

Protein sequence databases may be used to study and compare the sequences of an individual, or group of proteins of interest. SWII-PROT (Bairoch and Apweiler 2000) is a common repository for this information and may be used to determine the function of specific proteins as well as understand its domain structures and any post-translational modifications it may undergo upon synthesis. These databases may also be used to determine sequence conservation between groups of related proteins. The program PROSITE (Hofmann*, et al.* 1999) is the most popular for this alongside its ability to identify biologically relevant or active sites within the protein of interest. The PRINTs (Attwood*, et al.* 2000) software catalogues regions of conservation within families of proteins to predict confirmation and functions of newly discovered proteins. Understanding already established protein sequencing is key in underpinning novel protein structure and large databases that combine all current knowledge of protein sequencing information prove invaluable for protein identification projects. The PFAM (protein families) database (Finn*, et al.* 2016) is just one example of a large dataset of protein annotations and sequence alignments.

5.3.3 Macromolecular structures

The PDB (Berman*, et al.* 2000, Bernstein*, et al.* 1977) is perhaps the primary archive that exists for the study of 3D structures of proteins, RNA, DNA and a variety of complexes. In August

2000, there were approximately 13,000 structures solved by x-ray crystallography and NMR and in some cases, theoretical modeling alone. Structural analyses, schematic diagrams and information regarding interactions between different molecules can all be found in these repositories and may be used to elucidate structural and evolutionary relationships between novel and pre-established protein structures. There exist also specialised databases, for example the Nucleic Acids Database (NDB) (Berman*, et al.* 1992) for all nucleic acid structures. Additionally, ReLiBase (Hendlich 1998) may be used to explore receptor-ligand complexes structures and functions.

5.3.4 Gene expression studies

Experiments to evaluate the expression levels of individual genes has become an increasingly popular tool for assessing changes in target genes that may be affected by disease or injury. Levels of RNA can be quantified relatively quickly and easily and allow conclusions to be made about translation of target proteins within cells of interest. Whilst this may be carried out on a very small scale using qRT-PCR methodology (see Chapter 3), larger scale applications of this technique include cDNA microarray (Cheung*, et al.* 1999, Eisen and Brown 1999), Affymetrix Gene Chip (Lipshutz*, et al.* 1999) and SAGE (Velculescu 1999) technology. Relative levels of target genes may be determined using cDNA microarray technologies whilst absolute expression levels may be established with Affymetrix Gene Chip and SAGE methodologies. For humans, established examples of gene expression databases include The Molecular Portraits of Breast Tumours (Perou*, et al.* 2000) and Lymphoma and Leukemia Molecular Profiling (Golub*, et al.* 1999) and offer detailed databases with which to explore gene expression experiments in human cancer cell lines. The Cancer Genome Atlas (TCGA) is one database most commonly used for human cancers (http://cancergenome.nih.gov/). Other pieces of software including Genevestigator (NEBION, Switzerland) (Hruz*, et al.* 2008) and Braineac (www.braineac.org) are now other repositories for gene expression levels that allow complex query searches to determine changes in gene expression in the context of specific diseases or in target tissues/organs. The use of bioinformatics in this context may also serve as a preliminary target-finding resource as a way of determining gene targets of interest that may change in disease and can be identified for further validation in the lab in the future.

A great deal of work has been undertaken to simplify the way in which groups of genes can be classified or grouped together based on shared similarities within their expression profiles. Clustering genes by their expression profiles may allow groups of proteins to be determined that may be expressed together in response to certain cellular perturbations (Luscombe*, et al.* 2001), for example in the presence of a specific disease phenotype. Other attributes including structure, function and cellular localization of each gene product may also be considered. In this context, a “bigger picture” may be established with respect to the roles of certain gene products and changes

in their functionality with different cellular conditions. In the medical sciences, gene expression analysis may be used to provide insight into the gene expression biology within cells affected by various diseases (Friend 1999). Cancer (Golub*, et al.* 1999) and arteriosclerosis (Hiltunen*, et al.* 1999) are examples of this, whereby changes in expression in the context of these diseases may be compared to that of the healthy individual. Furthermore, identification of the genes that are expressed differentially in these conditions may prove useful in prediction of the causes that underlie the disease of interest, as well as potential biomarkers or even drug targets in this system (Luscombe*, et al.* 2001). Elucidating the transcriptional regulators that may underpin observed gene expression changes might also prove useful in determining disease risk factors or areas of interest for investigation of disease pathological mechanisms and pathways. Expression analysis of this kind may also prove beneficial in determining the response of trial pharmacological intervention (Colantuoni*, et al.* 2000, Debouck and Metcalf 2000) and in doing so, may also offer insight into potential side effects or toxicological risk that may arise upon administration.

Ultimately, assuming persistence in the growth of technological expertise, the use of systems biology combined with bioinformatics methods and large scale sequencing data are predicted to become a tool within the healthcare system. Post-natal genotyping for example may be more readily carried out as a tool to determine susceptibility or even immunity from certain diseases or pathogens. Indeed, a future of "personalised" medicine may become possible whereby vaccinations and treatment strategies may be prescribed on an individual basis as determined by genetic history and predicted predisposition to specific conditions (Sander 2000).

Overall, bioinformatics essentially aims to understand, analyse and categorise complex datasets of information so as to determine a greater depth of biological understanding in a given research field. Databases of this kind dictate a need for proper classification, encoding and storage for further meta-analysis. Meta-analysis requires sophisticated methods for data interrogation so as to decipher it in a meaningful functional sense. In this way, existing data may prove beneficial to any particular project where similar genes and gene sets may be implicated.

5.4 Bioinformatics and Alzheimer's disease

5.4.1 Functional protein sequences

AD is characterised by protein-based pathologies and bioinformatics tools to study protein sequences and their functionality are becoming increasingly more popular more recently. One particular study for example in 2008 collected 74 already established proteins known to be involved in the pathogenesis of AD and studied their sequences with the help of databases that store

functional protein sequences available for public use. Multiple sequence alignment algorithms could then be applied to this group of proteins to identify any similarities that may exist between the proteins of interest. The phylogenetic tree of distance between these proteins was established based on sequence similarity and disparity. In this particular study, of the 74 protein sequences studied, the presenilin-1 (PS-1), presenilin-2 (PS-2) and amyloid precursor protein (APP) were found to exhibit the minimum distance between each other. This data implicated these 3 proteins as key in the evolution of AD and suggested significant roles in the development of this disease (Rao*, et al.* 2008).

This study went on to postulate that, owing to their significance in the pathogenesis of AD, missense mutation in the *APP*, *PS-1* or *PS-2* genes might have significant implications on the processing of the APP protein and ultimately the generation of the toxic Aβ peptide. Indeed, accumulation of the Aβ peptide into mature insoluble plaques within the brain is known to trigger inflammatory responses via microglial activation and the release of pro-inflammatory cytokines. This work has been supported by reports of increased interleukin-1 (IL-1) and tumor-necrosis factor (TNF-α) in plasma and cerebrospinal fluid levels of patients with AD (Cacabelos*, et al.* 1991, Fillit*, et al.* 1991). As such, informatics may be used in this manner to elucidate target proteins to uncover new proteins of interest with regard a wider context of AD. Piecing together findings to create a bigger picture may be achieved with informatics, which coupled with lab validation may result in new hypotheses and conclusions regarding the mechanisms of this disease.

5.4.2 The use of bioinformatics as a tool for drug repurposing in Alzheimer's disease

The process by which drug therapies are designed and make their way from bench to bedside is an extremely long and costly one, not least because of the challenges associated with identifying and isolating novel compounds. Natural products are particularly favorable; indeed approximately 75% of all Food and Drug Administration (FDA) approved small molecules are either natural products themselves or derivatives of natural products (Newman and Cragg 2012). There are many attractions of natural products not least due to their complexity and protein binding specificity (Newman and Cragg 2012). There is however limitations in that they take a great of time to identify and require time-consuming purification methodologies to isolate.

Drug repurposing is a process by which new indications for pre-existing drugs can be identified for other diseases. This method is often safer, cheaper and saves a great deal more time (Siavelis*, et al.* 2016). This method uses a number of bioinformatics tools to compare chemical structures of known drugs, molecular docking, gene analyses, network simulations and chemo genomics data processing (Liu*, et al.* 2013). Microarray profiles in particular are used routinely in this

process as they can generate lists of up and down regulated genes. These lists can then be formulated into drug-drug, disease-disease and drug-disease comparisons.

If a compound is found to be consistently anti-correlated with AD, this reinforces its significance as a pharmacological target. Compounds may also be selected based on structural comparisons and similarities they may share with other identified compounds. Finally, pathway enrichment analysis may be used alongside network analysis methodologies to assess the efficacy of a drug compound against AD. From this work, a more manageable list of compounds can be compiled, based on mode of action and structural data that can then go on to be further validated in a lab based environment (Siavelis*, et al.* 2016).

One particular study, assessed gene signatures from five different gene expression experiments derived from AD human hippocampus samples. This study by Siavelis and colleagues resulted in a list of 27 drugs that were structurally different to those drugs that were currently in clinical use against AD (in particular they differed from acetylcholinesterase inhibitors and NMDA channel blockers, as discussed in chapter 1). This research proposed that protein kinase C (PKC) (mediates several cellular functions) (Mellor and Parker 1998), histone deacetylase (HDAC) (associated with epigenetic modification) (Smith 2008), arginase (ARG) (converts arginine to ornithine and urea) (Durante*, et al.* 2007), and glycogen synthase kinase 3 (GSK3) (participates in Wnt and insulin pathways) (Forde and Dale 2007) inhibitors might be beneficial in the reversal of the Alzheimer's induced gene expression pattern and thus show the potential to tackle the disease phenotype. These inhibitors may work as anti-Alzheimer's agents and this study indicated they might elicit their action via an epidermal growth factor receptor (EGFR) mediated pathway. Having identified target compounds in this manner, further work can be carried out in the lab to assess the efficacy of these lead compounds and their potential as AD therapeutics. Naturally, there are a number of challenges to overcome with this method of screening. Re-purposing of drugs in this manner will likely encounter complexities regarding dosage, toxicity and in the context of AD, whether these compounds can effectively cross the BBB. Despite this, more thorough research into multi modal use of certain compounds may prove a more time and money-effective strategy.

Whilst the efforts to treat AD are naturally still very much challenging, the use of bioinformatics tools on this occasion highlights the resources that are now available and the ways they can be exploited for scientific research. The advantages of such large repositories of information that are now publically available allow for a much more streamlined method of drug discovery. Understanding new uses for already established drug compounds in the context of AD may prove vital in treating this condition (Siavelis*, et al.* 2016).

5.4.3 Identification of biomarkers

Understanding ways in which AD can be treated relies heavily on confirming early diagnoses with which treatment strategies can be initiated. Diagnosis has proved particularly challenging with AD and often treatment initiatives begin too late making them not as effective as they could be. Biomarkers are fast becoming a focus of intensive research; finding a biomarker that can be easily and relatively cheaply detected in patients, as part of a screening initiative may prove crucial in detecting the early stages of AD. With application of computational methods large datasets can be screened for specific gene expression patterns or mutations associated with disease onset, early markers of change, or even identifier risk genes in individuals more predisposed to the condition.

One particular study, aimed at elucidating the mechanisms that underpin AD pathology by investigating microarray data of mRNA in cortex samples from patients with AD as compared to healthy age-matched controls using the Gene Expression Omnibus (GEO) (Edgar*, et al.* 2002) database (Zhao*, et al.* 2016). This study aimed to identify potential changes in the expression of genes in AD patents that could then be integrated into wider networks to identify target genes that may help diagnose AD more efficiently. This study identified target genes *SEC22B* and *SEC63* regulated by miRNA-206; *RAB10* regulated by miRNA-369-3p and *FLT1* regulated by miRNA-30e-3p that may play important roles in the progression and development of AD. Having identified miRNAs known to significantly change in AD patients, this data may also offer potential targets for the design of novel therapeutic strategies. In addition, interaction analysis and network construction analysis revealed that RBA proteins are important in the regulation of levels of Aβ (Udayar*, et al.* 2013). Indeed RAB10 (Ras-Related GTP-Binding Protein 10) is able to decrease levels of Aβ and hints at a regulatory role of RAB10 to modulate the activity of the γ-secretase cleavage. Likewise elevated levels of FLT1 (Vascular Endothelial Growth Factor Receptor 1) in AD patients as identified in this study revealed that FLT1 contributes to deposits of Aβ within the brain as well as microglial autocrine processes (Ryu*, et al.* 2009). Chronic inflammation is a key feature in AD pathogenesis and is associated with the deposition of Aβ in the brain. FLT may help to mobilise microglia and regulate their role in the development of AD. As such identification of this component may be an important target for future efforts to treat AD (Zhao*, et al.* 2016).

Several other targets of interest have been identified in this way via meta-analysis of microarray data from AD patients can reveal changes in the expression of specific genes that may prove fundamental in identifying the onset and development of AD pathology. For this reason, bioinformatics offers a helpful approach at the beginning of research projects to identify genes of interest that can be elucidated further within the laboratory at a later date. High level screening in this way serves as a top down approach to finding important pathological mechanisms and

pathways that can be targeted with therapeutics in the future to aid the treatment and ultimately cure of this disease.

5.4.4 GWAS and AD

Genome-wide association studies (GWAS) have proven particularly beneficial in AD research. GWAS is an approach by which genetic variants in a large group of individuals is examined to determine whether specific genetic variants are associated with a particular trait of interest, in this instance, AD. GWAS investigations usually focus on the association between SNPs and diseases. Understanding association between specific genetic variations and disease may prove useful in identifying biomarkers for the early diagnosis of AD, particularly for those individuals who may carry risk factor genes. The Human Genome Project in 2003 and the international HapMap project in 2005 have made sequencing information more readily available to researchers. Harold and colleagues in 2009 undertook a two-stage GWAS to study genomic data from 16,000 individuals, the largest AD study to date. This study confirmed the earlier finding that APOE (Avramopoulos 2009) is still the most significant SNP. This study also discovered two genetic loci not previously associated with the development of AD; CLU and PICALM (Harold*, et al.* 2009). The *CLU* gene encodes the clusterin protein that is up regulated in a number of conditions that involve chronic injury or inflammation within the brain (Calero*, et al.* 2000). Moreover, levels of clusterin are reported to be elevated in AD patients within cortical areas directly affected by AD pathology. Elevated levels of clusterin are also reported within the CSF and the amyloid plaques themselves (Giannakopoulos*, et al.* 1998, Liang*, et al.* 2008, McGeer*, et al.* 1992). The second identified locus was PICALM (phosphatidylinositol-binding clathrin assembly protein). Expression of this protein, although ubiquitous, is predominantly found within neurons, most specifically at the pre- and post-synaptic structures (Harold*, et al.* 2009). The PICALM protein has been shown to play a role in the regulation of trafficking of protein. In the context of AD, PICALM is reported to traffic VAMP2, a SNARE protein key in the fusion of synaptic vesicles to the presynaptic membrane for neurotransmitter release (Harel*, et al.* 2008). AD patients are known to display reduced synaptic activity correlated with cognitive decline and so implicated PICALM heavily in the progression of this disease. Identification of these two genetic loci offer new targets to study in the search for biomarkers of AD and drug discovery targets. Currently there are very few known genetic risk factors for AD. Mutations in the genes that encode APP, PSN-1 and PSN-2 are known to cause rare early onset forms of the disease. However, the more common sporadic late onset form of the disease are a little more misunderstood with APOE as the only unequivocally established susceptibility gene (Avramopoulos 2009).

5.5 Conclusions

In conclusion, there is a wealth of information available to research scientists now that may serve to aid in the identification of novel protein targets, structural analysis of novel proteins and potential biomarkers for a variety of diseases. In the context of AD, there is still a huge amount of information to be gained with regard to risk factor genes, network analysis and drug discovery target identification and with the advent of several pieces of software to aid such research, the use of bioinformatics is more common than ever. In particular, integration of different data types via various bioinformatics approaches may serve to generate new networks and models why which pathogenesis may be initiated. This project aimed to employ some of these resources to investigate further the role of HS in AD and set the functionality of HS in a wider context of the disease, not limited only to its interaction and regulation of BACE-1.

5.6 Aims of chapter

- Investigate changes in the expression of genes encoding HS biosynthetic genes as determined with microarray analysis and curated into gene expression profiling databases.
- Determine how changes to HS may be regulated in different regions of the brain.
- Investigate the role of HS in the wider context of AD with pathway network analysis and association studies to explore alternative pathways in AD that may be regulated by HS.

5.7 Methods

For the bioinformatics work, three gene lists were compiled and used in data mining efforts. The first contained Gene IDs encoding the HS biosynthetic enzymes and their core proteins (Sarrazin*, et al.* 2011) (Esko and Selleck 2002). This list was also established with the use of KEGG (Version 80.1, Kaneshisa laboratories, Japan) (Kanehisa and Goto 2000, Kanehisa*, et al.* 2016) to determine the pathway for the synthesis of HS. The list also included the HS degradation enzymes HPSE and HPSE2 and SULF1 and SULF2. The second list, all previously established GWAS significant AD risk factor genes and the third list, the heparin interactome (a list of over 300 proteins that heparin is known to interact with) (Ori*, et al.* 2011). The gene lists are detailed in **Appendix C**.

5.7.1 STRING

STRING (Version 10.0) (Jensen*, et al.* 2009) is a database of known and predicted protein-protein interactions. STRING software was used initially as a way of searching for interactions between the selected proteins of interest in this project. STRING software was used to assess

interactions of different types, whether that was experimentally validated links, co-expression, gene fusion, data-mining etc. Each interaction was given a score based on the confidence of a specific interaction. All scores rank from 0 to 1 where 1 indicated the highest confidence and 0, the lowest. On this occasion, all interactions were investigated based only on human data, not any other organism. A confidence threshold of 0.4 was set to eliminate any "weak" interaction information. STRING software was used to investigate any potentially unexpected links between the proteins of interest and to explore possible relationships between specific groups/subgroups of proteins. No additional nodes (additional proteins separate to proteins of interest that may tie proteins of interest together) were added to networks for the sake of simplicity. This software was used primarily to assess connections between the HS biosynthetic enzymes and any previously unconsidered interactions that may exist.

5.7.2 Genevestigator®

Genevestigator® software (Genevestigator® Version 47326744, NEBION) was used to review expression of HS biosynthetic genes and the genes encoding core proteins in the context of both AD and from an anatomical standpoint. The Genevestigator® software allowed a quick look at curated microarray information previously collected and made publically available for meta-analysis. This software was therefore ideal as a means to assess whether changes in HS biosynthetic machinery gene expression occurs with AD and indeed how expression may vary across different regions of the brain. As a first look, this database mining approach was used to identify target genes of interest for future lab validation studies.

Gene expression data for the HS biosynthetic enzymes and core proteins were investigated in the context of AD as well as different anatomical locations within the brain. High level analysis of gene expression changes in response to these perturbations (disease or anatomy) could be explored with heat map analysis to determine whether a gene of interest was up- or down- regulated and data points could be further analysed with regard to experimental detail, sample numbers, p value statistical significance etc. With respect to microarray analysis of HS biosynthetic genes in the context of AD, one particular study was found to be most relevant to this project within the database and was carried out by Liang and colleagues in 2006 to assess microarray expression profiling of genes from AD brains and healthy age-matched controls. The experimental details of this study are outlined in detail in **Appendix D**.

Expression of the HS biosynthetic genes and core proteins with respect to anatomical region allowed investigation of variation in expression and was used to assess potential vulnerability to certain areas with respect to changes in the structure of HS and the implications this may have on

AD pathology. Anatomical analysis was carried out independently to the AD phenotype and was obtained only from healthy individuals.

5.7.3 Ingenuity Pathway Analysis (IPA®)

The "core analysis" function was used in the IPA® (Ingenuity System Inc., USA) software to interpret the genes of interest in the context of biological pathways and networks. Both up- and down- regulated identifiers were defined as value parameters for the analysis. The software generated networks that were ordered according to a score of significance. The Fisher exact test p-value was used to assess significance of certain connections and canonical pathways. This pathway analysis software was able to generate networks whereby the differently regulated genes could all be placed into higher network systems based on previously known association and interactions, but independently of already established canonical pathways. Genes of interest explored with this system included the HS biosynthetic genes, their core proteins, the heparin interactome of 300+ proteins and AD risk genes previously identified in GWAS.

This software was used to display the most significant canonical pathways that may exist within a particular dataset uploaded into the software. The significance of interactions was determined based upon the probability of association between molecules within the dataset being studied. Furthermore, upstream regulator analysis was used to identify potential upstream regulators that may be responsible for the gene expression changes as observed in other work.

This work hoped to establish any novel associations with HS and other proteins implicated in AD, outside of the established BACE-1 interaction pathway. Naturally, these associations are largely based on predictions and as such, further work would be needed to validate potential interactions/ pathways within the lab. Hence, this work was largely preliminary and hoped to establish connections that may strengthen the view that HS has roles in AD pathogenesis in a wider context to that already known, and that might provide new directions for future research.

5.8 Results

5.8.1. STRING

Analysis with STRING software revealed a strong interaction network between the HS biosynthetic enzymes and core proteins, consistent with expectations for these related genes. All interactions between the proteins of interest were assigned a specific colour depending upon the

type of interaction (**Figure 5.1**). For the majority of interactions observed in this instance, the lime green line represented a ”text mining” interaction whereby interactions were based on two proteins found to be mentioned within the literature together frequently. As expected, this type of interaction was common within this group of proteins and largely cross-linked between different families of enzymes within the HS biosynthetic pathway. The pink interaction lines represented interactions that had been experimentally determined and were discovered between EXT1 and EXT2 (protein-protein interaction in humans) and also between NDST1 and EXT2 (protein-protein interaction in mice). Experimentally determined interactions were also reported between all members of the SDC family (protein-protein interactions in humans) and also between GPC4 and GPC6. The turquoise line between proteins distinguished interactions based on previously established curated database data. These interactions were largely known pathways regarding HS biosynthesis including N-deacetylation/N-sulfotransferase activity by the NDSTs, sulfation at the 6-O, 3-O and 2-O position by the HS6STs, HS3STs and HS2ST respectively and polymerisation of the HS chain by the EXTs. The large nodes within the network represented those proteins where 3D structure was either confirmed or predicted and smaller nodes represented those proteins with no known 3D structure. On this occasion, all proteins studied displayed a large node, indicative of a known, or at least partly known 3D structure with the exception of the HS6ST family and GLCE whose nodes were small indicative of unknown 3D structures. With this set of proteins, the EXTs and XYLTs displayed fewer interactions vs. the modification enzymes within the HS biosynthetic machinery. Coloured nodes represented all query nodes (**Figure 5.1**).

Following this, GWAS identified risk proteins were also included in the search to determine whether there were any interactions between known AD risk factor genes/proteins and the HS biosynthetic machinery proteins. With the two lists combined, the STRING generated network revealed a much less tightly connected network. Both protein list groups remained reasonably isolated from each other. Indeed, the only points of contact between the two groups were Interactions found between the SDC family and APOE. Any other connections found were largely co-mentions in the literature between known HS core proteins. With regard to the AD risk protein list, little experimental evidence was determined with reported interactions mainly arising from literature searches (**Figure 5.2**).

5.8.2 Genevestigator®

Genevestigator® software was then used to determine how the presence of the AD phenotype might affect the expression of the genes that encode HS related enzymes and core proteins. Heat maps were generated to assess whether expression of each gene of interest was either up- or down-regulated in the presence of AD vs. healthy controls. Changes were

representative of log_2 fold changes of expression. Green squares within the heat map indicated a down-regulation and red indicated an up-regulation of expression relative to healthy controls. Each gene is listed along the top of the heat map horizontally whilst the region of the brain studied is listed vertically on the left hand side. The data presented in the heat map are all representative of a single study whereby several regions of the brain were studied in a number of individuals with AD. The heat map generated for HS biosynthetic genes in the presence of the AD phenotype revealed strong changes in expression of a number of genes in a number of different regions within the brain, several of which were significant (**Figure 5.3**)(**Table 5.2**).

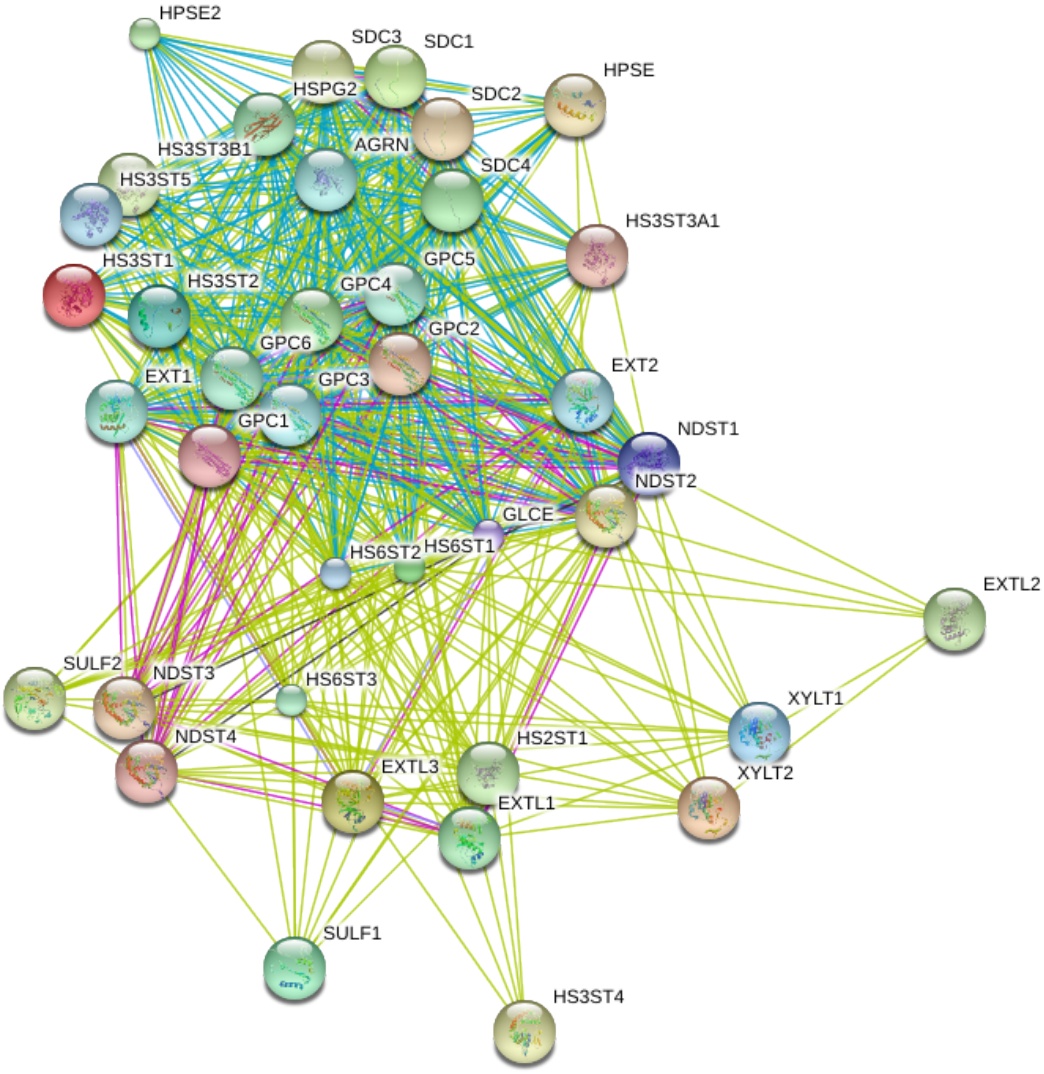

Figure 5.1: Output interaction network as generated by STRING software to display interactions between HS biosynthetic enzymes and core proteins. STRING software was used to assess interactions of different varieties. On this occasion, all interactions were investigated based only on human data, not any other organism. A confidence threshold of 0.4 was set to eliminate any "weak" interaction information. All interactions between the proteins of interest were assigned a specific colour depending upon the type of interaction. Lime green lines represent "text mining" interaction, Pink interaction lines represent interactions that had been experimentally determined. Turquoise lines between proteins distinguish interactions based on previously established curated database data. The large nodes within the network represent those proteins where 3D structure was either confirmed or predicted and smaller nodes represented those proteins with no known 3D structure.

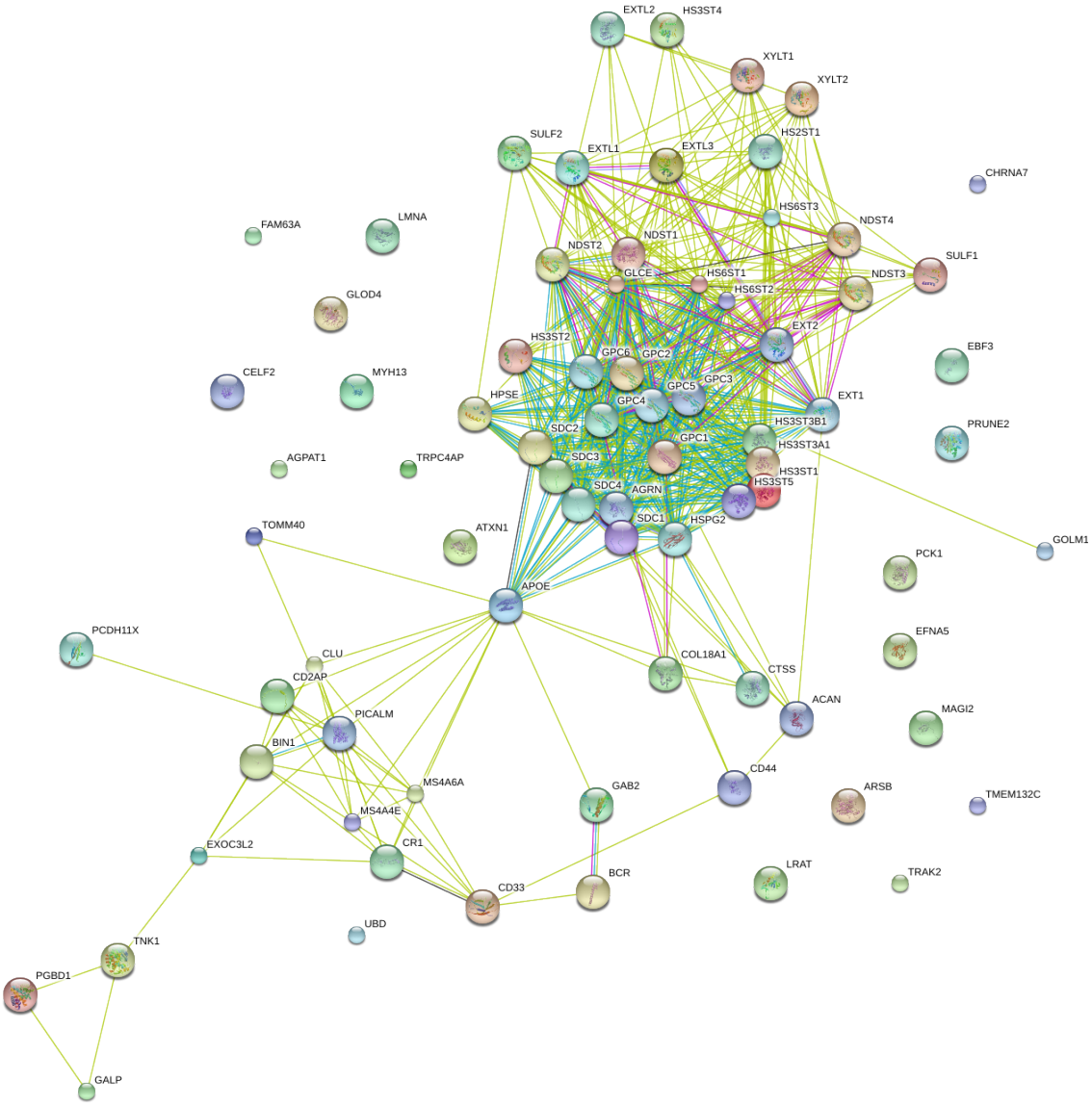

Figure 5.2: Output interaction network as generated by STRING software to display interactions between HS biosynthetic enzymes, core proteins and GWAS identified AD risk proteins. STRING software was used to assess interactions of different varieties. On this occasion, all interactions were investigated based only on human data, not any other organism. A confidence threshold of 0.4 was set to eliminate any "weak" interaction information. All interactions between the proteins of interest were assigned a specific colour depending upon the type of interaction. Lime green lines represent a "text mining" interaction Pink interaction lines represent interactions that had been experimentally determined. Turquoise lines between proteins distinguish interactions based on previously established curated database data. The large nodes within the network represent those proteins where 3D structure was either confirmed or predicted and smaller nodes represented those proteins with no known 3D structure.

Investigation of the raw data behind the heat map generated revealed significant up- and down-regulation of expression of the genes encoding the HS biosynthetic enzymes and core proteins in all of the brain regions studied. In the case of the HS biosynthetic enzymes, data generated from this microarray profiling experiment revealed strong down-regulation of the *EXT* and *EXTL* genes

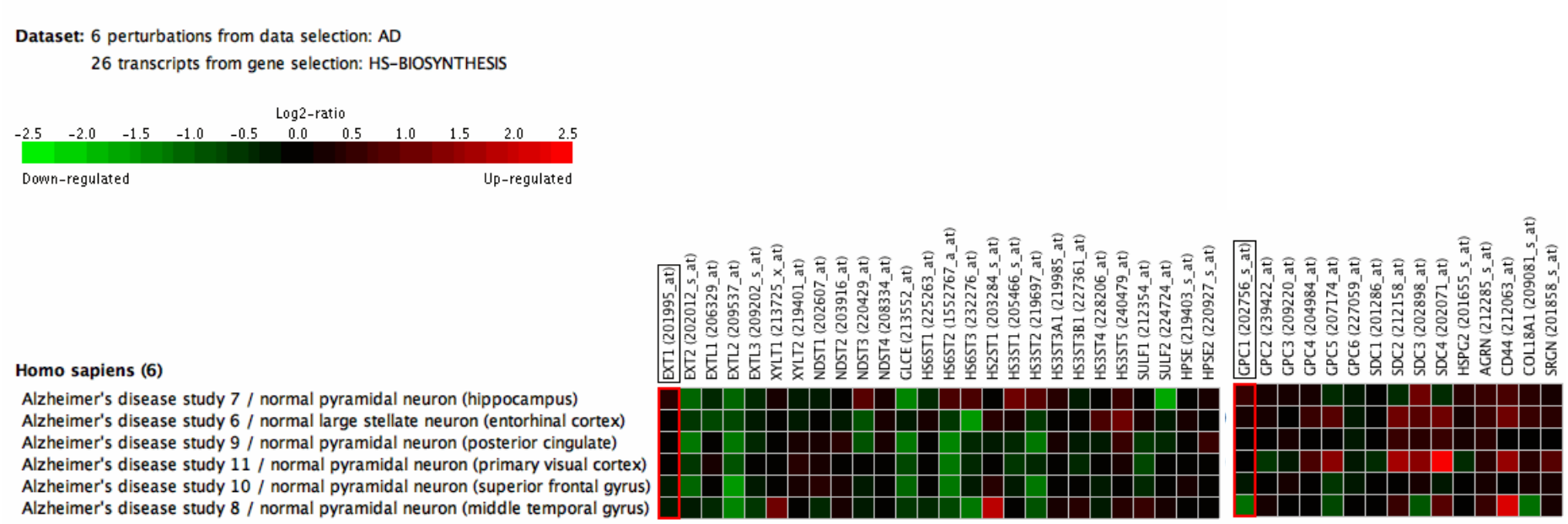

Figure 5.3: Heat map displaying fold changes in expression of the genes encoding HS biosynthetic enzymes and core proteins in the presence of the AD phenotype in 6 different brain regions. Individual genes are listed across the top of the map (genes encoding HS biosynthetic enzymes and core proteins) with experiment type/region listed vertically along the left. Logged normalised fold changes in expression levels were used to generate this map; colours range from red (high expression) to green (low expression). p values and fold changes were generated and viewed upon selection (see table 5.2). Regulation of expression varied significantly across the different brain regions studied on this occasion. HS biosynthetic machinery displayed robust down regulation vs. the core proteins that was more prominently up regulated. Heat map generated with Genevestigator® software and is based upon original data collected by Liang et al; 2006.

across all of the brain regions studies. Conversely, this experiment revealed strong trends for up-regulation of expression of the *SULF* and *HPSE* genes across the brain regions sampled in this study. Furthermore, expression of the HS biosynthetic genes was differentially regulated across the different brain regions with variable expression patterns displayed in each of the areas sampled. With respect to the core proteins, a much more substantial up-regulation of expression of the genes encoding core proteins was observed in the presence of the AD phenotype relative to healthy controls with much fewer genes displaying decreased expression. In particular, the primary visual cortex (PVC) and superior frontal gyrus (SFG) brain regions displayed the most prominent up regulation in expression across all genes studied. Conversely the hippocampus displayed the most prominent down-regulation of gene expression on this occasion. The *SRGN* and *AGRN* genes were found to be strongly up-regulated across all brain regions studied, the only genes to display this consistent expression change. Raw data values for these fold changes are detailed in **Table 5.2**.

Following the finding that the expression of the genes encoding HS biosynthetic enzymes and core proteins is altered in the presence of the AD phenotype. This software was used to determine how expression might be regulated across different regions of the brain in healthy individuals, AD is known to spread in a temporal and spatial fashion across different regions of the brain and the Genevestigator® software was used to determine whether regulation of the expression of HS biosynthetic machinery and core proteins in specific brain regions may determine resulting vulnerability of certain regions to AD pathology.

The Genevestigator® software curated several absolute expression datasets for the expression of the genes encoding HS biosynthetic enzymes and core proteins relative to different anatomical regions. This study was limited to the brain only and a heat map generated to determine how expression varies across different regions of the brain. The heat map generated from this search displayed strong expression differences across the different HS biosynthetic enzymes. Red coloured squares indicated the highest expression potential whilst those paler in colour represented lower expression potential. The hierarchal clustering tool was used to group genes together that share similar expression potential profiles. Grouping genes in this way highlighted groups of genes that were switched on and off together in response to particular anatomical location or disease state. The Euclidian distance function was used with this search to cluster groups of genes.

The heat map generated revealed very high expression of some genes and in contrast, very low expression potential of other genes (**Figure 5.4**). On several occasions, differences in high and low expression potentials were shared between enzyme subfamilies, perhaps indicative of regional specificity of specific isoforms. The *HPSE2* gene for example displayed very high expression potential across nearly all brain regions studied whilst the *HPSE* gene displayed one of the lowest expression potential profiles of all the genes searched for. Furthermore, the *HS3ST3A1* and *HS3ST3B1* genes

Table 5.2: Raw data (logged normalised fold changes) as generated by Genevestigator® software based on expression profiling experiment by Liang et al (Liang, *et al.* 2007). Genes are detailed vertically with brain regions of AD and healthy patients listed vertically. Abbreviations: ECX: entorhinal cortex; HIP: hippocampus; MTG: middle temporal gyrus; PCX: prefrontal cortex; SFG: superior frontal gyrus; PVC: primary visual cortex. Green represents down regulation of expression, red represents up regulation. Data shown in bold represents fold changes in expression with AD (relative to healthy controls) that reached significant ($p<0.05$) table A displays all genes encoding HS biosynthetic enzymes, table B, those genes encoding HS core proteins.

A	ECX	HIP	MTG	PCX	SFG	PVC
EXT1	-1.03	1.28	-1.33	-1.10	-1.15	-1.07
EXT2	-1.42	**-2.00**	-1.23	**-2.20**	**-2.11**	**-1.39**
EXTL1	**-1.74**	**-1.31**	**-1.39**	1.05	1.05	**1.23**
EXTL2	**-1.74**	**-2.09**	**-2.59**	**-2.31**	**-2.62**	-1.45
EXTL3	-1.21	-1.25	**-1.69**	**-1.38**	**-1.23**	1.11
XYLT1	1.04	1.23	**2.15**	-1.05	-1.01	1.10
XYLT2	-1.19	-1.26	1.01	1.13	1.19	**1.29**
NDST1	1.05	-1.24	**-1.38**	1.19	**1.27**	1.20
NDST2	-1.24	1.03	1.21	1.32	1.15	1.02
NDST3	**-1.95**	**1.89**	-1.22	**-1.86**	-1.20	-1.06
NDST4	1.15	**1.19**	-1.07	**1.16**	1.09	1.14
GLCE	-1.33	**-3.00**	**-1.39**	**-2.36**	**-1.94**	**-1.67**
HS6ST1	1.20	**-1.39**	-1.37	-1.11	1.10	1.14
HS6ST2	-1.35	1.47	-1.43	**-1.96**	**-1.98**	**-1.90**
HS6ST3	**-2.87**	**1.67**	**-2.28**	-.1.24	-1.18	-1.20
HS2ST1	1.20	-1.01	**3.70**	-1.26	1.31	1.12
HS3ST1	1.19	**2.21**	-1.10	-1.49	-1.36	-1.28
HS3ST2	-1.68	1.50	**-1.84**	**-2.56**	**-2.32**	-1.06
HS3ST3A1	-1.07	**1.31**	**1.21**	**1.13**	1.13	-1.03
HS3ST3B1	1.02	-1.20	1.93	-1.25	1.06	-1.70
HS3ST4	**1.70**	-1.17	-1.13	-1.37	-1.26	1.05
HS3ST5	**2.16**	**1.56**	**1.23**	**1.61**	-1.15	1.17
SULF1	1.16	1.11	**1.63**	**-1.56**	1.03	**-1.47**
SULF2	-1.32	**-3.12**	1.18	-1.28	1.06	-1.06
HPSE	1.12	1.01	-1.07	1.01	**1.22**	1.03
HPSE2	1.03	**1.26**	1.08	**1.46**	1.14	1.10

B	ECX	HIP	MTG	PCX	SFG	PVC
GPC1	**-2.04**	-1.16	-1.09	1.41	1.14	1.00
GPC2	1.07	1.01	**-1.56**	**1.23**	1.14	1.04
GPC3	1.07	1.15	-1.29	**1.15**	1.03	**1.18**
GPC4	-1.06	-1.09	**1.83**	1.30	**1.65**	1.02
GPC5	**-1.65**	-1.68	**3.32**	-1.43	**2.13**	1.24
GPC6	1.04	-1.15	-1.18	-1.21	1.10	-1.17
SDC1	1.02	1.01	**-1.56**	-1.08	-1.10	1.02
SDC2	1.38	-1.12	**3.30**	-1.50	**2.52**	**1.57**
SDC3	**-2.14**	1.08	**2.37**	**2.14**	**1.91**	**1.38**
SDC4	**1.87**	-1.02	**6.86**	-1.43	**2.63**	1.31
HSPG2	-1.12	-1.03	-1.37	**1.29**	1.20	1.19
AGRN	**1.51**	1.10	1.21	**1.51**	**1.50**	**1.27**
CD44	**9.90**	-1.09	**5.36**	**1.86**	**2.53**	-1.02
COL18A1	**-2.28**	1.11	**1.35**	1.55	**1.68**	1.06
SRGN	1.17	1.22	**2.01**	1.31	**1.34**	1.11

displayed very low expression potential in nearly all brain regions studied, indicative perhaps of redundancy of these isoforms within the brain. Other *HS3ST* genes including *HS3ST4* and *HS3ST2* displayed much higher expression potentials and were clustered with other genes sharing a similar profile including *NDST3, HS6ST1-3* and *EXTL2*. Whilst this data did not distinguish between expression changes that may occur in the presence of the AD phenotype, as investigated above, this search provided novel grouping of some of the HS biosynthetic genes that may be expressed together in select regions of the brain and highlighted those whose low expression potential may be indicative of less downstream consequences on structure of HS and its ligand binding affinities (**Figure 5.4**).

Finally, this search confirmed those regions of the brain implicated in AD such as the hippocampus and middle temporal gyrus that share high expression potential of HS biosynthetic enzymes and thus may strengthen our notion of a regulatory role of HS in AD pathogenesis in patients. The anatomical clustering was also carried out as described above but to look for expression potential profiling of the genes that encode the HS core proteins (**Figure 5.5**). Hierarchal clustering of the genes that express the HS core proteins revealed very high expression potential of the *GPC5* and *SDC3* genes and very low expression potential of the *SDC1* and *GPC3* genes. Clustering in this manner would suggest very tightly regulated expression of specific enzyme isoforms in different regions of the brain. *GPC1, SDC2, SDC4* and *AGRN* genes all displayed higher expression potential vs. other HS core protein genes. As with the HS biosynthetic genes, expression potential across the different brain regions was highly variable and indicated tight regulation in select locations of the brain that may predict vulnerability to different pathologies, not limited to AD (**Figure 5.5**). In contrast to the heat map generated with genes encoding HS biosynthetic enzymes (**Figure 5.4**), those genes that encode HS core proteins appeared to display an overall lower expression potential across the brain regions studied.

5.8.3 Ingenuity Pathway Analysis (IPA®)

IPA® was used to explore potential relationships and connections between the proteins of interest that we had explored in previous studies with STRING and Genevestigator®. The GWAS identified AD risk genes, those genes that encode the HS biosynthetic enzymes and those that encode the HS core proteins. Finally, the heparin interactome list was also added to searches for the sake of completion as this work was only at a preliminary stage and it was not known what connections might exist between proteins of interest.

For this work, the GWAS identified genes, HS biosynthetic genes, core protein genes and heparin interactome lists were compiled into one list into IPA®. Search results for this query were

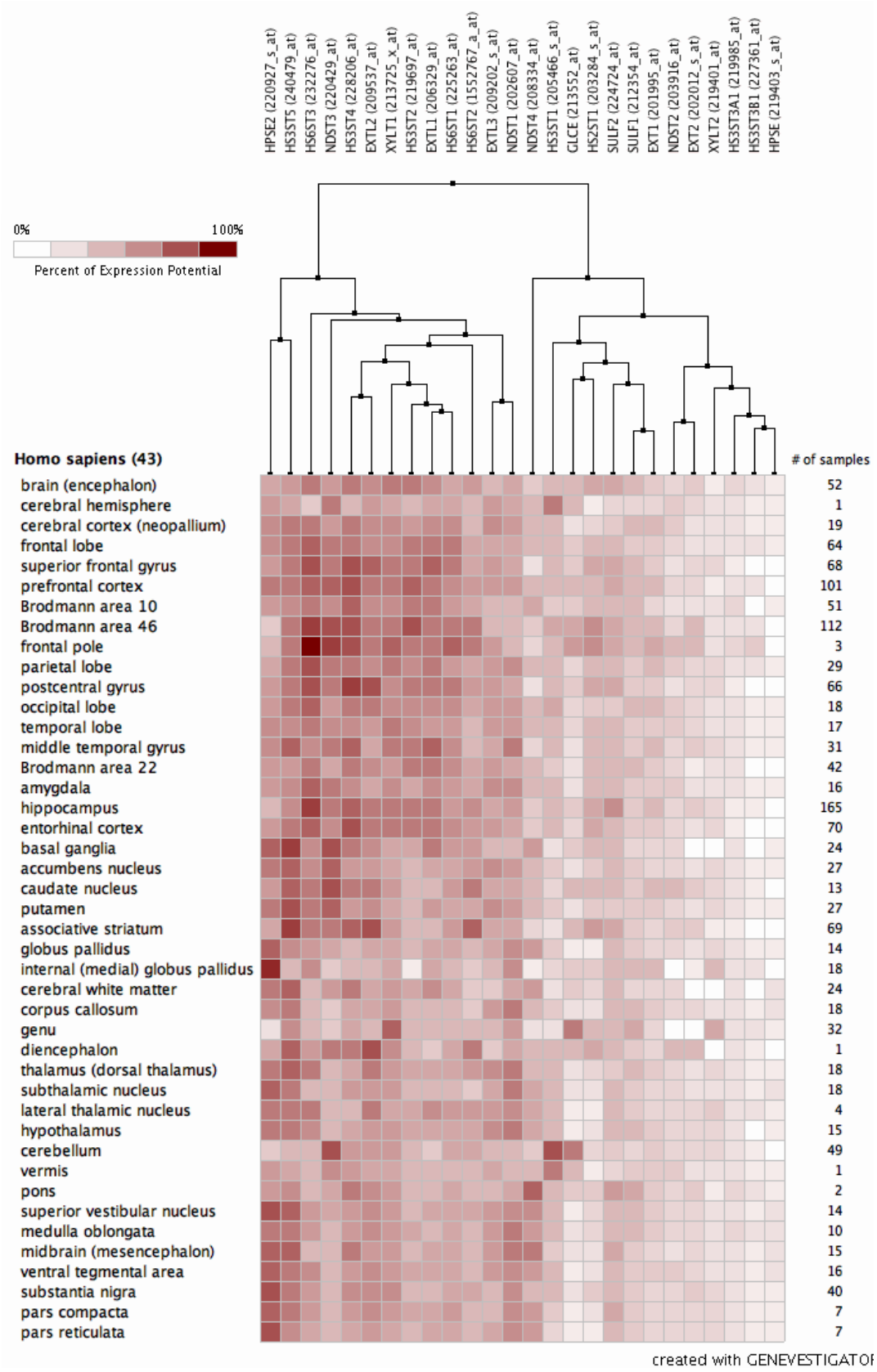

Figure 5.4: Hierarchal clustering of expression potential of genes encoding HS related enzymes in different anatomical locations within the brain as generated by Genevestigator® software. Anatomical regions are listed vertically and gene names horizontally. Dark red colour represents high expression potential and paler squares, lower expression potential. The number of samples assayed in each brain region is listed on the right vertically. Euclidian distance function was used to determine clustering of genes that shared similar expression profiles.

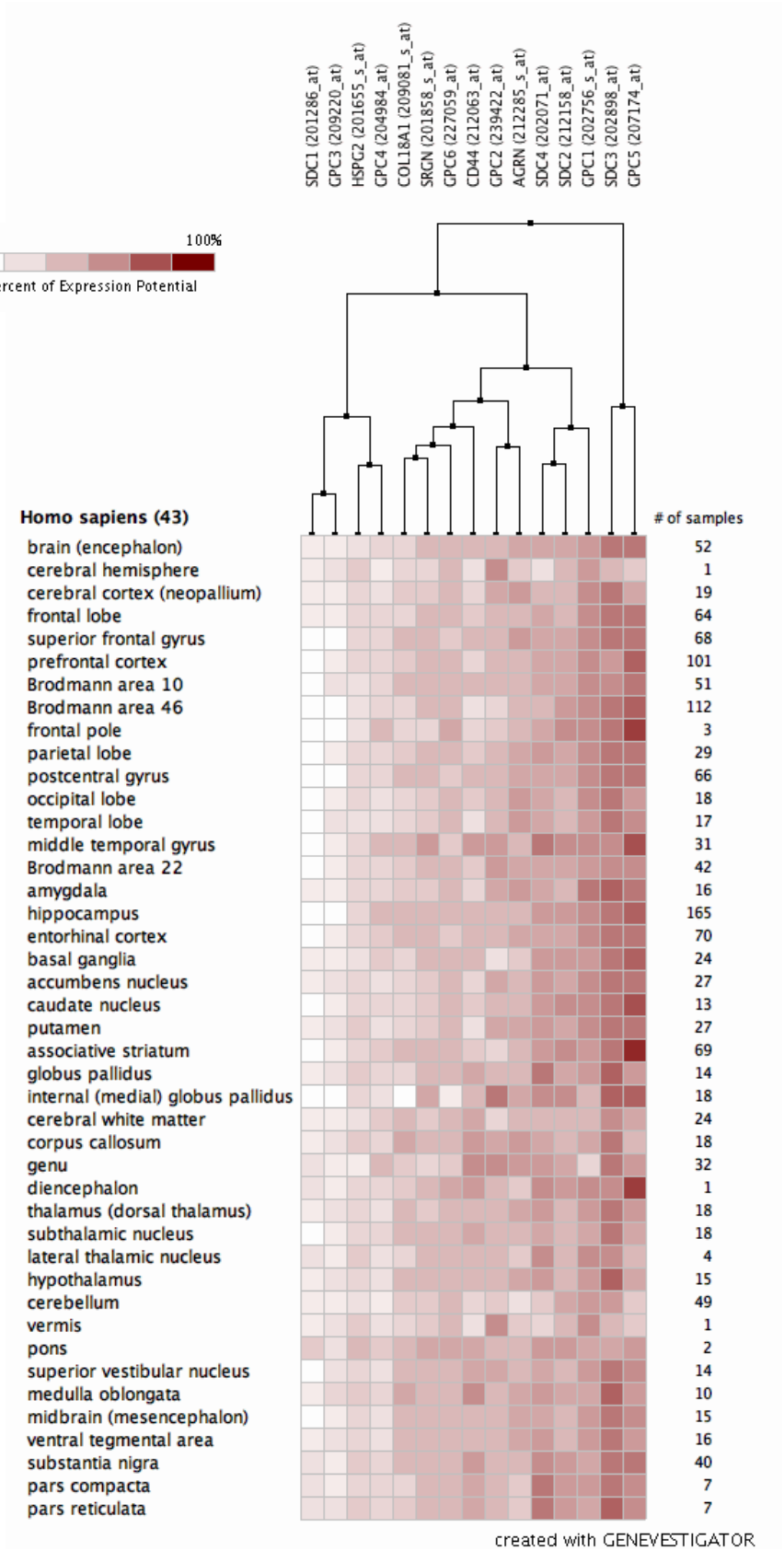

Figure 5.5: Hierarchal clustering of expression potential of genes encoding HS core proteins in different anatomical locations within the brain as generated by Genevestigator® software. Anatomical regions are listed vertically and gene names horizontally. Dark red colour represents high expression potential and paler squares, lower expression potential. The number of samples assayed in each brain region is listed on the right vertically. Euclidian distance function was used to determine clustering of genes that shared similar expression profiles.

filtered to show only connection evidence from human nervous system based data, not any other species or other regions of the body. As the number of genes was so high and the main focus of this work AD, it was decided for the sake of simplification to only include that data generated from the human CNS. It was hoped that any possible networks built from this work might be used as a basis on which to form validation experiments within the lab. Database searching with these lists generated a number of canonical pathways associated with the search proteins uploaded into the IPA® software. The top scoring canonical pathways determined with this search included hepatic fibrosis, granulocyte adhesion, bladder cancer signaling and the coagulation system. Interestingly, other canonical pathways found included axonal guidance, the neuroprotective role of THOP1 in AD, NFkB signaling and amyloid processing. This search was then filtered to those diseases and functions associated with the list of proteins of interest. Of the 476 proteins searched for on IPA®, 200 of them were associated with neurological disease in some way. Whilst the GWAS identified risk protein list would naturally be associated with the onset of neurological diseases, this gene list was only very short, suggesting a number of interactions came from the heparin interactome list. A bar chart was generated to display the diseases and functions associated with this target list search (**Figure 5.6**).

In the bar chart generated to display all associated diseases and functions linked to the target gene list, immune cell trafficking, inflammatory response, cell death, inflammatory disease, neurological disease and psychological disorders scored highly and reached the set threshold ($p<0.05$) for significance. This search indicated that these genes were associated with a number of canonical pathways and functional categories. This finding thus stressed a complexity of the functional network that underlies the etiology and development of AD. The downstream effectors associated with this gene list was large and varied and indicated a role of HS associated proteins that may have functionality with other networks involved in the pathogenesis of AD, specifically inflammation, cell death and neurological dysfunction. Those genes encoding the HS biosynthetic enzymes were not found to directly associate with these diseases but rather only the heparin interactome and GWAS identified AD risk factor genes.

No details regarding expression potential of these proteins were included within the IPA® search. This was partly because there was not a complete data set with this information for all of the target proteins investigated. As such, it was not possible to determine the downstream consequences of changes in the expression of specific proteins. Despite this, interactions and possible networks within the target protein lists could be predicted and the role of HS and heparin interacting proteins set into a wider context for AD pathology. Of the canonical pathways found to be associated with the target proteins, all were found to largely interact and displayed substantial cross over with respect to members of specific pathways and their functionality. That being said, the biosynthesis of HS was not found to share any overlap with the other established pathways and sat in isolation with respect to other physiological function within the body (**Figure 5.7**). This figure

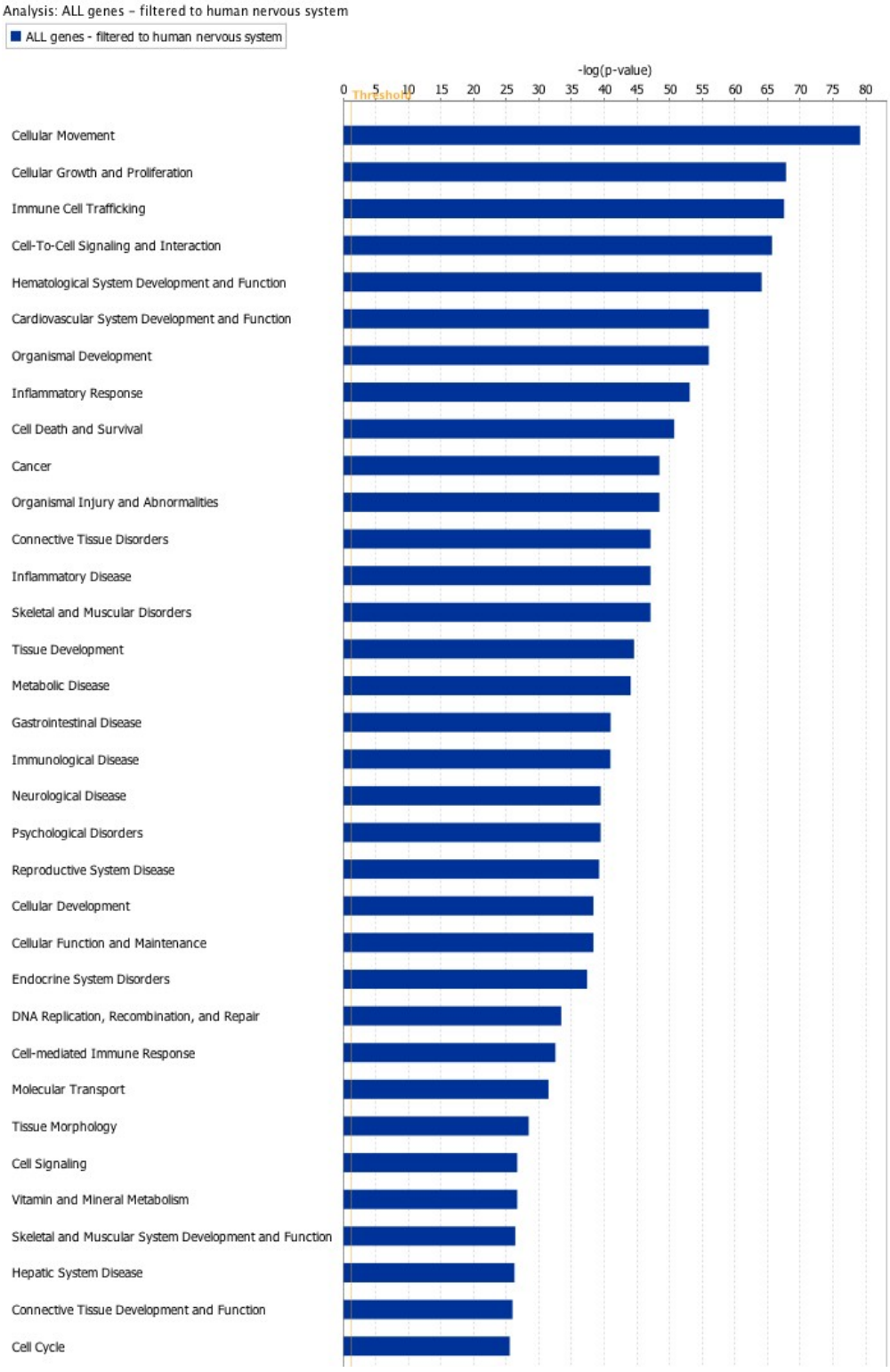

Figure 5.6: Diseases and functions associated with the target protein list as generated by IPA® software. Gene lists for HS biosynthetic enzymes, core proteins, GWAS identified AD risk genes and the heparin interactome were compiled into one target list and submitted to IPA® for network analysis. This bar chart displays the most significant diseases and functions associated wit the target gene list. The bigger the blue bar, the more significant the association was found to be. The orange line depicts the threshold of significance that set ($p<0.05$). Of the diseases and functions found to be represented, neurological disease, psychological disorder, and inflammatory based function was noted for their associations with AD.

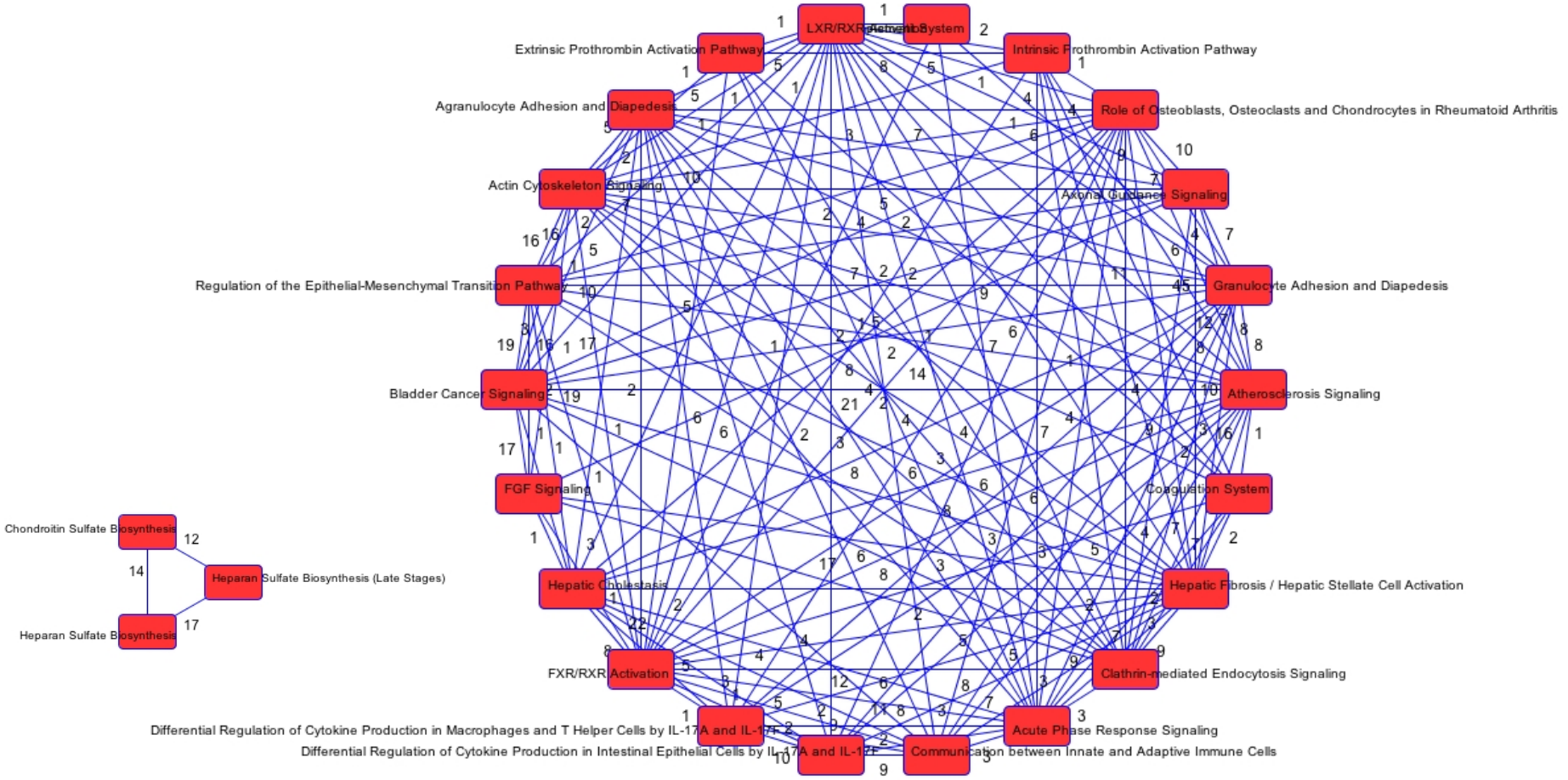

Figure 5.7: Overlap between the most significant canonical pathways associated with the HS biosynthetic enzymes, core proteins; GWAS identified risk genes and heparin interactome proteins. Figure as generated by IPA® shown those canonical pathways that share the same target protein members. Blue lines between red nodes depict over lap and the number above each blue line represents the number of overlapping components. Interestingly, the synthetic and modification pathways of HS and CS do not overlap at all with any of the other established canonical pathways but rather remain in isolation.

depicted the significant canonical pathways associated with the target gene list and the overlap between these pathways (the number above each line depicted the number of components that were shared). Whilst there was no shared interaction between the biosynthesis of HS and other physiological functionality, indirectly the biosynthesis of HS is hugely important for interaction with its ligand-binding partners. The data generated in this project has confirmed the importance of HS biosynthesis, the resulting HS structures and the ways in which they interact with their binding partners. This preliminary work thus highlighted a need to update network associations such that the biosynthesis and modification of HS may be implicated in the downstream consequences of ligand interaction. In the context of AD, the lab work from this project has gone some way to validate some of these connections. IPA® was used in combination to generate a predicted model of network interactions linking AD pathological pathways and HS. From the list of interactive networks generated by the IPA® software, the top (most significant) was chosen for further work. This network was chosen as a base on which to generate a larger compilation of laboratory proven association and functionality alongside those interactions predicted by the literature and other experimental data.

IPA® interaction predictions were coupled with the data generated from this project to create a prediction of a potential association network whereby the role of HS is implicated in the pathogenesis of AD in a wider context to that already established with its interaction with BACE-1. This work is preliminary and further work is required to confirm hypotheses and further elucidate the many other nodes of interaction that are sure to exist in this somewhat simplified model. For simplification, the interactions as predicted by the IPA® software in the top scoring network have been tabulated below to detail the interaction between each pair of nodes (**Table 5.3**). **Figure 5.8** was generated to combine the IPA® generated connections alongside the data generated from this project within the lab. This is a working model and puts forward a hypothesis for a wider functionality of HS in the pathogenesis of AD.

This network pathway as generated by the IPA® software includes nodes from the GWAS identified risk factor genes (PLAU) and several heparin interactome proteins (SERPINE2, FURIN, TGFB1). This network also allowed the integration of HS biosynthetic enzymes themselves. Coupled with the data generated within the lab in this project, a model for some of the pathways that could be involved in AD pathogenesis is hypothesised. As described previously, these interactions undoubtedly do not occur in isolation but rather within a much more complex framework of functional and regulatory pathways. Despite this, early work as described here implicated HS in AD not only in the context of its interaction with BACE-1 but also perhaps for other roles in the pathogenesis of AD.

Table 5.3: Interactions between nodes as predicted by the IPA® software. The top scoring network as generated by IPA® following search of protein lists describing HS biosynthetic enzymes, core proteins, GWAS associated risk factors and the heparin interactome generated a network scheme for the below proteins. This network incorporated proteins from several of the gene lists searched against and predicted the relationships between each node within the network.

Node 1	← Interaction →	Node 2
PLAU	Interaction of PLAU with SERPINE2	SERPINE2
SERPINE2	SERPINE2 increases inhibition of FURIN	FURIN
FURIN	FURIN increases cleavage of pro-BACE-1 to BACE-1	BACE-1
BACE-1	BACE-1 increases expression of LRP1	LRP1
LRP1	LRP1 plays a role in removal of Aβ from the brain	Aβ
Aβ	Aβ induces increased expression of IL6	IL6
FURIN	FURIN increases cleavage of pro-TGFB1 to TGFB1	TGFB1
TGFB1	TGFB1 induces increased expression of IL6	IL6
TGFB1	TGFB1 induces increased levels of beta-estradiol	Bet-estradiol
IL6	IL6 decreases levels of beta-estradiol	Beta-estradiol
Beta-estradiol	Beta-estradiol can modulate levels of HS	Sulfotransferases
Sulfotransferases	Sulfotransferases add sulfate groups to HS	Heparan sulfate
TGFB1	TGBF1 stimulates microglial activation	Microglial activation
Microglial activation	Activated microglia co-localise with mature amyloid plaques	Mature plaques

5.9 Discussion

5.9.1 STRING

Analysis with STRING software revealed a strong interaction network between the HS biosynthetic enzymes and core proteins. This observed close interaction was not surprising since these proteins all share common functional purpose to produce proteoglycans. Indeed, the majority of interactions observed represented interactions based on text mining whereby proteins of interest had appeared in the literature together. Again, this is expected with respect to these proteins appearing in the same mechanistic pathway. In contrast however, there were very few interactions displayed that represented experimentally determined association. The observed experimentally derived interaction between EXT1 and EXT2 is a previously established interaction between the two

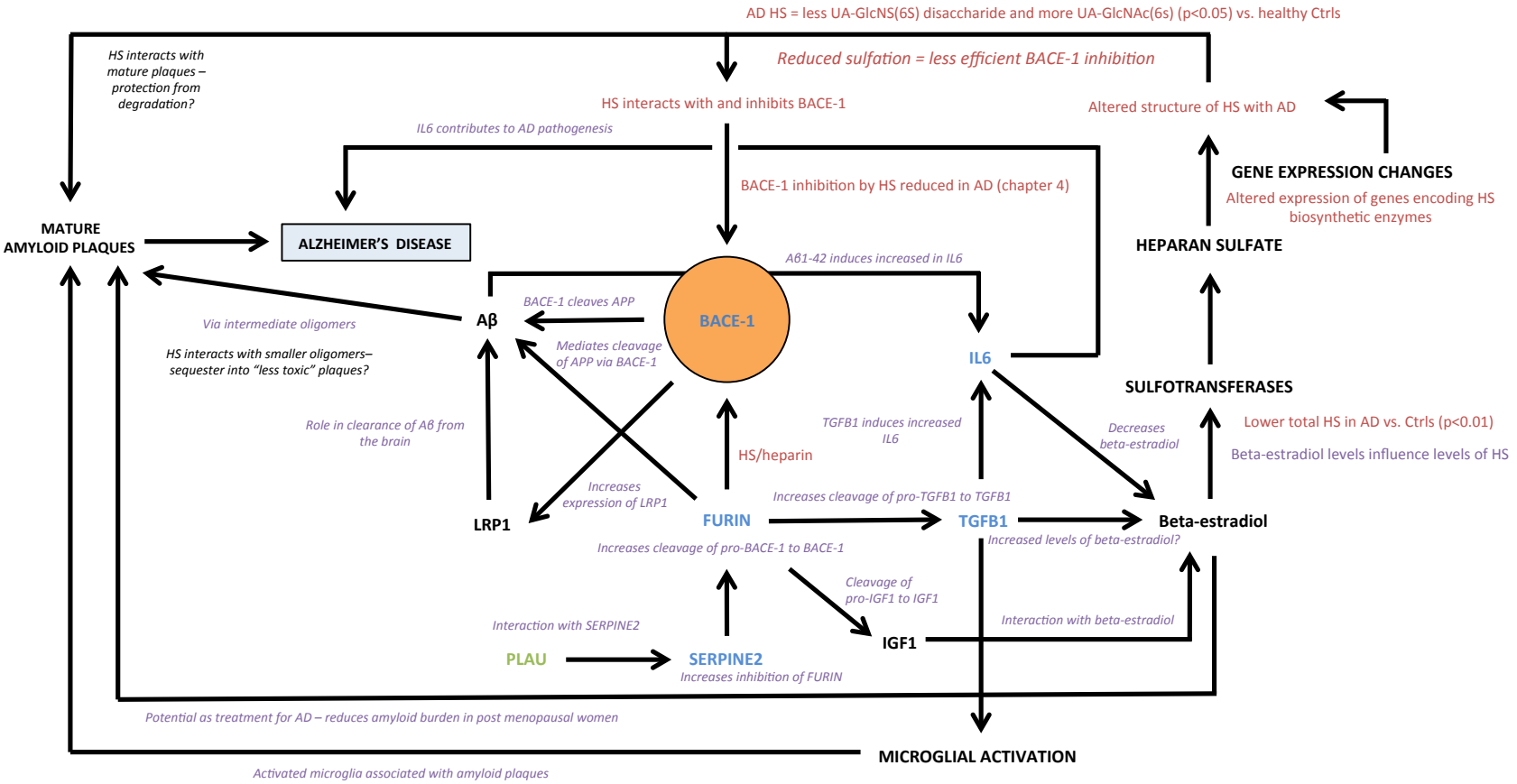

Figure 5.8: Predicted model of interaction between HS biosynthetic machinery, core proteins, GWAS identified risk proteins and heparin interactome as based on IPA generated interaction predictions and data generated within the lab in this project. The above network depicts a model generated as a combination of lab validated data and interaction predictions. More work is needed to confirm all associations as shown here however this network places HS structure and functionality in the wider context of AD, not just as an interactor of BACE-1 but also linking other pathogenic pathways associated with AD such as inflammation. Colours: Blue; heparin interactome, Green; GWAS identified AD risk genes, Red; lab validated findings, Purple; IPA® interactions.

enzyme isoforms and describes the complex formed by these to catalyse the extension of the HS chain during biosynthesis (McCormick*, et al.* 2000). In addition an interaction between NDST1 and EXT2 was recorded in mice in embryonic development research whereby levels of EXT1 and EXT2 were shown to affect the levels of NDST1 within the cell and ultimately had consequences for the final structure of HS that is generated (Presto*, et al.* 2008). Whilst this interaction has not been confirmed in humans as yet, this evidence suggests tight regulation of the synthesis of HS and the ways in which its final structure might be controlled. It was already previously established how the role of each family of enzymes works to polymerise and modify the HS chain. However, as yet there is still a great deal to learn regarding the mechanisms that regulate the final structure of HS and its ligand binding potential. Whilst we would expect the association of the HS biosynthetic machinery components on account of their common functionality, the notion of direct association between enzymes of different families are suggestive of a very complex pathway to regulate the final outcome in terms of HS structure. Moreover, the absence of any experimentally derived interaction data between more proteins within the HS biosynthetic pathway highlights the gaps in our understanding of this pathway.

With regard to the core proteins, experimentally determined interactions were also reported between all members of the SDC family (protein-protein interactions in humans). These interactions are based upon the research by Dews and colleagues in 2007 whereby the transmembrane domains (TMDs) of the SDC family have been shown to display homotypic and heterotypic interactions. This work suggested that these TMDs might play important roles in the interactions of full-length SDC family members (Dews and Mackenzie 2007). As before, evidence for interactions within a particular family may not be particularly surprising. That being said, this evidence does goes some way to further strengthen the notion of a more complex route of HS synthesis whereby the activity of particular enzymes and core proteins is not achieved in isolation but in combination with other factors.

STRING analysis was also carried out with the addition of the GWAS identified AD risk proteins. With this list combined with the HS biosynthesis list, STRING did not reveal tight interaction between the two lists. The only point of contact between the two groups was recorded between the SDC family and APOE. Kim and colleagues in 2014 described the role of the SDC family in the mediation of APOE isoform dependent neurite outgrowth and synaptic plasticity and their potential role in AD (Kim*, et al.* 2014). Furthermore, SDC2 has been reported to induce the maturation of dendritic spines within the brain (Ethell and Yamaguchi 1999), thus implicating the SDC family in the regulation of synaptic plasticity and demonstrating a direct association between the two gene lists.

Taken together, the use of STRING software on this occasion did not highlight a great deal of interaction between the proteins of interest. Naturally, that does not mean to say that these interactions do not exist but rather highlights a gap in our understanding with regard to the ways in which, if at all, HS biosynthetic machinery components interact and the implications this may have on wider AD risk factors. This search was somewhat limited in that the HS biosynthetic machinery is targeted to a very specific function. Indirectly, the role of these enzymes is vastly important as their activity determines the final structure of HS that in turn has consequences for ligand binding affinity. Indeed, considering final HS structural outcomes will be key no doubt in understanding the functionality of many downstream components associated with the pathogenesis of AD. Considering the interaction of individual components of the synthesis chain is likely to yield less interactive data being that it is the collective outcome that will have a more considerable effect on downstream ligand binders.

It is worth commenting that since HS is not a protein and is not directly encoded by a gene, it is under-represented in this approach. There is direct evidence of HS interacting with, various proteins, and this could also be taken into account in future extension of these studies. Indeed in further work in the future it will be useful to study the potential interactions of the heparin interactome proteins to assess whether any wider pathways and connections can be drawn implicating them in AD pathogenesis and its risk factors.

5.9.2 Genevestigator®

The Genevestigator® software was used to determine how the presence of the AD phenotype might affect the expression of the genes that encode HS biosynthetic enzymes and core proteins. It should be noted that this aspect of the informatics work was actually carried out prior to commencing any work within the lab as a way of preliminarily determining a) whether these changes were occurring at all in the presence of AD and b) which regions of the brain were most susceptible to these changes. Sampling of an appropriate brain region for this project was paramount and this aspect of the informatics work informed the choice that was made. The hippocampus is the brain region first implicated in AD pathogenesis (Padurariu*, et al.* 2012) yet its major roles in memory formation and consolidation make it a popular region to study and as such it is very difficult to obtain samples. The Genevestigator® work as described here highlighted the significant expression changes that occur in the middle temporal gyrus, a region of the temporal lobe (one of the 4 lobes of the cerebral cortex) and is an area key in the formation of memory and language known to be affected in AD (Convit*, et al.* 2000). The changes in expression of the HS biosynthetic enzymes and core proteins as determined with this previously published study suggested change in the structure of HS might also occur in the presence of AD and as such, proved

to be a suitable region of the brain to sample from patients to carry out the work as described in chapters 2-4.

The changes in the expression of HS genes in the presence of the AD phenotype as determined in this study were ultimately largely consistent with those changes established in the lab in chapter 3. As within any sampling from human sources, variability between individuals is significant and difficult to control. It was therefore promising to replicate most of the findings as displayed with the Genevestigator software. Strong up-regulation in the expression of the *SULF* genes across the brain regions studied was consistent with the TaqMan® array analysis as undertaken in chapter 3 and confirms the notion of a less sulfated HS in AD patients that might display reduced inhibition of BACE-1 and thus lead to the elevated generation of the toxic Aβ peptide. Down regulation of the *HS6ST* genes as displayed in this Genevestigator® search also strengthens our hypothesis that changes in the expression of HS biosynthetic genes could be an upstream causation of HS structural changes as observed in AD patient brain samples compared to healthy controls.

In addition, the use of the Genevestigator® software as demonstrated here allowed easy scanning of the different brain regions and the variability that may occur in HS synthesis regulation. As already hypothesised, it may be that variation in spatial vulnerability to AD pathogenesis as observed in the brain may be at least partly explained by alterations to the structure of HS. These changes will naturally be determined by expression profiles of the appropriate genes and as this informatics work indicated, may be very different in different regions of the brain. Future work to explore structural changes to HS in different regions of the brain would be interesting. Indeed, it would be interesting to explore whether the expression profiles in these regions can be "matched up" to their downstream effects. If so, expression patterns of these genes may prove beneficial as markers for vulnerability to AD pathogenesis in individuals.

With respect to the core proteins, a much more substantial up regulation of expression of the genes encoding core proteins was observed in the presence of the AD phenotype relative to healthy controls with much fewer genes displaying decreased expression. Despite this, the hippocampus stood out as displaying reasonably prominent down-regulation of core protein gene expression vs. other brain regions studied. This might be indicative of variable regulation across different brain regions and may go some way to explain why the hippocampus is affected first in AD disease development. Future work to look further into this will be crucial to confirm this; however, differential patterns of gene expression as observed in this work creates a strong argument for a tightly regulated process that may determine vulnerability to onset of disease.

In a similar manner, the expression of the genes encoding HS biosynthetic enzymes and core proteins was investigated in different brain regions in a physiological non-diseased state. AD is known to develop in a temporal and spatial fashion across different brain regions and variation in healthy baseline expression of these genes, it was hypothesised, may go some way to predict susceptibility to AD development, and indeed other neurological diseases. The heat map generated from this search displayed strong expression differences across the different HS biosynthetic enzymes. The clustering tool was also used to group genes that may be switched on and off together in response to a particular anatomical location or disease state. The observation on this occasion of differential expression across the isoforms of different enzyme families was suggestive of regional specificity and offers insight into the ways in which HS synthesis and modification may be regulated in different parts of the body. This finding was consistent with previous research that has established variable expression of HS enzyme isoforms (Lindahl*, et al.* 1998, Warda*, et al.* 2006). Whilst not necessarily surprising, variable expression of the isoforms as observed here may explain why AD pathogenesis develops in spatially variable fashion and does not develop ubiquitously throughout the brain (Galton*, et al.* 2001).

In addition, the use of the clustering tool allowed grouping of sets of genes that may be switched on and off together in the presence of the AD phenotype. Whilst a great deal more work would be needed to confirm this, the notion of groups of genes responding to a certain cellular state may offer clues into ways in which the structure of HS is controlled. Future work to investigate shared transcription factors for example between these groups of genes may offer some insight into the mechanisms that control downstream functionality of HS. Whilst we did not have time to look into this, the groups of genes generated with this tool in Genevestigator® may prove an interesting starting point for future studies.

5.9.3 Ingenuity Pathway Analysis (IPA®)

IPA® was used to explore potential relationships and connections between the proteins of interest that we had identified in our previous studies - the GWAS identified AD risk genes, those genes that encode the HS biosynthetic enzymes and those that encode the HS core proteins. Finally the heparin interactome list was also added to searches for the sake of completion as this work was only at a preliminary stage and it was not known what connections might exist between proteins of interest.

The top scoring canonical pathways determined with this search included hepatic fibrosis, granulocyte adhesion, bladder cancer signaling, axonal guidance and the coagulation system. The broad spectrum of canonical pathways associated with the gene lists used in this search were not surprising on account of the heparin interactome being such a large list of proteins. HS is found

ubiquitously all over the body, and due to its variable structural motifs (as described previously), the number of factors it is able to interact with is wide and varied. Indeed, HS is able to bind to chemokines, growth factors, coagulation cofactors, matrix proteins, and many more enzymes (Pomin and Mulloy 2015). As a result it is not surprising that these proteins would be involved in such a wide variety of canonical pathways. Similarly, of the 476 proteins searched, 200 of them were associated with neurological diseases in some way. Whilst GWAS identified risk genes would naturally be associated with neurological disease, this list was relatively short, and hence a number of heparin interactome and core proteins were also associated with neurological disease. Chemokines may be an obvious tie to neurological disease on account of the state of chronic inflammation associated with a number of neurological disorders (Samuels 2004). The finding here that a number of already established canonical pathways are associated with these target proteins, strengthened the notion of a very complex association network between these proteins and their wider role within the body. Likewise, whilst we have established a role for HS in interaction with BACE-1 and amyloid pathology, this work has indicated that HS may be key in other mechanisms that contribute to the pathogenesis of AD.

Moreover, the crossover between established canonical pathways confirms the complexity of the functionality exhibited by the HS-related proteins and the heparin interactome. The very nature of HS and its ability to bind numerous ligands makes its role within the body, particularly in the context of disease, particularly challenging to fully elucidate. The synthesis of HS itself sat in isolation with respect to other physiological function within the body. This finding seemed somewhat surprising on account of the importance of synthesis of HS and the consequences this has on ligand binding affinities and thus functions. Indirectly, the synthesis of HS is hugely important indeed the data generated in this project has confirmed the importance of HS biosynthesis and the resulting HS structures and the ways in which they interact with their binding partners. For that reason, this preliminary work highlighted a need to integrate the synthesis of GAGs and the downstream consequences this may have on the signaling and functionality of other associated proteins. The network of interactions generated here thus aimed to consolidate data as gathered in the lab in this project and the predictions of interactions made by the IPA® software. The resultant network therefore is only at this point a model that aims to predict the wider context of HS functionality in pathogenesis and development of AD.

This model (**Figure 5.8**) predicted a regulation of the BACE-1 enzyme via SERPINE2 and FURIN proteins. PLAU, a GWAS identified AD risk factor SNP is known to interact with SERPINE2 (Ozturk*, et al.* 2007) and one might predict that mutations within the PLAU gene may result in aberrant interaction with SERPINE2. Furthermore, SERPINE2, a serine protease inhibitor, is an inhibitor of FURIN, a protein that is able to activate a number of other proteins (including BACE-1) via cleavage. Indeed, FURIN is able to increase the activity of BACE-1 by cleavage of the Pro-BACE-1

pro-peptide. As such, this model predicted a process by which the activity of BACE-1 (in addition to its overexpression with AD (Decourt and Sabbagh 2011)) may be enhanced as a result of enhanced FURIN activity. Similarly, SERPINE2 is a member of the heparin interactome and as such, one might question the role of HS in attenuating or promoting the activity of this protein. FURIN is also able to activate TGFB1, via cleavage of pro-TGFB1 (transforming growth factor beta), a cytokine belonging to the transforming growth factor superfamily of proteins. Previous research has reported that dysfunction of the TGFB signaling pathway may contribute to AD by accelerating the deposition and fibrilisation of the Aβ peptide (Das and Golde 2006). It is important to note that TGFB is another heparin interactome protein and its functionality may be perturbed as a consequence of altered HS structure.

Downstream of TGFB, IL6 was shown to interact with this cytokine and literature based searches indicated that TGFB is able to induce elevated levels of IL6 (Turner*, et al.* 1990). IL6 is another heparin interactome protein and is consistently implicated in AD in the literature. Aberrant immune regulation and inflammatory processes is tightly associated with the development and persistence of AD (Akiyama*, et al.* 2000). Indeed, elevated levels of IL-6 have been reported in AD patients (Khemka*, et al.* 2014) and have been shown to stimulate the synthesis of APP. Purified interleukin-6 receptor (sIL-6R) added together with IL-6 has been shown to rapidly increase the levels of cell-associated and secreted APP (Ringheim*, et al.* 1998). Chronic inflammation is a known component of AD and this network association with IL-6 may go some way to predict a means by with an inflammatory state is imposed within the brain upon development of AD. Naturally, we do not know whether inflammatory states causes the AD pathology itself (as suggested above) or whether it exacerbates the pathology (or perhaps a combination of the two); however interaction of heparin interactome proteins with other factors known to associate with AD separate to BACE-1 indicates a complex functionality of HS in AD.

Also downstream to TGFB activity, it has been suggested that this cytokine may induce elevated levels of beta-estradiol (estrogen). Indeed, recent research has suggested a cross talk between TGFB and beta-estradiol such that estrogen receptor signaling was enhanced by the expression of TGFB. This finding no doubt has numerous implications for a variety of diseases including kidney function, atherosclerosis and breast cancer (Matsuda*, et al.* 2001) however may also be important in the context of AD. Estrogens in particular have been more recently studied for their efficacy as treatments of AD in light of their potential neuroprotective roles. Indeed, beta-estradiol has been shown to protect central nervous cells from oxidative stress (Behl*, et al.* 1995) including that induced by the presence of Aβ peptides and as such could prove beneficial in the treatment of AD and consequences of oxidative stress as implicated in this disease (Simpkins*, et al.* 2010). This is thus a very interesting pathway to study further, not least because of its potentially protective role in AD but also in light of its association with heparin interactome proteins.

Furthermore, the IPA® software predicted an interaction between beta-estradiol and sulfotransferases. Indeed, previous research confirmed that estradiol β-D-Xyloside is an efficient primer for the synthesis of HS and as such may be a modulator for the quantities of HS present within cells (Lugemwa and Esko 1991). Xylosides containing an aromatic ring (p-nitrophenol, 4-methylumbelliferone, and estradiol) primed heparan sulfate most efficiently. It has been suggested that the priming of HS by estradiol β-D-xyloside may be a result of the structural similarities between estradiol and a domain within the HSPG core proteins. Data generated in the lab as described in chapter 2 reported significantly reduced levels of total HS within brain samples from AD patients compared to healthy controls and this predicted interaction of TGFB and beta-estradiol, as established by IPA®, may go some way to explain a possible mechanism. These network components might also have implications on the level of sulfotransferase activity present along an HS chain; hence it is still largely uncertain how HS chain modification is regulated.

Based on a combination of early predictions made by IPA® and the data generated within the lab in this project, one might predict that alteration to PLAU as initiated by AD, may induce altered SERPINE2 functionality such that it is less able to inhibit FURIN. Enhanced FURIN activity may result in elevated BACE-1 activity which coupled with accelerated activity as a result of altered HS inhibition efficacy (as established in chapter 4), leads to an initiation of inflammatory pathways that exacerbate the effects of AD pathology and perpetuate the persistence of activated microglia and cytokines such as IL-6 that are associated with AD. This all may be accompanied by enhanced beta-estradiol signaling which may have downstream consequences on HS synthesis and modification which will drive the aberrant BACE-1 inhibition and aid the persistence of enhanced APP processing and Aβ turnover.

The lab data as presented here that confirmed a change in the structure of HS in brain tissue from AD patients might be associated with some of the upstream factors described above. It has been shown that structural alterations to HS have dramatic implications for its ability to bind BACE-1 and ultimately the generation of Aβ within cells, and the transfection studies in chapter 4 implicate subtle changes in sulfatase and sulfotransferase expression in the modulation of generation of this peptide. As such, it would seem there is a strong argument for importance of synthesis of HS in a number of physiological and disease-state pathways within the body. The network as described here goes some way to attempt to set the role of HS into a wider disease mechanism context. Naturally, this work is only preliminary and a great deal more work is required to establish how the role of HS may further be important in pathways such as inflammation that are known to exacerbate AD, and also its interaction with those risk factors already identified for the onset of AD. Despite this, the integration of GWAS associated risk factor proteins; heparin interactome proteins and data from the lab regarding the HS biosynthetic pathway highlight a model by which a better understanding of the complexity of AD may be approached.

5.10 Conclusions

There is no doubt that the use of informatics still requires a great deal more work to make any firm conclusions regarding HS and a wider role in AD. Despite this, the studies carried out here have highlighted the sheer complexity of any HS mediated pathway on account of the wide variety of ligands that it may bind and the canonical pathways with which it may be associated. The factors contributing to full-blown pathogenesis are multiple and varied and as such, understanding all of the mechanisms that underpin AD is a huge challenge in itself. That being said, the heparin interactome, HS biosynthetic machinery and pre-established GWAS identified risk proteins may serve as a useful tool in elucidating some of the crossover points between these myriad pathways. Inflammation it would seem is a particularly interesting area of cross talk between HS interacting proteins and amyloid pathology and one that future studies will need to further investigate. Whilst we may not have had time to explore the avenues highlighted with this work, there is no doubt that HS is a key player in AD pathology. Furthermore, if we are to think of HS as a wide acting, ubiquitous regulator within the body, one might consider it to function within an extremely "robust" system. In this sense, robustness may refer to the ability of HS to modulate its structure such that it may efficiently bind to an otherwise unavailable ligand to restore baseline conditions without risk of losing binding efficacy with another partner. Re-establishing "cellular equilibrium" following challenge is mediated to a great extent by HS and to that end, a great deal more focus on the regulation of HS synthesis may be warranted. Understanding the consequences of altered HS synthesis and modification may prove vital in understanding the aberrant pathways that may consequently be set into motion to initiate disease. The finding that HS synthesis is so poorly represented in network analysis suggests a need for a much greater focus on the seemingly subtle yet potentially significant alterations in HS structure. Moreover, the changes to HS as illustrated in this project in the context of AD and its amyloid pathology are not unique and could serve to be interesting targets of research for a number of other diseases.

Chapter 6: Final discussion and conclusions

6. Conclusions and final discussion

6.1 HS changes in AD and has altered BACE-1 inhibition efficacy

This project showed that the structure of HS purified from AD patient brain tissue is significantly less sulfated when compared to HS purified from healthy age-matched controls (chapter 2), suggesting that structural changes to HS occur as a consequence of the AD phenotype. In addition, this project showed that these changes in the composition of HS are likely a result of altered expression of the genes that encode HS-related enzymes responsible for the modification of the HS chain (chapter 3). Finally, the changes in HS structure elucidated here are implicated in altered BACE-1 inhibition efficacy (chapter 4) and as such may provide a mechanism by which AD development and progression is exacerbated within the brain of AD patients.

The changes in the structure of HS as observed in this project have confirmed the hypothesis that the function of HS as a naturally occurring "brake" on BACE-1 activity is attenuated by changes in its structure. This results in removal of the brake and potentially elevated APP processing as a consequence. In doing so, we have established a novel mechanism by which AD pathology may be initiated and exacerbated within the brains of AD patients. In addition, this work may serve to explain why those unaffected by AD are naturally protected from the onset of AD - if HS structure is maintained with ageing in a form that continues to put a brake on aberrant BACE-1 activity, APP processing could be maintained at a healthy level.

It should be noted that, the changes in the structure of HS as reported here have only been pursued with specific reference to function in regard to its interaction with the BACE-1 enzyme. It has already been shown that HS also interacts with, and influences in some cases, other features of AD pathology including interaction with the mature plaques themselves (Zhan*, et al.* 1995), the Aβ peptide (Castillo*, et al.* 1997, Cotman*, et al.* 2000). As such, in future studies it may be interesting to assess how the observed structural changes that occur with AD may also affect these additional functions. Previous research has indicated that interaction of HS with mature plaques may indeed protect them from degradation (Biroc*, et al.* 1993). Should this interaction be dependent upon sulfation motifs within HS (as we would expect), one might argue that AD induced structural changes may also enhance/inhibit this functionality. Likewise, the role of HS and HSPGs as a promoter of fibrilisation of smaller oligomers into mature fibrils (Snow*, et al.* 1994) may also be dependent upon structural features within the HS chain. It has also been established that GAG-amyloid interactions occur with a number of different affinities, all of which depend on the details of the amyloid fibril architecture. As such, it would appear there is a complex relationship between GAGs and the

amyloid species with regard to AD pathology development (Stewart*, et al.* 2016). Understanding the implications of HS structural alterations in all facets of its role in AD may help elucidate the ways in which AD pathology is self perpetuated.

This study investigated the structure of HS purified from the middle temporal gyrus region of the brain, an area of the cortex known to be implicated in AD and the spread of pathology. This area was selected based on previously established changes in the expression of HS biosynthetic genes in this region with AD, alongside known vulnerability of this region to AD pathology. Naturally, this study could be extended to explore possible changes in the structure of HS in other affected brain regions, including the hippocampus. This is the first area known to be affected by AD pathology and is also the key region implicated in memory formation and consolidation (Fox*, et al.* 1996). As such, understanding the changes in HS that may occur here will prove particularly interesting and may offer insights into temporal and spatial changes in HS correlated with the spread of this disease. Procuring samples of AD hippocampus is particularly challenging in light of its key functional roles in a number of cognitive functions. As such, selection of the middle temporal gyrus was an appropriate region to study first in the context of AD pathology. Now this preliminary study has uncovered significant changes in HS that occur with AD, there is a strong argument to pursue studies on other regions of the brain. In the same manner, informatics work that confirmed variable baseline expression of HS biosynthetic genes in different regions of the brain (chapter 5) may serve to predict regional vulnerability to the features of AD. It would be interesting in future studies to determine whether these differences in baseline expression can also predict HS structural variability and ultimately susceptibility of an individual to the onset of AD. In combination with this, establishing how BACE-1 activity inhibition by HS is altered in the hippocampus would be an interesting avenue to pursue; is the activity of BACE-1 in the presence of endogenous HS in this region enhanced to an even greater extent in AD patients vs. healthy controls?

The changes in the expression of HS biosynthetic genes as confirmed in this study have offered an upstream mechanism by which the reported changes in the structure of HS could be initiated. Elevated expression of the *SULF1* gene as reported in AD patients and reduced expression of the *HS6ST2* and *HS6ST3* genes is indicative of reduced sulfation at the 6-O position. This finding was supported by reduced sulfation of HS as confirmed with compositional analysis. Further work is needed to establish exactly how changes in HS gene expression affect downstream regulation of HS structure. Indeed, more work is also necessary to determine whether there is correlation between expression and activity of these enzymes. Despite this however, these changes in AD patients strongly indicate a mechanism by which HS structure is altered and ultimately, via modulation of BACE-1 activity, regulates production of the toxic Aβ peptide. Moreover, changes in expression patterns of these genes may serve as a very preliminary biomarker in which vulnerability to AD could be predicted in patients. Recently, a significant SNP within the *HS6ST1* gene was linked with

albuminuria, associated with the onset of diabetes (Teumer*, et al.* 2016). Moreover, the HS6ST1 gene has also been implicated in idiopathic hypogonadotrophic hypogonadism and the absence of puberty in adolescents (Tornberg*, et al.* 2011). Other HS related genes implicated in disease include GWAS studies to implicate the *NDST3* gene in schizophrenia and bipolar disorder (Lencz*, et al.* 2013) and *SUMF1* (sulfatase modifying factor 1) in autism (Glessner*, et al.* 2009). These findings strengthen the notion of HS biosynthetic genes as early markers for disturbances in key pathways associated with a range of diseases.

Interesting to note, Nagai and colleagues have previously reported regulation of the expression and cellular localisation of the HS6ST3 enzyme by BACE-1 (Nagai*, et al.* 2007). It is unknown as yet how these two proteins may be linked however it has been postulated that BACE-1 may cleave a currently unidentified protein that HS6ST3 in some way interacts with, or that BACE-1 may be able to interact with and regulate the secretory pathway by which HS6ST3 is transported. Interestingly this interaction was specific to HS6ST3 and not the other HS6ST enzyme isoforms. Moreover, inhibition of BACE-1 activity was able to increase the total levels of HS 6-O sulfation. Elevated 6-O sulfated in this manner may reflect a self perpetuating cycle by which effective HS mediated inhibition of BACE-1 can be exploited to maintain its own suppression. That being said, elevated 6-O sulfation may also serve to enhance fibril formation and stability (Castillo*, et al.* 1997, Lindahl*, et al.* 1999). Either way, the highly complex interaction between HS, its biosynthetic machinery, and the BACE-1 enzyme is further complicated by the myriad mechanisms by which AD pathogenesis is perpetuated. Further understanding the interaction between BACE-1 and HS6ST3 may prove key in underpinning BACE-1 regulation. Furthermore, our observation of down-regulation of the *HS6ST3* gene with AD may have direct implications on BACE-1 regulation independently of gross HS-mediated affects.

The established change in expression of the core proteins onto which HS chains may be bound also calls into question their role in development of AD pathology. The significant up-regulation of the *AGRN* gene sits well with earlier research that established its role as a protector against degradation via the presence of protease inhibitor domains (Gupta-Bansal*, et al.* 1995). The role of the HS chains that may decorate the AGRN core protein however is yet to be elucidated. Future studies to purify AGRN proteins from brain samples of AD patients and extraction of the HS chains that are attached may offer more information about HS covalently bound to core proteins and the ways they may influence functions related to the core protein itself. The structural changes as reported here do not distinguish between HS chains free in the cell and those attached to a core protein. Distinguishing between the two may identify important changes key in understanding their respective functionalities. Variability between patients was expected and as such, larger sample sizes in the future may be necessary to smooth out variability and strengthen some of the trends for

changes in expression as reported in chapter 3. More robust changes with AD may become apparent with larger group sizes.

In addition, this study confirmed that altered changes in the structure of HS in AD as induced (we hypothesise) by altered expression of the genes that encode the HS biosynthetic enzyme machinery results in reduced BACE-1 inhibition efficacy. Elevated activity of the BACE-1 enzyme is the known cause of elevated production of the Aβ peptide. This study has verified that HS may serve as the "brake" that regulates the activity of BACE-1. In the presence of the AD phenotype, this brake is less efficient (as a consequence of attenuated HS inhibition), resulting in elevated processing of the APP protein to form the Aβ peptide. This finding strengthens the notion that BACE-1 activity is a strong target for future design of therapeutics against AD and the role of HS; a physiologically active GAG provides the optimal template on which to create future therapies. This study has gone some way to highlight the "ideal" structures necessary for efficacious BACE-1 inhibition. Finding ways to mirror these structures, in combination with attenuation of the previously established anti-coagulant activities of heparin derivatives, may provide a route for development of small (important for crossing the BBB), non toxic, potent inhibitors of BACE-1, specific to only BACE-1 and not other proteases, and these may have significant therapeutic potential.

The somewhat preliminary *in vitro* work carried out in this project to assess how modulation of HS biosynthesis is able to regulate production of the Aβ peptide has gone some way to address the hypothesis of a "personalised" heparin derivative to treat the amyloid pathologies of AD. The knockdown of the *SULF1* and *SULF2* genes in cultured HEKSweAPP cells resulted in reduced accumulation of the $A\beta_{1\text{-}42}$ peptide and offered a plausible mechanism by which toxic peptide formation could be halted within cells (chapter 4). Furthermore, the data collected here offers a strong argument for the role of the sulfatase enzymes, as key players in the fine-tuning of HS structure with consequences on overall functionality of HS. Indeed, reduction of $A\beta_{1\text{-}42}$ as reported here confirms the notion of 6-O sulfation being important for BACE-1 interaction and inhibition (Scholefield*, et al.* 2003). Furthermore, the significant changes as reported here with knockdown of the *SULF* genes may put forward an argument for the importance of fine tuning of the HS chain following modification over gross structural changes. Knockdown of the *HS6ST* genes in this context produced less conclusive results regarding affects on $A\beta_{1\text{-}42}$ processing; this is likely due to issues of redundancy among the 3 different isoforms. Combinatorial knockdown of *HS6ST1*, *HS6ST2* and *HS6ST3* together will be something to pursue in future studies to explore the effects of more robust gene knockdown to reduce 6-O sulfation. It may be that combination knockdown will yield more substantial results with respect to modulation of $A\beta_{1\text{-}42}$ production. In addition a great deal more research is needed to determine the functionality of HS biosynthetic enzymes and the ways they function in combination with each other. It would be interesting to determine whether knockdown

of *HS6ST* gene expression completely for example forces the compensatory up-regulation of other genes and drives the equilibrium of synthesis via a different modification pathway e.g. enhanced activity of the HS2ST or HS3ST family of enzymes. Furthermore qRT-PCR analysis to explore potential expression changes of other gene families following knockdown of selected HS biosynthetic genes may offer interesting information concerning the regulation of HS synthesis and modification. It seems likely that regulatory mechanisms are in place to counter disturbances in the biosynthetic pathways that generate HS.

The work carried out to assess BACE-1 inhibition efficacy in the SULF KO mouse models went some way to recapitulate more exaggerated modulated structures of HS as discussed above. Indeed, this work reported a significant improvement in BACE-1 inhibition in mice in the absence of SULF2 in isolation, as well as those lacking both the *Sulf1* and *Sulf2* gene activity. Future studies may utilise other mouse knockout models as a way of generating more exaggerated gene knockdown to assess how regulation of HS synthesis takes place and the implications this has on the generation of the toxic Aβ species. Such animals could also be crossed with AD model mice to explore the effects on development of amyloid pathology.

Understanding the spatial arrangement of sulfation in HS may also prove to be key in understanding the ways in which it is able to interact with BACE-1 and how alterations in this spatial arrangement are implicated in BACE-1 inhibition efficacy. Developing other sequencing methodologies may help to further elucidate structural features of HS key in the interaction of HS with BACE-1. Compositional analysis as employed in this study allowed comparison of the ratios of specific disaccharides within HS from AD and age-matched control brain samples. However the sequence in which these disaccharides are observed in the HS chains could not be determined. In a similar manner, the structural analysis as employed in this study (chapter 2) could not distinguish the identity of the uronic acid residue. Changes in the structure of HS via epimerisation of the GlcA to IdoA residues (via the action of the C5 epimerase enzyme) have been postulated to have dramatic effects on the regulation of the modification events that occur subsequently (Rudd and Yates 2012). Changes in the expression of the *GLCE* gene as reported in chapter 3 with AD relative to age-matched healthy controls may be indicative of additional structural changes to a proportion of HS chains that could confer significant alterations in the subsequent sulfation motifs that are created. Using compositional analysis methods that can identify the identity of the uronic acid epimer (e.g. nitrous acid cleavage) would be of interest in future studies. Understanding the consequences of epimerisation to the HS chain in the context of AD may further strengthen the findings reported here that confirm structural changes as key in the regulation of BACE-1 and processing of APP to form the $A\beta_{1\text{-}42}$ peptide. Enhanced epimerisation of AD HS as potentially indicated by the gene expression data described here may suggest further structural changes implicated in BACE-1 inhibition efficacy and disease development. Taken together, understanding more about the “key

players" in terms of the HS biosynthetic machinery may provide ideas for reflecting susceptibility to the onset and development of AD.

This project has established that the compositional profile of HS derived from AD patient brain tissue is different to that of healthy age-matched controls and as such offers a mechanism by which the onset of AD may be promoted or accelerated. Furthermore, the known interaction of HS with other features of AD in addition to BACE-1 may serve to explain the persistence of this pathology in patient brains as disease development continues. This work coupled with review of the literature would suggest a "Yin-Yang" relationship whereby HS may both enhance the pathology associated with AD and protect against some of its toxic affects. The interaction of BACE-1 as investigated here is undoubtedly only a facet of the much wider and more complex role that HS is known to play in AD. That being said, targeting the activity of BACE-1 in this manner is a central pathway eliciting the very early "seeds" of AD pathology. Understanding the role of HS in this pathway thus serves as a strong drug design target in the future by nature of its significant position in greater disease development. The observed changes in HS as discussed in this study will surely affect several downstream ligand-binding targets of HS, though those affecting its interaction with the BACE-1 enzyme could certainly prove the most efficacious as a focus for drug design.

Targeting this key, and very well established, pathway in AD pathology might face criticism in light of several failed pharmaceutical efforts to create clinically effective anti-amyloid therapeutics. Despite this, the approach of this study to investigate the role of an already naturally occurring "brake" on BACE-1 activity immediately overcomes several of the failures of those compounds that reached but failed at clinical trials. Designing new drug strategies based on natural products already well tolerated by the body may prove to be key in treating AD.

6.2. HS changes with ageing and this has implications for BACE-1 inhibition efficacy

As a side issue, this project also aimed to investigate the variable of ageing in the context of HS and BACE-1 inhibition efficacy. This work was carried out to explore whether age, the biggest risk factor for the onset of AD, initiated similar pathways in the regulation of HS and its interaction with the BACE-1 enzyme. Somewhat unexpectedly, the data collected from this work indicated a separate mechanism by which HS is regulated with normal physiological ageing. Structural changes as induced with age (as discussed in chapter 2) were found to differ greatly from those recorded in AD patient HS samples indicating age and AD induced HS changes are different. Aged mouse HS samples were found to be more potent inhibitors of BACE-1 activity vs. their younger control counterparts, whereas one might have expected aged HS samples to display reduced BACE-1 inhibition properties

similar to that of the AD samples. This contradictory result however may suggest a separate protective mechanism is initiated whereby normal physiological aging in healthy individuals maintains an appropriate level of BACE-1 inhibition, thus avoiding elevated APP processing and enhanced levels of Aβ. Moreover, when studying the ageing phenotype, HS at lower concentrations exhibited the most potent BACE-1 inhibition. Future studies to investigate BACE-1 inhibition potency at even lower concentrations may prove interesting with regard to exploring the potential for aged HS to *both* inhibit and activate BACE-1 at varying concentrations.

Naturally this hypothesis needs a great deal more work to confirm and fully elucidate, not least in human tissue. This early data however, as described in this project, would suggest that there might be some protective regulatory processes that may actually shape HS such that it is better able to modulate the activity of BACE-1 to a normal physiological level. As with the studies in human AD tissue, gene expression studies to explore the potential upstream regulation of these structural changes as described with this ageing model will also be important. Differences in gene expression profiles with AD and with normal ageing may go some way to highlight separate regulatory pathways by which physiological ageing and disease are separated. Moreover, exploring how groups of HS-related genes may be regulated, for example via shared transcriptional regulators may offer new insight into how separate HS structural regulatory pathways may be maintained and balanced. We might predict that enhanced BACE-1 inhibition (as detailed in chapter 4) may be elicited via altered HS structures distinct to those observed in the presence of the AD phenotype, such that the ability of HS to interact with and block the activity of BACE-1 is significantly altered.

6.3. Bioinformatics tools set the role of HS in the wider context of AD

The roles of HS in the pathogenesis of and progression of AD are undoubtedly very complex and varied, and the work carried out here with bioinformatics has highlighted the need for future studies to further elucidate the pathways associated with the development of AD and the ways in which these pathways are connected. In particular, the preliminary work as carried out here indicated strong association with the HS biosynthetic machinery; GWAS identified risk genes and the heparin interactome with inflammatory pathways. Chronic inflammation is a known feature that accompanies AD pathology and finding ways to interconnect the numerous pathways associated with the development of this disease may be paramount in identifying key targets for potential therapeutic strategies. A great deal more work is needed before firm conclusions can be made regarding the role of heparin binding proteins and the network of interactions that both bring about, and aid in the persistence of, AD pathology. Moreover, the informatics work as carried out here not only allowed preliminary identification of areas prone to change in HS (as determined by Genevestigator studies prior to lab work) but also highlighted the absence of HS structural

regulation as a predictor for altered associations between proteins within a network. The work of this project has implicated the structure of HS and the way in which it is synthesised as central to its downstream affects and interaction with key proteins in disease mechanisms pathways. Whilst the biosynthesis of HS (and the means by which its biosynthesis is controlled) was not associated with the major canonical pathways as identified in this study, it seems unlikely that changes to this biosynthesis could *not* have significant implications on these pathways. As such, one might propose that a greater emphasis needs to be placed upon HS biosynthesis and the ways in which its structure might be modulated and the consequences this could have on important physiological and indeed disease pathways. Whilst more work is needed to establish firm conclusions regarding the interactive networks that link the heparin interactome, HS synthesis and GWAS identified AD risk factors, it is certain that these associations do exist, and understanding them, may shed some much needed light on disease progression and ways in which treatment of AD may be tackled in the future.

References

Adams MD, Soares MB, Kerlavage AR, Fields C, & Venter JC (1993) Rapid cDNA sequencing (expressed sequence tags) from a directionally cloned human infant brain cDNA library. *Nat Genet.* 4(4):373-380.

Adlard PA & Bush AI (2006) Metals and Alzheimer's disease. *J Alzheimers Dis.* 10(2-3):145-163.

Ai X*, et al.* (2007) SULF1 and SULF2 regulate heparan sulfate-mediated GDNF signaling for esophageal innervation. *Development.* 134(18):3327-3338.

Aikawa J & Esko JD (1999) Molecular cloning and expression of a third member of the heparan sulfate/heparin GlcNAc N-deacetylase/ N-sulfotransferase family. *J Biol Chem.* 274(5):2690-2695.

Aikawa J, Grobe K, Tsujimoto M, & Esko JD (2001) Multiple isozymes of heparan sulfate/heparin GlcNAc N-deacetylase/GlcN N-sulfotransferase. Structure and activity of the fourth member, NDST4. *J Biol Chem.* 276(8):5876-5882. Epub 2000 Nov 5821.

Aisen PS, Schmeidler J, & Pasinetti GM (2002) Randomized pilot study of nimesulide treatment in Alzheimer's disease. *Neurology.* 58(7):1050-1054.

Akiyama H*, et al.* (2000) Inflammation and Alzheimer's disease. *Neurobiology of aging* 21(3):383-421.

Allan LM, Ballard CG, Rowan EN, & Kenny RA (2009) Incidence and prediction of falls in dementia: a prospective study in older people. *PLoS One* 4(5):e5521. doi: 5510.1371/journal.pone.0005521. Epub 0002009 May 0005513.

Alva G & Cummings JL (2008) Relative tolerability of Alzheimer's disease treatments. *Psychiatry (Edgmont).* 5(11):27-36.

Ambrosius M, Kleesiek K, & Gotting C (2008) Quantitative determination of the glycosaminoglycan Delta-disaccharide composition of serum, platelets and granulocytes by reversed-phase high-performance liquid chromatography. *J Chromatogr A.* 1201(1):54-60. doi: 10.1016/j.chroma.2008.1006.1007. Epub 2008 Jun 1011.

Ard MD, Cole GM, Wei J, Mehrle AP, & Fratkin JD (1996) Scavenging of Alzheimer's amyloid beta-protein by microglia in culture. *J Neurosci Res.* 43(2):190-202.

Arriagada PV, Growdon JH, Hedley-Whyte ET, & Hyman BT (1992) Neurofibrillary tangles but not senile plaques parallel duration and severity of Alzheimer's disease. *Neurology.* 42(3 Pt 1):631-639.

Attwood TK*, et al.* (2000) PRINTS-S: the database formerly known as PRINTS. *Nucleic Acids Res* 28(1):225-227.

Avramopoulos D (2009) Genetics of Alzheimer's disease: recent advances. *Genome Med* 1(3):34.

Backstrom G*, et al.* (1979) Biosynthesis of heparin. Assay and properties of the microsomal uronosyl C-5 epimerase. *J Biol Chem.* 254(8):2975-2982.

Bairoch A & Apweiler R (2000) The SWISS-PROT protein sequence database and its supplement TrEMBL in 2000. *Nucleic Acids Res* 28(1):45-48.

Baker W*, et al.* (2000) The EMBL nucleotide sequence database. *Nucleic Acids Res* 28(1):19-23.

Ballard C & Corbett A (2010) Management of neuropsychiatric symptoms in people with dementia. *CNS Drugs.* 24(9):729-739. doi: 710.2165/11319240-000000000-000000000.

Bame KJ, Danda J, Hassall A, & Tumova S (1997) Abeta(1-40) prevents heparanase-catalyzed degradation of heparan sulfate glycosaminoglycans and proteoglycans in vitro. A role for heparan sulfate proteoglycan turnover in Alzheimer's disease. *J Biol Chem.* 272(27):17005-17011.

Bartus RT, Dean RL, 3rd, Beer B, & Lippa AS (1982) The cholinergic hypothesis of geriatric memory dysfunction. *Science.* 217(4558):408-414.

Beckman M, Freeman C, Parish CR, & Small DH (2009) Activation of cathepsin D by glycosaminoglycans. *FEBS J* 276(24):7343-7352.

Behl C, Widmann M, Trapp T, & Holsboer F (1995) 17-beta estradiol protects neurons from oxidative stress-induced cell death in vitro. *Biochem Biophys Res Commun* 216(2):473-482.

Benes P, Vetvicka V, & Fusek M (2008) Cathepsin D--many functions of one aspartic protease. *Crit Rev Oncol Hematol.* 68(1):12-28. doi: 10.1016/j.critrevonc.2008.1002.1008. Epub 2008 Apr 1018.

Benjannet S*, et al.* (2001) Post-translational processing of beta-secretase (beta-amyloid-converting enzyme) and its ectodomain shedding. The pro- and transmembrane/cytosolic domains affect its cellular activity and amyloid-beta production. *J Biol Chem.* 276(14):10879-10887. Epub 12001 Jan 10810.

Benson DA*, et al.* (2000) GenBank. *Nucleic Acids Res* 28(1):15-18.

Berchtold NC & Cotman CW (1998) Evolution in the conceptualization of dementia and Alzheimer's disease: Greco-Roman period to the 1960s. *Neurobiol Aging.* 19(3):173-189.

Bergamaschini L*, et al.* (2004) Peripheral treatment with enoxaparin, a low molecular weight heparin, reduces plaques and beta-amyloid accumulation in a mouse model of Alzheimer's disease. *The Journal of neuroscience : the official journal of the Society for Neuroscience* 24(17):4181-4186.

Berman HM*, et al.* (1992) The nucleic acid database. A comprehensive relational database of three-dimensional structures of nucleic acids. *Biophys J* 63(3):751-759.

Berman HM*, et al.* (2000) The Protein Data Bank. *Nucleic Acids Res* 28(1):235-242.

Bernfield M*, et al.* (1999) Functions of cell surface heparan sulfate proteoglycans. *Annu Rev Biochem* 68:729-777.

Bernstein FC*, et al.* (1977) The Protein Data Bank. A computer-based archival file for macromolecular structures. *Eur J Biochem* 80(2):319-324.

Bilikiewicz A & Gaus W (2004) Colostrinin (a naturally occurring, proline-rich, polypeptide mixture) in the treatment of Alzheimer's disease. *J Alzheimers Dis.* 6(1):17-26.

Bink RJ*, et al.* (2003) Heparan sulfate 6-o-sulfotransferase is essential for muscle development in zebrafish. *J Biol Chem.* 278(33):31118-31127. Epub 32003 Jun 31111.

Birks J (2006) Cholinesterase inhibitors for Alzheimer's disease. *Cochrane Database Syst Rev.* (1):CD005593.

Biroc SL, Payan DG, & Fisher JM (1993) Isoforms of agrin are widely expressed in the developing rat and may function as protease inhibitors. *Brain Res Dev Brain Res.* 75(1):119-129.

Bishop JR, Schuksz M, & Esko JD (2007) Heparan sulphate proteoglycans fine-tune mammalian physiology. *Nature.* 446(7139):1030-1037.

Blasko I*, et al.* (2004) Experimental traumatic brain injury in rats stimulates the expression, production and activity of Alzheimer's disease beta-secretase (BACE-1). *J Neural Transm (Vienna).* 111(4):523-536. Epub 2004 Feb 2004.

Braak H & Braak E (1991) Neuropathological stageing of Alzheimer-related changes. *Acta Neuropathol* 82(4):239-259.

Brenner S*, et al.* (2000) Gene expression analysis by massively parallel signature sequencing (MPSS) on microbead arrays. *Nat Biotechnol.* 18(6):630-634.

Brody DL & Holtzman DM (2008) Active and passive immunotherapy for neurodegenerative disorders. *Annu Rev Neurosci* 31:175-93.(doi):10.1146/annurev.neuro.1131.060407.125529.

Brookmeyer R, Johnson E, Ziegler-Graham K, & Arrighi HM (2007) Forecasting the global burden of Alzheimer's disease. *Alzheimers Dement.* 3(3):186-191. doi: 110.1016/j.jalz.2007.1004.1381.

Brooks DJ (2009) Imaging amyloid in Parkinson's disease dementia and dementia with Lewy bodies with positron emission tomography. *Mov Disord* 24(Suppl 2):S742-747. doi: 710.1002/mds.22581.

Bruinsma IB*, et al.* (2010) Sulfation of heparan sulfate associated with amyloid-beta plaques in patients with Alzheimer's disease. *Acta Neuropathol.* 119(2):211-220. doi: 210.1007/s00401-00009-00577-00401. Epub 02009 Jul 00428.

Brunden KR, Trojanowski JQ, & Lee VM (2009) Advances in tau-focused drug discovery for Alzheimer's disease and related tauopathies. *Nat Rev Drug Discov.* 8(10):783-793.

Buckner RL*, et al.* (2005) Molecular, structural, and functional characterization of Alzheimer's disease: evidence for a relationship between default activity, amyloid, and memory. *J Neurosci.* 25(34):7709-7717.

Buee L, Bussiere T, Buee-Scherrer V, Delacourte A, & Hof PR (2000) Tau protein isoforms, phosphorylation and role in neurodegenerative disorders. *Brain Res Brain Res Rev.* 33(1):95-130.

Buee L*, et al.* (1993) Binding of vascular heparan sulfate proteoglycan to Alzheimer's amyloid precursor protein is mediated in part by the N-terminal region of A4 peptide. *Brain Res.* 627(2):199-204.

Bullock SL, Fletcher JM, Beddington RS, & Wilson VA (1998) Renal agenesis in mice homozygous for a gene trap mutation in the gene encoding heparan sulfate 2-sulfotransferase. *Genes Dev.* 12(12):1894-1906.

Cacabelos R, Barquero M, Garcia P, Alvarez XA, & Varela de Seijas E (1991) Cerebrospinal fluid interleukin-1 beta (IL-1 beta) in Alzheimer's disease and neurological disorders. *Methods Find Exp Clin Pharmacol* 13(7):455-458.

Cale JM, Shaw CE, & Bird IM (1998) Optimization of a reverse transcription-polymerase chain reaction (RT-PCR) mass assay for low-abundance mRNA. *Methods Mol Biol* 105:351-371.

Calero M*, et al.* (2000) Apolipoprotein J (clusterin) and Alzheimer's disease. *Microsc Res Tech* 50(4):305-315.

Capila I & Linhardt RJ (2002) Heparin-protein interactions. *Angew Chem Int Ed Engl.* 41(3):391-412.

Castillo GM, Ngo C, Cummings J, Wight TN, & Snow AD (1997) Perlecan binds to the beta-amyloid proteins (A beta) of Alzheimer's disease, accelerates A beta fibril formation, and maintains A beta fibril stability. *J Neurochem.* 69(6):2452-2465.

Chen RL & Lander AD (2001) Mechanisms underlying preferential assembly of heparan sulfate on glypican-1. *J Biol Chem.* 276(10):7507-7517. Epub 2000 Dec 7505.

Cheung VG*, et al.* (1999) Making and reading microarrays. *Nat Genet* 21(1 Suppl):15-19.

Chomczynski P & Sacchi N (1987) Single-step method of RNA isolation by acid guanidinium thiocyanate-phenol-chloroform extraction. *Anal Biochem.* 162(1):156-159.

Colantuoni C, Purcell AE, Bouton CM, & Pevsner J (2000) High throughput analysis of gene expression in the human brain. *Journal of neuroscience research* 59(1):1-10.

Conrad HE (2001) Nitrous acid degradation of glycosaminoglycans. *Curr Protoc Mol Biol.* Chapter(17):Unit17.22A. doi: 10.1002/0471142727.mb0471141722as0471142732.

Convit A*, et al.* (2000) Atrophy of the medial occipitotemporal, inferior, and middle temporal gyri in non-demented elderly predict decline to Alzheimer's disease. *Neurobiology of aging* 21(1):19-26.

Conway CD*, et al.* (2011) Heparan sulfate sugar modifications mediate the functions of slits and other factors needed for mouse forebrain commissure development. *J Neurosci.* 31(6):1955-1970. doi: 1910.1523/JNEUROSCI.2579-1910.2011.

Cotman SL, Halfter W, & Cole GJ (2000) Agrin binds to beta-amyloid (Abeta), accelerates abeta fibril formation, and is localized to Abeta deposits in Alzheimer's disease brain. *Mol Cell Neurosci.* 15(2):183-198.

Cui H*, et al.* (2011) Effects of heparin and enoxaparin on APP processing and Abeta production in primary cortical neurons from Tg2576 mice. *PLoS One* 6(7):e23007.

Cui H*, et al.* (2011) Effects of heparin and enoxaparin on APP processing and Abeta production in primary cortical neurons from Tg2576 mice. *PLoS One* 6(7):e23007. doi: 23010.21371/journal.pone.0023007. Epub 0022011 Jul 0023029.

Cui H, King AE, Jacobson GA, & Small DH (2016) Peripheral treatment with enoxaparin exacerbates amyloid plaque pathology in Tg2576 mice. *Journal of neuroscience research*.

Cummings JL, Vinters HV, Cole GM, & Khachaturian ZS (1998) Alzheimer's disease: etiologies, pathophysiology, cognitive reserve, and treatment opportunities. *Neurology.* 51(1 Suppl 1):S2-17; discussion S65-17.

D'Andrea MR & Nagele RG (2010) Morphologically distinct types of amyloid plaques point the way to a better understanding of Alzheimer's disease pathogenesis. *Biotech Histochem.* 85(2):133-147. doi: 110.3109/10520290903389445.

Das P & Golde T (2006) Dysfunction of TGF-beta signaling in Alzheimer's disease. *J Clin Invest* 116(11):2855-2857.

Dauwels J, Vialatte F, & Cichocki A (2010) Diagnosis of Alzheimer's disease from EEG signals: where are we standing? *Curr Alzheimer Res.* 7(6):487-505.

Deakin JA & Lyon M (2008) A simplified and sensitive fluorescent method for disaccharide analysis of both heparan sulfate and chondroitin/dermatan sulfates from biological samples. *Glycobiology.* 18(6):483-491. doi: 410.1093/glycob/cwn1028. Epub 2008 Mar 1031.

Deane R, Bell RD, Sagare A, & Zlokovic BV (2009) Clearance of amyloid-beta peptide across the blood-brain barrier: implication for therapies in Alzheimer's disease. *CNS Neurol Disord Drug Targets.* 8(1):16-30.

Debouck C & Metcalf B (2000) The impact of genomics on drug discovery. *Annu Rev Pharmacol Toxicol* 40:193-207.

Decourt B & Sabbagh MN (2011) BACE1 as a potential biomarker for Alzheimer's disease. *Journal of Alzheimer's disease : JAD* 24 Suppl 2:53-59.

Dews IC & Mackenzie KR (2007) Transmembrane domains of the syndecan family of growth factor coreceptors display a hierarchy of homotypic and heterotypic interactions. *Proc Natl Acad Sci U S A* 104(52):20782-20787.

Dhoot GK*, et al.* (2001) Regulation of Wnt signaling and embryo patterning by an extracellular sulfatase. *Science.* 293(5535):1663-1666.

Dickson DW (1997) The pathogenesis of senile plaques. *J Neuropathol Exp Neurol.* 56(4):321-339.

Drummond KJ, Yates EA, & Turnbull JE (2001) Electrophoretic sequencing of heparin/heparan sulfate oligosaccharides using a highly sensitive fluorescent end label. *Proteomics.* 1(2):304-310.

Duan J & Kasper DL (2011) Oxidative depolymerization of polysaccharides by reactive oxygen/nitrogen species. *Glycobiology.* 21(4):401-409. doi: 410.1093/glycob/cwq1171. Epub 2010 Oct 1028.

Dubois B*, et al.* (2007) Research criteria for the diagnosis of Alzheimer's disease: revising the NINCDS-ADRDA criteria. *Lancet Neurol.* 6(8):734-746.

Dunckley T*, et al.* (2006) Gene expression correlates of neurofibrillary tangles in Alzheimer's disease. *Neurobiol Aging.* 27(10):1359-1371. Epub 2005 Oct 1319.

Durante W, Johnson FK, & Johnson RA (2007) Arginase: a critical regulator of nitric oxide synthesis and vascular function. *Clin Exp Pharmacol Physiol* 34(9):906-911.

Edgar R, Domrachev M, & Lash AE (2002) Gene Expression Omnibus: NCBI gene expression and hybridization array data repository. *Nucleic Acids Res* 30(1):207-210.

Eggert S*, et al.* (2004) The proteolytic processing of the amyloid precursor protein gene family members APLP-1 and APLP-2 involves alpha-, beta-, gamma-, and epsilon-like cleavages: modulation of APLP-1 processing by n-glycosylation. *J Biol Chem.* 279(18):18146-18156. Epub 12004 Feb 18117.

Eisen MB & Brown PO (1999) DNA arrays for analysis of gene expression. *Methods Enzymol* 303:179-205.

Ermolieff J, Loy JA, Koelsch G, & Tang J (2000) Proteolytic activation of recombinant pro-memapsin 2 (pro-beta-secretase) studied with new fluorogenic substrates. *Biochemistry.* 39(40):12450-12456.

Esko JD (2001) Special considerations for proteoglycans and glycosaminoglycans and their purification. *Curr Protoc Mol Biol.* Chapter(17):Unit17.12. doi: 10.1002/0471142727.mb0471141702s0471142722.

Esko JD & Lindahl U (2001) Molecular diversity of heparan sulfate. *J Clin Invest.* 108(2):169-173.

Esko JD & Selleck SB (2002) Order out of chaos: assembly of ligand binding sites in heparan sulfate. *Annu Rev Biochem* 71:435-471. Epub 2001 Nov 2009.

Ethell IM & Yamaguchi Y (1999) Cell surface heparan sulfate proteoglycan syndecan-2 induces the maturation of dendritic spines in rat hippocampal neurons. *J Cell Biol* 144(3):575-586.

Farlow M (2002) A clinical overview of cholinesterase inhibitors in Alzheimer's disease. *Int Psychogeriatr* 14(Suppl 1):93-126.

Farlow M, Anand R, Messina J, Jr., Hartman R, & Veach J (2000) A 52-week study of the efficacy of rivastigmine in patients with mild to moderately severe Alzheimer's disease. *Eur Neurol* 44(4):236-241.

Farlow MR, Alva G, Meng X, & Olin JT (2010) A 25-week, open-label trial investigating rivastigmine transdermal patches with concomitant memantine in mild-to-moderate Alzheimer's disease: a post hoc analysis. *Curr Med Res Opin.* 26(2):263-269. doi: 210.1185/03007990903434914.

Feldman HH, Schmitt FA, & Olin JT (2006) Activities of daily living in moderate-to-severe Alzheimer disease: an analysis of the treatment effects of memantine in patients receiving stable donepezil treatment. *Alzheimer Dis Assoc Disord.* 20(4):263-268.

Feyerabend TB, Li JP, Lindahl U, & Rodewald HR (2006) Heparan sulfate C5-epimerase is essential for heparin biosynthesis in mast cells. *Nat Chem Biol.* 2(4):195-196. Epub 2006 Mar 2012.

Feyzi E, Saldeen T, Larsson E, Lindahl U, & Salmivirta M (1998) Age-dependent modulation of heparan sulfate structure and function. *J Biol Chem.* 273(22):13395-13398.

Fialkow L, Wang Y, & Downey GP (2007) Reactive oxygen and nitrogen species as signaling molecules regulating neutrophil function. *Free Radic Biol Med.* 42(2):153-164. Epub 2006 Oct 2028.

Fillit H*, et al.* (1991) Elevated circulating tumor necrosis factor levels in Alzheimer's disease. *Neurosci Lett* 129(2):318-320.

Finn RD*, et al.* (2016) The Pfam protein families database: towards a more sustainable future. *Nucleic Acids Res* 44(D1):D279-285.

Fischer F, Molinari M, Bodendorf U, & Paganetti P (2002) The disulphide bonds in the catalytic domain of BACE are critical but not essential for amyloid precursor protein processing activity. *J Neurochem.* 80(6):1079-1088.

Ford-Perriss M*, et al.* (2002) Variant heparan sulfates synthesized in developing mouse brain differentially regulate FGF signaling. *Glycobiology.* 12(11):721-727.

Forde JE & Dale TC (2007) Glycogen synthase kinase 3: a key regulator of cellular fate. *Cell Mol Life Sci* 64(15):1930-1944.

Forlenza OV*, et al.* (2011) Disease-modifying properties of long-term lithium treatment for amnestic mild cognitive impairment: randomised controlled trial. *Br J Psychiatry.* 198(5):351-356. doi: 310.1192/bjp.bp.1110.080044.

Forsberg E & Kjellen L (2001) Heparan sulfate: lessons from knockout mice. *J Clin Invest.* 108(2):175-180.

Fox NC*, et al.* (1996) Presymptomatic hippocampal atrophy in Alzheimer's disease. A longitudinal MRI study. *Brain.* 119(Pt 6):2001-2007.

Freeman WM, Walker SJ, & Vrana KE (1999) Quantitative RT-PCR: pitfalls and potential. *BioTechniques* 1999 Jan;26(1):112-122.

Frese MA, Milz F, Dick M, Lamanna WC, & Dierks T (2009) Characterization of the human sulfatase Sulf1 and its high affinity heparin/heparan sulfate interaction domain. *J Biol Chem.* 284(41):28033-28044. doi: 28010.21074/jbc.M28109.035808. Epub 032009 Aug 035807.

Friend SH (1999) How DNA microarrays and expression profiling will affect clinical practice. *BMJ* 319(7220):1306-1307.

Fryer RM*, et al.* (2002) Global analysis of gene expression: methods, interpretation, and pitfalls. *Exp Nephrol* 10(2):64-74.

Fu H*, et al.* (2012) Complement component C3 and complement receptor type 3 contribute to the phagocytosis and clearance of fibrillar Abeta by microglia. *Glia.* 60(6):993-1003. doi: 1010.1002/glia.22331. Epub 22012 Mar 22321.

Fukumoto H, Cheung BS, Hyman BT, & Irizarry MC (2002) Beta-secretase protein and activity are increased in the neocortex in Alzheimer disease. *Arch Neurol.* 59(9):1381-1389.

Fukumoto H*, et al.* (2004) Beta-secretase activity increases with aging in human, monkey, and mouse brain. *The American journal of pathology* 164(2):719-725.

Funderburgh JL (2000) Keratan sulfate: structure, biosynthesis, and function. *Glycobiology.* 10(10):951-958.

Galimberti D & Scarpini E (2011) Disease-modifying treatments for Alzheimer's disease. *Ther Adv Neurol Disord.* 4(4):203-216. doi: 210.1177/1756285611404470.

Galton CJ*, et al.* (2001) Differing patterns of temporal atrophy in Alzheimer's disease and semantic dementia. *Neurology* 57(2):216-225.

Gauthier S*, et al.* (2009) Effect of tramiprosate in patients with mild-to-moderate Alzheimer's disease: exploratory analyses of the MRI sub-group of the Alphase study. *J Nutr Health Aging.* 13(6):550-557.

Ghadiali RS, Guimond SE, Turnbull JE, & Pisconti A (2016) Dynamic changes in heparan sulfate during muscle differentiation and ageing regulate myoblast cell fate and FGF2 signalling. *Matrix Biol*.

Ghosh AK, Brindisi M, & Tang J (2012) Developing beta-secretase inhibitors for treatment of Alzheimer's disease. *J Neurochem.* 120(Suppl 1):71-83. doi: 10.1111/j.1471-4159.2011.07476.x. Epub 02011 Nov 07428.

Ghosh AK & Osswald HL (2014) BACE1 (beta-secretase) inhibitors for the treatment of Alzheimer's disease. *Chem Soc Rev.* 43(19):6765-6813. doi: 6710.1039/c6763cs60460h.

Giannakopoulos P*, et al.* (1998) Possible neuroprotective role of clusterin in Alzheimer's disease: a quantitative immunocytochemical study. *Acta Neuropathol* 95(4):387-394.

Giulian D*, et al.* (1998) The HHQK domain of beta-amyloid provides a structural basis for the immunopathology of Alzheimer's disease. *J Biol Chem.* 273(45):29719-29726.

Glenner GG & Wong CW (2012) Alzheimer's disease: initial report of the purification and characterization of a novel cerebrovascular amyloid protein. 1984. *Biochem Biophys Res Commun.* 425(3):534-539. doi: 510.1016/j.bbrc.2012.1008.1020.

Glessner JT*, et al.* (2009) Autism genome-wide copy number variation reveals ubiquitin and neuronal genes. *Nature* 459(7246):569-573.

Goedert M*, et al.* (1996) Assembly of microtubule-associated protein tau into Alzheimer-like filaments induced by sulphated glycosaminoglycans. *Nature.* 383(6600):550-553.

Goldberg R*, et al.* (2013) Versatile role of heparanase in inflammation. *Matrix Biol* 32(5):234-240.

Golub TR*, et al.* (1999) Molecular classification of cancer: class discovery and class prediction by gene expression monitoring. *Science* 286(5439):531-537.

Gotz J, Ittner LM, Fandrich M, & Schonrock N (2008) Is tau aggregation toxic or protective: a sensible question in the absence of sensitive methods? *Journal of Alzheimer's disease : JAD* 14(4):423-429.

Griciuc A*, et al.* (2013) Alzheimer's disease risk gene CD33 inhibits microglial uptake of amyloid beta. *Neuron.* 78(4):631-643. doi: 610.1016/j.neuron.2013.1004.1014. Epub 2013 Apr 1025.

Griffin WS (2006) Inflammation and neurodegenerative diseases. *Am J Clin Nutr.* 83(2):470S-474S.

Griffin WS (2008) Perispinal etanercept: potential as an Alzheimer therapeutic. *J Neuroinflammation.* 5:3.(doi):10.1186/1742-2094-1185-1183.

Grobe K*, et al.* (2002) Heparan sulfate and development: differential roles of the N-acetylglucosamine N-deacetylase/N-sulfotransferase isozymes. *Biochim Biophys Acta.* 1573(3):209-215.

Groffen AJ*, et al.* (1998) Primary structure and high expression of human agrin in basement membranes of adult lung and kidney. *Eur J Biochem.* 254(1):123-128.

Guimond SE*, et al.* (2009) Rapid purification and high sensitivity analysis of heparan sulfate from cells and tissues: toward glycomics profiling. *J Biol Chem.* 284(38):25714-25722. doi: 25710.21074/jbc.M25109.032755. Epub 032009 Jul 032713.

Gupta-Bansal R, Frederickson RC, & Brunden KR (1995) Proteoglycan-mediated inhibition of A beta proteolysis. A potential cause of senile plaque accumulation. *J Biol Chem.* 270(31):18666-18671.

Gura T (2008) Hope in Alzheimer's fight emerges from unexpected places. *Nat Med.* 14(9):894. doi: 810.1038/nm0908-1894.

Habuchi H*, et al.* (2003) Biosynthesis of heparan sulphate with diverse structures and functions: two alternatively spliced forms of human heparan sulphate 6-O-sulphotransferase-2 having different expression patterns and properties. *Biochem J.* 371(Pt 1):131-142.

Habuchi H*, et al.* (2000) The occurrence of three isoforms of heparan sulfate 6-O-sulfotransferase having different specificities for hexuronic acid adjacent to the targeted N-sulfoglucosamine. *J Biol Chem.* 275(4):2859-2868.

Hagner-McWhirter A, Li JP, Oscarson S, & Lindahl U (2004) Irreversible glucuronyl C5-epimerization in the biosynthesis of heparan sulfate. *J Biol Chem.* 279(15):14631-14638. Epub 12004 Jan 14612.

HajMohammadi S*, et al.* (2003) Normal levels of anticoagulant heparan sulfate are not essential for normal hemostasis. *J Clin Invest* 111(7):989-999.

Handel TM, Johnson Z, Crown SE, Lau EK, & Proudfoot AE (2005) Regulation of protein function by glycosaminoglycans--as exemplified by chemokines. *Annu Rev Biochem* 74:385-410.

Haniu M*, et al.* (2000) Characterization of Alzheimer's beta -secretase protein BACE. A pepsin family member with unusual properties. *J Biol Chem.* 275(28):21099-21106.

Hansebo G, Kihlgren M, Ljunggren G, & Winblad B (1998) Staff views on the Resident Assessment Instrument, RAI/MDS, in nursing homes, and the use of the Cognitive Performance Scale, CPS, in different levels of care in Stockholm, Sweden. *Journal of advanced nursing* 28(3):642-653.

Hara H, Mouri A, Yonemitsu Y, Nabeshima T, & Tabira T (2011) Mucosal immunotherapy in an Alzheimer mouse model by recombinant Sendai virus vector carrying Abeta1-43/IL-10 cDNA. *Vaccine.* 29(43):7474-7482. doi: 7410.1016/j.vaccine.2011.7407.7057. Epub 2011 Jul 7429.

Hardy J, Duff K, Hardy KG, Perez-Tur J, & Hutton M (1998) Genetic dissection of Alzheimer's disease and related dementias: amyloid and its relationship to tau. *Nat Neurosci.* 1(5):355-358.

Hardy JA & Higgins GA (1992) Alzheimer's disease: the amyloid cascade hypothesis. *Science.* 256(5054):184-185.

Harel A, Wu F, Mattson MP, Morris CM, & Yao PJ (2008) Evidence for CALM in directing VAMP2 trafficking. *Traffic* 9(3):417-429.

Harold D*, et al.* (2009) Genome-wide association study identifies variants at CLU and PICALM associated with Alzheimer's disease. *Nat Genet* 41(10):1088-1093.

Hasegawa M, Crowther RA, Jakes R, & Goedert M (1997) Alzheimer-like changes in microtubule-associated protein Tau induced by sulfated glycosaminoglycans. Inhibition of microtubule binding, stimulation of phosphorylation, and filament assembly depend on the degree of sulfation. *J Biol Chem.* 272(52):33118-33124.

Hayano S*, et al.* (2012) Roles of heparan sulfate sulfation in dentinogenesis. *J Biol Chem.* 287(15):12217-12229. doi: 12210.11074/jbc.M12111.332924. Epub 332012 Feb 332920.

He W*, et al.* (2004) Reticulon family members modulate BACE1 activity and amyloid-beta peptide generation. *Nat Med.* 10(9):959-965. Epub 2004 Aug 2001.

He X, Chang WP, Koelsch G, & Tang J (2002) Memapsin 2 (beta-secretase) cytosolic domain binds to the VHS domains of GGA1 and GGA2: implications on the endocytosis mechanism of memapsin 2. *FEBS Lett.* 524(1-3):183-187.

He X, Li F, Chang WP, & Tang J (2005) GGA proteins mediate the recycling pathway of memapsin 2 (BACE). *J Biol Chem.* 280(12):11696-11703. Epub 12004 Dec 11621.

Hendlich M (1998) Databases for protein-ligand complexes. *Acta Crystallogr D Biol Crystallogr* 54(Pt 6 Pt 1):1178-1182.

Hernandez F, Perez M, Lucas JJ, & Avila J (2002) Sulfo-glycosaminoglycan content affects PHF-tau solubility and allows the identification of different types of PHFs. *Brain Res.* 935(1-2):65-72.

Hiltunen MO, Niemi M, & Yla-Herttuala S (1999) Functional genomics and DNA array techniques in atherosclerosis research. *Curr Opin Lipidol* 10(6):515-519.

Hofmann K, Bucher P, Falquet L, & Bairoch A (1999) The PROSITE database, its status in 1999. *Nucleic Acids Res* 27(1):215-219.

Holst CR*, et al.* (2007) Secreted sulfatases Sulf1 and Sulf2 have overlapping yet essential roles in mouse neonatal survival. *PLoS One.* 2(6):e575.

Hong L*, et al.* (2000) Structure of the protease domain of memapsin 2 (beta-secretase) complexed with inhibitor. *Science.* 290(5489):150-153.

Hong L & Tang J (2004) Flap position of free memapsin 2 (beta-secretase), a model for flap opening in aspartic protease catalysis. *Biochemistry.* 43(16):4689-4695.

Hossain MM*, et al.* (2010) Direct detection of HSulf-1 and HSulf-2 activities on extracellular heparan sulfate and their inhibition by PI-88. *Glycobiology* 20(2):175-186.

Hruz T*, et al.* (2008) Genevestigator v3: a reference expression database for the meta-analysis of transcriptomes. *Adv Bioinformatics* 2008:420747.

Hsiao LL, Stears RL, Hong RL, & Gullans SR (2000) Prospective use of DNA microarrays for evaluating renal function and disease. *Curr Opin Nephrol Hypertens.* 9(3):253-258.

Hu X*, et al.* (2008) Genetic deletion of BACE1 in mice affects remyelination of sciatic nerves. *FASEB J.* 22(8):2970-2980. doi: 2910.1096/fj.2908-106666. Epub 102008 Apr 106615.

Hu X*, et al.* (2006) Bace1 modulates myelination in the central and peripheral nervous system. *Nat Neurosci.* 9(12):1520-1525. Epub 2006 Nov 1512.

Hu X*, et al.* (2007) Transgenic mice overexpressing reticulon 3 develop neuritic abnormalities. *EMBO J.* 26(11):2755-2767. Epub 2007 May 2753.

Humphries DE*, et al.* (1999) Heparin is essential for the storage of specific granule proteases in mast cells. *Nature.* 400(6746):769-772.

Huse JT, Pijak DS, Leslie GJ, Lee VM, & Doms RW (2000) Maturation and endosomal targeting of beta-site amyloid precursor protein-cleaving enzyme. The Alzheimer's disease beta-secretase. *J Biol Chem.* 275(43):33729-33737.

Hussain I*, et al.* (2003) Characterization of the ectodomain shedding of the beta-site amyloid precursor protein-cleaving enzyme 1 (BACE1). *J Biol Chem.* 278(38):36264-36268. Epub 32003 Jul 36211.

Hutton M*, et al.* (1998) Association of missense and 5'-splice-site mutations in tau with the inherited dementia FTDP-17. *Nature.* 393(6686):702-705.

Huynh MB*, et al.* (2012) Age-related changes in rat myocardium involve altered capacities of glycosaminoglycans to potentiate growth factor functions and heparan sulfate-altered sulfation. *J Biol Chem.* 287(14):11363-11373. doi: 11310.11074/jbc.M11111.335901. Epub 332012 Feb 335901.

Huynh MB*, et al.* (2012) Glycosaminoglycans from aged human hippocampus have altered capacities to regulate trophic factors activities but not Abeta42 peptide toxicity. *Neurobiol Aging.* 33(5):1005.e1011-1022. doi: 1010.1016/j.neurobiolaging.2011.1009.1030. Epub 2011 Oct 1027.

Hyman BT & Gomez-Isla T (1997) The natural history of Alzheimer neurofibrillary tangles and amyloid deposits. *Neurobiol Aging.* 18(4):386-387; discussion 389-392.

Imbimbo BP & Giardina GA (2011) gamma-secretase inhibitors and modulators for the treatment of Alzheimer's disease: disappointments and hopes. *Curr Top Med Chem* 11(12):1555-1570.

Jack CR, Jr.*, et al.* (2011) Introduction to the recommendations from the National Institute on Aging-Alzheimer's Association workgroups on diagnostic guidelines for Alzheimer's disease. *Alzheimers Dement.* 7(3):257-262. doi: 210.1016/j.jalz.2011.1003.1004. Epub 2011 Apr 1021.

Jensen LJ*, et al.* (2009) STRING 8--a global view on proteins and their functional interactions in 630 organisms. *Nucleic Acids Res* 37(Database issue):D412-416.

Jeon SY, Bae K, Seong YH, & Song KS (2003) Green tea catechins as a BACE1 (beta-secretase) inhibitor. *Bioorg Med Chem Lett.* 13(22):3905-3908.

Jia J*, et al.* (2009) Lack of L-iduronic acid in heparan sulfate affects interaction with growth factors and cell signaling. *J Biol Chem.* 284(23):15942-15950. doi: 15910.11074/jbc.M809577200. Epub 809572009 Mar 809577231.

Jick H, Zornberg GL, Jick SS, Seshadri S, & Drachman DA (2000) Statins and the risk of dementia. *Lancet.* 356(9242):1627-1631.

John S, Thangapandian S, Sakkiah S, & Lee KW (2011) Potent BACE-1 inhibitor design using pharmacophore modeling, in silico screening and molecular docking studies. *BMC Bioinformatics.* 12(Suppl 1):S28. doi: 10.1186/1471-2105-1112-S1181-S1128.

Kalus I*, et al.* (2015) Sulf1 and Sulf2 Differentially Modulate Heparan Sulfate Proteoglycan Sulfation during Postnatal Cerebellum Development: Evidence for Neuroprotective and Neurite Outgrowth Promoting Functions. *PLoS One* 10(10):e0139853.

Kalus I*, et al.* (2009) Differential involvement of the extracellular 6-O-endosulfatases Sulf1 and Sulf2 in brain development and neuronal and behavioural plasticity. *J Cell Mol Med.* 13(11-12):4505-4521. doi: 4510.1111/j.1582-4934.2008.00558.x.

Kamimura K*, et al.* (2006) Specific and flexible roles of heparan sulfate modifications in Drosophila FGF signaling. *J Cell Biol.* 174(6):773-778.

Kandimalla KK, Scott OG, Fulzele S, Davidson MW, & Poduslo JF (2009) Mechanism of neuronal versus endothelial cell uptake of Alzheimer's disease amyloid beta protein. *PLoS One* 4(2):e4627. doi: 4610.1371/journal.pone.0004627. Epub 0002009 Feb 0004627.

Kanehisa M & Goto S (2000) KEGG: kyoto encyclopedia of genes and genomes. *Nucleic Acids Res* 28(1):27-30.

Kanehisa M, Sato Y, Kawashima M, Furumichi M, & Tanabe M (2016) KEGG as a reference resource for gene and protein annotation. *Nucleic Acids Res* 44(D1):D457-462.

Kanekiyo T, Liu CC, Shinohara M, Li J, & Bu G (2012) LRP1 in brain vascular smooth muscle cells mediates local clearance of Alzheimer's amyloid-beta. *J Neurosci.* 32(46):16458-16465. doi: 16410.11523/JNEUROSCI.13987-16412.12012.

Kang J*, et al.* (1987) The precursor of Alzheimer's disease amyloid A4 protein resembles a cell-surface receptor. *Nature.* 325(6106):733-736.

Kapp OH*, et al.* (1995) Alignment of 700 globin sequences: extent of amino acid substitution and its correlation with variation in volume. *Protein Sci.* 4(10):2179-2190.

Keenan TD*, et al.* (2014) Age-dependent changes in heparan sulfate in human Bruch's membrane: implications for age-related macular degeneration. *Invest Ophthalmol Vis Sci.* 55(8):5370-5379. doi: 5310.1167/iovs.5314-14126.

Kennedy ME*, et al.* (2016) The BACE1 inhibitor verubecestat (MK-8931) reduces CNS beta-amyloid in animal models and in Alzheimer's disease patients. *Sci Transl Med* 8(363):363ra150.

Kennett EC & Davies MJ (2007) Degradation of matrix glycosaminoglycans by peroxynitrite/peroxynitrous acid: evidence for a hydroxyl-radical-like mechanism. *Free Radic Biol Med.* 42(8):1278-1289. Epub 2007 Jan 1223.

Kevil C, Carter P, Hu B, & DeBenedetti A (1995) Translational enhancement of FGF-2 by eIF-4 factors, and alternate utilization of CUG and AUG codons for translation initiation. *Oncogene.* 11(11):2339-2348.

Khemka VK*, et al.* (2014) Raised serum proinflammatory cytokines in Alzheimer's disease with depression. *Aging Dis* 5(3):170-176.

Kim DY, Ingano LA, Carey BW, Pettingell WH, & Kovacs DM (2005) Presenilin/gamma-secretase-mediated cleavage of the voltage-gated sodium channel beta2-subunit regulates cell adhesion and migration. *J Biol Chem.* 280(24):23251-23261. Epub 22005 Apr 23214.

Kim J, Yoon H, Basak J, & Kim J (2014) Apolipoprotein E in synaptic plasticity and Alzheimer's disease: potential cellular and molecular mechanisms. *Mol Cells* 37(11):767-776.

Kim J*, et al.* (2016) miR-186 is decreased in aged brain and suppresses BACE1 expression. *J Neurochem* 137(3):436-445.

Kinnunen T*, et al.* (2005) Heparan 2-O-sulfotransferase, hst-2, is essential for normal cell migration in Caenorhabditis elegans. *Proc Natl Acad Sci U S A.* 102(5):1507-1512. Epub 2005 Jan 1525.

Kitazume S*, et al.* (2001) Alzheimer's beta-secretase, beta-site amyloid precursor protein-cleaving enzyme, is responsible for cleavage secretion of a Golgi-resident sialyltransferase. *Proc Natl Acad Sci U S A.* 98(24):13554-13559. Epub 12001 Nov 13556.

Kohen R & Nyska A (2002) Oxidation of biological systems: oxidative stress phenomena, antioxidants, redox reactions, and methods for their quantification. *Toxicol Pathol.* 30(6):620-650.

Kreuger J & Kjellen L (2012) Heparan sulfate biosynthesis: regulation and variability. *J Histochem Cytochem.* 60(12):898-907. doi: 810.1369/0022155412464972. Epub 0022155412462012 Oct 0022155412464974.

Kreuger J, Salmivirta M, Sturiale L, Gimenez-Gallego G, & Lindahl U (2001) Sequence analysis of heparan sulfate epitopes with graded affinities for fibroblast growth factors 1 and 2. *J Biol Chem.* 276(33):30744-30752. Epub 32001 Jun 30713.

Kreuger J, Spillmann D, Li JP, & Lindahl U (2006) Interactions between heparan sulfate and proteins: the concept of specificity. *J Cell Biol.* 174(3):323-327.

Kurella M*, et al.* (2001) DNA microarray analysis of complex biologic processes. *J Am Soc Nephrol.* 12(5):1072-1078.

Kurup S*, et al.* (2007) Characterization of anti-heparan sulfate phage display antibodies AO4B08 and HS4E4. *J Biol Chem.* 282(29):21032-21042. Epub 22007 May 21021.

LaFerla FM, Green KN, & Oddo S (2007) Intracellular amyloid-beta in Alzheimer's disease. *Nat Rev Neurosci.* 8(7):499-509.

Lai J*, et al.* (2003) Loss of HSulf-1 up-regulates heparin-binding growth factor signaling in cancer. *J Biol Chem.* 278(25):23107-23117. Epub 22003 Apr 23109.

Laird FM*, et al.* (2005) BACE1, a major determinant of selective vulnerability of the brain to amyloid-beta amyloidogenesis, is essential for cognitive, emotional, and synaptic functions. *J Neurosci.* 25(50):11693-11709.

Lamanna WC*, et al.* (2006) Heparan sulfate 6-O-endosulfatases: discrete in vivo activities and functional co-operativity. *Biochem J.* 400(1):63-73.

Lamanna WC, Frese MA, Balleininger M, & Dierks T (2008) Sulf loss influences N-, 2-O-, and 6-O-sulfation of multiple heparan sulfate proteoglycans and modulates fibroblast growth factor signaling. *J Biol Chem.* 283(41):27724-27735. doi: 27710.21074/jbc.M802130200. Epub 802132008 Aug 802130206.

Lamanna WC*, et al.* (2007) The heparanome--the enigma of encoding and decoding heparan sulfate sulfation. *J Biotechnol.* 129(2):290-307. Epub 2007 Feb 2008.

Lammich S, Schobel S, Zimmer AK, Lichtenthaler SF, & Haass C (2004) Expression of the Alzheimer protease BACE1 is suppressed via its 5'-untranslated region. *EMBO Rep.* 5(6):620-625. Epub 2004 May 2028.

Langsdorf A, Do AT, Kusche-Gullberg M, Emerson CP, Jr., & Ai X (2007) Sulfs are regulators of growth factor signaling for satellite cell differentiation and muscle regeneration. *Dev Biol.* 311(2):464-477. Epub 2007 Sep 2007.

Lencz T*, et al.* (2013) Genome-wide association study implicates NDST3 in schizophrenia and bipolar disorder. *Nat Commun* 4:2739.

Lever R & Page CP (2002) Novel drug development opportunities for heparin. *Nat Rev Drug Discov.* 1(2):140-148.

Leveugle B*, et al.* (1997) Heparin promotes beta-secretase cleavage of the Alzheimer's amyloid precursor protein. *Neurochem Int* 30(6):543-548.

Leveugle B*, et al.* (1998) Heparin oligosaccharides that pass the blood-brain barrier inhibit beta-amyloid precursor protein secretion and heparin binding to beta-amyloid peptide. *J Neurochem.* 70(2):736-744.

Leveugle B, Scanameo A, Ding W, & Fillit H (1994) Binding of heparan sulfate glycosaminoglycan to beta-amyloid peptide: inhibition by potentially therapeutic polysulfated compounds. *Neuroreport.* 5(11):1389-1392.

Lewis J*, et al.* (2001) Enhanced neurofibrillary degeneration in transgenic mice expressing mutant tau and APP. *Science.* 293(5534):1487-1491.

Li H, Yamagata T, Mori M, & Momoi MY (2002) Association of autism in two patients with hereditary multiple exostoses caused by novel deletion mutations of EXT1. *J Hum Genet* 47(5):262-265.

Li JP*, et al.* (2005) In vivo fragmentation of heparan sulfate by heparanase overexpression renders mice resistant to amyloid protein A amyloidosis. *Proc Natl Acad Sci U S A* 102(18):6473-6477.

Li JP*, et al.* (2003) Targeted disruption of a murine glucuronyl C5-epimerase gene results in heparan sulfate lacking L-iduronic acid and in neonatal lethality. *J Biol Chem.* 278(31):28363-28366. Epub 22003 Jun 28364.

Li T*, et al.* (2007) Moderate reduction of gamma-secretase attenuates amyloid burden and limits mechanism-based liabilities. *J Neurosci.* 27(40):10849-10859.

Liang WS*, et al.* (2008) Altered neuronal gene expression in brain regions differentially affected by Alzheimer's disease: a reference data set. *Physiol Genomics* 33(2):240-256.

Liang WS*, et al.* (2007) Gene expression profiles in anatomically and functionally distinct regions of the normal aged human brain. *Physiol Genomics.* 28(3):311-322. Epub 2006 Oct 2031.

Liang WS*, et al.* (2008) Alzheimer's disease is associated with reduced expression of energy metabolism genes in posterior cingulate neurons. *Proc Natl Acad Sci U S A.* 105(11):4441-4446. doi: 4410.1073/pnas.0709259105. Epub 0709252008 Mar 0709259110.

Lichtenthaler SF*, et al.* (2003) The cell adhesion protein P-selectin glycoprotein ligand-1 is a substrate for the aspartyl protease BACE1. *J Biol Chem.* 278(49):48713-48719. Epub 42003 Sep 48724.

Lin X*, et al.* (2000) Disruption of gastrulation and heparan sulfate biosynthesis in EXT1-deficient mice. *Dev Biol.* 224(2):299-311.

Lindahl B, Eriksson L, & Lindahl U (1995) Structure of heparan sulphate from human brain, with special regard to Alzheimer's disease. *Biochem J.* 306(Pt 1):177-184.

Lindahl B, Eriksson L, Spillmann D, Caterson B, & Lindahl U (1996) Selective loss of cerebral keratan sulfate in Alzheimer's disease. *J Biol Chem.* 271(29):16991-16994.

Lindahl B, Westling C, Gimenez-Gallego G, Lindahl U, & Salmivirta M (1999) Common binding sites for beta-amyloid fibrils and fibroblast growth factor-2 in heparan sulfate from human cerebral cortex. *J Biol Chem.* 274(43):30631-30635.

Lindahl U, Backstrom G, Thunberg L, & Leder IG (1980) Evidence for a 3-O-sulfated D-glucosamine residue in the antithrombin-binding sequence of heparin. *Proc Natl Acad Sci U S A.* 77(11):6551-6555.

Lindahl U, Jacobsson I, Hook M, Backstrom G, & Feingold DS (1976) Biosynthesis of heparin. Loss of C-5 hydrogen during conversion of D-glucuronic to L-iduronic acid residues. *Biochem Biophys Res Commun.* 70(2):492-499.

Lindahl U, Kusche-Gullberg M, & Kjellen L (1998) Regulated diversity of heparan sulfate. *J Biol Chem.* 273(39):24979-24982.

Linhardt RJ, Turnbull JE, Wang HM, Loganathan D, & Gallagher JT (1990) Examination of the substrate specificity of heparin and heparan sulfate lyases. *Biochemistry.* 29(10):2611-2617.

Lippa CF*, et al.* (2000) AMY plaques in familial AD: comparison with sporadic Alzheimer's disease. *Neurology.* 54(1):100-104.

Lipshutz RJ, Fodor SP, Gingeras TR, & Lockhart DJ (1999) High density synthetic oligonucleotide arrays. *Nat Genet* 21(1 Suppl):20-24.

Liu C*, et al.* (2014) Molecular mechanism of substrate specificity for heparan sulfate 2-O-sulfotransferase. *J Biol Chem.* 289(19):13407-13418. doi: 13410.11074/jbc.M13113.530535. Epub 532014 Mar 530520.

Liu CC*, et al.* (2016) Neuronal heparan sulfates promote amyloid pathology by modulating brain amyloid-beta clearance and aggregation in Alzheimer's disease. *Sci Transl Med* 8(332):332ra344.

Liu CC*, et al.* (2016) Neuronal heparan sulfates promote amyloid pathology by modulating brain amyloid-beta clearance and aggregation in Alzheimer's disease. *Sci Transl Med.* 8(332):332ra344. doi: 310.1126/scitranslmed.aad3650.

Liu J & Pedersen LC (2007) Anticoagulant heparan sulfate: structural specificity and biosynthesis. *Appl Microbiol Biotechnol* 74(2):263-272.

Liu Z*, et al.* (2013) In silico drug repositioning: what we need to know. *Drug Discov Today* 18(3-4):110-115.

Liu Z & Perlin AS (1994) Evidence of a selective free radical degradation of heparin, mediated by cupric ion. *Carbohydr Res.* 255:183-191.

Lugemwa FN & Esko JD (1991) Estradiol beta-D-xyloside, an efficient primer for heparan sulfate biosynthesis. *J Biol Chem* 266(11):6674-6677.

Lum DH, Tan J, Rosen SD, & Werb Z (2007) Gene trap disruption of the mouse heparan sulfate 6-O-endosulfatase gene, Sulf2. *Mol Cell Biol.* 27(2):678-688. Epub 2006 Nov 2020.

Luscombe NM, Greenbaum D, & Gerstein M (2001) What is bioinformatics? An introduction and overview. *Yearb Med Inform* (1):83-99.

Maccarana M, Casu B, & Lindahl U (1993) Minimal sequence in heparin/heparan sulfate required for binding of basic fibroblast growth factor. *J Biol Chem.* 268(32):23898-23905.

Mackenzie IR, Hao C, & Munoz DG (1995) Role of microglia in senile plaque formation. *Neurobiol Aging.* 16(5):797-804.

Maeda N (2015) Proteoglycans and neuronal migration in the cerebral cortex during development and disease. *Front Neurosci* 9:98.

Maltseva I, Chan M, Kalus I, Dierks T, & Rosen SD (2013) The SULFs, extracellular sulfatases for heparan sulfate, promote the migration of corneal epithelial cells during wound repair. *PLoS One* 8(8):e69642.

Martinez A & Perez DI (2008) GSK-3 inhibitors: a ray of hope for the treatment of Alzheimer's disease? *J Alzheimers Dis.* 15(2):181-191.

Massena S*, et al.* (2010) A chemotactic gradient sequestered on endothelial heparan sulfate induces directional intraluminal crawling of neutrophils. *Blood* 116(11):1924-1931.

Matsuda T, Yamamoto T, Muraguchi A, & Saatcioglu F (2001) Cross-talk between transforming growth factor-beta and estrogen receptor signaling through Smad3. *J Biol Chem* 276(46):42908-42914.

Mazanetz MP & Fischer PM (2007) Untangling tau hyperphosphorylation in drug design for neurodegenerative diseases. *Nature reviews. Drug discovery* 6(6):464-479.

McCormick C, Duncan G, Goutsos KT, & Tufaro F (2000) The putative tumor suppressors EXT1 and EXT2 form a stable complex that accumulates in the Golgi apparatus and catalyzes the synthesis of heparan sulfate. *Proc Natl Acad Sci U S A.* 97(2):668-673.

McGeer PL, Kawamata T, & Walker DG (1992) Distribution of clusterin in Alzheimer brain tissue. *Brain Res* 579(2):337-341.

McKhann G*, et al.* (1984) Clinical diagnosis of Alzheimer's disease: report of the NINCDS-ADRDA Work Group under the auspices of Department of Health and Human Services Task Force on Alzheimer's Disease. *Neurology.* 34(7):939-944.

McLaurin J, Franklin T, Zhang X, Deng J, & Fraser PE (1999) Interactions of Alzheimer amyloid-beta peptides with glycosaminoglycans effects on fibril nucleation and growth. *Eur J Biochem.* 266(3):1101-1110.

McShane R, Areosa Sastre A, & Minakaran N (2006) Memantine for dementia. *Cochrane Database Syst Rev.* (2):CD003154.

Meirovitz A*, et al.* (2013) Heparanase in inflammation and inflammation-associated cancer. *FEBS J* 280(10):2307-2319.

Mellor H & Parker PJ (1998) The extended protein kinase C superfamily. *Biochem J* 332 (Pt 2):281-292.

Merry CL*, et al.* (2001) The molecular phenotype of heparan sulfate in the Hs2st-/- mutant mouse. *J Biol Chem.* 276(38):35429-35434. Epub 32001 Jul 35416.

Minges KE, Whittemore R, & Grey M (2013) Overweight and obesity in youth with type 1 diabetes. *Annu Rev Nurs Res* 31:47-69.

Mirra SS, Hart MN, & Terry RD (1993) Making the diagnosis of Alzheimer's disease. A primer for practicing pathologists. *Arch Pathol Lab Med.* 117(2):132-144.

Mirra SS*, et al.* (1991) The Consortium to Establish a Registry for Alzheimer's Disease (CERAD). Part II. Standardization of the neuropathologic assessment of Alzheimer's disease. *Neurology.* 41(4):479-486.

Moon AF*, et al.* (2012) Dissecting the substrate recognition of 3-O-sulfotransferase for the biosynthesis of anticoagulant heparin. *Proc Natl Acad Sci U S A.* 109(14):5265-5270. doi: 5210.1073/pnas.1117923109. Epub 1117922012 Mar 1117923119.

Morimoto-Tomita M, Uchimura K, Werb Z, Hemmerich S, & Rosen SD (2002) Cloning and characterization of two extracellular heparin-degrading endosulfatases in mice and humans. *J Biol Chem.* 277(51):49175-49185. Epub 42002 Oct 49173.

Murayama KS*, et al.* (2006) Reticulons RTN3 and RTN4-B/C interact with BACE1 and inhibit its ability to produce amyloid beta-protein. *Eur J Neurosci.* 24(5):1237-1244. Epub 2006 Sep 1238.

Nadanaka S & Kitagawa H (2008) Heparan sulphate biosynthesis and disease. *J Biochem.* 144(1):7-14. doi: 10.1093/jb/mvn1040. Epub 2008 Mar 1026.

Nagai N*, et al.* (2007) Regulation of heparan sulfate 6-O-sulfation by beta-secretase activity. *J Biol Chem* 282(20):14942-14951.

Nagai N*, et al.* (2013) Involvement of heparan sulfate 6-O-sulfation in the regulation of energy metabolism and the alteration of thyroid hormone levels in male mice. *Glycobiology.* 23(8):980-992. doi: 910.1093/glycob/cwt1037. Epub 2013 May 1020.

Nagamine S*, et al.* (2012) Organ-specific sulfation patterns of heparan sulfate generated by extracellular sulfatases Sulf1 and Sulf2 in mice. *J Biol Chem.* 287(12):9579-9590. doi: 9510.1074/jbc.M9111.290262. Epub 292012 Feb 290261.

Narindrasorasak S*, et al.* (1991) High affinity interactions between the Alzheimer's beta-amyloid precursor proteins and the basement membrane form of heparan sulfate proteoglycan. *J Biol Chem.* 266(20):12878-12883.

Newman DJ & Cragg GM (2012) Natural products as sources of new drugs over the 30 years from 1981 to 2010. *J Nat Prod* 75(3):311-335.

Nielsen HM*, et al.* (2010) Astrocytic A beta 1-42 uptake is determined by A beta-aggregation state and the presence of amyloid-associated proteins. *Glia.* 58(10):1235-1246. doi: 1210.1002/glia.21004.

O'Callaghan P*, et al.* (2008) Heparan sulfate accumulation with Abeta deposits in Alzheimer's disease and Tg2576 mice is contributed by glial cells. *Brain Pathol.* 18(4):548-561. doi: 510.1111/j.1750-3639.2008.00152.x. Epub 02008 Apr 00111.

O'Connor T*, et al.* (2008) Phosphorylation of the translation initiation factor eIF2alpha increases BACE1 levels and promotes amyloidogenesis. *Neuron.* 60(6):988-1009. doi: 1010.1016/j.neuron.2008.1010.1047.

Ogishima T*, et al.* (2005) Increased heparanase expression is caused by promoter hypomethylation and up-regulation of transcriptional factor early growth response-1 in human prostate cancer. *Clin Cancer Res* 11(3):1028-1036.

Okayama T*, et al.* (1998) Formal design and implementation of an improved DDBJ DNA database with a new schema and object-oriented library. *Bioinformatics* 14(6):472-478.

Ori A, Wilkinson MC, & Fernig DG (2011) A systems biology approach for the investigation of the heparin/heparan sulfate interactome. *J Biol Chem* 286(22):19892-19904.

Otsuki S*, et al.* (2010) Extracellular sulfatases support cartilage homeostasis by regulating BMP and FGF signaling pathways. *Proc Natl Acad Sci U S A.* 107(22):10202-10207. doi: 10210.11073/pnas.0913897107. Epub 0913892010 May 0913897117.

Ozturk A, Minster RL, DeKosky ST, & Kamboh MI (2007) Association of tagSNPs in the urokinase-plasminogen activator (PLAU) gene with Alzheimer's disease and associated quantitative traits. *Am J Med Genet B Neuropsychiatr Genet.* 144B(1):79-82.

Padurariu M, Ciobica A, Mavroudis I, Fotiou D, & Baloyannis S (2012) Hippocampal neuronal loss in the CA1 and CA3 areas of Alzheimer's disease patients. *Psychiatr Danub* 24(2):152-158.

Pagani I*, et al.* (2012) The Genomes OnLine Database (GOLD) v.4: status of genomic and metagenomic projects and their associated metadata. *Nucleic Acids Res* 40(Database issue):D571-579.

Pallerla SR*, et al.* (2008) Altered heparan sulfate structure in mice with deleted NDST3 gene function. *J Biol Chem.* 283(24):16885-16894. doi: 16810.11074/jbc.M709774200. Epub 709772008 Apr 709774201.

Paresce DM, Ghosh RN, & Maxfield FR (1996) Microglial cells internalize aggregates of the Alzheimer's disease amyloid beta-protein via a scavenger receptor. *Neuron.* 17(3):553-565.

Parish CR (2006) The role of heparan sulphate in inflammation. *Nat Rev Immunol.* 6(9):633-643. Epub 2006 Aug 2018.

Patey SJ, Edwards EA, Yates EA, & Turnbull JE (2006) Heparin derivatives as inhibitors of BACE-1, the Alzheimer's beta-secretase, with reduced activity against factor Xa and other proteases. *J Med Chem.* 49(20):6129-6132.

Perou CM*, et al.* (2000) Molecular portraits of human breast tumours. *Nature* 406(6797):747-752.

Pomin VH & Mulloy B (2015) Current structural biology of the heparin interactome. *Curr Opin Struct Biol* 34:17-25.

Poorkaj P*, et al.* (1998) Tau is a candidate gene for chromosome 17 frontotemporal dementia. *Ann Neurol.* 43(6):815-825.

Powell AK, Yates EA, Fernig DG, & Turnbull JE (2004) Interactions of heparin/heparan sulfate with proteins: appraisal of structural factors and experimental approaches. *Glycobiology.* 14(4):17R-30R. Epub 2004 Jan 2012.

Pratt T, Conway CD, Tian NM, Price DJ, & Mason JO (2006) Heparan sulphation patterns generated by specific heparan sulfotransferase enzymes direct distinct aspects of retinal axon guidance at the optic chiasm. *J Neurosci.* 26(26):6911-6923.

Presto J*, et al.* (2008) Heparan sulfate biosynthesis enzymes EXT1 and EXT2 affect NDST1 expression and heparan sulfate sulfation. *Proc Natl Acad Sci U S A* 105(12):4751-4756.

Qu BX*, et al.* (2010) Analysis of three plasmid systems for use in DNA A beta 42 immunization as therapy for Alzheimer's disease. *Vaccine.* 28(32):5280-5287. doi: 5210.1016/j.vaccine.2010.5205.5054. Epub 2010 Jun 5284.

Rakover I, Arbel M, & Solomon B (2007) Immunotherapy against APP beta-secretase cleavage site improves cognitive function and reduces neuroinflammation in Tg2576 mice without a significant effect on brain abeta levels. *Neuro-degenerative diseases* 4(5):392-402. Epub 2007 May 2025.

Rao AA*, et al.* (2008) Bioinformatic analysis of functional proteins involved in obesity associated with diabetes. *Int J Biomed Sci* 4(1):70-73.

Reddy VP, Zhu X, Perry G, & Smith MA (2009) Oxidative stress in diabetes and Alzheimer's disease. *Journal of Alzheimer's disease : JAD* 16(4):763-774. doi: 710.3233/JAD-2009-1013.

Reijmers RM*, et al.* (2010) Impaired lymphoid organ development in mice lacking the heparan sulfate modifying enzyme glucuronyl C5-epimerase. *J Immunol.* 184(7):3656-3664. doi: 3610.4049/jimmunol.0902200. Epub 0902010 Mar 0902205.

Rej R, Jaseja M, & Perlin AS (1989) Importance for blood anticoagulant activity of a 2-sulfate group on L-iduronic acid residues in heparin. *Thromb Haemost.* 61(3):540.

Reuter MS*, et al.* (2014) NDST1 missense mutations in autosomal recessive intellectual disability. *Am J Med Genet A* 164A(11):2753-2763.

Revesz T*, et al.* (2002) Sporadic and familial cerebral amyloid angiopathies. *Brain Pathol.* 12(3):343-357.

Ribe EM*, et al.* (2005) Accelerated amyloid deposition, neurofibrillary degeneration and neuronal loss in double mutant APP/tau transgenic mice. *Neurobiol Dis.* 20(3):814-822. Epub 2005 Aug 2024.

Ringheim GE*, et al.* (1998) Enhancement of beta-amyloid precursor protein transcription and expression by the soluble interleukin-6 receptor/interleukin-6 complex. *Brain Res Mol Brain Res* 55(1):35-44.

Ringvall M*, et al.* (2000) Defective heparan sulfate biosynthesis and neonatal lethality in mice lacking N-deacetylase/N-sulfotransferase-1. *J Biol Chem.* 275(34):25926-25930.

Robakis NK, Ramakrishna N, Wolfe G, & Wisniewski HM (1987) Molecular cloning and characterization of a cDNA encoding the cerebrovascular and the neuritic plaque amyloid peptides. *Proc Natl Acad Sci U S A.* 84(12):4190-4194.

Rong J, Habuchi H, Kimata K, Lindahl U, & Kusche-Gullberg M (2001) Substrate specificity of the heparan sulfate hexuronic acid 2-O-sulfotransferase. *Biochemistry.* 40(18):5548-5555.

Ropero S*, et al.* (2004) Epigenetic loss of the familial tumor-suppressor gene exostosin-1 (EXT1) disrupts heparan sulfate synthesis in cancer cells. *Hum Mol Genet.* 13(22):2753-2765. Epub 2004 Sep 2722.

Rudd TR & Yates EA (2012) A highly efficient tree structure for the biosynthesis of heparan sulfate accounts for the commonly observed disaccharides and suggests a mechanism for domain synthesis. *Mol Biosyst* 8(5):1499-1506.

Ryu JK, Cho T, Choi HB, Wang YT, & McLarnon JG (2009) Microglial VEGF receptor response is an integral chemotactic component in Alzheimer's disease pathology. *The Journal of neuroscience : the official journal of the Society for Neuroscience* 29(1):3-13.

Sabelli PA & Shewry PR (1995) Northern analysis and nucleic acid probes. *Methods Mol Biol* 49:213-228.

Salawu FK, Umar JT, & Olokoba AB (2011) Alzheimer's disease: a review of recent developments. *Ann Afr Med.* 10(2):73-79. doi: 10.4103/1596-3519.82057.

Salloway S*, et al.* (2011) A phase 2 randomized trial of ELND005, scyllo-inositol, in mild to moderate Alzheimer disease. *Neurology.* 77(13):1253-1262. doi: 1210.1212/WNL.1250b1013e3182309fa3182305. Epub 3182011 Sep 3182314.

Samuels MA (2004) Inflammation and neurological disease. *Curr Opin Neurol* 17(3):307-309.

Sander C (2000) Genomic medicine and the future of health care. *Science* 287(5460):1977-1978.

Sandwall E*, et al.* (2010) Heparan sulfate mediates amyloid-beta internalization and cytotoxicity. *Glycobiology.* 20(5):533-541. doi: 510.1093/glycob/cwp1205. Epub 2010 Jan 1095.

Santa-Maria I, Hernandez F, Del Rio J, Moreno FJ, & Avila J (2007) Tramiprosate, a drug of potential interest for the treatment of Alzheimer's disease, promotes an abnormal aggregation of tau. *Mol Neurodegener.* 2:17.

Sarrazin S, Lamanna WC, & Esko JD (2011) Heparan sulfate proteoglycans. *Cold Spring Harb Perspect Biol* 3(7).

Scheff SW & Price DA (1993) Synapse loss in the temporal lobe in Alzheimer's disease. *Ann Neurol.* 33(2):190-199.

Schenk D*, et al.* (1999) Immunisation with amyloid-beta attenuates Alzheimer's-disease-like pathology in the PDAPP mouse. *Nature* 400(6740):173-177.

Scholefield Z*, et al.* (2003) Heparan sulfate regulates amyloid precursor protein processing by BACE1, the Alzheimer's ?-secretase. *J Cell Biol.* 163(1):97-107. doi:110.1083/jcb.200303059.

Schreml J*, et al.* (2014) The missing "link": an autosomal recessive short stature syndrome caused by a hypofunctional XYLT1 mutation. *Hum Genet* 133(1):29-39.

Schubert D, Schroeder R, LaCorbiere M, Saitoh T, & Cole G (1988) Amyloid beta protein precursor is possibly a heparan sulfate proteoglycan core protein. *Science.* 241(4862):223-226.

Schworer R, Zubkova OV, Turnbull JE, & Tyler PC (2013) Synthesis of a targeted library of heparan sulfate hexa- to dodecasaccharides as inhibitors of beta-secretase: potential therapeutics for Alzheimer's disease. *Chemistry.* 19(21):6817-6823. doi: 6810.1002/chem.201204519. Epub 201202013 Apr 201204513.

Selkoe DJ (1991) The molecular pathology of Alzheimer's disease. *Neuron.* 6(4):487-498.

Shaffer LM*, et al.* (1995) Amyloid beta protein (A beta) removal by neuroglial cells in culture. *Neurobiol Aging.* 16(5):737-745.

Shaklee PN & Conrad HE (1984) Hydrazinolysis of heparin and other glycosaminoglycans. *Biochem J.* 217(1):187-197.

Shao C, Shi X, Phillips JJ, & Zaia J (2013) Mass spectral profiling of glycosaminoglycans from histological tissue surfaces. *Anal Chem* 85(22):10984-10991.

Shi Q*, et al.* (2009) Reduced amyloid deposition in mice overexpressing RTN3 is adversely affected by preformed dystrophic neurites. *J Neurosci.* 29(29):9163-9173. doi: 9110.1523/JNEUROSCI.5741-9108.2009.

Shi X & Zaia J (2009) Organ-specific heparan sulfate structural phenotypes. *J Biol Chem* 284(18):11806-11814.

Shi XP*, et al.* (2001) The pro domain of beta-secretase does not confer strict zymogen-like properties but does assist proper folding of the protease domain. *J Biol Chem.* 276(13):10366-10373.

Shimkets RA*, et al.* (1999) Gene expression analysis by transcript profiling coupled to a gene database query. *Nat Biotechnol.* 17(8):798-803.

Shimo T*, et al.* (2004) Indian hedgehog and syndecans-3 coregulate chondrocyte proliferation and function during chick limb skeletogenesis. *Dev Dyn.* 229(3):607-617.

Shioi J, Anderson JP, Ripellino JA, & Robakis NK (1992) Chondroitin sulfate proteoglycan form of the Alzheimer's beta-amyloid precursor. *J Biol Chem.* 267(20):13819-13822.

Shioi J, Refolo LM, Efthimiopoulos S, & Robakis NK (1993) Chondroitin sulfate proteoglycan form of cellular and cell-surface Alzheimer amyloid precursor. *Neurosci Lett.* 154(1-2):121-124.

Shukla D*, et al.* (1999) A novel role for 3-O-sulfated heparan sulfate in herpes simplex virus 1 entry. *Cell* 99(1):13-22.

Siavelis JC, Bourdakou MM, Athanasiadis EI, Spyrou GM, & Nikita KS (2016) Bioinformatics methods in drug repurposing for Alzheimer's disease. *Brief Bioinform* 17(2):322-335.

Siemers E*, et al.* (2005) Safety, tolerability, and changes in amyloid beta concentrations after administration of a gamma-secretase inhibitor in volunteers. *Clin Neuropharmacol.* 28(3):126-132.

Simpkins JW, Yi KD, Yang SH, & Dykens JA (2010) Mitochondrial mechanisms of estrogen neuroprotection. *Biochimica et biophysica acta* 1800(10):1113-1120.

Singer O*, et al.* (2005) Targeting BACE1 with siRNAs ameliorates Alzheimer disease neuropathology in a transgenic model. *Nat Neurosci.* 8(10):1343-1349. Epub 2005 Aug 1328.

Skidmore MA*, et al.* (2006) High sensitivity separation and detection of heparan sulfate disaccharides. *J Chromatogr A.* 1135(1):52-56. Epub 2006 Oct 2010.

Skidmore MA, Guimond SE, Dumax-Vorzet AF, Yates EA, & Turnbull JE (2010) Disaccharide compositional analysis of heparan sulfate and heparin polysaccharides using UV or high-sensitivity fluorescence (BODIPY) detection. *Nat Protoc.* 5(12):1983-1992. doi: 1910.1038/nprot.2010.1145. Epub 2010 Dec 1982.

Smeds E*, et al.* (2003) Substrate specificities of mouse heparan sulphate glucosaminyl 6-O-sulphotransferases. *Biochem J.* 372(Pt 2):371-380.

Smith CL (2008) A shifting paradigm: histone deacetylases and transcriptional activation. *Bioessays* 30(1):15-24.

Smits NC*, et al.* (2006) Phage display-derived human antibodies against specific glycosaminoglycan epitopes. *Methods Enzymol* 416:61-87.

Snow AD*, et al.* (1990) Early accumulation of heparan sulfate in neurons and in the beta-amyloid protein-containing lesions of Alzheimer's disease and Down's syndrome. *Am J Pathol.* 137(5):1253-1270.

Snow AD*, et al.* (1994) An important role of heparan sulfate proteoglycan (Perlecan) in a model system for the deposition and persistence of fibrillar A beta-amyloid in rat brain. *Neuron.* 12(1):219-234.

Snow AD & Wight TN (1989) Proteoglycans in the pathogenesis of Alzheimer's disease and other amyloidoses. *Neurobiol Aging.* 10(5):481-497.

Snow AD, Willmer J, & Kisilevsky R (1987) Sulfated glycosaminoglycans: a common constituent of all amyloids? *Lab Invest.* 56(1):120-123.

Snow AD, Willmer JP, & Kisilevsky R (1987) Sulfated glycosaminoglycans in Alzheimer's disease. *Hum Pathol.* 18(5):506-510.

Solomon B (2007) Antibody-mediated immunotherapy for Alzheimer's disease. *Curr Opin Investig Drugs.* 8(7):519-524.

Solomon B, Koppel R, Frankel D, & Hanan-Aharon E (1997) Disaggregation of Alzheimer beta-amyloid by site-directed mAb. *Proc Natl Acad Sci U S A.* 94(8):4109-4112.

Stefani M & Liguri G (2009) Cholesterol in Alzheimer's disease: unresolved questions. *Curr Alzheimer Res.* 6(1):15-29.

Stewart KL*, et al.* (2016) Atomic Details of the Interactions of Glycosaminoglycans with Amyloid-beta Fibrils. *J Am Chem Soc* 138(27):8328-8331.

Sugahara K & Kitagawa H (2000) Recent advances in the study of the biosynthesis and functions of sulfated glycosaminoglycans. *Curr Opin Struct Biol.* 10(5):518-527.

Sugahara K*, et al.* (2003) Recent advances in the structural biology of chondroitin sulfate and dermatan sulfate. *Curr Opin Struct Biol.* 13(5):612-620.

Sugaya N, Habuchi H, Nagai N, Ashikari-Hada S, & Kimata K (2008) 6-O-sulfation of heparan sulfate differentially regulates various fibroblast growth factor-dependent signalings in culture. *J Biol Chem.* 283(16):10366-10376. doi: 10310.11074/jbc.M705948200. Epub 705942008 Feb 705948214.

Tahara K*, et al.* (2006) Role of toll-like receptor signalling in Abeta uptake and clearance. *Brain.* 129(Pt 11):3006-3019. Epub 2006 Sep 3019.

Talmage DA (2008) Mechanisms of neuregulin action. *Novartis Found Symp* 289:74-84; discussion 84-93.

Tamagno E*, et al.* (2002) Oxidative stress increases expression and activity of BACE in NT2 neurons. *Neurobiol Dis.* 10(3):279-288.

Tao C*, et al.* (2013) Molecular characterization, expression profiles, and association analysis with hematologic parameters of the porcine HPSE and HPSE2 genes. *J Appl Genet* 54(1):71-78.

Tariot PN*, et al.* (2004) Memantine treatment in patients with moderate to severe Alzheimer disease already receiving donepezil: a randomized controlled trial. *JAMA.* 291(3):317-324.

Tatusova TA, Karsch-Mizrachi I, & Ostell JA (1999) Complete genomes in WWW Entrez: data representation and analysis. *Bioinformatics* 15(7-8):536-543.

Terry RD*, et al.* (1991) Physical basis of cognitive alterations in Alzheimer's disease: synapse loss is the major correlate of cognitive impairment. *Ann Neurol.* 30(4):572-580.

Tesco G*, et al.* (2007) Depletion of GGA3 stabilizes BACE and enhances beta-secretase activity. *Neuron.* 54(5):721-737.

Teumer A*, et al.* (2016) Genome-wide Association Studies Identify Genetic Loci Associated With Albuminuria in Diabetes. *Diabetes* 65(3):803-817.

Timmer NM*, et al.* (2009) Amyloid beta induces cellular relocalization and production of agrin and glypican-1. *Brain Res.* 1260:38-46.(doi):10.1016/j.brainres.2008.1012.1063. Epub 2009 Jan 1017.

Toida T*, et al.* (1997) Structural differences and the presence of unsubstituted amino groups in heparan sulphates from different tissues and species. *Biochem J.* 322(Pt 2):499-506.

Toma L, Berninsone P, & Hirschberg CB (1998) The putative heparin-specific N-acetylglucosaminyl N-Deacetylase/N-sulfotransferase also occurs in non-heparin-producing cells. *J Biol Chem.* 273(35):22458-22465.

Tornberg J*, et al.* (2011) Heparan sulfate 6-O-sulfotransferase 1, a gene involved in extracellular sugar modifications, is mutated in patients with idiopathic hypogonadotrophic hypogonadism. *Proc Natl Acad Sci U S A* 108(28):11524-11529.

Trojanowski JQ & Lee VM (2005) Pathological tau: a loss of normal function or a gain in toxicity? *Nat Neurosci.* 8(9):1136-1137.

Tun H, Marlow L, Pinnix I, Kinsey R, & Sambamurti K (2002) Lipid rafts play an important role in A beta biogenesis by regulating the beta-secretase pathway. *J Mol Neurosci.* 19(1-2):31-35.

Turnbull JE & Field RA (2007) Emerging glycomics technologies. *Nat Chem Biol.* 3(2):74-77.

Turnbull JE & Gallagher JT (1991) Sequence analysis of heparan sulphate indicates defined location of N-sulphated glucosamine and iduronate 2-sulphate residues proximal to the protein-linkage region. *Biochem J* 277 (Pt 2):297-303.

Turnbull JE, Hopwood JJ, & Gallagher JT (1999) A strategy for rapid sequencing of heparan sulfate and heparin saccharides. *Proc Natl Acad Sci U S A.* 96(6):2698-2703.

Turner M, Chantry D, & Feldmann M (1990) Transforming growth factor beta induces the production of interleukin 6 by human peripheral blood mononuclear cells. *Cytokine* 2(3):211-216.

Turner RT, 3rd*, et al.* (2002) Specificity of memapsin 1 and its implications on the design of memapsin 2 (beta-secretase) inhibitor selectivity. *Biochemistry.* 41(27):8742-8746.

Tyagi S (2000) Taking a census of mRNA populations with microbeads. *Nat Biotechnol.* 18(6):597-598.

Udayar V*, et al.* (2013) A paired RNAi and RabGAP overexpression screen identifies Rab11 as a regulator of beta-amyloid production. *Cell Rep* 5(6):1536-1551.

van Horssen J*, et al.* (2002) Accumulation of heparan sulfate proteoglycans in cerebellar senile plaques. *Neurobiol Aging.* 23(4):537-545.

van Horssen J, Wesseling P, van den Heuvel LP, de Waal RM, & Verbeek MM (2003) Heparan sulphate proteoglycans in Alzheimer's disease and amyloid-related disorders. *Lancet Neurol.* 2(8):482-492.

van Horssen J*, et al.* (2002) Collagen XVIII: a novel heparan sulfate proteoglycan associated with vascular amyloid depositions and senile plaques in Alzheimer's disease brains. *Brain Pathol.* 12(4):456-462.

van Kuppevelt TH, Dennissen MA, van Venrooij WJ, Hoet RM, & Veerkamp JH (1998) Generation and application of type-specific anti-heparan sulfate antibodies using phage display technology. Further evidence for heparan sulfate heterogeneity in the kidney. *J Biol Chem* 273(21):12960-12966.

Vassar R, Kovacs DM, Yan R, & Wong PC (2009) The beta-secretase enzyme BACE in health and Alzheimer's disease: regulation, cell biology, function, and therapeutic potential. *J Neurosci.* 29(41):12787-12794. doi: 12710.11523/JNEUROSCI.13657-12709.12009.

Velculescu VE (1999) Essay: Amersham Pharmacia Biotech & Science prize. Tantalizing transcriptomes--SAGE and its use in global gene expression analysis. *Science* 286(5444):1491-1492.

Vellas B*, et al.* (2011) Prevention trials in Alzheimer's disease: an EU-US task force report. *Prog Neurobiol.* 95(4):594-600. doi: 510.1016/j.pneurobio.2011.1008.1014. Epub 2011 Sep 1010.

Velliquette RA, O'Connor T, & Vassar R (2005) Energy inhibition elevates beta-secretase levels and activity and is potentially amyloidogenic in APP transgenic mice: possible early events in Alzheimer's disease pathogenesis. *J Neurosci.* 25(47):10874-10883.

Verbeek MM, Eikelenboom P, & de Waal RM (1997) Differences between the pathogenesis of senile plaques and congophilic angiopathy in Alzheimer disease. *J Neuropathol Exp Neurol.* 56(7):751-761.

Verbeek MM*, et al.* (1999) Agrin is a major heparan sulfate proteoglycan accumulating in Alzheimer's disease brain. *Am J Pathol.* 155(6):2115-2125.

Verma M, Vats A, & Taneja V (2015) Toxic species in amyloid disorders: Oligomers or mature fibrils. *Ann Indian Acad Neurol.* 18(2):138-145. doi: 110.4103/0972-2327.144284.

Vina J & Lloret A (2010) Why women have more Alzheimer's disease than men: gender and mitochondrial toxicity of amyloid-beta peptide. *Journal of Alzheimer's disease : JAD* 20(Suppl 2):S527-533.

Vlodavsky I*, et al.* (2012) Significance of heparanase in cancer and inflammation. *Cancer Microenviron* 5(2):115-132.

von Arnim CA*, et al.* (2005) The low density lipoprotein receptor-related protein (LRP) is a novel beta-secretase (BACE1) substrate. *J Biol Chem.* 280(18):17777-17785. Epub 12005 Mar 17774.

Walter J*, et al.* (2001) Phosphorylation regulates intracellular trafficking of beta-secretase. *J Biol Chem.* 276(18):14634-14641. Epub 12001 Jan 14629.

Wang J, Tanila H, Puolivali J, Kadish I, & van Groen T (2003) Gender differences in the amount and deposition of amyloidbeta in APPswe and PS1 double transgenic mice. *Neurobiol Dis.* 14(3):318-327.

Wang Z*, et al.* (2005) Positive association of heparanase expression with tumor invasion and lymphatic metastasis in gastric carcinoma. *Mod Pathol* 18(2):205-211.

Warda M*, et al.* (2006) Isolation and characterization of heparan sulfate from various murine tissues. *Glycoconj J* 23(7-8):555-563.

Weingarten MD, Lockwood AH, Hwo SY, & Kirschner MW (1975) A protein factor essential for microtubule assembly. *Proc Natl Acad Sci U S A* 72(5):1858-1862.

Wen Y, Onyewuchi O, Yang S, Liu R, & Simpkins JW (2004) Increased beta-secretase activity and expression in rats following transient cerebral ischemia. *Brain Res.* 1009(1-2):1-8.

Winterbourn CC (2008) Reconciling the chemistry and biology of reactive oxygen species. *Nat Chem Biol.* 4(5):278-286. doi: 210.1038/nchembio.1085.

Wisniewski T & Konietzko U (2008) Amyloid-beta immunisation for Alzheimer's disease. *Lancet neurology* 7(9):805-811.

Wong GT*, et al.* (2004) Chronic treatment with the gamma-secretase inhibitor LY-411,575 inhibits beta-amyloid peptide production and alters lymphopoiesis and intestinal cell differentiation. *J Biol Chem.* 279(13):12876-12882. Epub 12004 Jan 12876.

Xu D*, et al.* (2005) Characterization of heparan sulphate 3-O-sulphotransferase isoform 6 and its role in assisting the entry of herpes simplex virus type 1. *Biochem J* 385(Pt 2):451-459.

Yan R, Han P, Miao H, Greengard P, & Xu H (2001) The transmembrane domain of the Alzheimer's beta-secretase (BACE1) determines its late Golgi localization and access to beta -amyloid precursor protein (APP) substrate. *J Biol Chem.* 276(39):36788-36796. Epub 32001 Jul 36720.

Yang CN*, et al.* (2011) Mechanism mediating oligomeric Abeta clearance by naive primary microglia. *Neurobiol Dis.* 42(3):221-230. doi: 210.1016/j.nbd.2011.1001.1005. Epub 2011 Jan 1018.

Yates EA, Guimond SE, & Turnbull JE (2004) Highly diverse heparan sulfate analogue libraries: providing access to expanded areas of sequence space for bioactivity screening. *J Med Chem.* 47(1):277-280.

Yiannopoulou KG & Papageorgiou SG (2013) Current and future treatments for Alzheimer's disease. *Ther Adv Neurol Disord.* 6(1):19-33. doi: 10.1177/1756285612461679.

Yosizawa Z, Sato T, & Schmid K (1966) Hydrazinolysis of alpha-1-acid glycoprotein. *Biochim Biophys Acta.* 121(2):417-420.

Young ID, Willmer JP, & Kisilevsky R (1989) The ultrastructural localization of sulfated proteoglycans is identical in the amyloids of Alzheimer's disease and AA, AL, senile cardiac and medullary carcinoma-associated amyloidosis. *Acta Neuropathol* 78(2):202-209.

Yue M, Hanna A, Wilson J, Roder H, & Janus C (2011) Sex difference in pathology and memory decline in rTg4510 mouse model of tauopathy. *Neurobiology of aging* 32(4):590-603.

Zcharia E*, et al.* (2004) Transgenic expression of mammalian heparanase uncovers physiological functions of heparan sulfate in tissue morphogenesis, vascularization, and feeding behavior. *FASEB J* 18(2):252-263.

Zec RF & Burkett NR (2008) Non-pharmacological and pharmacological treatment of the cognitive and behavioral symptoms of Alzheimer disease. *NeuroRehabilitation* 23(5):425-438.

Zhan SS, Veerhuis R, Kamphorst W, & Eikelenboom P (1995) Distribution of beta amyloid associated proteins in plaques in Alzheimer's disease and in the non-demented elderly. *Neurodegeneration.* 4(3):291-297.

Zhang GL, Zhang X, Wang XM, & Li JP (2014) Towards understanding the roles of heparan sulfate proteoglycans in Alzheimer's disease. *Biomed Res Int* 2014:516028.(doi):10.1155/2014/516028. Epub 512014 Jul 516023.

Zhang RL*, et al.* (1995) The temporal profiles of ICAM-1 protein and mRNA expression after transient MCA occlusion in the rat. *Brain Res.* 682(1-2):182-188.

Zhang X*, et al.* (2007) Hypoxia-inducible factor 1alpha (HIF-1alpha)-mediated hypoxia increases BACE1 expression and beta-amyloid generation. *J Biol Chem.* 282(15):10873-10880. Epub 12007 Feb 10815.

Zhang Y*, et al.* (2015) Detection of subjects and brain regions related to Alzheimer's disease using 3D MRI scans based on eigenbrain and machine learning. *Front Comput Neurosci.* 9:66.(doi):10.3389/fncom.2015.00066. eCollection 02015.

Zhang Y*, et al.* (2014) A lifespan observation of a novel mouse model: in vivo evidence supports abeta oligomer hypothesis. *PLoS One.* 9(1):e85885. doi: 85810.81371/journal.pone.0085885. eCollection 0082014.

Zhao Y, Tan W, Sheng W, & Li X (2016) Identification of Biomarkers Associated With Alzheimer's Disease by Bioinformatics Analysis. *Am J Alzheimers Dis Other Demen* 31(2):163-168.

Appendix

Appendix A

Optimisation of HS extraction and purification steps for disaccharide analysis with strong anion exchange chromatography

Initially, HS extraction and purification was carried out on mouse brain tissue and with commercially available disaccharide standards to ensure that the procedure could be carried out fully without loss of the HS material. HS extraction and purification protocol yielded reasonably low detection of disaccharides. As there were only limited quantities of brain sample available from the brain bank, optimisation was necessary to enhance detection of small quantities of HS so that multiple experiments could be carried out with each donated sample, as well as generating large enough peaks so as to be accurately analysed without error.

The protocol steps as outlined in Chapter 2 were necessary for appropriate extraction and purification of HS from tissue. Any issues/potential losses of material from each of the main steps were highlighted and solutions found where necessary. These are outlined below. Importantly, with exception of TLC optimisation that was carried out as a separate experiment, the other modifications to the protocol were carried out in combination with one another.

DEAE step optimisation

There were difficulties with pelleting the beads appropriately and some were lost as a result, during elution steps. This would have negatively impacted HS product yield as the sugar is bound to the beads until the final elution steps. As such any beads lost in preceding wash steps precluded recovery of purified HS product. To solve this, beads were spun at a greater speed (3000 rpm) for a longer period of time (5 min) and all wash steps (10ml) and elution steps (1ml x2) were carried out in greater volume and decanted off the beads rather than pipetted off. This prevented loss of beads and as a result improved the yield of HS collected at this step.

Graphite column optimisation

In this step of the protocol, there was some graphite contamination in the final sample of HS recovered. In addition there were issues removing all of the organic solvents used to elute the HS from the graphite beads. Graphite contamination was shown to interfere with the labeling process that followed, as it could not be sufficiently dissolved in the DMSO: acetic acid mixture. Furthermore, graphite carried over in this manner resulted in a reduced product yield, as HS remained bonded to the graphite beads and could not be successfully dissociated. As a solution, the

graphite columns were spun at a lower speed (1.5 x g) to prevent the graphite passing through the matrix filter at the bottom of the column into the sample. Furthermore an increased number of water washes and speed vac steps were incorporated into the protocol to ensure complete removal of all organic solvents that would otherwise interrupt the successive labeling and clean up steps.

TLC step optimisation

A study was run to assess efficiency of the TLC method for removing free BODIPY label that would otherwise saturate the fluorescence detection on the HPLC system. 4 samples of HS standards 1-8 were labeled with the BODIPY hydrazide tag (10µl) of 160µg/ml stock) and run on the TLC plates as described previously (**Chapter 2**). Different sections of the plate relative to original sample placement were taken for each experiment and run over the Propac PA-1 column to assess which standards were collected from which region of the plate.

Previously, silica filings from the TLC plate were taken from -2cm of sample spot to +2cm (TLC1). Results of this study however found that a high proportion of standard UA-GlcNAc was found within the region 2-4cm from sample placement (TLC2) (**Figure 1**). To ensure all of the standard disaccharides were collected without loss, a greater proportion of the silica filings from the plate must be collected. This prevented loss of final HS product at HPLC analysis. Together, the combination of these alterations to the protocol provided enhanced detection of the HS disaccharides significantly by approximately 5 fold. The TLC step proved to be the most significantly optimized step with dramatic increases in the detection of HS disaccharide standard. Optimisation of this protocol therefore improved the quality of the chromatograms for each sample and enhanced detection of even very small quantities of individual disaccharides.

Ethanol precipitation optimisation

The last step is included in this protocol to ensure final removal of any impurities that may have co-purified with the HS. Initially, there were some significant losses of the UA-GlcNAc disaccharides. This disaccharide is totally unsulfated and as such only binds relatively weakly to the positively charged strong anion exchange column. It appeared to be dissociated almost immediately from the column. This may have been a result of insufficient water wash steps after ethanol precipitation such that carry over of the sodium acetate meant the sample could be easily dissociated from the column. Increased wash steps effectively removed the salt and prevented loss

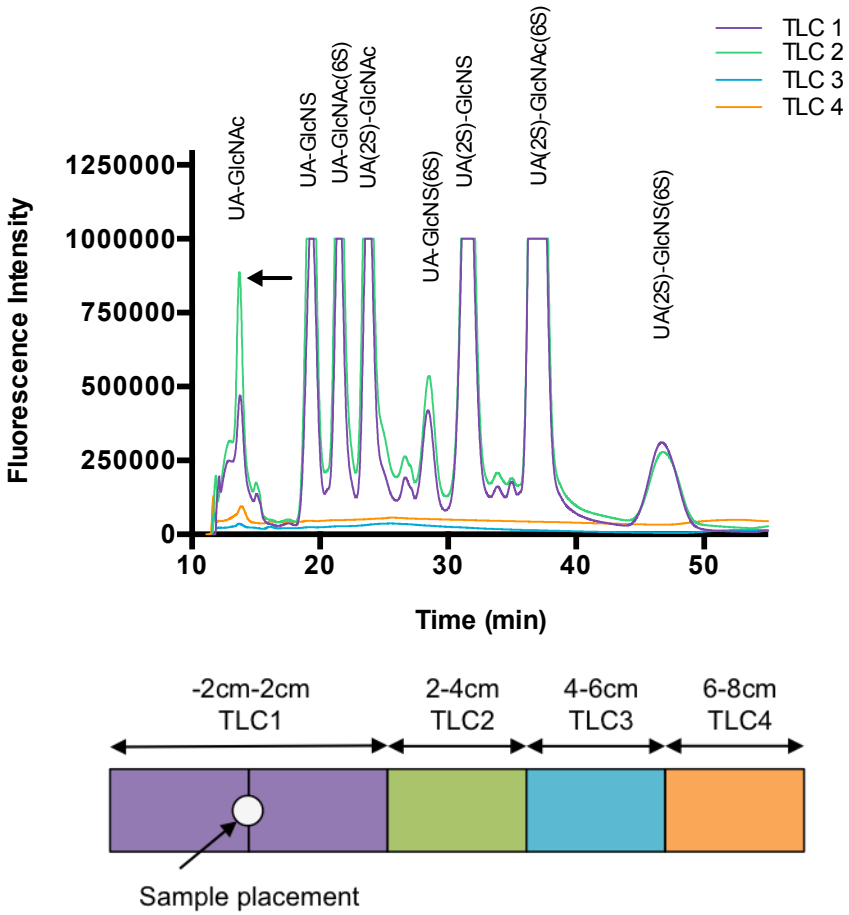

Figure A1: Optimisation of TLC step in compositional analysis of purified HS from human AD and Ctrl BA21 brain regions. Different regions of the TLC (as shown) were taken and analysed to determine how labeled HS disaccharide standards run along the TLC plate. As indicated by the arrow on the chromatogram, a great deal of the UA-GlcNAc disaccharide is present within the "TLC2" region of the plate, a region previously uncollected before optimisation. This is the smallest of the disaccharides and hence we would expect it to travel further up the plate. In future HS purifications and labeling, filings from the TLC plate were collected as far as 6cm from the bottom of the plate to ensure total recovery of all HS disaccharides.

of unsulfated HS disaccharides from the column inappropriately. This dramatically improved the yield of the UA-GlcNAc standard that could be detected and analysed as part of compositional analysis studies.

Results

Together, these small changes to the protocol dramatically increased the detection of purified HS after strong anion exchange chromatography. **Figure 2** shows data for preparation of disaccharides by the original or improved protocols. In some instances there was nearly a 5-fold improvement in the amount of purified HS that could be analysed.

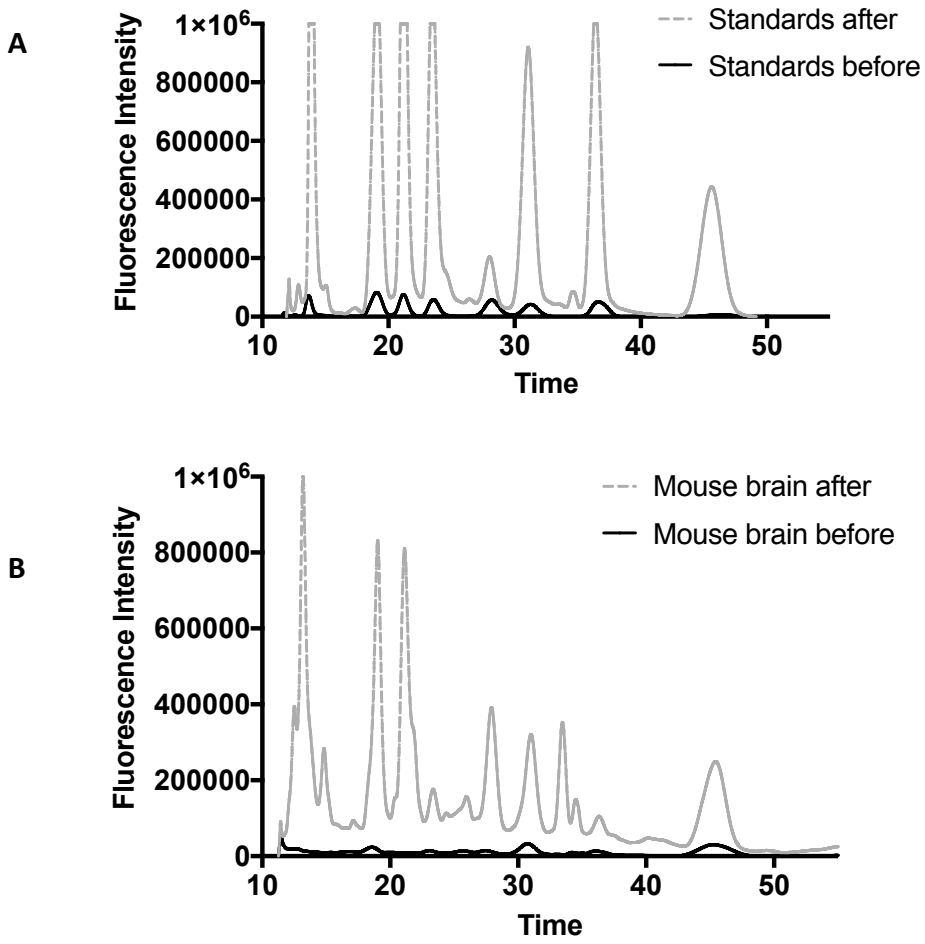

Figure A2: Original and optimised protocols for HS extraction and labeling of commercially available disaccharide standards (A) and HS derived from mouse brain samples (B). Fluorescence strong anion exchange HPLC of commercially available disaccharide standards and HS derived from mouse brain samples. These were prepared as per original protocol measures and injected over a Propac PA-1 column and eluted with a linear gradient of sodium chloride (0-1M over 30min) and isocratic NaOH (150mM). Peaks were detected using an inline fluorimeter, λ_{exc} = 488nm and λ_{emm} = 520nm. From left to right disaccharides present a progressively greater level of sulfation. Chromatograms display improved profiles following optimisation of the original protocol. A much greater signal intensity was established following improvement to the protocol.

Appendix B

SULF KO mouse brain compositional analysis data

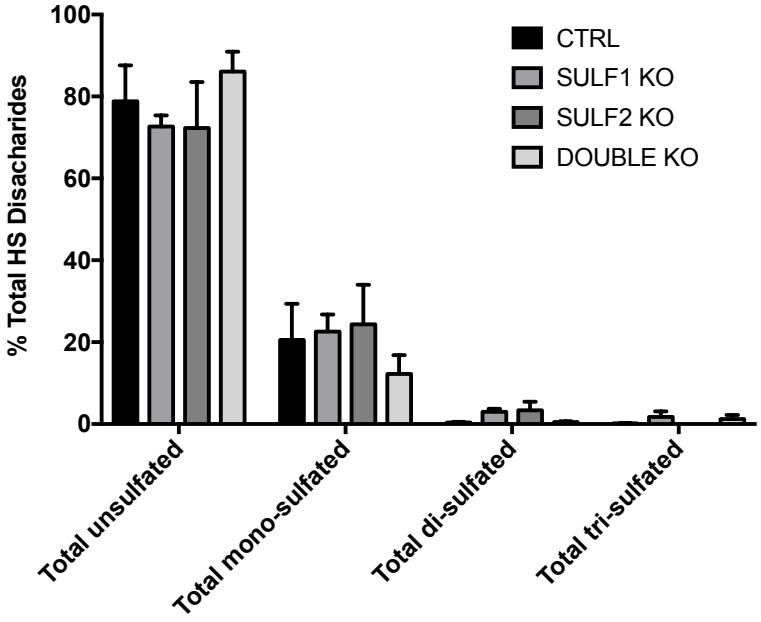

Figure B1: Composition of HS disaccharides displaying different numbers of sulfate groups does not differ upon knockdown of the *Sulf1* or *Sulf2* gene. HS isolated from control, SULF1 KO, SULF2 KO and DOUBLE KO mouse brain samples were digested with a mixture of heparin lyases (heparinase I, II and III mixture) and resultant disaccharides were labeled with BODIPY hydrazide and subjected to strong anion exchange chromatography on a Propac PA-1 column and eluted with a linear gradient of sodium chloride (0-1M over 30 min) and isocratic sodium hydroxide (150mM). Peaks were detected using an inline fluorimeter, λ_{exc} = 488nm and λ_{emm} = 520nm. Peak areas for each disaccharide were measure and disaccharide analysis is expressed as a % of mono- di- and tri- sulfated motifs within the HS analysed. Data shown are from control (n=3), SULF1 KO (n=3), SULF2 KO (n=3) and DOUBLE KO (n=3). Error bars represent mean (±S.E.M).

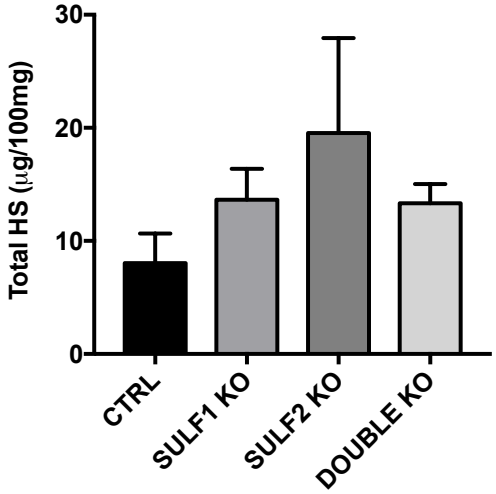

Figure B2: Total HS levels do not change upon knockdown of the *Sulf1* or *Sulf2* gene. HS isolated from control, SULF1 KO, SULF2 KO and DOUBLE KO mouse brain samples were digested with a mixture of heparin lyases (heparinase I, II and III mixture) followed by exhaustive clean up enzymatic digestion to remove other GAGs, DNA, RNA and protein. Resultant disaccharides were finally quantified and total HS levels were normalised to µg/100mg of wet tissue starting material. Data shown are from control (n=3), SULF1 KO (n=3), SULF2 KO (n=3) and DOUBLE KO (n=3). Error bars represent mean (±S.E.M).

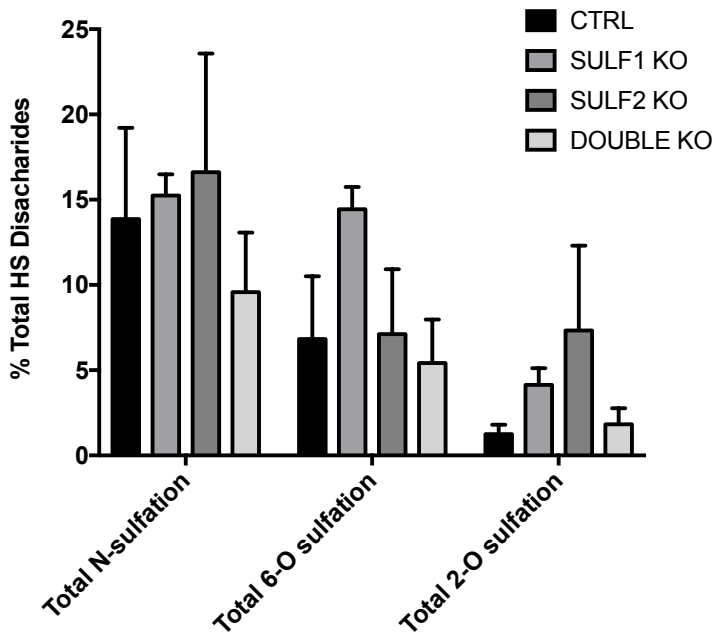

Figure B3: Composition of HS disaccharides sulfated at different locations do not differ upon knockdown of the *Sulf1* or *Sulf2* gene. HS isolated from control, SULF1 KO, SULF2 KO and DOUBLE KO mouse brain samples were digested with a mixture of heparin lyases (heparinase I, II and III mixture) and resultant disaccharides were labeled with BODIPY hydrazide and subjected to strong anion exchange chromatography on a Propac PA-1 column and eluted with a linear gradient of sodium chloride (0-1M over 30 min) and isocratic sodium hydroxide. Peaks were detected using an inline fluorimeter, λ_{exc} = 488nm and λ_{emm} = 520nm. Peak areas for each disaccharide were measure and disaccharide analysis is expressed as a % of N-, 6-O and 2-O sulfated motifs within the HS analysed. Data shown are from control (n=3), SULF1 KO (n=3), SULF2 KO (n=3) and DOUBLE KO (n=3). Error bars represent mean ± S.E.M.

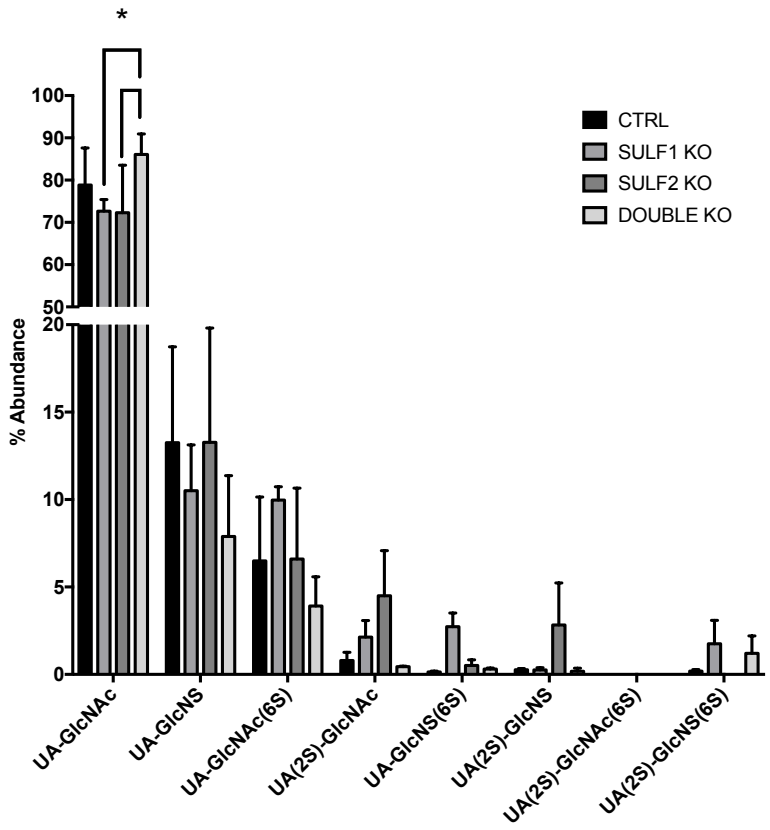

Figure B4: Composition of HS disaccharides changes upon knockdown of the *Sulf1* or *Sulf2* gene. HS isolated from Ctrl, SUlF1 KO, SULF2 KO and double KO mouse brain samples were digested with a mixture of heparin lyases (heparinase I, II and III mixture) and resultant disaccharides were labeled with BODIPY fluorescent hydrazide and subjected to strong anion exchange chromatography on a Propac PA-1 column and eluted with a linear gradient of sodium hydroxide (0-1M over 30 min). Peaks were detected using an inline fluorimeter, λ_{exc} = 488nm and λ_{emm} = 520nm. Peak areas for each disaccharide were measure and disaccharide analysis is expressed as a % of total HS analysed. Data shown are from Ctrl (n=3), SULF1 KO (n=3), SULF2 KO (n=3) and Double KO (n=3). Error bars represent mean ± S.E.M. Student's t-test * p<0.05, ** p<0.01, *** p<0.001.

Appendix C

Gene/protein lists created for bioinformatics work

List 1: HS biosynthetic enzymes and core proteins

This list included all HS biosynthetic enzymes including the core proteins onto which HS chains may be covalently bound. This list was generated with the use of KEGG (Version 80.1, Kaneshisa laboratories, Japan) to determine the established pathway for the synthesis of HS. This list also included the HS degradation enzymes including HPSE and HPSE2 and SULF1 and 2. With regard to core proteins, only the "full time" HSPGs were selected. The "part time" HSPGs, including betaglycan and Neuropilin-1 were not included in this list (Sarrazin*, et al.* 2011).

EXT1	HS6ST3	GPC3
EXT2	HS2ST1	GPC4
EXTL1	HS3ST1	GPC5
EXTL2	HS3ST2	GPC6
EXTL3	HS3ST3A1	SDC1
XYLT1	HS3ST3B1	SDC2
XYLT2	HS3ST4	SDC3
NDST1	HS3ST5	SDC4
NDST2	SULF1	HSPG2
NDST3	SULF2	AGRN
NDST4	HPSE	CD44
GLCE	HPSE2	COL18A1
HS6ST1	GPC1	SRGN
HS6ST2	GPC2	

List 2: GWAS determined AD risk proteins

APOE	PCK1	CELF2
LRAT	PGBD1	TMEM132C
FAM1138	TNK1	TRPC4AP
ATXN1	TRAK2	ARSB
CD33	UBD	CANDI
PCDH11X	CLU	EFNA5
ACAN	PICALM	MAGI2
BCR	CHRNA7	PRUNE2
CTSS	BIN1	TOMM40
EBF3	CD2AP	GAB2
FAM63A	CR1	EXOC3L2
GALP	EPHAI	AGPAT1
LMNA	MS4A4E	ATP6VOA4
LOC651924	MS4A6A	GLOD4
MYH13	GOLM1	RG56

List 3: Heparin interactome proteins

This list was obtained from the work of Ori et al in 2011 (Ori*, et al.* 2011). The interactome list was obtained from Supplementary data, Table 1. All details of functionality of these proteins can be found in this publication also.

4F2
5NTD
A1AT
A1BG
A2MG
A4
AACT
AAMP
ABCBB
ABCG2
ABCG5
ABP1
ADA1B
AGRP
AIMP1
ALDR
AMBP
AMRP
ANGI
ANGT
ANT3
ANXA1
ANXA2
ANXA3
ANXA5
ANXA6
APLP1
APLP2
APOA5
APOB
APOE
APOH
AQP1
ARGI1
ARTN
ASIP
AT1A1
AT1B1
AT1B3
AT2B1
ATP7B
ATPA
ATRN
ATS1
ATS3
ATS5
ATS8
ATS9
B2MG
B3AT
B4E216
BACE1
BMP2
BMP3
BMP4
BMP6
BMP7
BTC
C1QA
C1QB
C1QC
C4BPA
CAC1S
CADH8
CAP7
CATB
CATG
CBG
CBPB2
CBPD
CC134
CCD80
CCL1
CCL11
CCL13
CCL15
CCL17
CCL19
CCL2
CCL21
CCL22
CCL23
CCL24
CCL25
CCL27
CCL28
CCL3
CCL4
CCL5
CCL7
CCL8
CD031
CD1D
CD36
CD47
CEL
CERU
CF015
CFAB
CFAD
CFAH
CFAI
CHRD
CJ058
CLUS
CMA1
CO1A1
CO1A2
CO2
CO2A1
CO3
CO3A1
CO4A
CO4A1
CO4A2
CO5
CO5A1
CO5A3
CO6
CO6A3
CO7
CO8A
CO8B
CO8G
CO9
CO9A1
COBA1
COBA2
COCA1
CODA1
COEA1
COIA1
COJA1
COLQ
COMP
COMT
CONA1
COPA1
CRCM1
CRLD2
CSF2
CTGF
CTR2
CXB1
CXCL2
CXCL6
CXCL7
CXL10

CXL11
CXL13
CXL16
CYC
CYR61
DCC
DHB11
DHB12
DHB13
DHB7
DPP4
ECE1
ECM2
EFNA1
EFNA3
EFNA5
ELN
ELNE
ENOA
ENPP1
ENPP3
ERBB2
FA10
FA11
FA12
FA55A
FA9
FBLN7
FBN1
FBN2
FBS1
FCGRN
FETUB
FGF1
FGF10
FGF12
FGF14
FGF16
FGF17
FGF18
FGF2
FGF20
FGF22
FGF3
FGF4
FGF5
FGF6
FGF7
FGF8
FGF9
FGFP1
FGFP3
FGFR1
FGFR2
FGFR3
FGFR4
FIBA
FIBB
FIBG
FINC
FST
FSTL1
FURIN
G6B
GDN
GDNF
GELS
GHR
GP182
GPNMB
GROA
GTR2
HBEGF
HDGF
HEP2
HFE
HGF
HMGB1
HPT
HRG
IAPP
IBP2
IBP3
IBP4
IBP5
IBP6
IC1
IFNG
IHH
IIGP5
IL10
IL12B
IL2
IL3
IL4
IL5
IL6
IL7
IL8
IMPG2
INHBA
INSR
IPSP
ITA1
ITA5
ITAM
ITAV
ITB1
ITB3
ITIH3
ITM2B
KALM
KGFL1
KGFL2
KNG1
LAMA1
LAMA2
LAMA3
LAMA4
LAMA5
LAMC2
LCAP
LDLR
LEG9
LGR4
LIFR
LIPC
LIPE
LIPL
LIS1
LPHN2
LTBP1
LYAM1
LYAM3
MBL2
MDR1
MDR3
MET
MIF
MK
MMP14
MMP2
MMP7
MMP9
MOT1
MOT8
MRP6
MYL9
NAV2
NCAM1
NET1
NICA
NOGG
NRG1
NRP1
NRTN
NTCP
OCLN
OZF
PA2G5
PA2GA
PAI1
PAIRB
PCFT
PCOC2
PCSK5
PCSK6
PDCD5
PDGFA
PDGFB
PDIA1

PDIA6
PEBP1
PECA1
PEDF
PERM
PF4V
PGBM
PGS1
PIGR
PLBL1
PLF4
PLGF
PLMN
PON1
PON2
PON3
POSTN
PPIB
PRDX4
PRELP
PRG2
PRIO
PRL
PROC
PROP
PSN1
PTC1
PTN
PTPRC
Q5IT36
Q5JAR4
Q8IV69
Q9HCS8
RL22
RL29
ROBO1
RSPO1
RSPO2
RSPO3
RSPO4
RSSA
S12A9
S20A2
S22A1
S22A7
S22AI
S38A3
S38A4
S39A4
S4A4
SAA
SAMP
SCN5A
SDF1
SEM5A
SEM5B
SFRP1
SHH
SIAT1
SLIT1
SLIT2
SLPI
SNG1
SODC
SODE
SORT
SOST
STAB2
STEA4
STIM1
SYUA
TAU
TEN1
TENA
TENX
TFPI1
TFR1
TFR2
TGBR3
TGFB1
TGFB2
TGM2
THIO
THRB
THYG
TIMP3
TIP
TNF13
TNFA
TPA
TR11B
TRFE
TRFL
TRY1
TRYB1
TRYB2
TSG6
TSP1
TSP2
TSP3
TSP4
TTHY
UROK
VEGFA
VEGFB
VGFR1
VGFR2
VTDB
VTNC
VWF
WNT1
X3CL1
XCL1
XDH
ZNT1
ZPI

Appendix D

Genevestigator protocol

Briefly, 33 AD brain samples (15 males and 18 females) were collected at three Alzheimer's disease Centers (ADCs) in America; Washington University, Duke University and Arizona University ADCs. Alzheimer's samples were taken from patients with a mean age of 79.9 ± 6.9yr and were selected based on both clinical and neurological criteria. Post mortem at death allowed histopathological confirmation of AD and of the samples selected, CERAD scores ranged from moderate to frequent and Braak stages ranged from V to VI (Braak and Braak 1991). Control samples were collected from the Sun Health research Institute, an ADC and were clinically classified as neurologically normal (Liang*, et al.* 2007). 10 males and 4 females made up the healthy control sample group and were gender and age-matched to AD samples at death. Average age for this group was 79.8 ± 9.1yr. Post mortem at death confirmed CERAD scores of infrequent and Braak staging of I to II (Liang*, et al.* 2007).

Heterogeneity within tissue was eliminated prior to expression profiling by laser capture microscopy on all brain regions. 6 brain regions were targeted in total, with 14 biological replicates taken for each region. The entorhinal cortex (BA 28 and 34), hippocampus, middle temporal gyrus (BA 21 and 37), posterior cingulate (BA 23 and 31), primary visual cortex (BA 17) and superior frontal gyrus (BA 10 and 11) were all selected as regions of interest (Dunckley*, et al.* 2006). The 6 regions chosen were based on their vulnerability to the pathological processes of associated with AD and ageing. Sections were dissected, frozen and sectioned and mounted onto slides (Dunckley*, et al.* 2006). Approximately 1,000 pyramidal neurons were collected from the cortical layer III from the white matter of each brain region per brain sample by laser capture microdissection with the Arcturus Autopix Automated laser Capture Microdissection System (Mouse View, CA) (Liang*, et al.* 2008). RNA was extracted according to manufacturer's instructions (Pico Pure RNA Isolation Kit, Arcturus), and DNA removed according to manufacturer's instructions (Qiagen RNAse free DNase Set, Valencia, CA). RNA samples underwent double round amplification before cleaning and biotin labeling as per manufacturer's instructions (Affymetrix GeneChip Two-Cycle Target labeling kit, Santa Clara, CA) (Liang*, et al.* 2007). For the microarray analysis, cocktails were hybridized to the Affymetrix Human Genome U133 plus 2.0 Array for 16h at 45'C in the Hybridization Oven 640. This array allowed the analysis over 38,500 pre-characterized human genes. After Incubation, arrays were washed according to manufacturer's instructions and finally scanned for signal intensity. All target gene signal intensities were normalized against the housekeeping gene GAPDH (Liang*, et al.* 2007).